Managed by Platinum Foundation
GANDHINAGAR INSTITUTE OF TECHNOLOGY
AICTE Approved | Affiliated with Gujarat Technological University

'GIT-Journal of Engineering and Technology'

ISSN 2249–6157
(Print & Online)

Published By,

Gandhinagar Institute of Technology
Khatraj - Kalol Road, Moti Bhoyan,
Tal. Kalol, Dist. Gandhinagar-382721
Phone: 9904405900, 02764-281860/61
E-mail: director@git.org.in, jet@git.org.in
Website: www.git.org.in

About Gandhinagar Institute of Technology

Gandhinagar Institute of Technology is established by Platinum Foundation in 2006. It offers under graduate programs in Mechanical Engineering, Information Technology, Computer Engineering, Electronics and Communication Engineering, Electrical Engineering and Civil Engineering and Post graduate program in MBA (Finance, Human Resource Development, and Marketing), M.E. in Mechanical Engineering with specialization in Thermal Engineering and Computer Aided Design & Computer Aided Manufacturing and M.E. in Computer Engineering with specialization in Software Engineering.

All these programs are approved by AICTE, New Delhi and affiliated to Gujarat Technological University. We have elaborate laboratory facilities and highly motivated and qualified faculty members. We are also arranging technical seminars, conferences, industry-institute interaction programs, workshops and expert lectures of eminent dignitaries from different industries and various reputed educational institutes.

Our students are innovative and have excellent acceptability to latest trends and technologies of present time. Our students have also participated in various technical activities as well as sports activities and have achieved various prices at state level. We have two annual publications, a National level research journal 'GIT-Journal of Engineering and Technology (ISSN 2249–6157)' and 'GIT-a Song of Technocrat' (college magazine).

Trustees

Shri Hareshbhai B. Rohera

Shri Ghanshyambhai V. Thakkar

Shri Deepakbhai N. Ravani

Shri Pravinbhai A. Shah

Smt Varshaben M. Pandhi

Shri Mahendrabhai R. Pandhi

Message from the Director

It gives me immense pleasure that the eleventh issue of our National journal 'GIT-Journal of Engineering and Technology' is being published with ISSN 2249 – 6157 for eleventh successive year. The annual journal contains peer reviewed technical papers submitted by the researchersfrom all domainsof engineering and technology. The issue is a result of imaginative and expressive skill and talent of GIT family. Research papers were invited from the researchers of all domains in engineering and technology across the India. More than 60 research papers were received. After peer reviewed 21 papers are selected and being published in this issue of the journal.

GIT was established in 2006 and during a short span of twelve years; it has accomplished the mission effectively for which it was established. Institute has been constantly achieving the glory of excellence in the field of curricular and co-curricular activities. For the eleventh consecutive year an annual technical symposium TechXtreme 2018 was successfully organized by the institute. More than 4500 students of various technical institutions across the Gujarat participated in the Techfest. Prizes worth Rs 2 lacs and trophies were given to the winners. Annual cultural event Jazba 2017 was organized with participation of more than 1500 students of the institute in various cultural events of Debate, Quiz, Essay writing, Rangoli, Music, Dance, Drama etc.

Institute awarded as best Engineering College for providing best placement to the students by ASSOCHAM. Institute was awarded by 94.3 MY FM for "Excellence in Faculty (Engineering & Technology)". Dr N M Bhatt, Director is awarded with GTU Pedagogical Innovation special for outstanding contribution for implementing curriculum of Design Engineering. Institute is 3 star Super RESOURCE centre for spoken tutorial project of IIT-Bombay funded by MHRD, Govt. of India. Institute has also arranged blood donation drives and fund for Sainik Welfare fund. Student Team Greenitious as Best Design Award for Effi-Cycle was awarded by SAE LD Collegiate Club. Institute has also hosted GTU Zonal Techfest 2015 and 2018 of Gandhinagar Zone. Team Renosters participated in ATV car design competition "BAJA STUDENT INDIA" held at NIT, Jamshedpur and got 20th position in all over India. Institute won ISHRAE "A-Quest" quiz competition at Zonal Level and appreciated by GTU for creating student innovation and Start-up Ecosystem in campus.

The Institute is also emphasis on academic development of its faculty members. During the year, many International and National papers has been published and presented by the faculty members. The faculty members have also been deputed to attend large number of seminars/workshops/training programs/symposiums.

Publication of the journal of national level is not possible without whole hearted support of committed and experienced Trustees of Platinum Foundation and I take an opportunity to express my deep feelings of gratitude to all of them for their constant support and motivation.

It's my privileged to compliment the staff members and the students for showing high level of liveliness throughout the year. I also congratulate the team of the GIT-Journal of Engineering and Technology for their untiring effort to bring out this eleventh issue of the journal.

Dr N M Bhatt
Director & Chief Editor

Index

Evaluation of Replacing HFC134a in Domestic VCR system

Nirav M Modi[a], Nimesh Gajjar[a], N M Bhatt[a*]

[a]*Gandhinagar Institute of Technology, Moti Bhoyan, Gandhinagar, Gujarat, India 382781*

Abstract

HFC134a is composed of carbon, fluorine and hydrogen and has been used as a replacement of CFC and HCFC refrigerant in medium and higher temperature household and commercial refrigeration systems and automotive air conditioning. It is a greenhouse gas and has significant effect in global warming which is the burning issue for world today. Research studies revealed that refrigerants which are being used in air conditioning and refrigeration industry for more than 200 years now are one of the major causes for it. Refrigerants like CFCs, HCFCs and HFCs which are commonly used till date contain chlorine and fluorine atoms which deplete Ozone layer and cause global warming effects like increasing average temperature of earth. Hence, Montreal and Kyoto Protocol are developed and adopted by many countries to reduce the usage of harmful refrigerants and its impact on the environment. These protocols put limits on consumption of higher Ozone Depleting Potential (ODP) and Global Warming Potential (GWP) value refrigerants and hence many need to be dropped out. In industry, currently R134a is widely used refrigerant in domestic and other small appliances, after traditional refrigerants were dropped out or phased out. R134a shows excellent thermodynamic performance and non-flammability characteristics and so popular in industry but not eco-friendly as having higher GWP and contribute to damage environment. So, this paper focuses on replacement options of R134a which have very low GWP value, lesser atmospheric life, and performance matching to R134a with minimal system changes, so they can be a longer-term solution. It has been evaluated that R152a and R600a have better thermodynamic performance but as they are flammable, they can be used with domestic system if sufficient safety precautions are taken. R1234yf will be a better alternative to R134a as it shows similar thermo-physical properties and has a very low 100-year GWP rating of 4, which is approximately 350 times lower than R134a.

Keywords: Global warming; ODP; GWP; Montreal/Kyoto Protocol; R134a; R600a; R1234yf.

Abbreviation	
AB	Alkyl benzene
GWP	Global Warming Potential
HCFCs	Hydro chlorofluorocarbons
HCs	Hydrocarbons
HFOs	Hydrofluro-olefins
MO	Mineral Oil
ODP	Ozone Depleting Potential
POE	Polyol Ester
PAO	Poly Alpha Oelfin
PAG	Polyalkylene Glycol
VCR	Vapour Compression Refrigeration
Subscripts	
c	condenser
e	evaporator

1. Introduction

The most common thermodynamic cycle used in refrigeration industry is Vapor Compression Refrigeration (VCR) cycle which is nearly 200 years old. In VCR systems refrigerant is used as circulating medium which absorbs and removes heat from the space to be cooled and subsequently rejects that heat elsewhere.Aside from technological advance, a major change to their use nowadays is the increased focus on reducing the impact of refrigerants on the environment. Today the same cycle is used but with variety of refrigerants. In the beginning, refrigerants were easily obtainable as they existed in nature.

By 1930s, safety issues were the major concerns and many fire and health related cases reported due to leakage of refrigerants. Safety refrigerants called CFCs were invented and began to use globally along with development of partially chlorinated refrigerants called HCFCs.

* N M Bhatt Tel.: +91-9904406000
E-mail address: nmbhatt19@gmail.com

In the early 1970s, it was noticed that CFC refrigerants which reach to the stratosphere are broken into highly reactive forms of chlorine by the ultraviolet radiation and take part in a series of chain reactions leading to ozone depletion. Hence these substances are recognized as ozone depleting substances (ODS) and global loss of ozone due to that substance with reference to R11 is recognized as ozone depleting potential (ODP). Montreal Protocol was developed in 1987 to phase down substances that deplete ozone layer. HFCs were considered as substitutes for the CFCs due to its zero ODP value but they have higher GWP and investigations have shown that its longer use will be the major contributor to global warming. Hence from October 2016 Montreal Protocol agrees to phase down HFCs too.

The release or loss of refrigerants from air conditioning and refrigeration system into atmosphere is one of the causes for increased greenhouse gases emissions [1, 2]. This phenomenon directly relates to the global environmental concerns such as global warming and ozone layer depletion. Substances such as chlorine and fluorine used to make chemical refrigerants are directly damages ozone layer when they release/loss from the system.

A refrigerant which meets or exceeds basic selection criteria such as toxicity and flammability makes them as short-term solutions, if they impact environmentally on the other end. Hence, other selection criteria such as zero ODP and lower GWP values shall be a primary focus while selection of refrigerant which reduces environmental impact and can be a long-term solution.

This paper evaluates alternative refrigerants of R134a in domestic VCR system which meets new stringent requirement of GWP and hence no/less environmental impacts.

2. R134a as a Refrigerant:

R134a is chlorine free HFC refrigerant which has zero ODP and widely used and tested comprehensively. It is also widely used for a blend with other refrigerants. R134a was initially the refrigerant choice to replace R12 in domestic refrigerators because it is chlorine-free, no-flammable, no/less toxic, has zero ODP and comparable cycle efficiency. The boiling point, vapor pressure characteristics and refrigeration cycle efficiency are quite similar to R12 but its volumetric capacity is less and not fully compatible with R12 lubrication system [3]. Today about 63% of newly produced domestic refrigeration system are charged with R134a and about 36% are charge with iso-butane. It is predicted that at least 75% of globally produced domestic refrigeration will use hydrocarbons in next 10 years. The iso-butane requires lesser charge than R134a and already widely accepted in Europe [4].

Table 1 Thermal Properties of R134a and R12 [5]

Parameters	R134a	R12
Critical Temperature (°C)	101.06	112
Critical Pressure (MPa)	4.05	4.115
Normal Boiling point (°C)	-26.1	-29.8
Molecular Weight (Kg/kmol)	102.02	120.93
Critical Density (kg/m^3)	511.9	558
ASHRAE Safety Class	A1	A1

2.1. Environmental Issues:

Global Warming Potential: R134a has suitable properties such as non-flammability, stability, and similar vapour pressure to the refrigerants CFCs and HCFCs but due to its very high GWP value, it is necessary to investigate more environmentally friendly refrigerants. Always lower GWP refrigerants are essential in VCR systems to reduce the impact of refrigerant on climate change.GWP is an index of a substance's ability to be greenhouse gas. It is a relative measure of how much heat a greenhouse gas traps in the atmosphere. It compares the amount of heat trapped by a certain mass of the gas to the amount of heat trapped by a similar mass of carbon dioxide for a 100-year time frame. R134a is one of the six chemicals that are signalled out by Kyoto protocol due to its very high GWP value (1430) to reduce global warming. Fig. 1(a) shows GWP value of R134a and other probable substitutes.

Atmospheric Life:HFC refrigerant emissions are released to the atmosphere throughout the lifecycle of equipment i.e., during equipment manufacture, installation, operation, maintenance, and at end-of-life. Longer a greenhouse gas stays in the atmosphere, higher will be the heating effect. R134a is fluorinated refrigerant and decompose persistent wastes in atmosphere and influence the climate for 14 years of atmospheric lifetime. As shown in Fig. 1(b), R134a shows comparatively longer atmospheric life than other refrigerants.

2.2. Regulations/Legislation:

Montreal Protocol: This protocol was adopted to prevent ozone layer by targeting refrigerant which have more than zero ODP value. On October 15, 2016, with the United States' leadership, 197 countries adopted an amendment to phase down HFCs under the Montreal Protocol in Kigali, Rwanda. Under the amendment, countries committed to cut the production and consumption of HFCs by more than 80 percent over the next 30 years [6, 7].
Kyoto Protocol: The most utilized refrigerant for domestic applications has been R134a until the Kyoto protocol established its phasing out due to its too high GWP (1430). In accordance with the United Nations Framework Convention on Climate Change (UNFCCC), the Kyoto Protocol targets refrigerants which have more than 150 GWP value for phase-out [8, 9].

3. Possible alternative of R134a:

In 2010, B. O. Bolaji experimentally examined R152a and R32 in a 120 liter refrigerator designed and developed to work with R134a. The results obtained showed that the design temperature and pull-down time set by International Standard Organization (ISO) for small refrigerator were achieved earlier using refrigerant R152a and R134a than using R32. It was concluded that the performance of R152a in the domestic refrigerator was constantly better than those of R134a and R32 throughout all the operating conditions and the average coefficient of performance (COP) obtained using R152a was 4.7% higher than R134a while average COP of R32 was 8.5% lower than R134a [10]. Chao-Chieh Yu, Tun-Ping Teng employed HC refrigerants as alternatives for R134a refrigerator. He evaluated the refrigeration performance and feasibility of using these alternative refrigerants HC1 (65% R290 + 35% R600a), HC2 (50% R290 + 50% R600a) and HC3 (00% R290 + 100% R600a) by conducting the no-load pull-down test and 24-hour on-load cycling test. The charged ratios were 30%, 40%, 50%, and 60% based on the charged mass of R134a for HC refrigerants. The results of the no-load pull-down test revealed that the optimal charged mass for all the HC refrigerants was 40% of that of R134a and efficiency factor (EF) of HC1, HC2, and HC3 were 9.1%, 12.2%, and 42.3% higher than that of R134a [11].E. Navarro, I.O. Martınez-Galvan, J. Nohales, J. Gonzalvez-Macia experimentally investigated compressor behaviour in terms of compressor efficiency, volumetric efficiency, losses to the ambient and oil-refrigerant properties using R1234yf, R290 and R134a. The operating parameter comprised two compressor speeds, evaporation temperatures from -15°C to 15°C and condensation temperatures from 40°C to 65°C. After investigation they concluded that R-290 has shown a significant improvement in compressor and volumetric efficiencies and the heat losses were considerably lower than for the other two refrigerants and R-1234yf improves its efficiencies compared to R-134a for pressure ratios higher than 8. R1234yf has discharge temperature was approximately 10 K lower than the discharge temperature of the other refrigerants [12]. Kyle M. Karber, Omar Abdelaziz, Edward A. Vineyard performed experiment for R-1234yf and R-1234ze as drop-in replacements for R134a in two household refrigerators – one baseline and one advanced technology. An experiment was conducted to evaluate and compare the performance of R134a to R-1234yf and R-1234ze, using AHAM standard HRF-1 to evaluate energy consumption. These refrigerants were tested as drop-in replacements, with no performance enhancing modifications to the refrigerators. In Refrigerator 1 and 2, R-1234yf had 2.7% and 1.3% higher energy consumption than R134a, respectively. This indicates that R-1234yf is a suitable drop-in replacement for R134a in domestic refrigeration applications. In Refrigerator 1 and 2, R-1234ze had 16% and 5.4% lower energy consumption than R134a, respectively. In order to replace R134a with R-1234ze in domestic refrigerators the lower capacity would need to be addressed, thus R-1234ze might not be suitable for drop-in replacement [13].

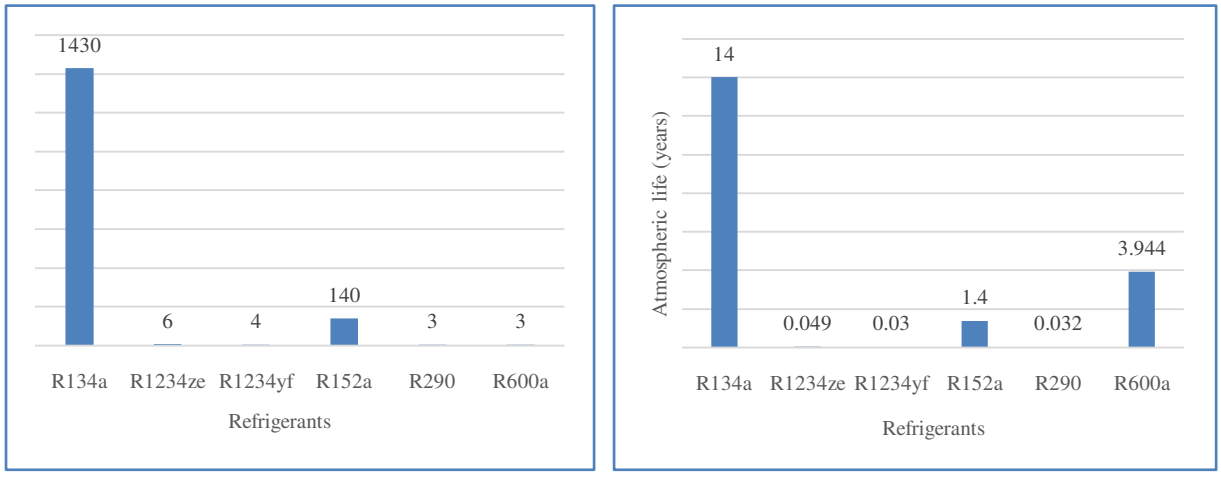

(a) (b)

Fig. 1. (a) GWP of various refrigerants and (b) Atmospheric life of various refrigerants [14]

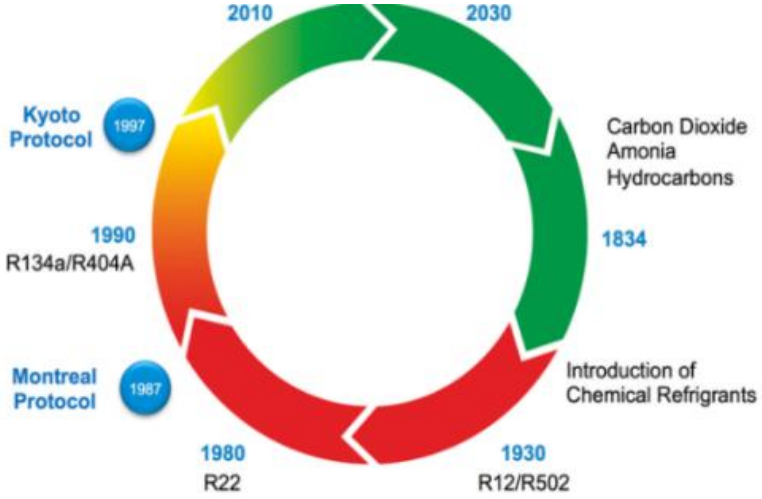

Fig. 2. Effect of Regulations

Fig. 2 shows transition history of various refrigerants due to different regulation to control impact on environment. Regulatory organizations put limits on usage of high GWP refrigerants and phase out in future. So, substituting over from higher GWP values to lower GWP values refrigerants so that they have minimal or less impact on environment.

From the discussion so far, it is clear that choices made in past were not sustainable refrigerants. Regarding long term sustainable refrigerants, three main parameters must be aligned to accomplish a real sustainable balance i.e. affordability, safety and environment friendliness. When choosing a new refrigerant for an application, all three parameters need to be considered together and balanced. If not, it will be impossible to achieve long term sustainable results.

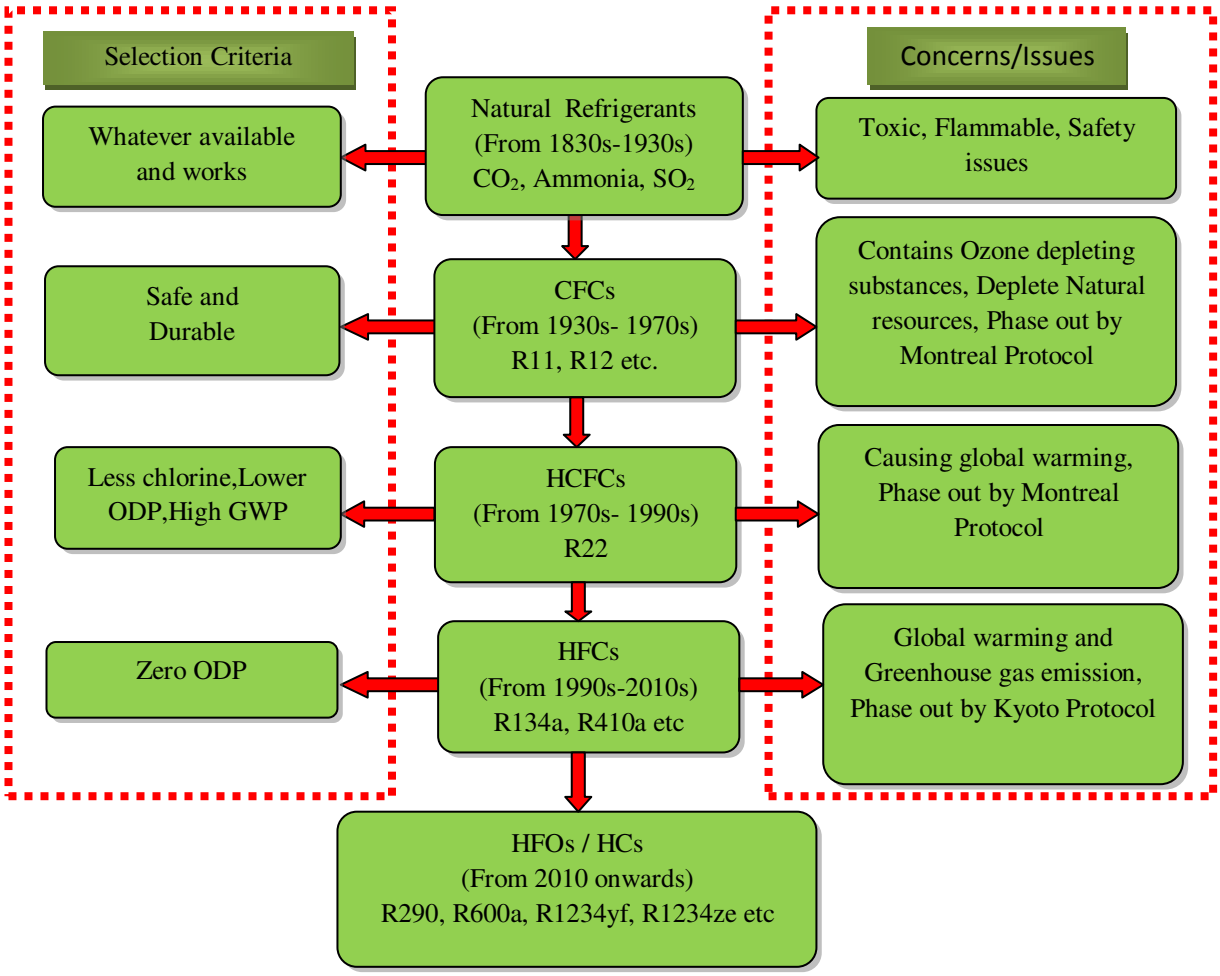

Fig. 3. Transitional History of Refrigerants [15]

3.1 Desirable Selection criteria:

In response to global HFC phase-down targets and proposals, it is necessary to discover proper alternative for existing and future equipment. Most of the newer zero-ODP, low-GWP alternatives suffer from one or more undesirable characteristics, such as greater flammability, toxicity. So, there are several demands to be met by a fluid to be suitable as a replacement of existing refrigerant [5]. Desirable selection criteria can be categorized in 7to three classes. In first criteria of health and safety for environment, refrigerant should have zero ODP, very low GWP, non-toxic and non/low flammable. Replacement refrigerant should have high critical point temperature, low enough freezing point, low pressure ratio, low viscosity, high thermal conductivity and comparable normal boiling point temperature as close to that of refrigerant to be replaced. Other criteria for replacement refrigerants are oil solubility/miscibility, high dielectric strength of vapour and easy leak detection [15, 16].

To reduce refrigerant's environmental impacts (such as global warming and greenhouse gas emissions) and to meet stringent codes requirements, usage HFCs group refrigerants need to eliminate. Hence great demand arises to develop and switch over to eco-friendly refrigerants groups like HFOs and HCs / natural refrigerants. Ultra-low GWP value, lesser atmospheric life and have better and/or similar kind of performance to R134a refrigerant, will be driving factors for a replacement options. Table 2. shows possible alternate refrigerants and its properties which may be used as a replacement of R134a in domestic application and may be a longer-term solution.

Table 2. Alternate Refrigerants Properties

Refrigerant Group	HFCs		HFOs		HCs / Blend	
Refrigerants	R134a	R152a	R1234ze	R1234yf	R290	R600a
Environmental Parameters						
ODP	0	0	0	0	0	0
GWP	1430	140	6	4	3	3
Atmospheric Life (years)	14	1.4	0.049	0.03	0.032	3.944
Thermodynamic Parameters						
Normal Boling Point ºC	-26.1	-24.02	-19	-29.45	-42.1	-11.67
Critical Temperature ºC	101.06	113.3	109.4	94.7	96.8	135.0
Critical Pressure MPa	4.05	4.52	3.63	3.3	4.256	3.645
Freezing Point ºC	-96.6	-117	-156.3	-152.2	-187.1	-159.6
Pressure Ratio Tc = 55ºC and Te = -25ºC	17.55	17.61	20.14	14.48	10.53	20.91
Other Parameters						
Toxicity	Lower	Lower	Lower	Lower	Lower	Lower
Flammability	No	Medium	Mildly	Mildly	Higher	Higher
ASHRAE Safety Class	A1	A2	A2L	A2L	A3	A3
Lubrication suitability	POE, PAG	POE, PAG	POE, PAG	POE, PAG	MO, AB	MO, AB

Careful study of Table 2 reveals that no refrigerant exists which can fulfill all basic selection criteria, but care shall be taken while selection to minimize impact on environment. GWP value and better pull down characteristics of R152a is favourable than R134a but it's classified as A2 safety class which is medium flammable so not suitable as an alternate solution [7]. HFO group refrigerants R1234ze and R1234yf have lower GWP value than R134a so can be considered as an alternative solution with consideration of mildly flammable. Their thermo-physical properties are also similar to R134a and hence can be considered as a most suitable drop-in replacement. Research study shows that R1234yf and R1234ze give marginally lesser COP for same operating conditions. These group of refrigerants are compatible with lubrication system of R134a and no major changes are required [6]. It can be seen from Table 2 that the pressure ratio for R1234yf is lower than that of R134a, R152a, R1234ze and R600a hence for same condenser temperature, R1234yf gives better performance compared to R1234ze when used as a drop-in replacement in R134a [10]. HCs are flammable refrigerants but can be used in small system where fluid charge is less with some safety precautions. They are not compatible with POE/PAG lubrication system hence system requires change [4]. R600a refrigerant is having higher suction vapor volume so require larger compressor size to meet the same refrigerating capacity than R134a. Moreover, there are chances of moisture carry over at compressor from surroundings due to below atmospheric working pressure on the suction side and can affect the performance of the system [4].

Table 3. Refrigerants Properties

Refrigerant Group	HFCs	HFOs		HCs / Blend	
Refrigerants	R152a	R1234ze	R1234yf	R290	R600a
Environment (ODP, GWP)	☹	☺	☺	☺	☺
Atmospheric Life	☹	☺	☺	☺	☺
Pressure and Temperature	☺	☺	☺	☹	☹
Thermal Performance (COP)	☺	☺	☺	☺	☺
Chemical Property	☹	☺	☺	☹	☹
Legislation (Montreal and Kyoto Protocol)	☹	☺	☺	☺	☺
Availability	☺	☺	☺	☺	☺
As a direct replacement	☹	☺	☺	☹	☹
Requirement satisfied ☺	Requirement unsatisfied ☹				

Conclusion:

By reviewing all possible options for alternate refrigerant with their merits and demerits, it can be observed that no refrigerant is ideal, but proper screening criteria can help to select future refrigerant, which may be a long-term solution. R1234yf shows similar performance to R134a and meets all other requirements so will be a better candidate for the long-term replacement of R134a with minimal or without changes into the existing system. Other Refrigerants like R152a and R600a shows better performances than R134a which can be used only in small systems with enough safety precautions as they are flammable.

References:

[1] Calm, J.M.,2001, Emissions and environmental impacts from air-conditioning and refrigeration systems, International Journal of Refrigeration 25, pp. 293–305
[2] Johnson, 1998, Global warming from HFC, environment impact assessment rev 18, pp. 485 – 492
[3] S. W. Crown et al., 1992, A Comparison Study of the Thermal Performance of R12 and R134a, International Refrigeration and Air Conditioning Conference, paper 155
[4] M. Mohanraj, S. Jayaraj, C. Muraleedharan, 2009, Environment friendly alternatives to halogenated refrigerants-A review, International journal of greenhouse gas control, 3, pp. 108 –119
[5] C P Arora, Third edition, Refrigeration and air conditioning, The McGraw-Hill companies, Pages (138-140)
[6] European Parliament and the Council of the European Union (EU), 2014, Regulation (EU) No 517/2014 on fluorinated greenhouse gases and repealing Regulation (EC) No 842/2006, Official Journal of the European Union
[7] Montreal Protocol on Substance that Deplete the Ozone Layer; United Nations Environment Programme: Montreal, Canada, 1998
[8] Samira Benhadid-Dib, Ahmed Benzaoui, 2012, Refrigerants and their environmental impact Substitution of hydro chlorofluorocarbon HCFC and HFC hydro fluorocarbon. Search for an adequate refrigerant, Energy Procedia 18, pp. 807 – 816
[9] Kyoto Protocol to the United Nations Framework Convention on Climate Change, United Nations Framework Convention on Climate Change, 1997
[10] B.O. Bolaji, 2010, Experimental study of R152a and R32 to replace R134a in a domestic refrigerator, Energy 35, pp. 3793-3798
[11] Chao-Chieh Yu, Tun-Ping Teng, Retrofit, 2014, Assessment of refrigerator using hydrocarbon refrigerants, Applied Thermal Engineering 66 (2014), pp. 507-518
[12] E. Navarro, I.O. Martınez-Galvan, J. Nohales, J. Gonza lvez-Macia, 2013, Comparative experimental study of an open piston compressor working with R-1234yf, R-134a and R-290, International Journal of Refrigeration 36, pp. 768-775
[13] Kyle M. Karber, Omar Abdelaziz, Edward A. Vineyard., 2012, Experimental Performance of R1234yf as a Drop-in Replacement for R134a in Domestic Refrigerator, International Refrigeration and Air Conditioning Conference at Purdue, July 16-19
[14] Guillermo Restrepo et al., 2007, Ranking of Refrigerants, Environmental Chemistry and Ecotoxicology, University of Bayreuth
[15] Calm J M, 2012, Refrigerants transition again, moving towards sustainability, ASHRAE/NIST conference 10, pp. 29-30
[16] Calm, J.M., 2008, The next generation of refrigerants - historical review, considerations, and Outlook, International journal of refrigeration 31, pp.1123-1133.

Simulation of Die and Punch for CNC Press Break

Vipal R Panchal[a*], Someshwar S Pandey[a], Hardik R Patel[a]

[a]*Gandhinagar Institute of Technology, Moti Bhoyan, Gandhinagar, Gujarat, India 382781*

Abstract

Minimization of response time and costs and maximization of the efficiency and quality in producing a product are imperative for survival in the competitive manufacturing industry. Sheet metal forming is a widely used and costly manufacturing process, to which these considerations apply. Mild Steel becomes favorable to compare to steel regards for some improvement in fabrication industries, increased engine efficiency and fuel economy. Wide range of mild steel product included doors, window, safety guard, control panel, seat frames and roof panels have been produced.
Research work was carried out to study the finite element (elastic-plastic) analysis of sheet metal forming process using the finite element software. For analyses of diing and punch shape of CNC press break in bending critical angle sheet by experimental work and compare with FEA taking ideal loading and boundary condition. Optimization of parameter of CNC press break such as die shape, punch shape and material thickness by FEA and identifying critical angle of sheet metal.

Keywords: CNC, Press Break, Die, Punch, Analysis.

Nomenclature

l	machine Length (mm)
D	diameter (mm)
g	gravity constant (m/s)
tc	duration (sec)
Greek symbols	
μ	coefficient of friction
η	efficiency

1. Work with assemblies

Working with assembly in solid work use different tool of mate like coincident, parallel, perpendicular etc.

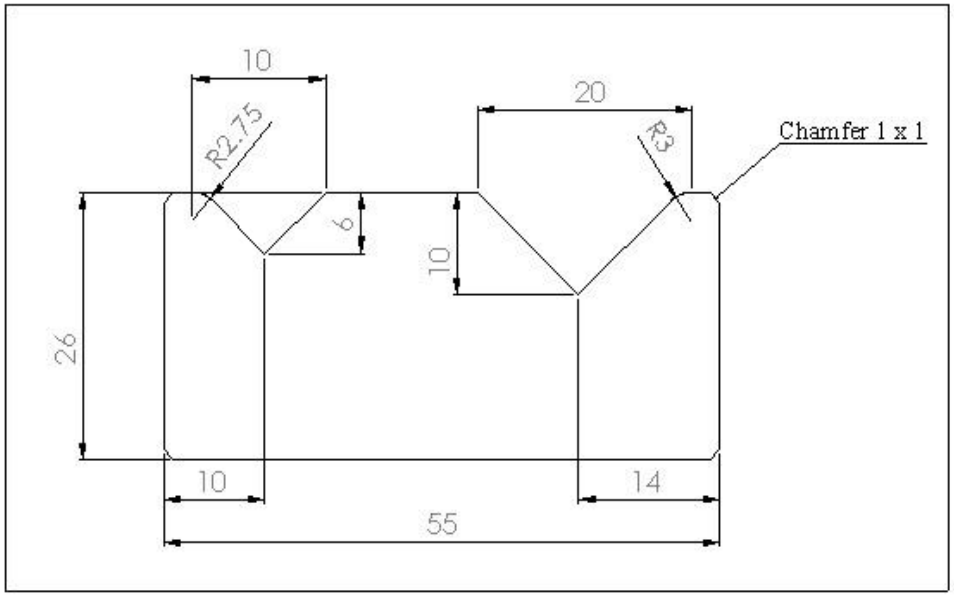

Fig.1 Detail Views of Die [13]

* Vipal Pachal Tel.: +91-9624071881
E-mail address: vipal.pachal@git.org.in

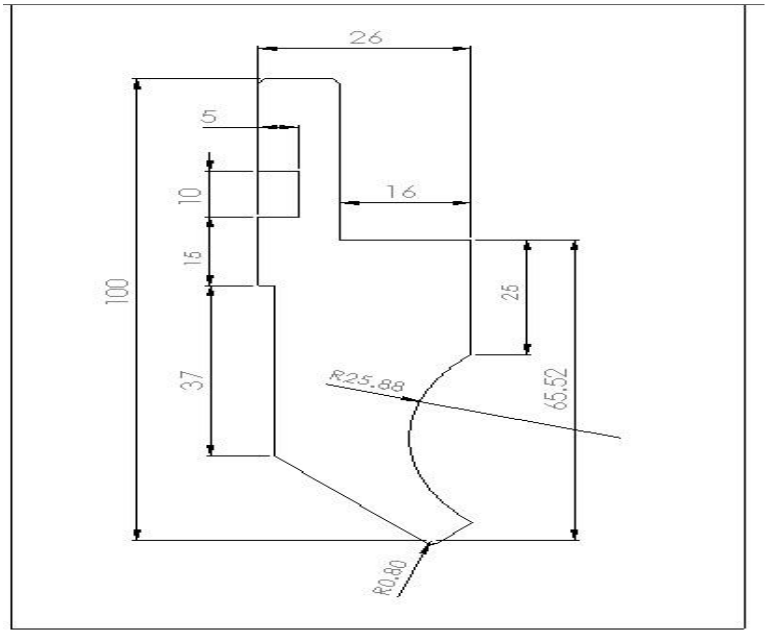

Fig.2 Detail View Drawing of Punch [13]

Fig. 1 and Fig.2 are presented detail drawing of die and punch of EHP sh 110 Servo Hybrid CNC Press Break.

Using parts features creates different components of Die and Punch. All assemblies such as die, punch and sheet were created using various components (part) by constrained there relative motion.
Using part modelling environment separate part files was generated for die, punch and sheet.
First to make geometry of both die and punch with as per practical data to measure length of both die and punch and amount to extruded part by using extrude command of feature operation.
Further using new sketch on base extruded component and draw sketch on existing extruded feature of identifying model width As shown in Fig. 3 and Fig. 4, there are different such as Front View and orientations of 3D model of Die and Punch such as isometric view.

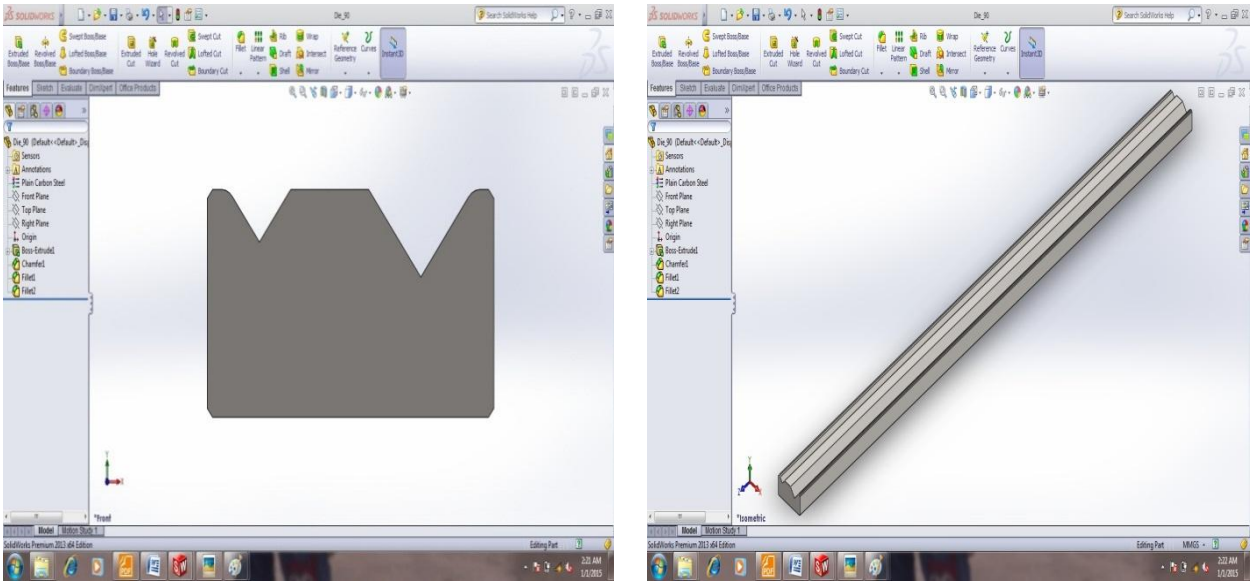

Fig.3 3 D Model of Die (Front and Isometric View)

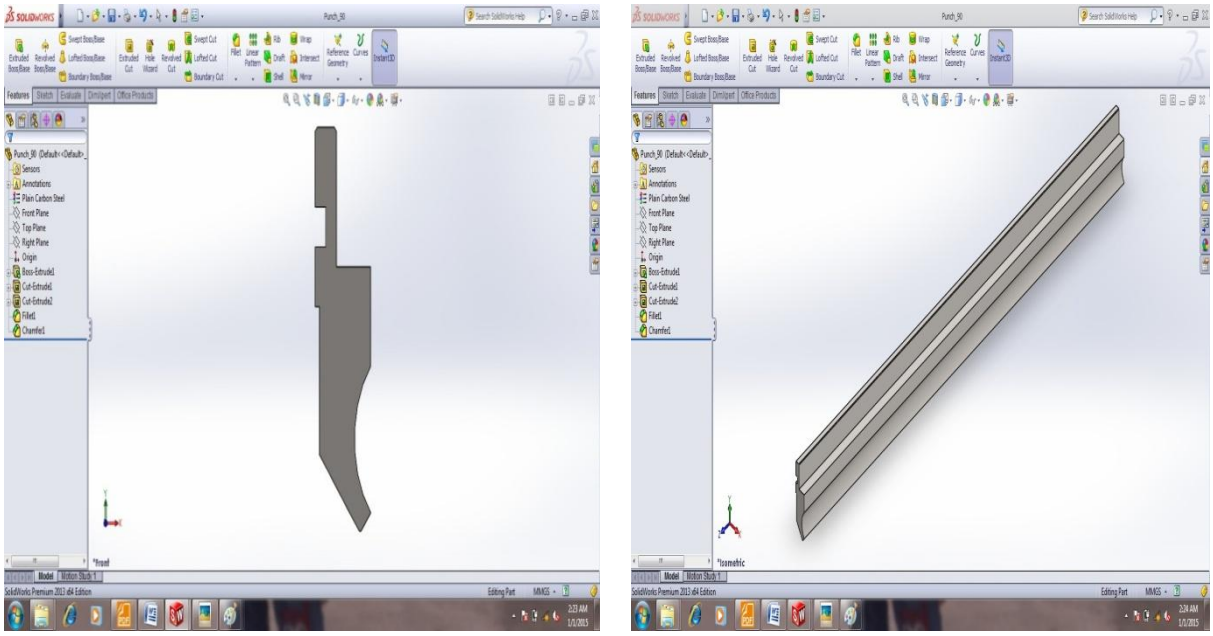

Fig..4 3 D Model of Punch (Front and Isometric View)

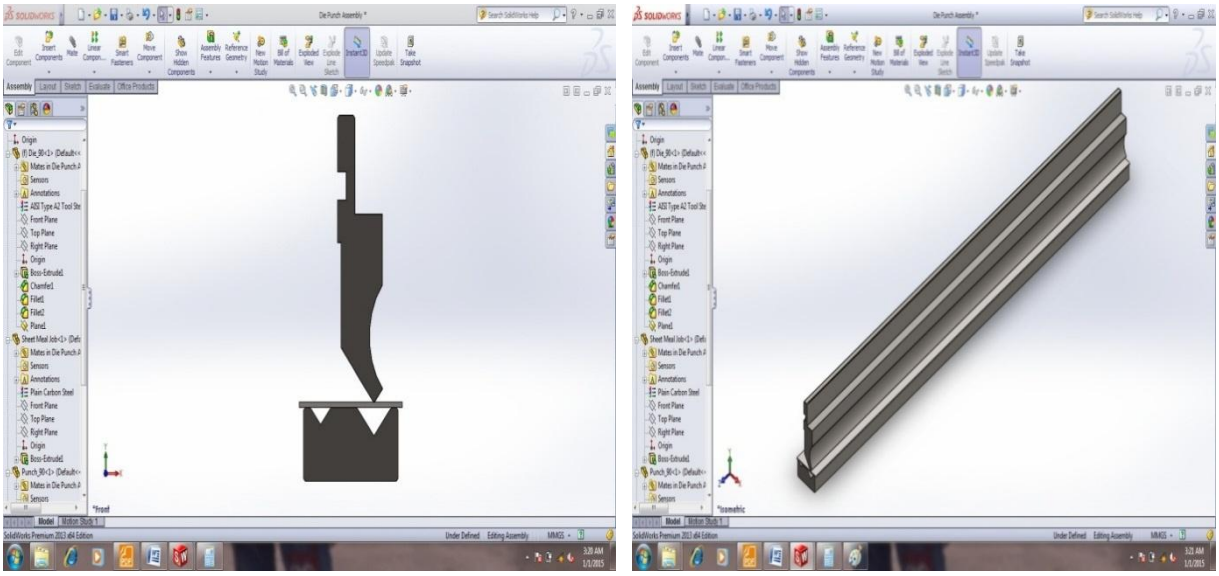

Fig.5 3Assembly Modelling of Die and Punch with Sheet Metal

2. Bending Calculation

Table 1 is presented calculation of bending force with respect different sheet metal thickness. These data standards available in company data base on maintaining pressure on ram of punch.

Table 4.1 Bending Calculation [13]

Thickness (t) mm	1	1.2	1.6	2	3	4	5
Bending Length (BL) mm	1000	1000	1000	1000	1000	1000	1000
Tensile Strength (UTS) kg/mm^2	42	42	42	42	42	42	42
V Opening (V) mm	4	4	4	4	4	4	4
Bending Force	21	33.26	69.88	126	378	840	1575

3. Finite Element Method

The Finite Element Method (FEM) is a numerical technique for analyzing engineering designs. FEM is accepted as the standard analysis method due to its generality and suitability for computer implementation. FEM divides the model into many small pieces of simple shapes called elements effectively replacing a complex problem by many simple problems that need to be solved simultaneously. The following figure shows CAD and its FEA model.

4. Proposed Study

In this analysis work, FE410 sheet with 8 mm thicknesses is taken for research study with "V "bending. A standard hydraulic press is selected for the "V" bending experiment; a sample specimen of 1000 x 60 x 2 mms is taken for the experiment.

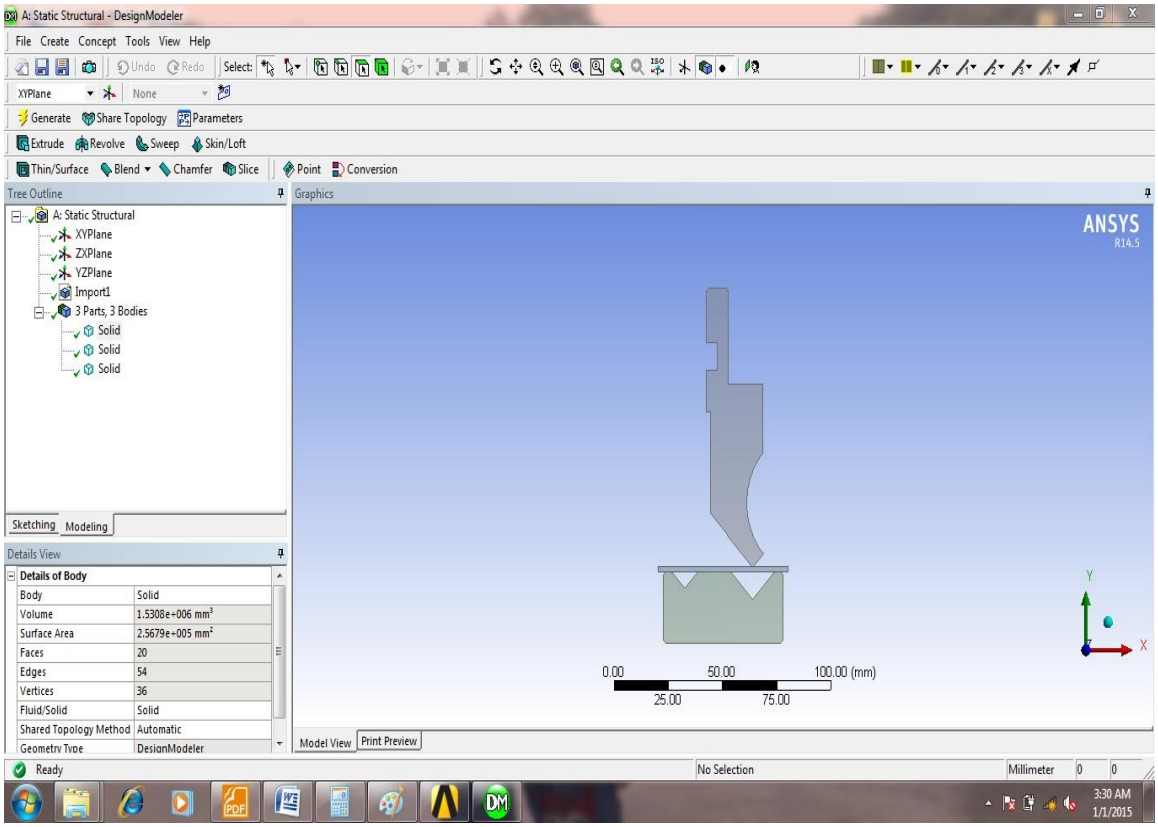

Fig. 6 Geometry of Die, Punch and Metal Sheet using static analysis

5. Die and Punch

Die and punch are made of tool steel which having , 6T die opening, and the punch as prescribed as above in with three different radii. Simply supporting is used for bending operation. The bending force for bending 2 mm thickness sheets is 126 N.

6. Computation Strategy for FEA

Finite element method is the best and prescribed for large deformation non-linear simulation like this metal forming process. Solid Work 2013 is one of the best explicit solvers available in the market; ANSYS 14.5 integrates this solver for all type of explicit solution.

7. Meshing Setup for FEA

Quad and Tetra elements were chosen for the meshing. Since ANSYS automatically selects the meshing algorithm and type of element required for the analysis model, it is easy to concentrate on the mesh density of accurate analysis.

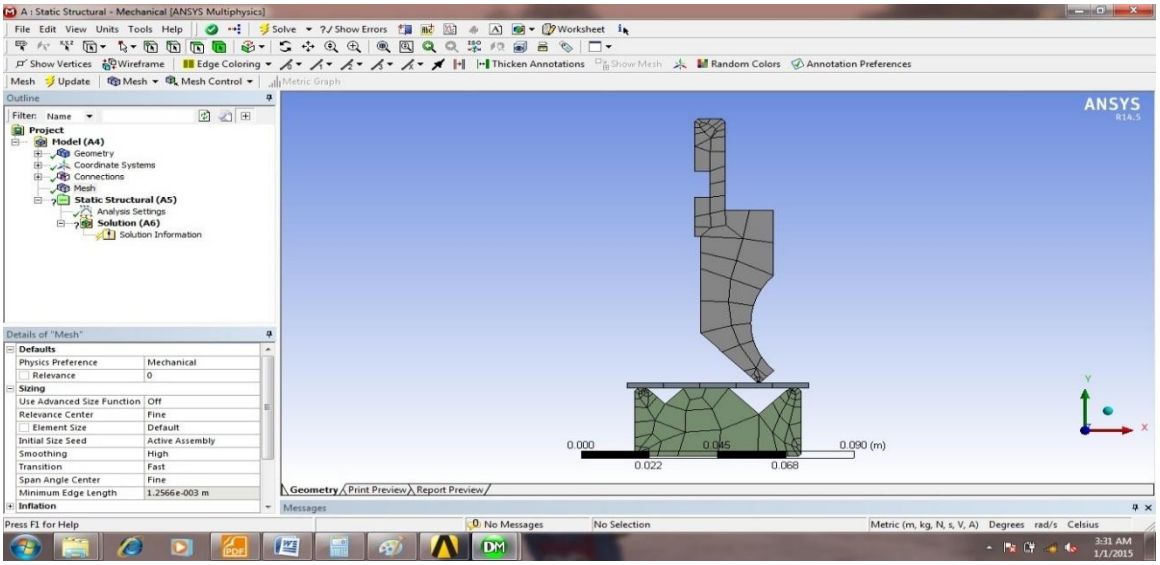

Fig.7 Meshing of Die, Punch and Metal Sheet using static analysis

8. Material Property for FEA

Proper explicit model of the low carbon steel is selected for sheet model and tool steel is applied for die and punch. The material library in the Autodyne software allows us to select the required material model. Proper hardening law is used for the material model; all the models are collected by the software from different research work of different scholars all around the globe. The hardening of the materials after the yield is an important factor of any forming process and not limited to this only for any plastic flow models. Different research works have been conducted to explore the material property after the yield limit and algorithm are formulated for identifying the hardening factors of the material.

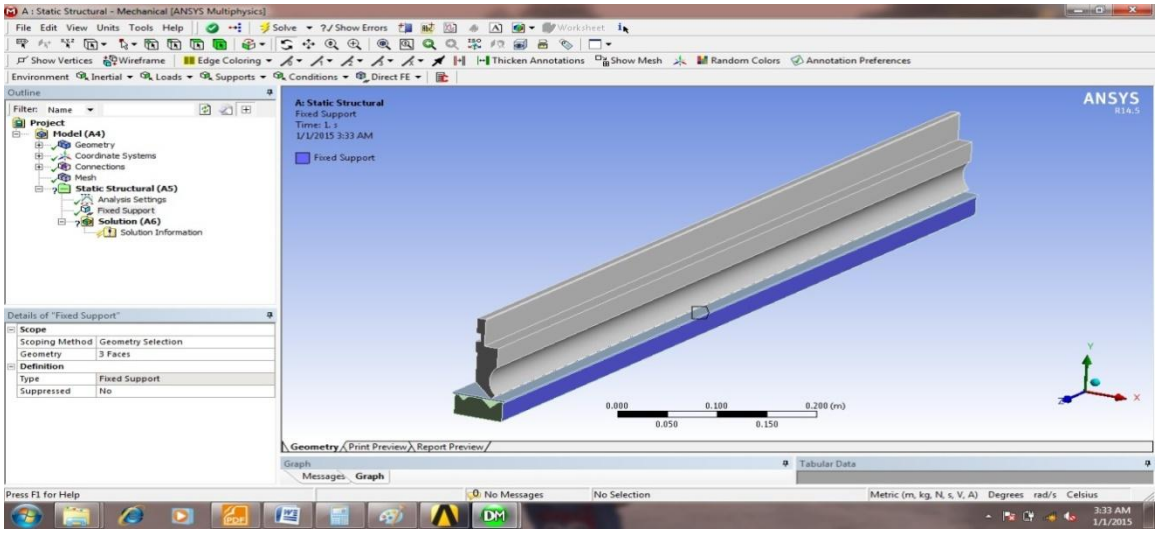

Fig. 8 Boundary Condition of Die, Punch and Metal Sheet using static analysis

9. Loading details for FEA

The loads for the model with respect to the radius of the punch are calculated as force as are given in table 1 Based on the pressure applying to the piston of the hydraulic cylinder, the pressure is converted to force for easier application in to finite element solution. We have considered 126 N for 2mm thickness sheet.

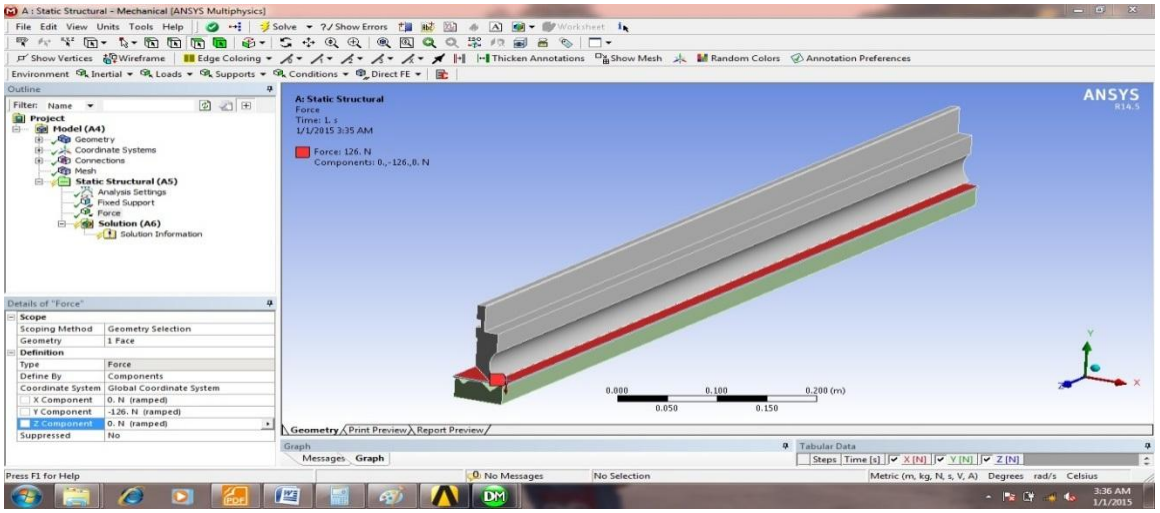

Fig. 9 Loading Condition of Die, Punch and Metal Sheet using static analysis

10. Results

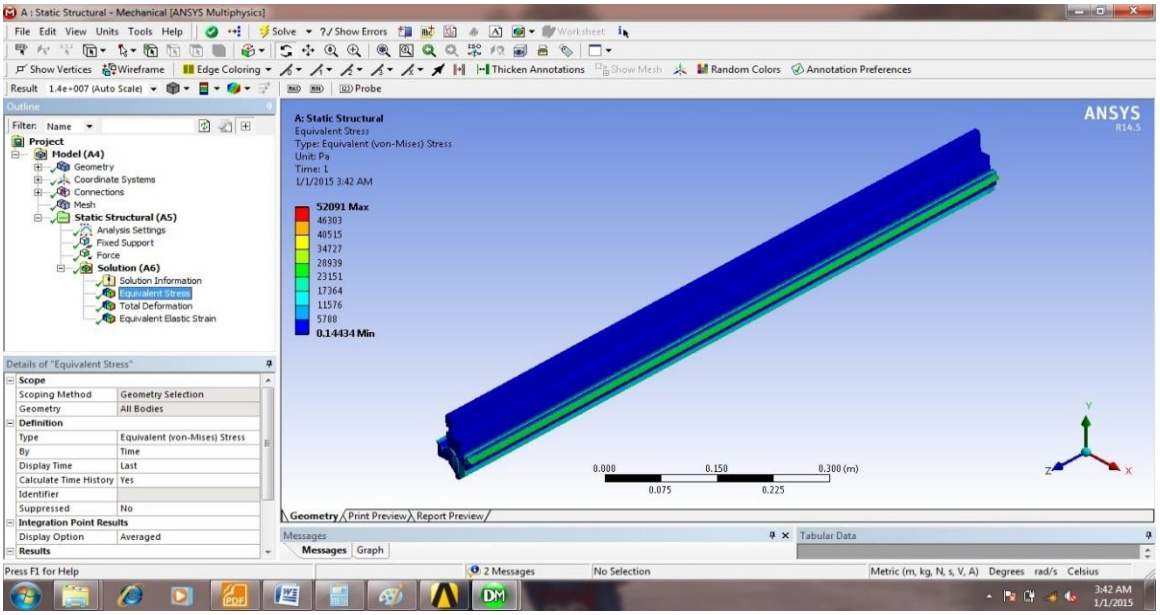

Fig.10 Von mises Stress Result

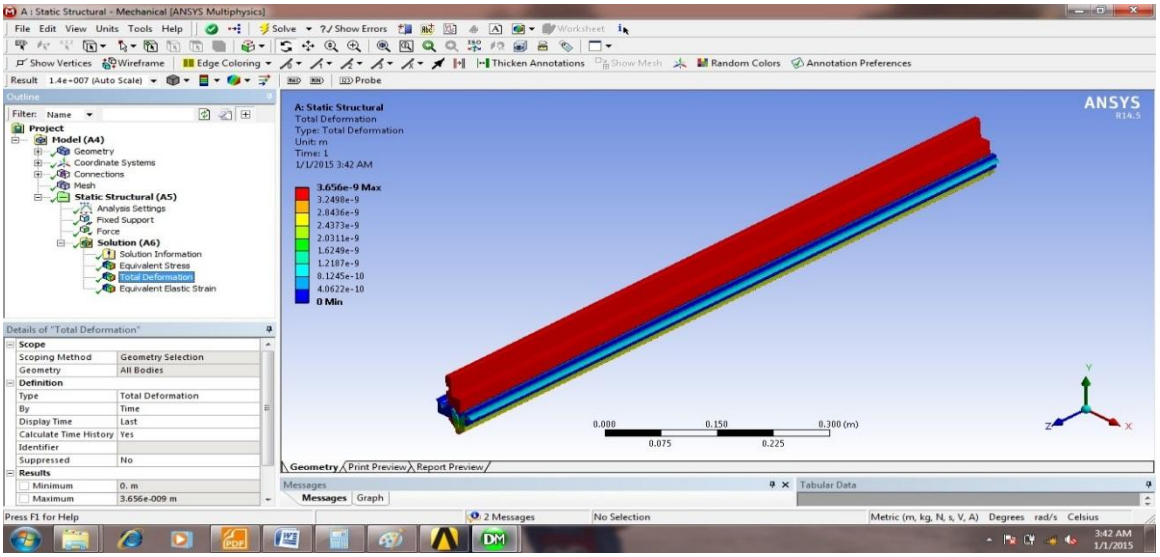

Fig. 11 Deflection Result

11. Practical Data from Company

From company data, Fig. 12 and Fig. 13 are shows Die and Punch of EHP 110 Servo Hybrid CNC Press Break. Company was purchasing standard die and punch form Euro stamp which is one of manufacture of press break die and punch.

Fig. 12 Die 2V 90º (Mfg. Euro Stamp) [14]

Fig. 13 Punch 90º (Mfg. Euro Stamp)[14]

Acknowledgment

I am extremely thankful to Asst. Prof. Someshwar S Pandey, Asst. professor in Mechanical Engineering Department, Gandhinagar Institute of Technology, Moti Bhoyan and Asst. Prof. Hardik R Patel, Asst. professor in Mechanical Engineering Department, Gandhinagar Institute of Technology, Moti Bhoyan are valuable cooperation, constant support with encouraging attitude at all stages of my work. I am highly obliged with him for his constructive criticism and valuable suggestions, which helped me to present the scientific results from an efficient and effective manner in this research.

Conclusion

The analysis performed in this research is based on some assumptions and restrictions. However, complete literature review and input parameter of Press Bend identification, thus, understanding of behavior of sheet metal bending are attained taking every possible detail into account. Therefore, the following are recommended for future work as extensions and elaborations of this research.

- Check effects of ram force on bending component for complex bending.
- Step taking to reduce chance of failing in bending process.
- Comparison of both data onto analysis.
- Applying proper optimization method of same.

References

[1] James A. Polyblank, Julian M. Allwood, Stephen R. Duncan, "Closed-loop control of product properties in metal forming: A review and prospectus"Journal of Materials Processing Technology 214 (2014) pp. 2333–2348.
[2] Kwansoo Chung, Hyunki Kim, Chulhwan Lee, "Forming limit criterion for ductile anisotropic sheets as a material property and its deformation path insensitivity. Part I: Deformation path insensitive formula based on theoretical models" International Journal of Plasticity 58 (2014) pp. 3–34.
[3] Peter Groche, Matthias Brenneis, "Manufacturing and use of novel sensoric fasteners for monitoring forming processes" Measurement 53 (2014) pp. 136–144.
[4] Omer El Fakir, Liliang Wang, Daniel Balint, John P. Dear, Jianguo Linand Trevor A. Dean, "Experimental and numerical studies of the solution Heat treatment, Forming, and in-die Quenching (HFQ) process on AA5754" International Journal of Machine Tools & Manufacture, http://dx.doi.org/10.1016/j.ijmachtools.2014.07.008
[5] G. Centeno, A. J. Martínez-Donaire, C. Vallellano, L. H. Martínez-Palmeth,D. Morales, C. Suntaxi, F. J. García-Lomas, "Experimental Study on the Evaluation of Necking and Fracture Strains in Sheet Metal Forming Processes" Procedia Engineering 63 (2013) pp. 650 – 658.
[6] S.M. Hafis, M.J.M. Ridzuan, Alina Rahayu, Mohamed, R.N. Farahana, S.Syahrullail, "Minimum quantity lubrication in cold work drawing process: Effects on forming load and surface roughness" Procedia Engineering 68 (2013) pp. 639 – 646.
[7] H. Meier, J. Zhu, B. Buff, R. Laurischkat, "CAx Process Chain for Two Robots Based Incremental Sheet MetalForming"45th CIRP Conference on Manufacturing Systems 2012.
[8] Mehdi Zohoor, Esmaeil Ghadiri Zahrani, "Experimental and numerical analysis of bending angle variation and longitudinal distortion in laser forming process" Scientia Iranica B (2012) 19 (4), pp.1074–1080.
[9] J. Avemann, R. Willy, G. Zhao, P. Groche, "Forming Process Integrated Induction Brazing"45thCIRP Conference on Manufacturing Systems 2012.

Book

[10]M.P. Groover, Fundamental of modern manufacturing Materials, Processes and systems, 4edition.
[11] R. Ganesh Narayanan, IITG, Reference Material

Website

[12]https:// www.hindustanhydraulic.com/catalogue.php
[13]https://www.eurostampsrl.it/index.php
[14] www.engilabs.com

Development in the Design of Automobile Mud Guard

Amit Patel[a*], Ashish Majithiya[a], Vrajesh Makwana[a]

[a]*Gandhinagar Institute of Technology, Moti Bhoyan, Gandhinagar, Gujarat, India 382781*

Abstract

Nowadays, the current mud guards are not effective enough to prevent the splashing of water to the rear vehicle or rear vehicle rider. All bikes and automobiles consist of mud guards or mud flaps. In spite of having mud guards, these vehicles fail to stop the splashing of water. Observing this minor but a critical problem, we have planned to work on the modification of present mud guards. This modification will be more effective and hence will be able to prevent comparatively more splashing of water from the rear wheel of the automobiles, especially Bikes. This modified design of the mud guard will be more convenient and effective for the vehicles in monsoon season

Keywords: Automobile, Mud Guard

1. Introduction

A mud guard, is also known as mud-flap which is used in combination with the vehicle fender to protect the vehicle, passengers, other vehicles, and pedestrians from mud and other flying debris thrown into the air by the rotating tire. It is also known as fender.Fender is the American English term for the part of an automobile, motorcycle or other vehicle body that frames a wheel well (the fender underside). Its primary purpose is to prevent sand, mud, rocks, liquids, and other road spray from being thrown into the air by the rotating tire [1,2,3].

1.1. Objectives of mud guards

- Prevention of splashing of water and other debris to the passenger driving behind the vehicle.
- Cleanliness of vehicles

Mud guard is the piece of material that is attached to the wheel well and sole purpose is to defray and minimize the spray or splash of water, mud, snow, rocks. Pickup Trucks, Sport Utility Vehicles, Suburban, Jeep, Tahoe, Expedition, Explorer are examples of what type of vehicles commonly upgrade to aftermarket splash guards.
A mudguard is a part of a car, motorcycle, scooter or bicycle. People use it to stop mud, water or other objects from coming up onto the vehicle or the person and also to protect the engine from mud. It stops road debris such as mud, pebbles, glass, sticks and many more from being shot as a projectile to other cars, motorcycles, and pedestrians.
Perhaps we have noticed that trucks have huge and thick mud-flaps. That is because when they leave a construction site, their tires sometimes come out with up to 2 inches of mud (never mind the gravel stuck in the tires threads). When these trucks hit the road, the heavy mud is shot out of the tire like a bullet. If trucks don't have mud-flaps, someone could be seriously injured. Mud-flaps are there to stop stones from scratching our paint off our car and also stopping mud and dirt spraying on the sides.
Driving in rain, snow, mud even dirt without protection can cause damage to your new vehicle or to those driving behind us. Many people view mud flaps to be unnecessary or may get in the way while 4x4ing.For many, this is just an excuse not to shop for them because of the confusion between the names for the product.
When we outfit your vehicle with front and rear Ultimate Mud Flaps we will have ultimate protection against rocks, mud, snow, rain and debris hitting our vehicle. Ultimate-Flaps will complement your vehicle's clean line and offer a tailored finish look. With Ultimate-Flaps on our vehicle, cars that are behind us will benefit from less debris and splash as we travel down the road.

1.2. Classification of Mud guards

1. According to the location
i. Front Wheel Mud guards
ii. Rear Wheel Mud guards

* Amit Patel Tel.: +91-7600010215
E-mail address: amit.patel@git.org.in

2. According to material (and their qualities)

i. Fiber
Abrasion resistance, Chemical, mildew & moth resistance, Elasticity, Flammability, Heat sensitivity, Shrinkage, Strength, Sunlight resistance, Wrinkle recovery

ii. Polymer
Chemical, mildew & moth resistance, Thermal and electrical insulators, Light Weight, Very high range of characteristics and color

iii. Plastic
Lightweight, Resistance to breakage, Insulating capacity (electrical, thermal and acoustic), Ease of handling and safety, Versatility, Recyclability, Usefulness, Simple, cheap manufacturing, Impermeability (water, light, gases)

iv. Steel
Formability, Durability, good tensile and yield strength

2. Current Scenario

Mudguard clearance of current bikes in market

Fig 2.1. Mudguard image of Yamaha FZ

Fig 2.2. Mudguard image Hero Splendor

As per analysis, the height of mud guards attached to the current models of the bikes are not effective enough to prevent the splashing of water and mud. The main factor necessary behind the process is Ground clearance between the ground and rear mud guard. More the clearance more is the possibility of splashing of water on to the rear vehicle. Data of the ground clearances of some bikes have been collected.

Table 2.1 Bike with their clearance between mudguard and road

Sr. no	Bike Model Name	Clearance (cm)
1	Bajaj Pulsar	45
2	Hero Splendor	42
3	Yamaha FZ	53
4	Honda Shine	43
5	Hero Passion	45

3. Experimental Work

3.1. Selection of bike

Lowest space between the mudguard and road is the prime criteria for the selection of bike. From the survey, minimum clearance has been found in the Hero Splendor. It will give minimum splashing of mud and water [4].

3.2. Experiment to measure maximum splashing height and length of water

All the experiments have been carried out in the open space. 5 cm level height was maintained by pouring mud and water. Experiments with different speeds and water levels have been carried out. To measure the splashing height, one object is provided at 85 cm from the rear wheel of bike.

Table 3.1 Experimental data of splashing height and length with different speed.

Sr. No	Speed of the vehicle (km/h)	Water/mud level (cm)	Splashing height (cm)	Splashing Length (cm)
1	25-30	5	95	162
2	35-40	5	114	185
3	45-50	5	130	215
4	55-60	5	143	228

Fig 3.1 Experiments of measuring height and length of splashing

3.3. Experiment to measure splashing height at different distances

For collecting length and height of splashing 3 object fixed at different distance. Distance between tire and object was kept 85 cm, 140 cm, and 190 cm from the rear tyre.

Table 3.2 Splashing height at different distance from the rear wheel

	Object 1 (A)	Object 2 (B)	Object 3 (C)
Distance from rear wheel (cm)	85	140	190
Splashing height on recorded object (cm)	60-65	110-115	40-45

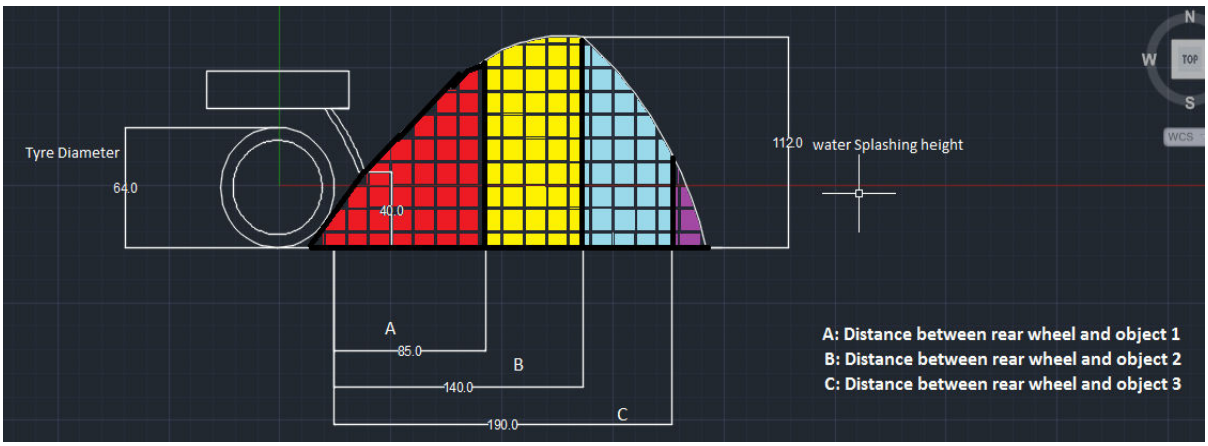

Fig.3.2 Graphical representation of splashing height and length.

4. Adding Supplementary Mudguard

It is necessary to cover more area of rear wheel which can be only done by augmenting the length of mud guard. Thus, practical was performed by attaching the supplementary guard at the fender of the vehicle. The extra guards of different dimensions are attached and the result was noted. The angle of extra guard was kept between 30 and 40 degree. After the supplementary mudguard the height of guard from the ground was 25 mm only. Measurements of splashing height and length was measured when object is 140 mm away from the rear wheel of bike.

Fig.4.1 Experiments after additional mudguard

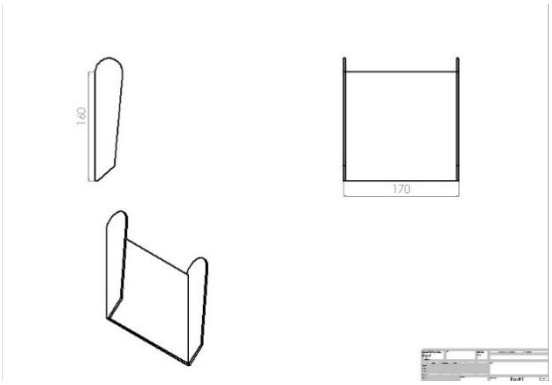

Fig.4.2 Design of additional supplementary mudguard

Length was kept with three different size and inclination of mudguard with 30 degree. Results were noted down. Again experiments have been done with same length of mudguard with inclination 40 degree. Speed was kept constant for all the experiments, i.e. 40-45 kmph.

Table:4.1 Experimental data of splashing height and length noted with additional mudguard

Sr. No	Length of mud guard (cm)	Inclination of supplementary guard	Maximum Length of splashing of water (cm)	Height of splashing of water (cm), while object at 140 cm away from the rear wheel.
1	5	30	160-162	90
2	10	30	60-70	50
3	15	30	20-30	15
4	5	35	170-172	95
5	10	35	65-68	54
6	15	35	25-29	18
7	5	40	172-178	97
8	10	40	70-76	56
9	15	40	29-36	20

It was clearly observed from the result table, that inclination of 40 degree is not preferable against 30 degree inclined additional mudguard.

Water splashing height was reduced from 130 cm to 90cm, 50cm and 15cm. Percentage reduction for above three length of additional mudguard was 31%, 62%, 89%. It was observed from the experimental data that provision of additional mudguard with 15 mm length and with 30 degree inclination will increase mudguard efficiency minimum by 85%.

Water splashing length was reduced from 215 cm to 162cm, 70cm and 30cm. Percentage reduction for above three length of additional mudguard was 25%, 68%, 87%. It was observed from the experimental data that provision of additional mudguard with 15 mm length and with 30 degree inclination will increase mudguard efficiency minimum by 87%.

Fig.4.3 Mudguard with supplementary mudguard

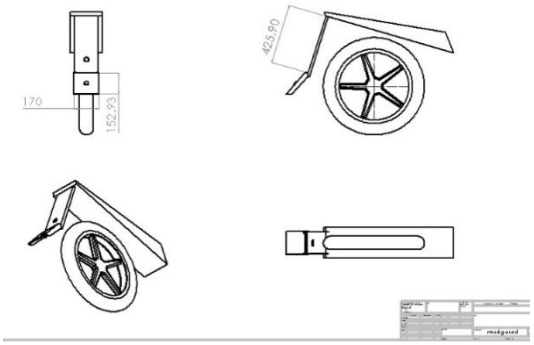

Fig.4.4 Mudguard design using Autocad software

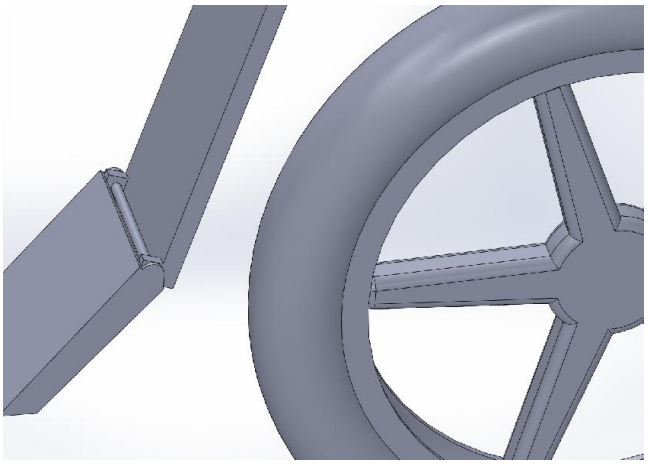

Fig.4.5 Conceptual design of Flip mudguard (Flexible type)

Here, permanent mudguard was used for the experiments and it was fastened by the bolts. But it can be design flexible manner. By providing linkage mechanism one can have flexible movement of mudguard. Flexible mudguard may be applicable to 4 wheeler and trucks also as it was the vehicle splashing mudguard in major quantity. Folding arrangement was also prepared for getting advantage of additional mudguard.

Conclusion

From the experiments, it is clear that just by adding an extra mudguard of 15 cm length, mudguard preventing efficiency increased by 85% and 87% So that, the water and debris splashed from rear tire will not harm the vehicle or two wheeler driver. In this experiments, fixed permanent mudguard is used, and advantage of using permanent guards is that the guard is easy to attach, maintenance free and no extra mechanism is required. As a future scope, flexible design of mudguard should be prepared. It will increase the cost of mechanism and instalment, but the use and operation of additional mudguard will be easy for users. Flip type mudguard is also possible with some open/close mechanism. Other than this folding mechanism sliding guard can be prepared with extra attachment. Due to additional mudguard the look of two wheeler is affected and this is the only disadvantage for users.

Reference:

[1] Liu J., Li L., Study of Motorcycle Fenders
[2] Mascarin A., Dieffenbach J., Fender Material Systems: A Lifecycle Cost Comparison
[3] O'Malley M., Plastic Fenders
[4] Ray R., Jawahar N., Study of Fluid Structure Interaction due to Water Splashing on the Rear Fender of Motorcycles

Modeling and Simulation of Distance Relay and It's Operation during Teed line and Load Encroachment

Piyush Pandya[a*], Naitik Trivedi[a],Naveen sharma[a]

[a]*Gandhinagar Institute of Technology, Moti Bhoyan, Gandhinagar, Gujarat, India 382781*

Abstract

Now adays in a long transmission line distance relay is widely used. The Distance Relay achieves selectivity on the basis of impedance. As the impedance is proportional to the distance to the fault point, relay directly indicates distance of fault location. Distance relay is always set for instantaneous operation in the first zone, delayed operation in second zone and provide back protection in third zone.Modelling of protective relays offer an economical and feasible alternative to find out the performance of relays and protection systems. MHO characteristics of distance relay are utilized in this paper used and Bergeron model of the transmission line are modelled in PSCAD/EMTDC software. To study about the operation of distance relay for various type of faults and relay performance during Teed line and load encroachment is done in this paper. A 230 kV, 300 km Transmission line systems are used in this paper.

Keywords: Distance relay, Load encroachment , Symmetrical and unsymmetrical fault, Teed line

1. Introduction

Distance relay is generally used for long transmission line and it gives the trip signal to the circuit breaker during any abnormal condition then circuit breaker isolate faulty portion from the healthy section.To study the behaviour of a distance relay during short-circuits, for designing new prototypes, to check and optimize the performance of relays that already installed in power system, to design new relaying algorithms and to check the performance of the new relay equipment it is necessary to model the distance relay.
To select the type of relay for the particular application and for analysis it's require modelling of relay. Researcher can improvise and realize different algorithm on it. Manufacturer also can inspect confirm how the relay would perform during systems disturbances and normal operating conditions and to make the necessary corrective adjustment on the relay settings. Each internal part can be observed during different operating condition. [5] In this paper, the concept of distance protection and impedance setting rule for three zones are given in second section. The simulation result of distance relay operation for different fault and different fault location are given in third Section The basic concept of Teed line and load encroachment and its effect is given in to fourth section. In fifth section conclusion are drawn.

1.1 Distance Relay

Distance relay are designed to protect transmission line against basic type of faults like L-G, LL-G, L-L and three phase faults. For detection of above mentioned faults, each one of the zones of distance relays require six units. Three units for detecting faults between the phases and the remaining three units for detecting phase to earth faults [2], [6]. The positive sequence impedance is the basis of the calculating the setting of distance relay. Table 1 indicates fault impedance calculation formula for below mentioned fault types.

Table 1. Fault impedance calculation for different faults

Types of Fault	Formula
A-g (Line to ground)	$Z_A = V_A/(I_A + 3kI_0)$
B-g (Line to ground)	$Z_B = V_B/(I_B + 3kI_0)$
C-g (Line to ground)	$Z_C = V_C/(I_C + 3kI_0)$
A-B (Line to Line)	$ZAB = VAB/(IA - IB)$
B-C (Line to Line)	$ZBC = VBC/(IB - IC)$
C-A (Line to Line)	$ZCA = VCA/(IC - IA)$

* Piyush Pandya Tel.: +91-9428143720
E-mail address: piyush.pandya@git.org.in

Where, k = (Z_0-Z_1) / Z_1, Z_0 and Z_1 are zero sequence and positive sequence impedances. The distance relay operates in three zones. Zone 1cover 80-85% of transmission line length in which it operates instantaneously. The zone 2 covers remaining line length and 50% of adjacent line length. Relay operates in zone 2 with 15 to 20 cycle time delay. Zone 3 covers remaining adjacent transmission line length. It is generally used to provide backup protection. Zone 3 operates with 50-60 cycle delay. [10]

1.2 Mho Relay Model Algorithm

In the condition of any fault in transmission line the voltage signals and current signals contain decaying dc components, higher order frequency components and lower order frequency components. In the sensed signal Higher order frequency components can be eliminated using low pass anti-aliasing filters with appropriate cut-off frequency, but the anti-aliasing filters cannot remove decaying dc components and rejects lower order frequency components, which affects the performance of digital relay. In order to overcome this, the Discrete Fourier transformation can be used to remove the dc-offset components. [9]

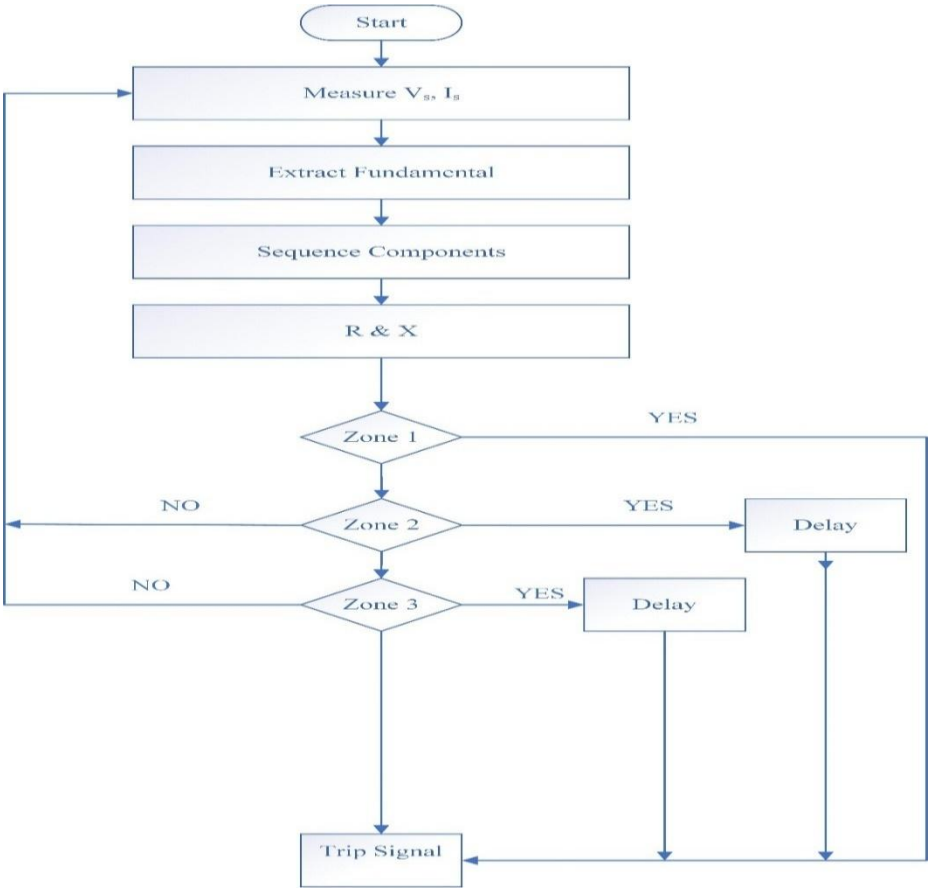

Fig. 1 Mho Relay modeling Algorithm

2. Proposed Scheme

In order to detect islanding condition controller needs to compare the DG output parameters with system parameters [5]. On the basis of this comparison islanding situation can be decided. Islanding detection techniques can be broadly classified into remote and local techniques. Further local techniques can be divided into passive, active and hybrid techniques as shown in figure 2.

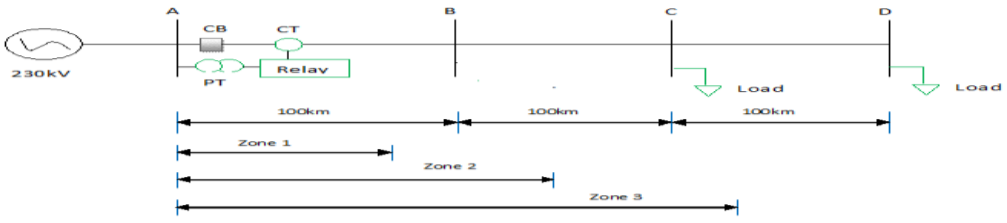

Fig.2 Simulated System

2.1 Single Line to ground Fault

Single line to ground fault is created in phase A with fault resistance 5 ohm. Its operation during zone 1, zone 2 and zone 3 is shown below. Fault occur at 40km from bus A in zone 1, 120km from bus A in zone 2,and 212 km from bus A in zone 3. The simulation time of occurrence of fault is 0.2 sec.[8]

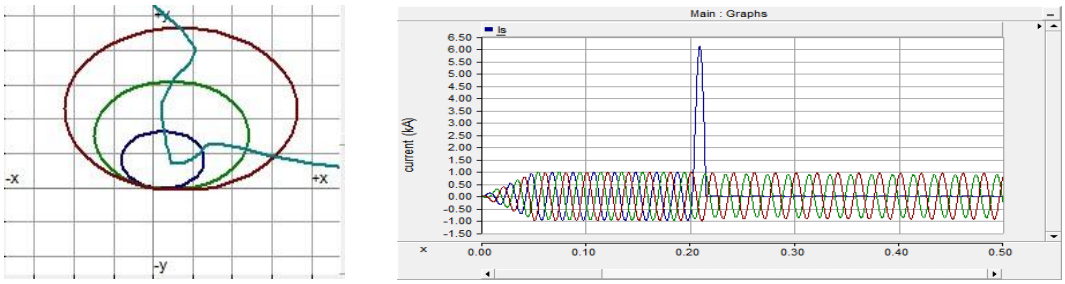

Fig.3 (a) Zone 1 operation (b)L-g Fault current for zone1

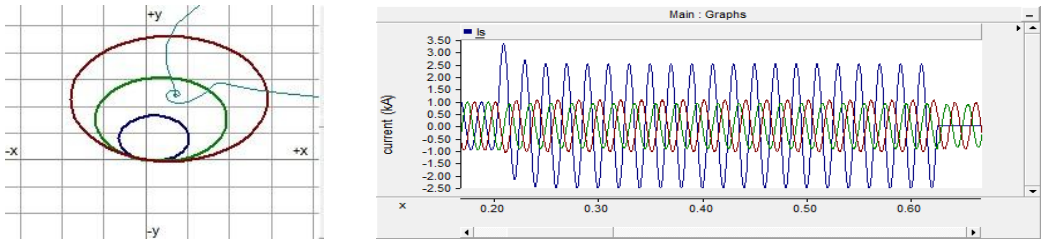

Fig.4 (a) Zone 2 operation (b) L-g Fault current for zone 2

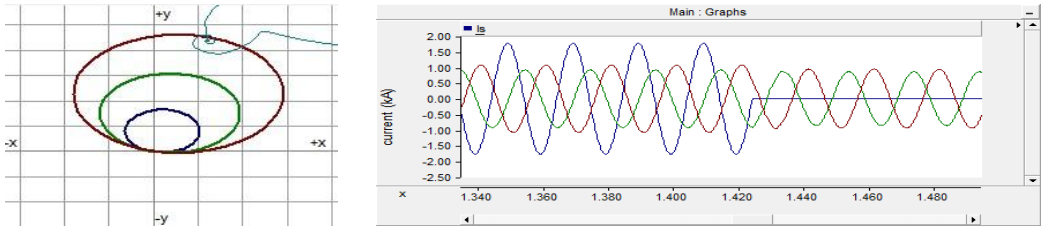

Fig.5 (a) Zone 3 operation(b) L-g Fault current for zone 3

Three phase fault is a balanced fault or symmetrical fault. It is the most severe fault which occurs in transmission line system. The operation of distance relay for fault occurs in various location is shown below.

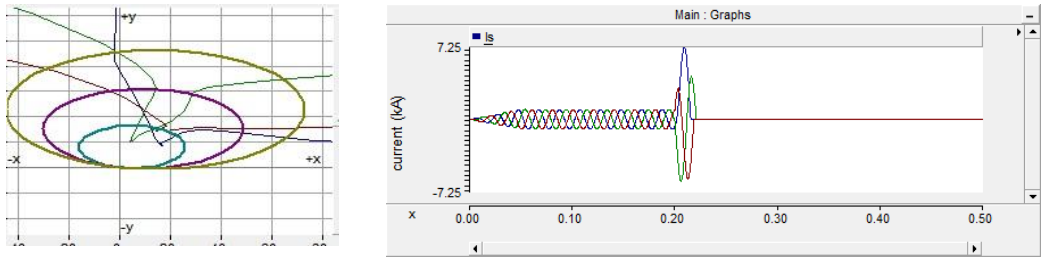

Fig.6 (a) Zone 1 operation (b) Three phase Fault current for zone1

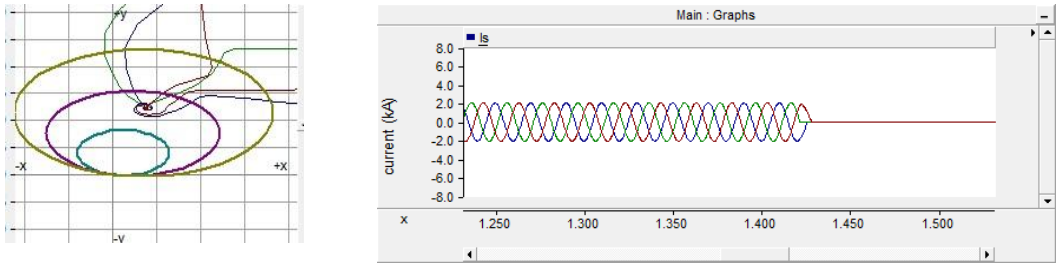

Fig.7(a) zone 2 at 120 km (b) zone2 operation with 20 cycle delay

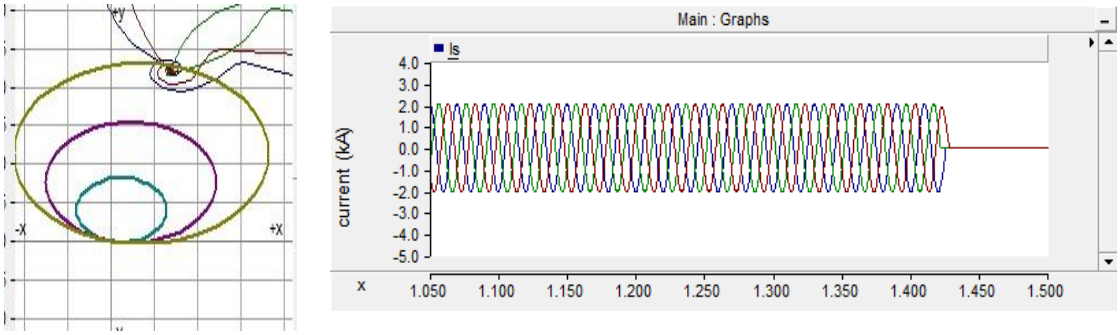

Fig.8(a) zone 3 at 212 km (b) zone 3 operation with 60 cycle delay

3. Teed Line And Load Encroachment

The protection of multi-terminal transmission lines is more complicated than two-terminal lines. Generally due to Intermediate In-feed from the third terminal or an out feed to the terminal they usually experience additional problems. Due to intermediate In-feed from the third terminal the distance relay measured more impedance rather than actual one. [1]

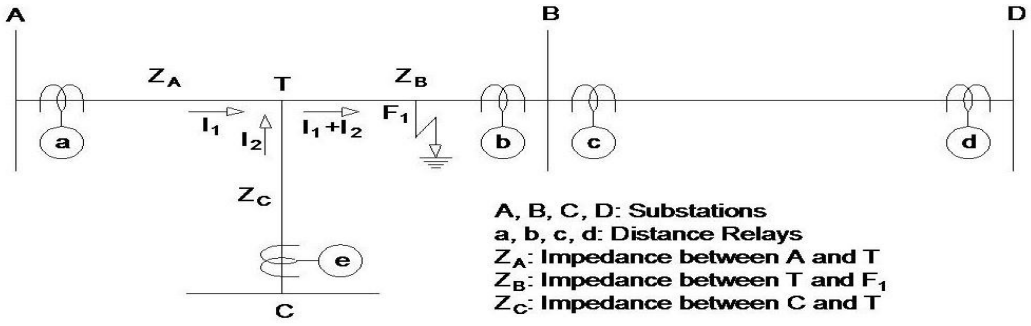

Fig.8 Teed line for fault at F_1 and Relay a

Consider the impedance seen by the relay 'a' at the substation A, when the fault occurs at F_1 .In the absence of an intermediate teed line, the relay will measure below impedance.

$$\text{True impedance to fault} = Z_A + Z_B$$

But with the intermediate current In-feed I_2, the apparent impedance seen by relay becomes,

$$\text{Measured impedance} = Z_A + Z_B + (I_2 / I_1)\, Z_B$$

So measured impedance is more than the true impedance. [3] So the fault appears to be farther away from the actual location. This means that the relay will under reach.

3.1 Simulation result of Teed line

In this paper 400kV Teed Line is considered at point T. The fault is created at 230 kV transmission line in zone 2. Due to teed line present, the distance relay at the substation A measure impedance more than that the actual so if the fault occurs in zone 2, distance relay will operate in zone 3 with time delay 60 cycle rather than in zone 2.

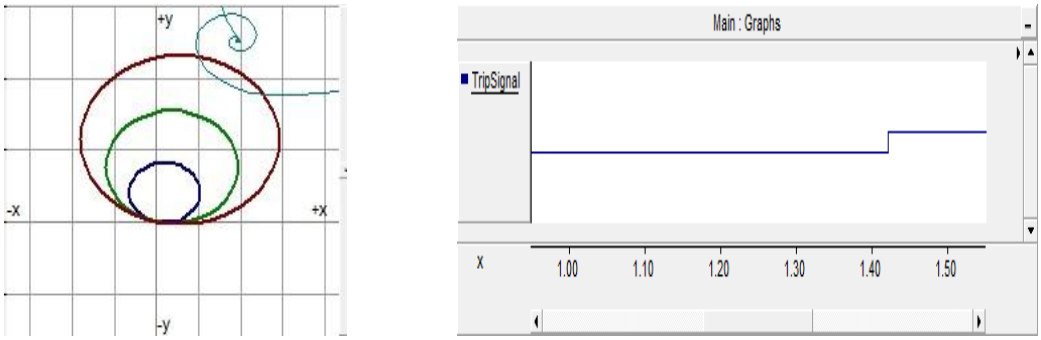

Fig.9 (a) Fault occurs in teed line at 120km, (b) Trip signal provide by relay for teed line

3.2 Simulation result of load encroachment

The change in transmission network structure or shifting the power flow from one line to another under steady-state operating conditions may cause the positive-sequence impedance to enter the zone 3 characteristic of a distance relay. This phenomenon is referred to as load encroachment. [3] If the load is increase from the maximum loadablility limit of distance relay then impedance seen by the relay during this overload condition will be less than their set impedance and so distance relay will mal operate in zone 3.
In this paper to create the load encroachment condition for relay at substation A, the load at bus D is increased gradually to twice its steady state value in 30 steps. For 230 kV transmission line and for 30^{o} power factor angle load if the load increased above the 564 MW and 326 MVAR, relay will mal operate in zone 3 due to load encroachment.

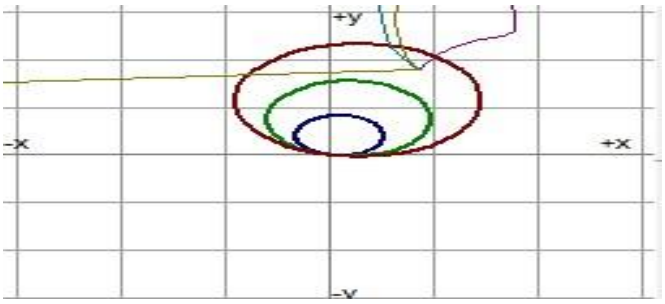

Fig.10 Zone 3 operation relay due to Load Encroachment

Conclusion

Modeling and simulation of distance relay are done using PSCAD/EMTDC software.The performance characteristics of mho relay was evaluated at different locations with different type of fault. The developed mho characteristics may be used for training young and inexperienced engineers and technicians. Due to the teed line present distance relay seen more impedance rather than actual so relay will be under reach. If load is increase from the maximum loadability of the relay then distance relay will maloperate.

Journal article:

[1] R. K. Aggarwal, D. V. Coury, A. T. Johns, and A Kalam, 1993. A practical approach to accurate fault location on extra high voltage teed feeders. IEEE–Transaction on Power Delivery, Vol. 8, pp. 874-883.
[2]Harikrishna M, 2010. Performance of quadrilateral relay on EHV transmission line Protection during various faults. ACEEE International journal on Control System and Instrumentation, Vol.1, No.1, July 2010
[3] M. Jin and T. S. Sidhu, 2008. Adaptive load encroachment prevention scheme for distance protection. Elect. Power Syst. Res., vol. 78, pp. 1693–1700.
[4] P.K. Dash., A.K. Pradhan, G. Panda, A.C. Liew, 2000. Adaptive relay setting for flexible AC transmission systems (FACTS). Power Delivery, IEEE Transactions on, Volume: 15 Issue: 1, pp. 38 -43

Book:

[5] Hamid Sherwali and Abdlrahem, 2010. Matlab - Modelling, Programming and Simulations, InTech publishers.
[6] Y.G. Paithankar, 1998. Transmission Network and Protection Theory and Practice, MARCEL DEKKAR INC.
[7] Phadke, Arun G., & James S. Thorp, 2009. Computer relaying for power systems. John wiley & Sons.
[8] PSCAD/EMTDC: Electromagnetic transients program including dc systems, 1994. Manitoba, H.V.D.C."Research Centre.

Symposium Proceedings:

[9] Abdlmnam A. Abdlrahem, Hamid H Sherwali, 2009. Modelling of Numerical Distance Relays Using Matlab, IEEE Symposium on Industrial Electronics and Applications, Kuala Lumpur, Malaysia.
[10] Rincon, Cesar, and Joe Perez, 2012. Calculating loadability limits of distance relays, Protective Relay Engineers, 65th Annual Conference for. IEEE.

Appendix

Parameter	Value	Unit
System Voltage	230	kV
System Frequency	50	Hz
Line Length (AB, BC, CD)	100	km
Positive Sequence Series Impedance of transmission line	123.6 + *j*508.4	Ω
Positive Sequence Cap. Reactance of transmission line	0.29473	MΩ × km
Zero Sequence Series Impedance of transmission line	451 + *j*1327.7	Ω
Zero Sequence Cap. Reactance of transmission line	0.51013	MΩ × km
Positive Sequence Impedance of Source	0.6 + *j*18.28	Ω
Fault Resistance	10	Ω

\

FLRW Metric and Lanczos Potential

Ravi Panchal[a*]

[a]*Gandhinagar Institute of Technology, Moti Bhoyan, Gandhinagar, Gujarat, India 382781*

Abstract

Lanczos potential is analogue to potential in general relativity. In this paper, the field of observer for FLRW metric has been found in such a way that the observer becomes shear-free and irrotational. Using it the Lanczos potential for FLRW metric has been obtained.

Keywords: Newman-Penrose Formalism; Lanczos Potential; FLRW metric

1. Introduction

In general relativity, Einstein's field equations relate matter and geometry of the space-time. Einstein has used anti-self-dual part of the Riemann tensor R_{hijk} to derive the field equations. By analyzing self-dual part of Riemann tensor, in 1962 Carnelius Lanczos [1] Have proved that the curvature tensor can be obtained by covariant derivative of a rank three tensorL_{ijk} , which is now known as Lanczos potential tensor. It is analogous to the fact from the electromagnetism that rank two tensor, that is, electromagnetic field tensor can be obtained using covariant derivative of rank one potential.
In order to obtain Lanczos potential tensor for a given geometry, it is required to solve Weyl-Lanczos relations; which are highly non-linear relationships between Weyl tensor and Lanczos potential tensor. Due to non-linear nature, there is no standard method for solving Weyl-Lanczos relations and the approach must be heuristic. At the same time the Lanczos potential tensor has fundamental importance in general relativity due to its analogy with potential of electromagnetism. In spite of the importance, a large class of solutions is still uncovered especially for the spacetimes of non-vacuum nature. In 1987, Novello and Velloso have given algorithm for finding Lanczos potential for perfect fluid spacetimes having various conditions on shear, rotation, etc. The difficulty in using this algorithm is to find field of observer u^i which is shear-free, irrotational etc. Another way to obtain Lanczos potential is using Newmann-Penrose version of Weyl-Lanczos relations and Newmann-Penrose field equations developed by Parga et al.[2] But, the non-vacuum spacetime involves tetrad components of Ricci tensor and that is why this approach becomes difficult. The rich analogy electromagnetism and gravity inspire researchers to find Lanczos potential for different geometries[3] –[11]. Due to complexity involved in Weyl-Lanczos relations, it is difficult to develop an algorithm for finding Lanczos potential for arbitrary spacetimes. But, a systematic approach of finding solution of them for a large class of spacetimes will lead us to a general procedure. For this reason, Hasmani and coworkers have been finding Lanczos potential for non-vacuum spacetimes [12],[13].This paper is part of the continuous process and here we have obtained Lanczos potential for non-vacuum FLRW metric. The notations and terminologies used in this paper are used from [14],[15] and for brevity they are not included in the paper.

1.1 Decomposition of Riemann Curvature Tensor

Let the spacetime having a metric g_{ij} with signature -2 and usual Levi-Civita connection for covariant differentiation. For a vector field A_i, the Riemann tensor can be defined as,

$$A_{k;ij} - A_{k;ji} = R_{ijk}{}^{l} A_l. \tag{1}$$

The following is standard decomposition of Riemann curvature tensor into its irreducible parts [7].

* Ravi Panchal Tel.: +91-9909239778
E-mail address: ravi.panchal712@gmail.com

$$R_{ijkl} = C_{ijkl} + E_{ijkl} + G_{ijkl}, \tag{2}$$

where

$$G_{ijkl} = \frac{1}{12}R\left(g_{ik}g_{jl} - g_{il}g_{jk}\right), \tag{3}$$

$$E_{ijkl} = \frac{1}{2}\left(g_{ik}S_{jl} + g_{jl}S_{ik} - g_{il}S_{jk} - g_{jk}S_{il}\right), \tag{4}$$

$$S_{ij} = R_{ij} - \frac{1}{4}Rg_{ij} \tag{5}$$

$$R_{ij} = R_{ipj}{}^{p}, R = R^{i}{}_{i} \tag{6}$$

and C_{ijkl} is the Weyl conformal tensor.

The algebraic properties satisfied by the Weyl tensor are similar to the properties satisfied by Riemann tensor. From equations (3)-(6) it can be observed that the tensors G_{ijkl} and E_{ijkl} can be obtained from tensor with fewer indices S_{ij}, R_{ij}, g_{ij} and R. In this way, Lanczos [1] thought that the Weyl tensor C_{ijkl} can also be obtained using tensor with less than four indices. The tensor field is now known as Weyl-Lanczos relations.

1.2 Lanczos Potential as Analogy between Electromagnetism and Gravity

The Jordan form of the field equations [16] is

$$C_{ijk}{}^{l}{}_{;l} = J_{ijk}, \tag{7}$$

where

$$J_{ijk} = R_{ki;j} - R_{kj;i} + \frac{1}{6}g_{kj}R_{;i} - \frac{1}{6}g_{ki}R_{;j}, \tag{8}$$

which is analogous to Maxwell's equations

$$F^{j}_{i\,;j} = J_{i}. \tag{9}$$

Also, F_{ij} satisfies

$$F_{ij;k} + F_{jk;i} + F_{ki;j} = 0. \tag{10}$$

Equations (9) and (10) give us guarantee for the existence of potential A_i; and using covariant derivative of the potential A_i, the electromagnetic field tensor F_{ij} can be generated as follows

$$F_{ij} = A_{i;j} - A_{j;i}. \tag{11}$$

The Weyl tensor C_{ijkl} satisfies symmetry property and differential equations similar to electromagnetic field tensor. Thus, one can think about possibilities of generating Weyl tensor from a simple tensor. It is possible to generate Weyl tensor using covariant derivative of the Lanczos tensor [10] using the following Weyl-Lanczos relations

$$\begin{aligned} C_{ijkl} = {} & L_{ijk;l} - L_{ijk;l} + L_{kli;j} - L_{kl;j;i} + L_{(il)}g_{jk} + L_{(jk)}g_{il} - L_{(ik)}g_{jl} - L_{(jl)}g_{ik} \\ & + \frac{2}{3}L^{pq}{}_{;pq}\left(g_{ik}g_{jl} - g_{il}g_{jk}\right), \end{aligned} \tag{12}$$

where the Lanczos potential tensor satisfies the following properties

$$L_{ijk} + L_{jik} = 0, \tag{13}$$

$$L_{ijk} + L_{jki} + L_{kij} = 0, \tag{14}$$

$$L_{i}{}^{j}{}_{j} = 0, \tag{15}$$

$$L_{ij}{}^{k}{}_{;k} = 0. \tag{16}$$

Property (15) is known as algebraic gauge conditions and property (16) is called differential gauge conditions. Lanczos potential tensor has total 64 components. Because of properties (13)-(16), the number of independent components of Lanczos potential tensor reduces to 10.

2. FLRW Metric and Lanczos Potential

Metric expression for FLRW metric is

$$ds^2 = -R^2\left(\frac{1}{1-kr^2}dr^2 + r^2(d\theta^2 + \sin^2\theta\, d\phi^2)\right) + dt^2, \tag{17}$$

where$R$ is a function of t and arbitrart constant k is known as a curvature index. For the FLRW metric, we chose null tetrad as

$$l^j = \frac{(1-kr^2)^{\frac{1}{2}}}{\sqrt{2}\,R}\delta_1^j + \frac{1}{\sqrt{2}}\delta_4^j, \qquad n^j = -\frac{(1-kr^2)^{\frac{1}{2}}}{\sqrt{2}\,R}\delta_1^j + \frac{1}{\sqrt{2}}\delta_4^j,$$

$$m^j = \frac{1}{\sqrt{2}\,rR}\delta_2^j + i\frac{\csc\theta}{\sqrt{2}\,rR}\delta_3^j, \qquad \overline{m}^j = \frac{1}{\sqrt{2}\,rR}\delta_2^j - i\frac{\csc\theta}{\sqrt{2}\,rR}\delta_3^j.$$

The following are non-vanishing spin coefficients [14]

$$\rho = -\frac{(1-kr^2)^{\frac{1}{2}}}{\sqrt{2}\,rR} - \frac{\dot{R}}{\sqrt{2}\,R}, \quad \mu = -\frac{(1-kr^2)^{\frac{1}{2}}}{\sqrt{2}\,rR} + \frac{\dot{R}}{\sqrt{2}\,R}, \quad \epsilon = -\gamma = \frac{\dot{R}}{2\sqrt{2}\,R}, \quad \beta = -\alpha = \frac{\cot\theta}{2\sqrt{2}\,rR}. \tag{18}$$

All components of Weyl scalar vanish. The non-zero components of complex tetrad components of Ricci tensor are

$$\Phi_{00} = \Phi_{22} = 2\Phi_{11} = \frac{1}{2}\left(\frac{k}{R^2} + \frac{\dot{R}^2}{R^2} - \frac{\dot{R}}{R}\right), \qquad \Lambda = \frac{1}{4}\left(\frac{k}{R^2} + \frac{\dot{R}^2}{R^2} + \frac{\dot{R}}{R}\right). \tag{19}$$

Since, some of the tetrad components of Ricci tensors are non-zero, the spacetime is non-vacuum.

For a choice of unit time-like velocity vector

$$u^j = \left\{0,0,\frac{i\csc\theta}{rR},0\right\},$$

the field of observer becomes expansion-free, shear-free and rotation-free; the non-vanishing components of acceleration vector are

$$a_1 = -\frac{1}{r} \qquad a_2 = -\cot\theta, \qquad a_4 = -\frac{\dot{R}}{R}$$

It is known that, if the field of observer u^j is expansion-free and rotation-free, then the Lanczos potential [10] is given by

$$L_{ijk} = a_i u_j u_k - a_j u_i u_k, \tag{20}$$

up to a gauge. To incorporate Lanczos gauge conditions, we consider

$$L_{ijk} = a_i u_j u_k - a_j u_i u_k - \frac{1}{3}(a_i g_{jk} - a_j g_{ik}), \tag{21}$$

Using (21), the Lanczos potential tensors for FLRW metric are as follows

$$L_{121} = \frac{\cot\theta\, R^2}{3(1-kr^2)}, \qquad L_{122} = -\frac{1}{3}rR^2, \qquad L_{133} = \frac{2}{3}r\,R^2\sin^2\theta,$$

$$L_{141} = \frac{R\dot{R}}{3(1-kr^2)}, \qquad L_{144} = \frac{1}{3r}, \qquad L_{233} = \frac{1}{3}r^2R^2\sin 2\theta,$$

$$L_{242} = \frac{1}{3}r^2R\dot{R}, \qquad L_{244} = \frac{\cot\theta}{3}, \qquad L_{343} = -\frac{2}{3}r^2R\dot{R}\sin^2\theta, \tag{22}$$

and thus the following are Lanczos potential scalars

$$L_1 = -\frac{1}{3}L_4 = \frac{1}{6\sqrt{2}}\left(\frac{(1-kr^2)^{\frac{1}{2}}}{rR} + \frac{\dot{R}}{R}\right), \qquad L_6 = -\frac{1}{3}L_3 = \frac{1}{6\sqrt{2}}\left(\frac{(1-kr^2)^{\frac{1}{2}}}{rR} - \frac{\dot{R}}{R}\right), \qquad L_2 = -L_5 = \frac{\cot\theta}{3\sqrt{2}\,rR},$$

where

$$L_0 = L_{ijk}\,l^i m^j l^k, \qquad L_4 = L_{ijk}\,l^i m^j m^k,$$
$$L_1 = L_{ijk}\,l^i m^j \overline{m}^k, \qquad L_5 = L_{ijk}\,l^i m^j n^k,$$
$$L_2 = L_{ijk}\,\overline{m}^i n^j l^k, \qquad L_6 = L_{ijk}\,\overline{m}^i n^j m^k,$$
$$L_3 = L_{ijk}\,\overline{m}^i n^j \overline{m}^k, \qquad L_7 = L_{ijk}\,\overline{m}^i n^j n^k.$$

The following is relationship of spin coefficients (18) and Lanczos scalars

$$L_1 = -\frac{1}{3}L_4 = -\frac{\rho}{6}, \qquad L_6 = -\frac{1}{3}L_3 = -\frac{\mu}{6}, \qquad L_2 = -L_5 = \frac{2}{3}\beta.$$

Thus, the Lanczos potential scalars depends on only three spin coefficients ρ, μ and β.

Conclusion

In this paper we have obtained Lanczos potential for FLRW metric using technique of general observers. We have successfully established the relation between Lanczos scalars and spin coefficients, which was conjectured by Parga et al.[2] It is hoped that the results will help researchers in obtaining Lanczos potential of non-vacuum type.

Acknowledgement

The author is thankful to Prof. A.H. Hasmani for reading the manuscript in detail and providing his valuable suggestions for the improvement of the manuscript

References

[1] Lanczos, C. 1962, The Splitting of the Riemann Tensor. Rev. Mod. Phys. 34, pp. 379.
[2] Ares de Parga, G., Chayoya A., A., O., and Lopez Bonilla, J. L., 1989, Lanczos Potential, Journal of Mathematical Physics 30, pp. 1294.
[3] O'donnell, P. and Pye, H., 2010, A brief historical review of the important developments in Lanczos potential theory. Electronic Journal of Theoretical Physics 7, pp. 327.
[4] Andersson, F. and Edgar, S.B., 2000, Spin coefficients as Lanczos scalars: Underlying spinor relations, Journal of Mathematical Physics 41, pp. 2990.
[5] Holgersson, D., 2004, Lanczos potentials for perfect fluid cosmologies, Linköping University Thesis.
[6] Ahsan, Z., and Bilal, M., 2010, A Solution of Weyl-Lanczos Equations for Arbitrary Petrov Type D Vacuum Spacetimes, International Journal of Theoretical Physics 49, pp. 2713.
[7] Dolan, P., and Muratori, B. D., 1998, The Lanczos Potential for Vacuum Space-Times with an Ernst Potential, Journal of Mathematical Physics 39, pp. 5406.
[8] Dolan, P., and Kim, C. W., 1994, Some Solutions of the Lanczos Vacuum Wave Equation, Proceedings of the Royal Society of London A: Mathematical, Physical and Engineering Sciences 447, pp. 577.
[9] Maher, W. F., and Zund, J. D., 1968, A Spinor Approach to the Lanczos Spin Tensor, Il Nuovo Cimento A 57, pp. 638.
[10] Novello, M., and Velloso, A. L., 1987, The Connection between General Observers and Lanczos Potential, General Relativity and Gravitation 19, pp. 1251.
[11] Roberts, M. D., 1995, The Physical Interpretation of the Lanczos Tensor. Il Nuovo Cimento B 110, pp. 1165.
[12] Hasmani, A. H., and Panchal, R., 2016, Lanczos Potential for Some Non-Vacuum Spacetimes, The European Physical Journal Plus 131, pp. 1.
[13] Hasmani, A. H., and Panchal, R., 2017, Lanczos Potential for Weyl Metric, PRAJNA - E-Journal of Pure & Applied Sciences, Accepted.
[14] Chandrasekhar, S., 1998. The mathematical theory of black holes, Oxford University Press.
[15] Newman, E., and Penrose, R., 1962, An Approach to Gravitational Radiation by a Method of Spin Coefficients, Journal of Mathematical Physics 3, pp. 566.
[16] Hawking, S.W. and Ellis, G.F.R., 1973, The large scale structure of space-time (Vol. 1). Cambridge university press.

Wastewater treatment of railway station using activated sludge process

Raj Vahheta[a], Anand Varindani[a*], Bhavyang Zapadiya[a], Kishan Patel[a], Jivandeep Vora[a], Nirav Vaghasia[a]

[a]*Alpha College of Engineering and Technology,At. Khatraj , Gandhinagar, Gujarat, India 382781*

Abstract

One of the major problems the country is facing is water shortage. Hence, it is imperative that water is conserved as much as possible and now a days water is used at railway stations for washing and cleaning the trains and railway stations. A substantial quantum of water is used in rail coaches, washing rails, washing trains and other human activities such as: - restrooms and toilet flushing and "it is definitely possible to save considerable quantity". In railway station, the wastewater is present in huge amount so this project is about an idea to reuse that type water by treating it to the level that it can be used for standard purposes in the railway stations .There are many types of process which is used in our project to treat the wastewater which is generated in railway station such as Preliminary, Primary, Secondary, Tertiary etc. And further through that treatment process the energy can be generated from methane gas which will be released in the wastewater treatment process. At the end of the wastewater treatment process if there is any remains of solid waste in our treatment unit, it will be used as a 'fertilizer.

Keywords: Activated sludge process, Gas production, Power generation, Railway station, Fertilizer

1. Introduction

The water quality of kalupur railway station has been found to deteriorate in respect of most of the parameters by continuous discharge of water for different types of purpose and waste waters in the Railway stations such as platform wastewater and wastewater generated during washing of rails and trains and other human activities, such as restrooms, toilet flushing. Very high content of oil & grease and phethogenic compounds in sewers are found in the wastewater. The enhancement of turbidity and colour is due to high total suspended solids in wastewater of railway station. High contents of phosphate, nitrate, chloride, BOD and compounds of phosphorus and nitrogen along with other components in the Railway wastewater have given rise to eutrophication. For execution of this plant we prefer the kalupur railway station. The area of kalupur railway station is 1.36 sq km. The travelers (population) passing throughout the day is 65,000 approximately. Approximately 250 trains are daily arriving at station out of which the water consumption to wash one bogie's washroom that is 50 liter per bogies. Approximately 15 train's washrooms are wash daily. So Total water use to wash 1 train is = 50 × 25 = 1250 liters/train.About 60% of the Suspended solids of sewage are removed by sedimentation, 75% by chemical coagulation and settling, and 90% by complete treatment, such as by the activated sludge or the trickling filters. At the end of the process the gas will produce by sludge in sludge digestor. The amount of gas produce is about 0.6 cubic.m per kg of volatile matter present in the sludge. The gas produce usually contains 65% methane, 30% carbon dioxide, and trace amount of other gases. Energy will produce from this generated gas. The sludge which remaining at the end of the process we use that remaining sludge as a fertilizer.

The advantages

- To reduce the cost of water which is supply by the municipality to railway station.
- To reduce the cost of electricity.
- At the end of the process, if we have some extra surcharge water than that water we are going to use for different purposes like in cooling water , gardening , toilet flushing, road washing etc.
- The energy will produce from methane gas with the help of sludge digestor.
- Sludge which remaining at the end of the process use as fertilizer.

* Anand Varindani Tel.: +91-8469062268
E-mail address: varindanianand@gmail.com

1.1 *Brief about units*

1. Preliminary treatment:-
   - We are providing screen bars as well as grit chamber.
   - The Main function of screen bar is to remove large particles
   - And grit chamber is provided to remove inorganic matter.

2. Primary treatment:-
   - The purpose of the Primary sedimentation tank (PST) is to remove organic matter.
   - Efficiency of removal of suspended solid is 60-70 %.
   - Efficiency of removal of BOD is 30-40 %.

3**.** Secondary treatment:-
   - Secondary treatment process is basically done by activated sludge process it is suspended growth process.
   - It consists of two tanks one is for aeration tank where microorganisms are grown second one is a clarifier where the settling of impurities take places.

4. Tertiary treatment**:-**
   - Simple Chlorination process.

1.2 Objetives

The main and important aspects and objective of this topic is to treat the wastewater which is generated in the railway station.
- The wastewater is to be treated and can also be further use in the standard purposes such as: - rail coaches, washing rails, washing trains and other human activities such as: - restrooms and toilet flushing and also to clean the railway station.
- From this treatment process methane gas can be generated and can also be further used as a energy source.
- And if there is any type remaining sewage there will an arrangement by which that type of solid waste can be further used as fertilizer.
- The design of the treatment unit will be done in such a way that the cost of the treatment could be lesser as much as possible.

1.3 *Scope*

Through this project sustainable quantum of water can be saved and could also make a difference in ‘saving water’ which will play an important role in environmental factor such as in enhancement of water quality.
- It can also be beneficial in an economical way such as saving the charges of water from municipality.
- Sufficient amount of methane gas will be produced or can be released by which the energy generation can be done and by that we can save the electricity charges.
- Usage of remaining sewage will be done as a fertilizer.
- It will also make a difference in saving water and therefore in the ‘water pollution acts’ as the water is to be treated it will help in decreasing the water pollution which is done at the railway station.

2. Discharge

The water consumption to wash one bogie’s washroom. that is 50 liter per bogies. if Approximately 15 train’s washrooms are wash daily.So for that

$= 50 \times 25 = 1250$ liters/train. (25 bogie per train)

Daily water consumption for washing train

$= 1250 \times 15 = 18750$ liters/day

≈ 18.75 kld.

Domestic waste water generation = 500 kld (from source)

= 518.75 kld

≈ 0.51 MLD

3. Details about units

Screen bars:-Screening is the first unit operation (physical unit operation) in wastewater treatment plants. A screen is device with openings generally of uniform size. The screening elements may consist of parallel bars, rods, gratings or wire mesh or perforated plates, and the screens may be of any shape although generally they are circular or rectangular.

Grit Chamber:- Grit has as a specific gravity ranging from 2.4 to 2.65. The design is based on Size & specific gravity of particle.

Primary Sedimentation tank (PST):- There are two types of tank i. Rectangular ii. Circular. We are not providing rectangular tank because they are economical for large plant so we are providing circular tank.

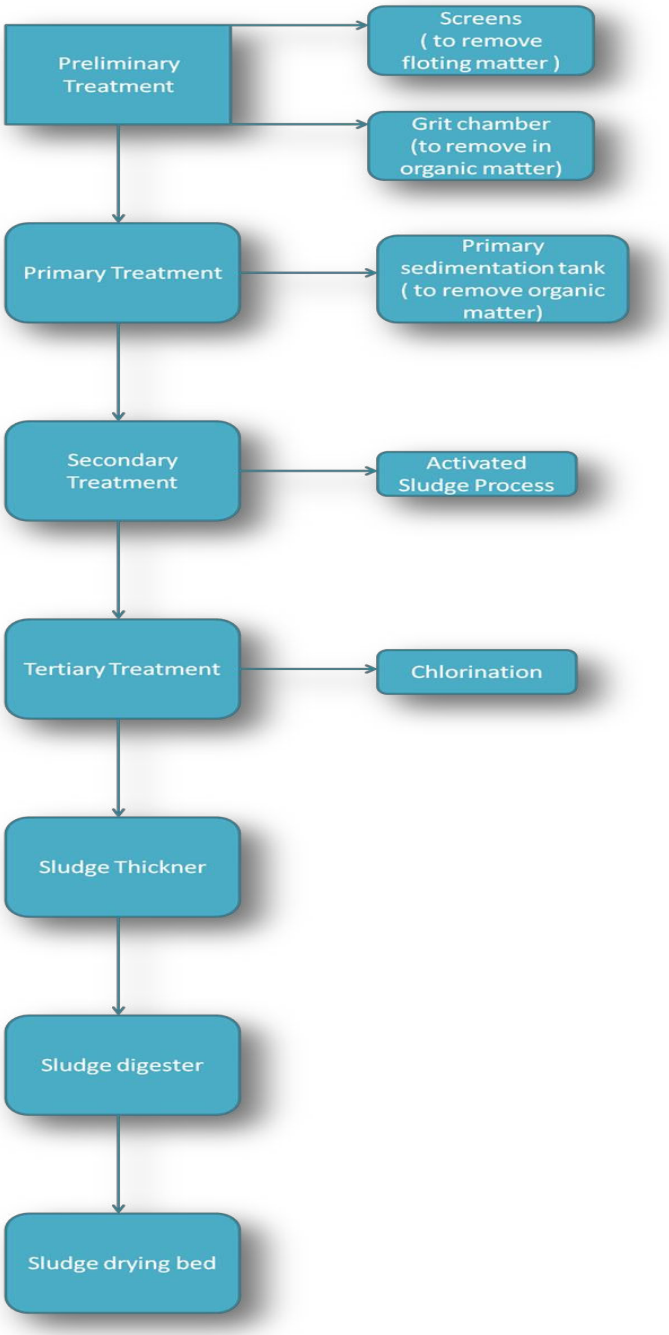

Fig.1 Flow chart of treatment plant

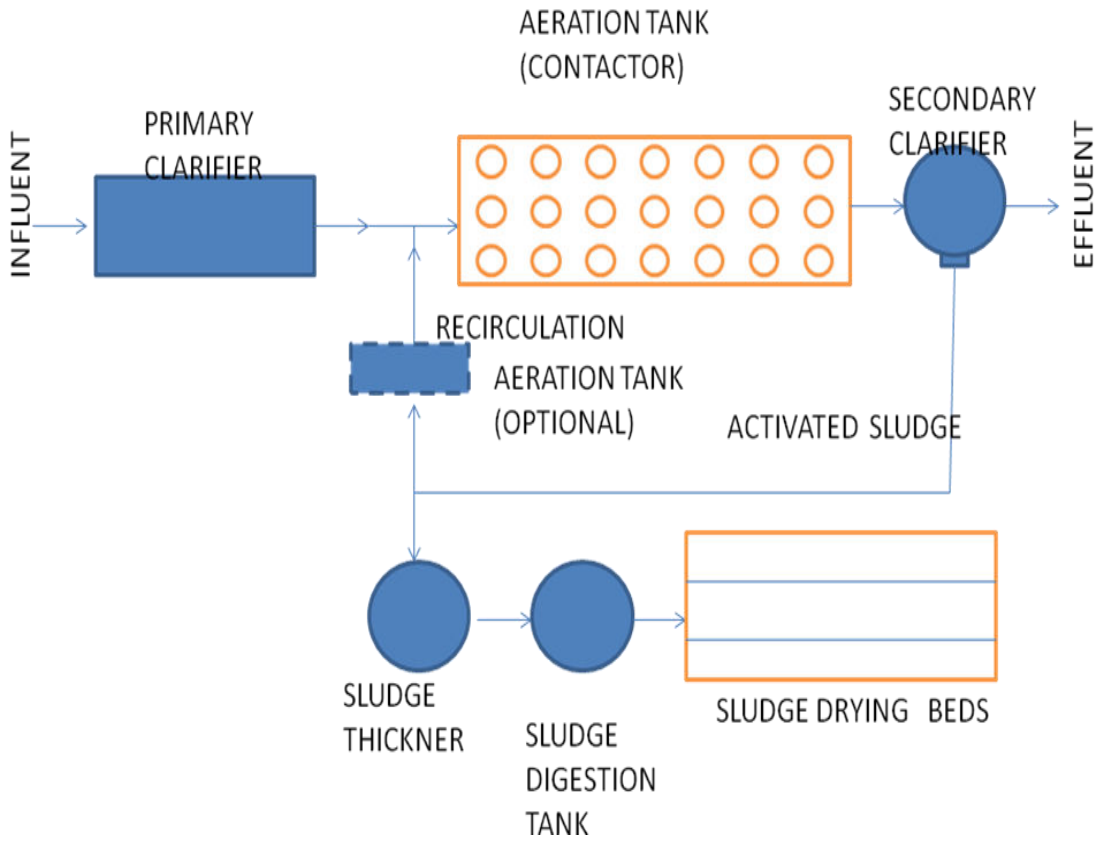

Fig.2 Flow dia. of activated sludge process

Secondary (biological) treatment:-

Activated Sludge Process:-

- The activated sludge is the sludge which is obtain by settling sewage in presence of abundant oxygen so as to be supercharged with favourable aerobic micro-organisms.
- In this process tank are provided
    1. Aeration tank
    2. Secondary clarifier
- The effluent from the primary settling tank is mixed with a dose of activated sludge and is aerated in an aeration tank for 4 to 8 hrs.
- Efficiency of BOD removal is 80-95 %
- Efficiency of bacteria removal is 90 – 95 %

Sludge digestor

- The Purpose of use this digestors is to produce Methane gas.
- It consists of a circular R.C.C tank with hoppered bottom and
- having a fixed or a floating type of root over its top.
- Digestors have two types of roof
    1. Floating type
    2. Fixed type
- Through this digestor gases are produce and this gases of decomposition are collected in a gas dome.
- The digested sludge which settles down to the hoppered bottom of the tank is removed under hydrostatic pressure, periodically, once a week or so.

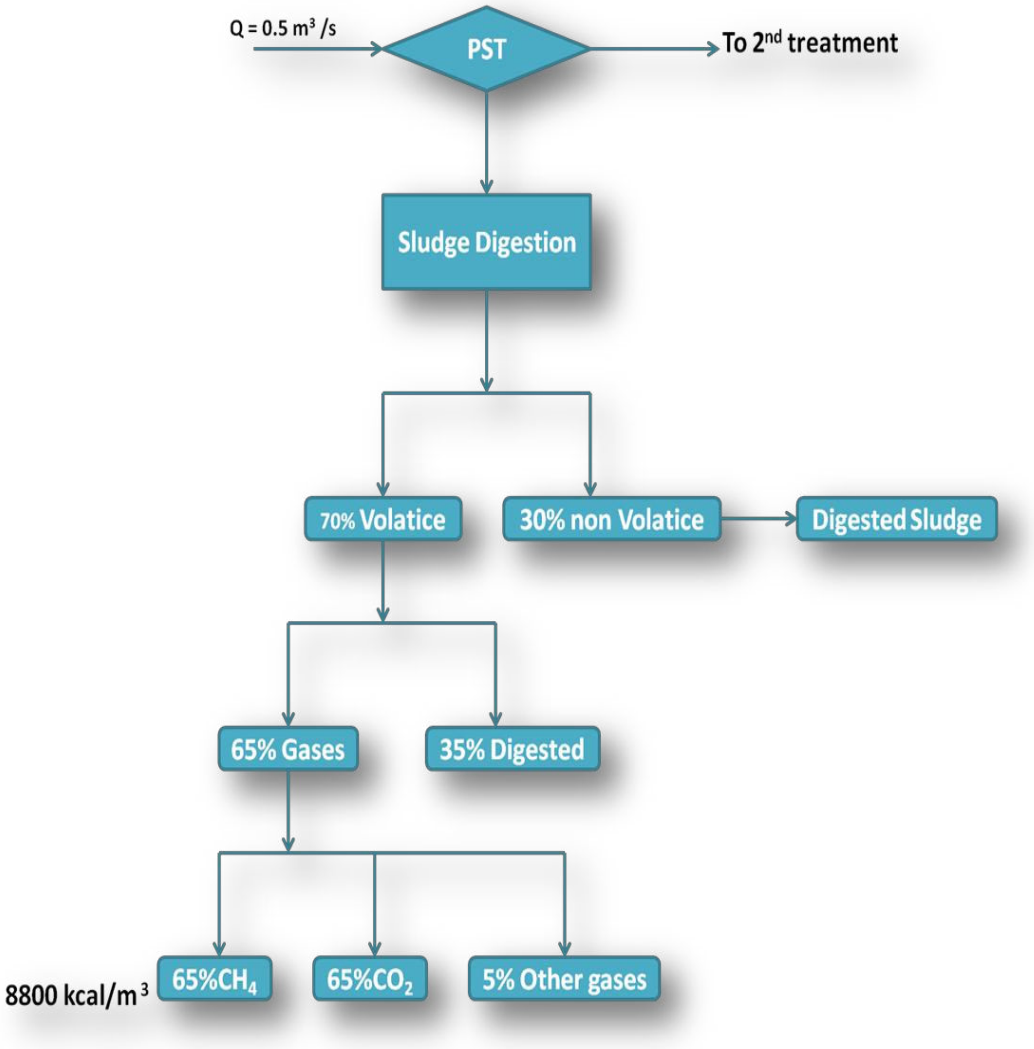

Fig.3 Layout of gas production

4. Gas Production

If it is possible to analyse the wastewater to be treated, and to determine the characteristics of the sludge, its gas producing ability may be estimated. About 60% of the Suspended solids of sewage are removed by sedimentation, 75% by chemical coagulation and settling, and 90% By complete treatment, such as by the activated sludge or the trickling filters, preceded and followed by sedimentation.The amount of gas produce is about 0.6 cubic.m per kg of volatile matter present in the sludge.The gas produce usually contains 65% methane, 30% carbon dioxide, and trace amount of other gases. The heat content of methane is approximately 3600 kJ/m3 (8800 kC/m3).

4.1 Cost of units

The prices given here are only indicative and meant to give an idea. All capacities given are in KLD (Kilo litres /day,
kilo= 1000 litres).

- 5.0 KLD STP = Rs.5.0 lakhs.
- 10 to 15 KLD = Rs.8.0 lakshs.
- 25 KLD = Rs.15.0 Lakhs.
- 35 KLD = Rs.18.0 Lakhs.
- 50 KLD = Rs.35.0 Lakhs.
- 75 KLD = Rs.40.0 Lakhs.
- 100 KLD = Rs.30.0 Lakhs. (All civil work for this size to be built by buyer)

Also please note:

- Prices given are exclusive of Value Added Tax and excise duties (if applicable)

- Supplier will charge a separate amount for installation and starting up the STP. This can cost an additional 5 to 10%
- Prices for MBR systems are not given since they involve a substantial import content and hence it would be better to approach companies that offer such a sytem for a price directly.

Conclusion

Although the initial installment cost is high but the maintenance cost is found to be very economical and hence can be put in use. There is significant reduction in BOD level as well as Total organic carbon content. Again there is significant high reduction in hardness Complete removal of colour and odour enhances its purification efficiency. Also about 100 % disinfection has been achieved after post treatment. There seen to be high reduction in metal ion and total dissolved solid content. Removal of alkanity of water also a major advantage. So from the above fact the whole treatment is seem to be economical and highly efficient for water treatment containing high organic as well as inorganic components and also gives nearly complete disinfection which may be used for Tap water.

References

[1] Sewage disposal and air pollution engineering, Author: Santosh Kumar Garg first edition:march,1979
[2] waste water engineering Author: Dr. B.C.Punmia, Er.Ashok.K.Jain, Dr.Arun K.Jain for design criteria and design units.
[3] Apha standard book for parameters test
[4] Indian standard specifications for drinking water IS:10500 waste water disposal , standards, ambient , air quality standards
[5] AWWA. In Water Quality and Treatment: A Handbook of Community Water Supplies, 4th Ed.; McGraw-Hill.
[6] Metcalf & Eddy, Inc. Wastewater Engineering: Treatment and Reuse, 4th Ed.; McGraw-Hill.

Estimation of Passenger Car Unit at Signalized Intersection

Harsh Dobariya[a], Dharam Bhatt[a], Sivam Bohare[a], Bhaumik Bhatt[a], Pranav Dholiya[a*]

[a]*Gandhinagar Institute of Technology, Moti Bhoyan, Gandhinagar, Gujarat, India 382781*

Abstract

The majority of roads in India are of single lane way and two lane way. Due to budget constrains, sometimes this road are constructed with one and half lane width (4.2m) and is called a intermediate lane road with traffic moving on both direction. To simplify the analysis of mixed traffic on such roads, different types of vehicles are converted into equivalent number of passenger car by using PCU. The results of the study will helpful to traffic engineers and practitioners as PCU values are often required in traffic flow and highway capacity study.

Keywords: Passenger car unit, signalized intersection, hetrogenous traffic flow, videography survey.

1. Introduction

India has the second largest road network 3.3 million km in the world, second only to the USA 6.6 million km. presently, there are nearly 30 million vehicles in India and about 2.5 million are added every year. The volume of traffic on roads increases at the rate of 12% per annum. Capacity augmentation and improvement in the level of service is normally achieved by widening existing roads (Gupta 2000). Today India is 32% urban, between 2010 and 2050 India will go from 32% urban to 52% urban and in 2070 75% urban (United Nations projections). The urban roads of India generally carry the heterogeneous traffic which is the combination of various vehicles like Cars, Buses, Trucks Motor cycles, Light goods vehicles, Auto Rickshaws, Pedal Cycles, Hand drawn carts, and Animal drawn carts etc. These all vehicles have different speeds, size, Load carrying capacities or passenger capacities etc. which affect the urban heterogeneous traffic flow. The problem is more in case of mixed traffic flow when speed differential among different categories of vehicles is quite substantial. It increases the desired number of overtaking considerably with limited opportunities to overtake. Prediction and knowledge of capacity is fundamental in design, planning, operation and layout of road network sections. The analysis and modelling for road links focused primarily on establishing speed-flow relationships for different road types and to study the influence on these relationships of geometric traffic and environmental condition. Road side environment and activities have an important role in reducing the speed in urban areas. Many activities at the road side can reduce speed significantly.Computer Simulation models can play an important role in the analysis and assessment of the road transport system and its component. Also these models are very useful to develop traffic stream models, car following theory, shock wavy analysis and queuing analysis. The simulation models are to be considered only after analytical techniques have not been found approximate.

1.1. Methodology

There is so many traffic problems are create at the signalized intersection in urban area because of a different mode of transportation at the signalized intersection. In this project first we visited different intersection and then we select intersection which has dance traffic. The places which have dance traffic are Pakavan cross road, Shivranjani circle, and income tax circles. We observed that there is no solution apply at Shivaranjani circle because there was already over bridge constructed at Shivaranjani circle. The main road of the Ahmedabad people is S.G High way (Sarkhej –Gandhinagar) so there is main junctions are approaching through the given and parallel to the city where pakwan cross road is the heavy traffic at office timing so we select pakwan cross road.

we choose pakwan junction because it's a connected to sarkhej to the Gandhinagar high way which is almost a huge traffic problem will be going to occur in future that why we select this junction. This is the National highway 8. And at the pakwan junction it's a big urban signalization traffic signal therefore it must be an important part of the road. For this we have find the PCU value at urban intersection.as per PCU value we will give better solution for reduce traffic.

* Pranav Dholiya Tel.: +91-9408752621
E-mail address: pravav.dholiya@git.org.in

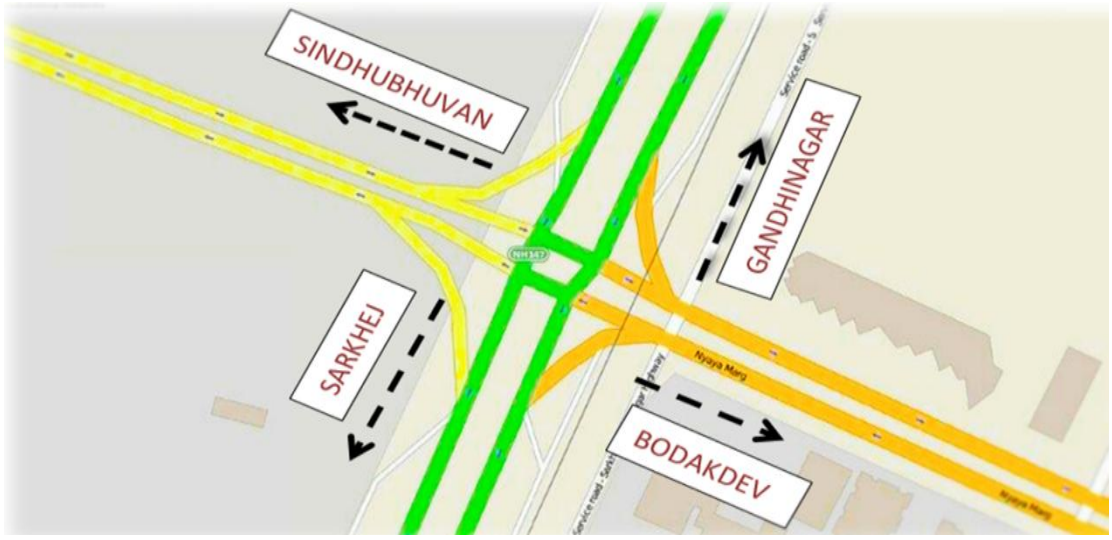

Fig 1 Pakwan Cross Road Circle

2 Field Surve

2.1 Traffic Signal condition at Roadway/approach

Table 1 Traffic Signal condition at Roadway/approach

Intersection	TrafficApproach From	Width(m)	Cycle time(s)	Green time(s)	Amber time(s)	Red time(s)
Pakwan Intersection (Ahmedabad)	Sarkhej	13.90	193	60	3	130
	Sidhu-Bhuvan	9.30	193	30	3	160
	Gandhinagar	13.90	193	60	3	130
	Bodakdev	8.60	193	40	3	150

2.2 Road Conditions

Table 2 Inventory Details of Road

	L/R	Sarkhej	Sindhu Bhuvan	Gandhinagar	Bodakdev
Footpath Width(m)	L	1.55	-	1.55	.90
	R	1.55	-	1.55	.90
Carriageway Width(m)	L	15.36	9.30	15.36	9.30
	R	15.36	9.30	15.36	9.30
Approach Width(m)		13.90	9.30	13.90	8.60
Traffic Signal	L/R	YES	NO	YES	YES
Street Light	L	YES	YES	YES	YES
	R	YES	YES	YES	YES
Bus Stand	L	YES	NO	NO	NO
	R	NO	NO	NO	NO
Parking	L	YES	NO	YES	YES
	R	YES	NO	YES	YES

3. Videography method

In this study speed measured by stop watch method and other variable find by Videography. Two point mark on the urban traffic stream on selected location the length of the road is taken 40m to 50m in between is known as mid-block section of the road the video will be played the time taken by different vehicles to cross 50m distance will be measured in seconds. For example, a car takes 5.00 seconds to cross 50m distance then the speed of this 26 car will be 36km/hr after completing the traffic survey the video is to played reputed and the results are accurate and reliable by this method another important traffic flow characteristics is the flow which is measured

in vehicles per hour this is also possible by videography method if we play the video again and again we can count the total numbers of different vehicles.

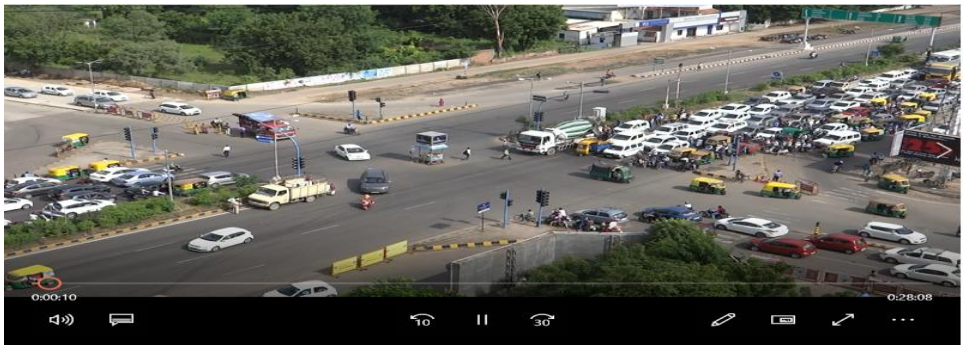

4 Data Require For Find Pcu By Various Method

4.1 Data Required For Area Occupancy Method

PCU=(Vc/Vi)/(Ac/Ai)

Where,

Vc and Vi=means speed of car and vehicle type irespectively

Ac and Ai= their respective projected rectangular area 1*w on the road

Table 3 Vehicle Details

Category	Vehicle	Dimension(m)	Projected Area (m^2)
Car	Car,jeep,van	3.72*1.44	5.39
Bus	Bus	10.10*2.43	24.74
Truck	Truck	7.50*2.35	17.62
LCV	Minibus	6.10*2.10	12.81
M- truck	Multi-axcel	2.35*12	28.60
Bikes	Scooter,motorbike	1.87*0.64	1.20
Cycle	Paddelcycle	1.90*0.45	0.85
Autos	Auto,tampo	3.20*1.40	4.48

4.2 Data ReruiredFor Homogeneous Coefficient Method

PCU=(Li/Ui)/(Lc/Uc)

Where,

Li = length of corresponding vehicle

Lc = length of the car

Ui = speed of the corresponding vehicle

Uc = speed of the car

4.3 *Data Analysis*

Table 4 Length and Speed of vehicle

CATAGORY	Length of the car Lc (m)	Lenth of the vehical Li(m)	Speed of the car uc (km/hr)	Speed of the vehical ui (km/hr)
Car	3.7	3.7	31.46	31.46
3W	3.7	2.85	31.46	25.71
2W	3.7	2.10	31.46	27.50
LCV	3.7	4.50	31.46	24.84
HCV	3.7	8.40	31.46	16.6

4.3.1 Area Occupancy Method

Table 5 Area Occupancy Method

Category of Vehicle	Area Occupancy Method	Homogeneous Coefficient Method
CAR	1	1
3W	0.81	0.95
2W	0.24	0.64
LCV	2.90	1.55
LHCV	6.33	

4.3.*2 Homogeneous Coefficient Method*

Table 6 Homogeneous Coefficient Method

CATAGORY	Length of the car	Lenth of the	Speed of the caruc	Speed of the vehical	Lc/uc	Li/ui	PCU
Car	3.7	3.7	31.46	31.46	0.42	0.42	1
3W	3.7	2.85	31.46	25.71	0.42	0.40	0.95
2W	3.7	2.10	31.46	27.50	0.42	0.24	0.64
LCV	3.7	4.50	31.46	24.84	0.42	0.65	1.55
HCV	3.7	8.40	31.46	16.6	0.42	1.82	4.30

4.4 *Result*

Table 7 Comparison of Methods

CATAGORY	Length of the car Lc	Lenth of the vehical	Speed of the car	Speed of the vehical ui
Car	3.7	3.7	31.46	31.46
3W	3.7	2.85	31.46	25.71
2W	3.7	2.10	31.46	27.50
LCV	3.7	4.50	31.46	24.84
HCV	3.7	8.40	31.46	16.6

5. Classified Volume Data

Sarkhej to Gandhinagar

Time 9:30 am to 11:00 am

Time	T/w	Car	LCV	Bus	ACM PCU	HCM PCU
5	90	42	3	2	84.96	112.85
10	97	40	4	0	74.88	108.28
15	85	45	2	1	77.53	106.8
20	86	42	3	3	90.33	114.59
25	102	30	3	0	63.18	99.93
30	94	25	4	0	59.16	91.36
35	89	39	4	0	71.96	102.16
40	85	39	3	2	80.76	106.65
45	87	25	5	1	66.71	92.73
50	80	49	1	0	71.1	101.75
55	84	34	2	0	59.96	90.86
60	104	33	4	1	75.89	110.06
65	96	42	3	2	86.4	116.69
70	97	40	1	0	66.18	103.63
75	78	41	3	0	68.42	95.57
80	70	33	2	0	55.6	80.9
90	130	58	6	2	119.26	159.1
Total	1554	657	53	14	1272.28	1793.91

Gandhinagar to Sarkhej

Time 9:30 am to 11:00 am

Time	T/w	Car	LCV	Bus	ACM PCU	HCM PCU
5	87	45	3	1	80.91	109.63
10	83	41	3	0	69.62	98.77
15	96	38	2	2	79.5	111.14
20	94	36	1	2	74.12	106.31
25	80	38	4	0	68.8	95.4
30	88	39	3	0	68.82	99.97
35	84	41	2	0	66.96	97.86
40	86	35	1	1	64.87	95.89
45	89	39	4	2	84.62	110.76

50	85	36	3	0	65.1	95.05
55	94	37	1	0	62.46	98.71
60	83	31	1	2	66.48	94.27
65	88	43	2	1	76.25	106.72
70	81	35	3	0	63.14	91.49
75	84	35	4	1	73.09	99.26
80	89	36	3	0	66.06	97.61
90	178	46	7	1	115.35	175.07
Total	1569	651	47	13	1246.15	1783.91

Sindhubhavan to Bodakdev

Time 9:30 am to 11:00 am

Time	T/w	Car	LCV	Bus	ACM PCU	HCM PCU
5	84	41	2	0	66.96	97.86
10	87	40	3	2	82.24	108.93
15	76	39	4	1	75.17	98.14
20	88	44	0	0	65.12	100.32
25	98	37	2	0	66.32	102.82
30	87	36	2	0	62.68	94.78
35	78	34	3	0	61.42	88.57
40	83	37	4	1	74.85	100.62
45	83	36	3	0	64.62	93.77
50	84	43	3	0	71.86	101.41
55	75	37	2	0	60.8	88.1
60	78	36	1	2	70.28	96.07
65	79	44	3	0	71.66	99.21
70	74	35	2	0	58.56	85.46
75	79	37	2	1	68.09	94.96
80	83	32	3	0	60.62	89.77
90	166	65	6	1	128.57	184.84
Total	1482	673	45	8	1209.82	1725.63

Bodakdev to Sindhubhavan

Time 9:30 am to 11:00 am

Time	T/w	Car	LCV	Bus	ACM PCU	HCM PCU
5	80	40	5	1	80.03	103.25

10	93	38	3	0	69.02	102.17
15	88	45	3	1	81.15	110.27
20	86	42	2	1	74.77	104.44
25	108	20	4	1	63.85	99.62
30	90	27	5	0	63.1	92.35
35	82	35	3	0	63.38	92.13
40	79	39	6	1	81.69	103.16
45	87	18	4	0	50.48	79.88
50	70	45	2	0	67.6	92.9
55	68	30	3	1	61.35	82.47
60	80	33	4	1	70.13	94.7
65	85	63	2	0	89.2	120.5
70	78	23	1	0	44.62	74.47
75	73	40	3	0	66.22	91.37
80	79	35	2	0	59.76	88.66
90	134	78	5	2	137.32	180.11
Total	1460	651	57	9	1223.67	1712.45

Sarkhej to Gandhinagar

Time 6:30 Pm to 8:00 PM

Time	T/w	Car	LCV	Bus	ACM PCU	HCM PCU
5	90	48	3	3	97.29	123.15
10	100	45	2	2	87.46	120.7
15	88	47	0	4	93.44	120.52
20	93	43	3	3	93.01	120.07
25	109	30	2	1	68.29	107.16
30	95	23	0	0	45.8	83.8
35	85	37	4	1	75.33	101.9
40	77	40	0	3	77.47	102.18
45	84	28	5	1	68.99	93.81
50	70	32	5	0	63.3	84.55
55	76	32	2	0	56.04	83.74
60	101	37	4	1	79.17	112.14
65	90	45	2	3	91.39	118.6
70	97	26	1	0	52.18	89.63
75	65	40	5	2	82.76	97.95

80	63	57	2	0	77.92	100.42
90	112	80	6	2	136.94	169.58
Total	1495	690	46	26	1346.78	1829.9

Gandhinagar to Sarkhej

Time 6:30 pm to 8:00 pm

Time	T/w	Car	LCV	Bus	ACM PCU	HCM PCU
5	95	45	2	2	86.26	117.5
10	87	39	4	1	77.81	105.18
15	88	43	3	2	85.48	112.57
20	80	42	4	3	91.79	112.3
25	97	28	1	0	54.18	91.63
30	81	29	2	1	60.57	88.24
35	82	35	4	0	66.28	93.68
40	70	37	2	3	78.59	97.8
45	86	29	4	1	67.57	94.54
50	75	52	1	0	72.9	101.55
55	81	37	2	2	74.9	100.54
60	103	31	5	0	70.22	104.67
65	90	51	2	6	116.38	137.5
70	93	29	2	0	57.12	91.62
75	78	41	3	3	87.41	108.47
80	79	33	2	2	70.42	95.26
90	148	54	5	2	116.68	165.07
Total	1513	655	48	28	1334.56	1818.12

Sindhunhavan to Bodakdev

Time 6:30 pm to 8:00 pm

Time	T/w	Car	LCV	Bus	ACM PCU	HCM PCU
5	88	45	2	1	78.25	108.72
10	81	42	5	2	88.6	110.19
15	78	44	3	0	71.42	98.57
20	83	47	4	3	97.51	119.22
25	96	23	2	2	64.5	96.14
30	91	26	2	1	59.97	91.64
35	88	38	1	0	62.02	95.87

40	73	40	4	1	75.45	97.22
45	75	23	1	2	56.56	81.15
50	71	47	3	0	72.74	97.09
55	77	33	2	3	76.27	98.28
60	89	37	4	0	69.96	100.16
65	95	60	3	1	97.83	129.75
70	87	26	2	0	52.68	84.78
75	70	35	1	1	61.03	85.65
80	73	39	3	2	77.88	98.97
90	110	54	2	5	117.85	149
Total	1425	659	44	24	1280.52	1742.4

Bodakdev to Sindhubhavan

Time: 6:30 pm to 8:00 pm

Time	T/w	Car	LCV	Bus	ACM PCU	HCM PCU
5	89	40	4	2	85.62	111.76
10	99	44	3	2	89.12	120.61
15	88	35	1	1	65.35	97.17
20	86	47	3	0	76.34	106.69
25	105	38	2	2	81.66	116.9
30	95	23	4	2	70.06	98.6
35	93	39	2	3	86.11	114.52
40	78	36	1	0	57.62	87.47
45	89	30	4	1	69.29	97.46
50	74	50	3	0	76.46	102.01
55	79	36	4	2	79.22	101.36
60	86	38	5	3	92.13	113.69
65	83	40	3	2	81.28	106.37
70	87	23	2	0	49.68	81.78
75	79	35	1	0	56.86	87.11
80	76	33	3	2	72.6	94.89
90	118	56	5	1	105.15	143.57
Total	1504	643	50	23	1294.55	1781.96

Conclusion

The analysis is based on the field study conducted on typical city road around pakwan cross road considering almost all classis of vehicles found in India. The PCU values for different categories of vehicles are determine by different methods. It has been observe that from the study of traffic volume and road way conditions that the

PCU value of vehicles significantly changes with the change in traffic volume and road design. This result shows that area occupancy method is the best method among all to find PCU value at heterogeneous traffic area.

References

[1] Al-Kaisy, A., Jung, Y., and Rakha, H. (2005). "Developing passenger car equivalency factors for heavy vehicles during congestion." Journal of Transportation Engineering, 131(7), pp. 514–523.
[2] Arasan, V.T., Dhivya, G. (2010). "Methodology for determination of concentration of heterogeneous traffic". Journal of Transportation Systems Engineering and Information Technology, 10 (4), pp. 50-61.
[3] Chandra, S., and Kumar, U. (2003). "Effect of Lane Width on Capacity under Mixed Traffic Conditions in India." Journal of Transportation Engineering, 129(2), pp. 155-160.
[4] Chandra, S., Mohan, M., and Gates, T. J. (2014). "Estimation of Critical Gap using Intersection Occupancy Time." 19th International Conference of Hong Kong Society for Transportation Studies, Z. Lang, ed., Hong Kong, pp. 313–320.

Acknowledgement

The success and final outcome of this project required a lot of guidance and assistance from many people and we are extremely privileged to have got this all along the completion of our project. All that we have done is only due to such supervision and assistance and we would not forget to thank them. We would not forget to remember Ahmedabad Traffic Police for their Support of providing informations. We are thankful to and fortunate enough to get constant encouragement, support and guidance from all Teaching staffs of civil engineering which helped us in successfully completing our project work.

Prevenzione- Data Leakage Prevention

Dipen Paresh Shah[a*]

[a]*Gandhinagar Institute of Technology, Moti Bhoyan, Gandhinagar, Gujarat, India 382781*

Abstract

While doing business sometimes it is necessary to hand over companies or organizations sensitive data to supposedly trusted third parties (Agents). Here, the one who is sharing the data is denoted by the term 'Distributor' and the one receives the data is termed as 'Agent'. It is quite necessary to create a secure environment or region in order to keep our sensitive information secure and to ensure Data Prevention and avoid Data Leakage Prevention to some extent. The main aim of the system is create a secure region where distributors and agents can share their data. Additionally, if someone modifies the data it will know to the distributor.

Keywords: Data Leakage Prevention , Cloud, Homomorphic Encryption , Distributor , Agent

1. **Introduction**

Data leakage is common across all industries, academic and government offices (all the sector). For the business purpose or research purpose the data must be shared among the differentent erprises or agents. Once data is given to the agents, it should not reach to the unauthorized person. If somebody among the agents leaks the data, it may lead to great loss. To avoid this loss it is necessary to detect the leakage and stop doing business with that agent. Currently, techniques based on 'watermarking' are used to detect the guilt of agent, but it has to modify the data which is not allowed in some cases. The Prevenzione focuses on the novel method of preventing your sensitive data by providing a secure platform and detecting the guilty who has leaked the data.

2. Objective and Scope of System

A data failure is the unintentional release of secure information to an unauthorized environment. For example, company may have partnerships with other companies that require sharing customer data. Similarly, a hospital may give patient records to researchers who will device new treatments. The goal is to estimate the leaked data came from the agents as opposed to other sources. Not only to we want to estimate the agents leaked data, but we would also like to find out if one of them was more likely to be the leaker. Algorithms are designed to know the source of the leaker.
Prevenzione that is to be developed provides the distributors and the agents with all the secured data management, Data Prevention and Data Leakage Detection to agents. The Prevenzione is supposed to have the following features.

- The System will be able to manage the data among distributors and agents.
- The System will view the data to the respective user.
- The System will provide secure platform to users.
- The System is capable of doing Guilty Person Analysis.

3. Existing System

Several systems are there which aims at providing security to data plus the whole system but though they fail at providing data security to its highest level and many loopholes were found in the existing system.

Watermarking:
The watermark is difficult for an attacker to remove, even when several individuals conspire together with independently watermarked copies of the data. It describes a digital watermarking method for use in audio, image; video and multimedia data. It is distortions such as cropping and scaling, compression, rotation, translation

* Dipen Shah Tel.: +91-7600459085
E-mail address: dipen.shah1996@gmail.com

These techniques were used for handling data leakage detection. But the drawback of this technique is that it requires some modification of data. Also in some cases the watermarks can be destroyed if the data recipient is malicious. Hence there is need to propose efficient technique to find data leakage.

4. Homomorphic Encryption

Homomorphic Encryptions basically perform to calculate complex mathematical operations to encrypted data without compromising the encryption, which allows computation on ciphertexts which generate the encrypted result. When decrypted, its match the result of process as if they had been performed on the plaintext. Cloud Computing platforms can perform tough computations on homomorphically encrypted data without ever having access to the unencrypted data. It can also be used to securely chain together different services without exposing sensitive data. It can also be used to create other secure systems such as secure voting systems, collision-resistant hash functions, and private information retrieval schemes.

4.1 Experimental Analysis for Prevenzione

In the proposed system, we develop 'Elgamal' algothim for finding guilty agents. For this purpose different data allocation strategies are used. We are using "Fake records" (used with the data to generate different hash value) which are not real but appear as real records in order to find the guilty agent. Here these Fake objects acts as a watermarks like in watermarking technique. It improves over the limitations of watermarking technique as it does not require any modification of original data. If it turns out an agent was given one or more fake objects that were leaked, then the distributor can be more confident that agent was guilty. Also in proposed system, we have implemented e-mail filtering technique in which unauthorized users will be unable to see and download the contents of the e-mails which is send by guilty agent. So Distributors sensitive data remains secure.
In figure 1 we can see design of eclipse IDE. As should be obvious the first content document ElGamal.txt has some ordinary content record. We compile this record utilizing apache ant, the outcome [figure 1] we get unique content document is changed over to figure content and the aftereffect of the figure content is currently changed over to plain content.

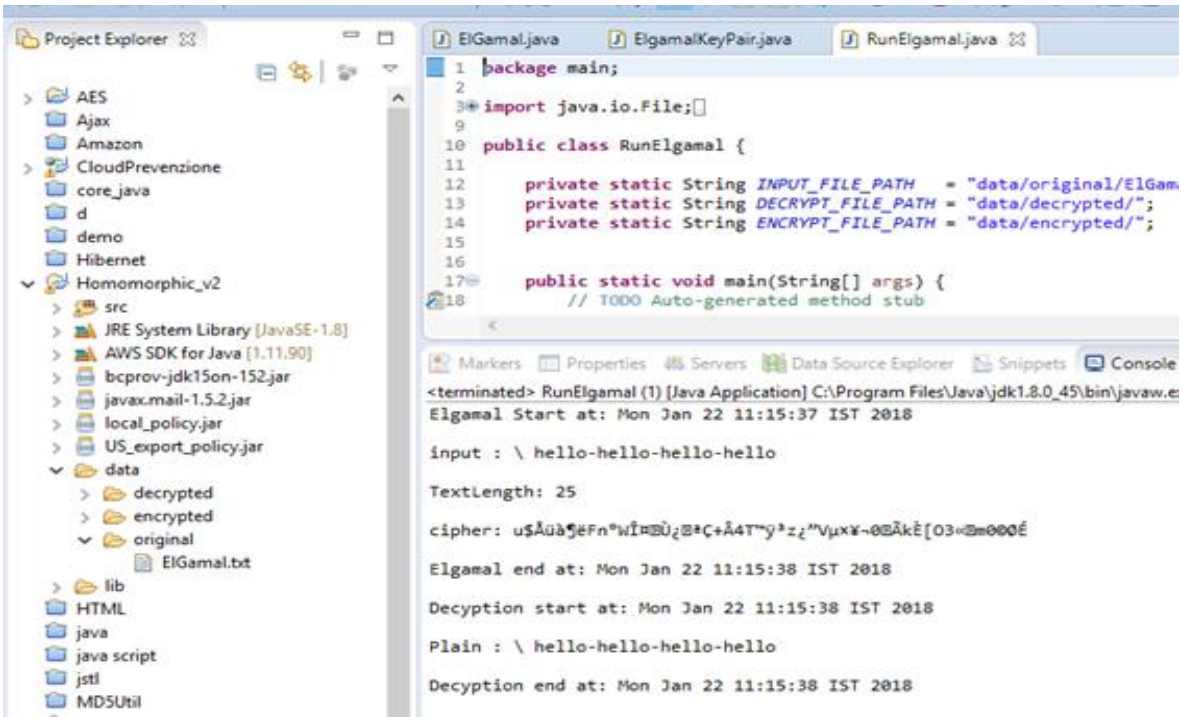

Fig 1 Elgamal Data Encryption/Decryption

Security is of prime concern while carrying out this online system. This system has implemented proper security measures such as creating secure space between client machine and server and proper access rights control is been implemented, So that the system will provide a secure environment to each system user on terminal to make work easy as well as return required information in easiest way.
In figure 2 we can see that it's generate before and after has value for the cipher text.So,when distributor send the sensitive data to agent, that time it's generate the hash value and other side agent modified or some change

in that sensitive data, that time it's change the has value. In Elgamal Encryption it's depend on the data hash value as we consider for securing the sensitive data in a region.

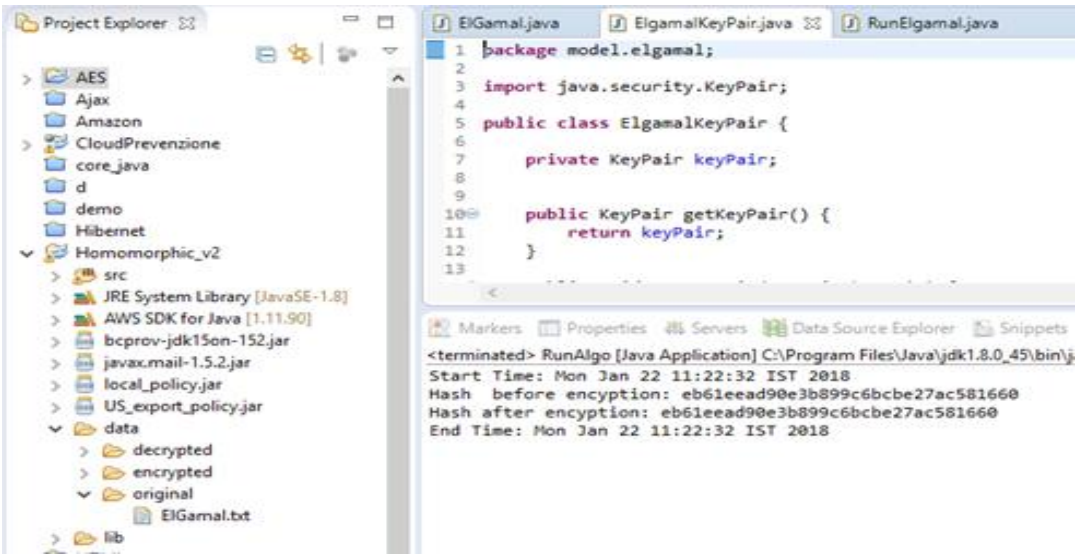

Fig 2 Elgamal Fake Object (Hash Value)

5. Prevenzione System

Prevenzione system is providing secure region where distributor and the other agent can share their sensitive data. This system is on the cloud platform with secure region. In this system the distributor will upload the data in cloud and then our algorithm applied on that data for security. And the other side agent can be show data and download that data too, but if the data is modified or change in that data and transfer to other region, so that will be notifying by the distributor. And for the security reason we have expand our' Elgamal' algorithm with the help of it generate the fake hash value and it will attach with the original data.

5.1. Distributor Module

Distributor will add the agent list according to his requirements and share the data to his agents. The data will be uploaded by the distributor and after that data can be shared and downloaded. The data will be sending in the encrypted form and stored in cloud platform.

At Distributor's side:

- The distributor (which will act as an admin in the system) will enter into the system by means of login.
- Then the distributor can upload the files which can be shared or downloaded.
- Distributor can view all the files uploaded.
- Distributor can share his data to his respective agents.
- Distributor get notify if the data is modified and send to other region.

5.2. Agent Module

Agent can view the data provided by the distributors and share the data .The encrypted data can be retained in its original form by means of key provided by the distributor. The data will be downloaded from cloud platform.

At Agent's side:

- Agent can enter the system by means of login or registration(if not registered)
- Agent can view the received files from the distributor.
- Agent can share the file.

5.3 Data Allocation

The main focus of our system is data allocation problem as how can the distributor intelligently give data to agent in order to improve the chances of detecting a guilty agent, Distributor can send the file to the authenticated Agent, Agent can edit the data etc. Agent views the secret key through mail. In order to increase the chances of detecting agents that leak data.

5.4 Fake Object

The distributor creates and adds fake objects (through 'ElGamal Encryption') to the data that he distributes to agents. Fake objects are objects generated by the distributor in order to increase the chances of detecting agents that leak data. The distributor may be able to add fake objects to the distributed data in order to improve his effectiveness in detecting guilty agents.

Conclusion

This application will provide a secure environment for data sharing by means of various encryption techniques. This will ensure Data Prevention and Data Leakage Prevention and also provide a relief to various sectors where data sharing take place.

Future work

Our future work includes the investigation of agent if the data is leaked from the trusted source. So we are planning to go for DLD (Data Leakage Detection) in further enhancements.

References

[1] Ruanaidh,JJKÓ.,W.J.Dowling,andF.M.Boland."Watermarking digital images forcopyright protection." IEE Proceedings-Vision, Imageand Signal Processing 143.4(1996):250-256.

[2] Hartung,Frank,andBernd Girod."Watermarkingof uncompressedandcompressedvideo."Signalprocessing 66.3(1998): pp. 283-301.

Using Optical Flow Handling Occlusion

Mukesh Parmar[a*], Birendra Zala[a], Svapnil Vakharia[a]

[a]*Gandhinagar Institute of Technology, Moti Bhoyan, Gandhinagar, Gujarat, India 382781*

Abstract

In video surveillance systems major performance decline is Occlusion. Occlusion should be detected very precisely by all automatic software system. Also automatic system continuously monitors the scene. When two objects are overlap, rear object will be hidden behind the front object. The hidden part of the rear object is called a occluded part the object. Human bodies are overlapped when they are walking in the scene. Illumination can be the reason for the occlusion because object identified by the intensity value of particle which belong to the object. Occlusion is not directly detected problem. Pixel of the occluded is detected which belong to the part of the same. Purpose of detection of Occlusion is mainly for the set occluded part in the image and gets the original image. Exquisite resampling and Optical flow are used for the improve the performance of the algorithm. Included phase in the algorithm is such like prediction, importance sampling and resampling. Optical flow is used for the finding important particle which can give both intensity and the direction of the particle.

Keywords: Occlusion, Particle Filter, Optical Flow

1. Introduction

Image processing is used for different operations for digital phase and doing operations on the image, for getting good result it will detect helpful data from it. We are providing the video, frames as input and the output will be concerned characteristics of image. The image processing system contains as two dimensional signals treated as image for live methods of signal dispensation will be apply to them. Nowadays, It is one of the best increasing technologies, with its applications in a variety of branches of a business. Frames are detected, recognized by using Visual surveillance system with image processing. This type of structure is largely used in applications such as safety for major construction forces areas which can be detected and monitored travel in cities creatures. Analysis of video has been done by the recording of the video.

The occlusion is one of the main problems of reduced performance in video surveillance systems. Every mechanized discovery systems must precisely control occlusion. Two object is moving in the environment they overlapping each other due to that reason rear object will not be detected. It is called Occlusion. It has three types self occlusion, inter-object occlusion, back ground occlusion. Due to occlusion different parts such like animal, tree, vehicles will be overlapped in a scene.

Monte Carlo Theorem is used as fundamental concept in Particle filter. Object recognition and Tracking find out the state using posterior probability [1],rectify by[2] used new type of particle filter using exquisite resampling to reach tracking.

2. Particle Filter

In this Section, We are giving algorithm detail. Figure[1] is show the flow chart of the system of particle filter Optical Flow. It has three basic step. 1.prediction 2. Weight calculation and sampling

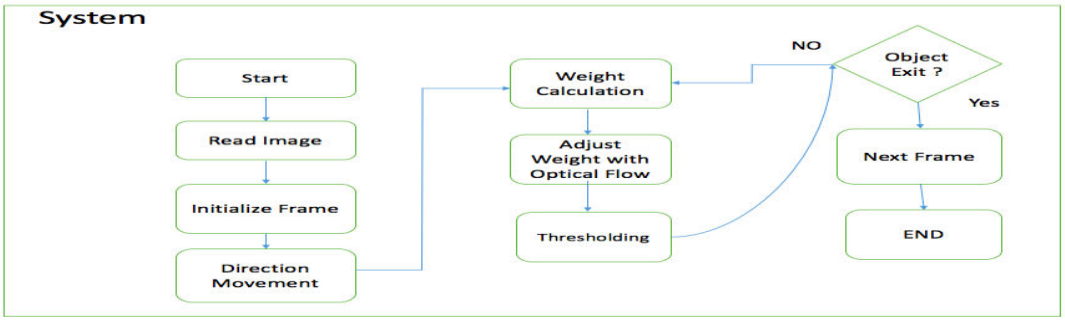

Figure [1] system

* Mukesh Parmar Tel.: +91-9904405915
E-mail address: mukesh.parmar@git.org.in

2.1 Particle Filter

Tracking objects in frame of picture has involvement of both systems non-linear and non Gaussian. Probabilistic framework used for find out the interference of tracking in frame[3].They are consecutive Monte Carlo strategies in light of point mass portrayals of likelihood densities, which are connected to any state display [4]. Molecule Filter is a speculation tracker, which approximates the sifted back conveyance by an arrangement of weighted particles. It weights particles in light of a probability score and after that engenders these particles as indicated by a movement.
Weight of every molecule ought to be changed relying upon perception for current casing. The essential Molecule Channel calculation comprises of 2 stages: Successive significance examining (Sister) and Choice advance. In Sister step it utilizes Successive Monte Carlo Re-enactment. For every molecule at time t, change priors are tested. For every molecule we at that point assess and standardize the significance weights. In determination steps (Resampling), we duplicate or dispose of particles concerning high or low significance weights to get a predefined number of particles. This choice advance is the thing that enables us to track moving articles proficiently. [4]

2.2 Prediction

The main phase of molecule channel is forecast organize. At the point when protest vanishes, rather than haphazardly spreading particles, we radially spread particles from where question vanished on account of the presumption that the question won't move faraway quickly. On the off chance that the question is incidentally blocked, the way we spread particles inquire about the objective more proficiently than looking all inclusive. While in long haul impediment, we have effectively spread particles all inclusive and this can abstain from missing the object.[6]Then, utilize the movement vector got from optical stream to modify the dissemination extend. An elevated expectation deviation of the movement vector demonstrates the question moves radically, consequently we have to grow the dispersion run as Figure 2(a). A low standard deviation demonstrates moving consistency, so the dissemination range could be contracted, as Figure. 2(b).[7]

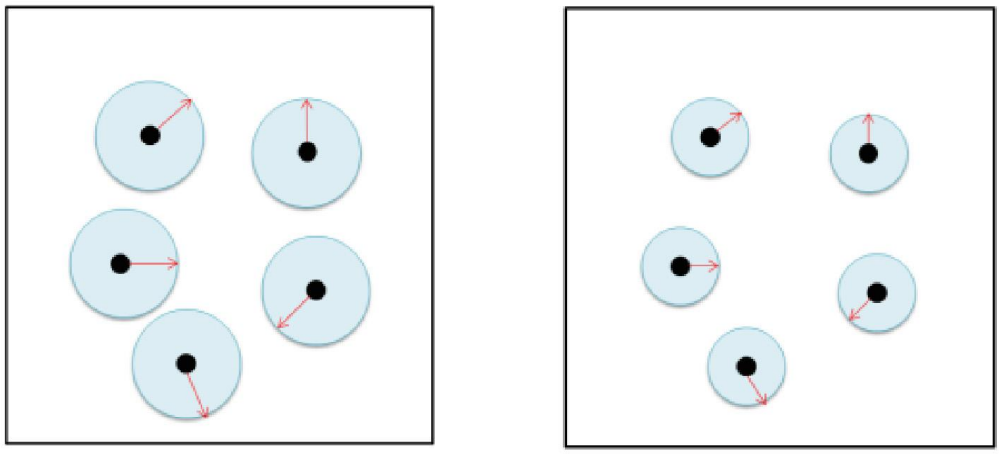

(a) (b)
Figure 2 (a) high deviation for diffusion (b) low deviation for range

We can also predict the moving direction by motion vector. It is reasonable that the object moves toward the same direction according to the last few seconds, as a result, we spread the particles toward the same direction if moving direction has consistency.[6]

2.3 Optical Flow

Movement estimation is requesting field among analysts to process autonomous estimation of movement at every pixel in the greater part of general. Movement estimation for the most part known as optical or optic stream. Movement is imperative part in picture groupings. Movement estimation is the way toward deciding movement vectors that depict the change starting with one 2-D picture then onto the next. Optical stream or optic stream is the example of obvious movement of items, edges and surface in a visual scene caused by the relative movement between an onlooker (an eye or a camera) and the scene. Molecule Channel - this molecule framework execution, the weighting framework will have two modes that can be initiated during a period that is helpful for the following framework. The principal mode will take the last yield of the Lucas Kanade tracker and

utilize those as contributions to the molecule framework estimations . The molecule framework is as yet experiencing the majority of the already portrayed advances which comprise of: 1. The next edge predicts the consistent speed movement 2. show Weight every molecule in light of its separation from the Lucas Kanade focusing on yield Utilizing the present edge. 3.The Gaussian arbitrary circulation for speed base. 4. Resample the particles in view of the weight. 5. Repeat stage first until finish .[11]

2.4 Sampling

Objective of this phase is find weight for each particle and also save important and discarded less important particle from. Color histogram of the target model is used as feature to determine the weights.It is called importance sampling.RGB histogram space used 8,8,8 bins also derived weights of the target model. Always centre pixel of the object is important compare to boundary pixel.[6]
The wake of getting the first weights by computing their Bhattacharyya coefficients, we find a way to refine them. Optical stream [8] is the evident movement of shine designs in the picture. In a perfect world, it would be the same as the movement field. Computing the normal of movement vector [9] got from optical stream, we can anticipate another inside from the last focus. Advancing the weights of particles around the middle which optical predicts is the initial step.
The second step is to set an edge. Low-weight particles diminish exactness, to maintain a strategic distance from it, we plan to dispense with those less imperative. An appropriate measure of decadence of the calculation is the viable example estimate Neff presented in [1]. Utilizing to acquire the powerful examples, pick the most minimal weight in those examples to set the limit. The weight which is lower than the limit is set to be zero .
At the point when every one of the weights are little and set to zeros, implies every one of the particles in the entire edge are not like the objective, at the end of the day, there exists no object.[1]
Elimination of the small weight particle and give the importance to the higher value weight particle .This objective of this phase. Prediction is also depend on the high value pixel. Disadvantage of Resampling algorithm has represented in the fig.N = number of particles [6]
Ci represents the cumulative sum of weights. Ui is a sequence of random variable which is uniformly distributed in the interval [0,1].We view Ui as a threshold, the CDF crossing over it is considered the more important one. As shown in , Because C2, C4 and C5 cross the threshold U2, U4 and U5.U2,U4,U5 are saved for the use of next prediction. From the figure we can found that particle 2 weight lesser than particle 1. Particle 4 weight is lesser than particle 3.Estimation accuracy will be decreased due to this fault .From using the resampling ,problem will be solved. [10]

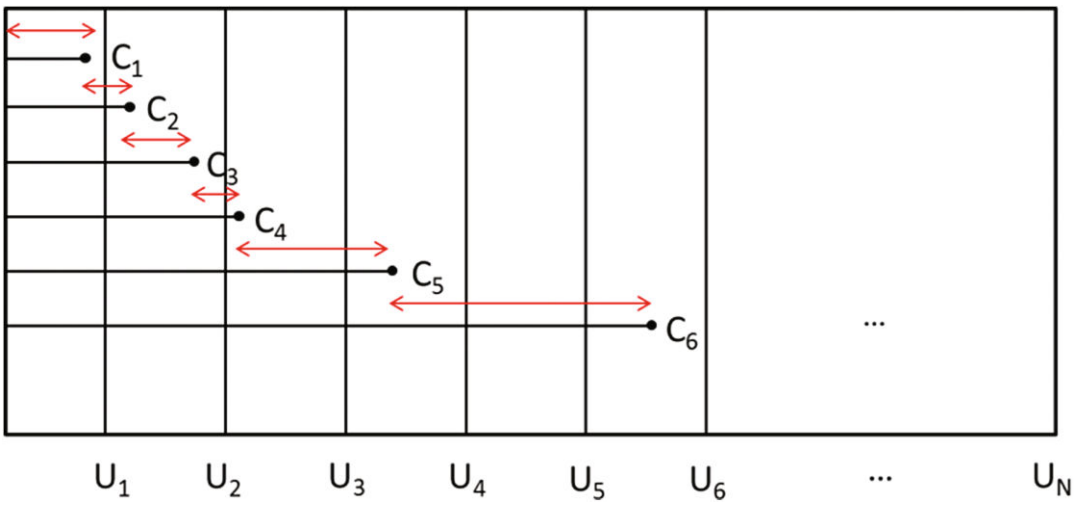

Figure.3 Algorithm of resampling

Find out the particle which has high weight in that interval. C1,C3 eligible candidate to be saved .From this pdf can be very accurate .

We generate the dynamic state space equation which given below:[6]

where vk and wk are nonzero mean Gaussian random variables,

x0 = 1, $\alpha = 0.5$, $\beta = 25$,$\gamma = 8$, sample numbers = 100, Time step = 50 s.

$$x x_{k+1} = \alpha x_k + \beta \frac{x_k}{1+x_k^2} + \gamma \cos(1.2\, k) + v_k \quad [6]$$

$$y_k = \frac{x_k^2}{20} + w_k \quad k= 1,2 .....$$

Comparison of Particle filter and Optical Flow

		Mean error	Accuracy
Experiment 1	Particle Filter	30.89	96.07 %
	Using Optical Flow	19.97	97.38 %
Experiment 2	Particle Filter	47.54	42.60 %
	Using Optical Flow	24.52	96.69 %
Experiment 3	Particle Filter	56	67.5 %
	Using Optical Flow	38.4	99 %

Conclusion

Particle filter is mainly based on estimation of posterior probability. It is also useful for pattern recognition and object tracking. Using adaptive particle for object tracking scheme along with exquisite resampling, we can improve prediction and resampling.
Refinement of particle weights are done by Optical Flow, using the dynamic state model for motion information. From that we can easily find out the future flow of the object. Proposed algorithm is improved and enhanced the image ,from the comparison table we can easily derive .

Acknowledgment

I am exceptionally appreciative and might want to express gratitude toward Prof. Darshana Mistry, for her recommendation and proceeded with help without them it would not have been feasible for me to finish this paper. I might want to thank every one of my companions, associate and colleagues for all the keen and mind fortifying talks.

References

[1] Arulampalam, M.S.” A tutorial on particle filters for online nonlinear/non-gaussian Bayesian tracking.” IEEE Trans. Signal Process. 50(2),pp. 174–188 (2002)
[2] Vermaak, J., Godsill, S.J., Perez, P.”Monte carlo filtering for multi target tracking and data association.” IEEE Trans. Aerosp. Electron. Syst 41(1), pp. 309–332 (2005)
[3] P. Li, T. Zhang, and A. E. C. Pece, “Visual contour tracking based on particle filters”, Image Vision Comput.,2003, 21(1):pp. 111 – 123.
[4] Md. Zahidul Islam, Chi-Min Oh and Chil-Woo Lee “Video Based Moving Object Tracking by Particle Filter” International Journal of Signal Processing, Image Processing and Pattern Vol. 2, No.1, March, 2009
[5] Lyudmila MIHAYLOVA, Paul BRASNETT, Nishan CANAGARAJAH and David BULL “Object Tracking by Particle Filtering Techniques in Video Sequences1” Department of Electrical and Electronic Engineering, University of Bristol, UK
[6] Lan-Rong Dung(&), Yu-Chi Huang, Ren-Yu Huang, and Yin-Yi Wu “An Adaptive Particle Filtering for Solving occlusion Problems of Video Tracking” Springer International Publishing Switzerland 2015 C. Stephanidis (Ed.): HCII 2015 Posters, Part I, CCIS 528, pp. 677–682, 2015.
[7] Shaohua Zhou, Rama Chellappa, Baback Moghaddam “Visual Tracking and Recognition Using Appearance-Adaptive Models in Particle Filters” IEEE Transactions on Image Processing, 13:11, pp. 1491-1506, 2004
[8] Horn, K., Schunck, B.G.: Determining optical flow. Artif. Intell. 17(1), pp. 185–203 (1981)
[9] Lucas, B.D., Kanade, T.: An iterative image registration technique with an application to stereo vision. In: The 7th International Joint Conference on Artificial Intelligence, vol. 81, pp. 674–679 (1981)
[10] Fu, X., Jia, Y.: An improvement on resampling algorithm of particle filters. IEEE Trans.Signal Process. 58(10), pp. 5414–5420 (2010)
[11] Dhara Patel,Saurabh Upadhyay,Optical Flow Measurement using Lucas kanade Method ”International Journal of Computer Applications (0975 – 8887) Volume 61– No.10, January2013

Use of Blockchain Technology for Image Recognition and Malware Detection

Varun Prakash Bhat[a*], Archana Singh[a]

[a]*Gandhinagar Institute of Technology, Moti Bhoyan, Gandhinagar, Gujarat, India 382781*

Abstract

This paper proposes an improvement in existing innovations for malware detection through image processing on Android Systems. The major problem is the implementation of a machine learning system on Android devices which can be taxing and complicated. Therefore firstly, we propose that the disassembly of the malware binaries into opcode sequences be taken place on a central server. Then, the server divides these opcode sequences between a set amount of Android devices for image recognition and malware detection. These devices act as end nodes for the blockchain network and perform the task of generating the variant images for their respective assigned sequences. The variant sequences are then uploaded onto the central server back again for classification, storage and distribution of malware information.

Keywords: blockchain; malware detection; opcode sequences; artificial intelligence; machine learning; image recognition

1. Introduction

Malwares are a real security threat. According to the McAfee Lab Threat Report[1], staggering counts of 57.6 million new samples were found in the 3rd quarter of 2017 alone. Due to such a rapid growth in malwares and their variants, the traditional method of 'see and report' where the user reports a suspicious file to their installed antivirus/antimalware company is cumbersome and tedious. The company itself requires a significant amount of time to analyse and react to such a threat. The reaction method too is slow. Conventionally, companies introduce patches and force-update their antivirus software when an internet connection is available. The duration between the introduction of the patch and its installation is enough for any malware to wreck havoc on the target system. In recent years, more and more research is made on binary malware variants. This is because these variants form a majority of the malware families. Methods such as K – Nearest Neighbour (KNN), Support Vector Machine (SVM), decision tree (DT), random forest (RF), Naïve Bayesian (NB), and clustering provide a machine learning solution for analysis of malware files.[2]

2. Literature Review

We provide a wholesome solution to the analysed problems which would greatly enhance the processing as well as implementation of such a malware detection system in Android devices. The proposed solution, "blockchain technology" will ensure that the above-mentioned problems be reduced, if not completely removed.

2.1 Blockchain Technology

Blockchain technology is an upcoming field which is primarily used for cryptocurrency mining. This technology is used to generate virtual currency by creating a huge network of systems which then solve cryptographic puzzles which later on earn them virtual currency in the form of BitCoins, Etherium, or any other preferred currency. Blockchains are very secure and have a very high Byzantine Fault tolerance. They are decentralized systems and can be used for a variety of functions ranging from transaction processing to documenting provenance in publically maintained ledgers.

The implementation of "blockchain" in malware image variant detection will provide the following advantages:-
1. Storage: Android devices have very limited storage. However, due to blockchain each Android device needs to store only a small portion of the malware opcode sequence which can be deleted once the image variant is deleted.
2. Processing power: Android devices also lack in processing power which makes it difficult to carry out heavy-duty tasks on CPUs. As a result of blockchain, the devices only need to perform variant analysis on a very small code hash. The hash would also contain the cryptographic hash of the previous block which can then be easily reassembled on the central server due to availability of transaction data.

* Varun Bhat Tel.: +91-9099348160
E-mail address: braindom.varun@gmail.com

3. Concurrent information: The problem with remote systems is that there is a chance of duplicate analysis taking place. However, due to an interconnected chain of systems the malware variants that already have been identified and classified need not be analysed again. This would save both time and resources and would also increase the total amount of files analysed.
4. Tamperproof: Since most of the software code is stored on a separate central server which is abstracted due to the sheer volume of connected android devices. This ensures that the code is essentially secure and virtually tamperproof which will increase the code security.

2.2 Malware image variant

Instead of regular decoding of malicious files, researchers found out a way to map the malware patterns. These patterns were then fed into a SVM (Support Vector Machine) for creating of learning models and systems. The malware binaries are divided into small opcode binaries. These opcode binaries are then converted into their grayscale, image variants. Then by using method such as KNN (K-Nearest Neighbhour) patterns are found that match previous known, malware patterns. In case the malware is unknown, it is fed into the SVM for training. The opcode is split into 2 parts where one is for experimentation while the other is for training. As compared to decoding methods, image variant methods have reported an experimental accuracy increase of upto 15% in detection of malwares.[2]

2.3 SVM (Support Vector Machine)

SVMs are training models that are used to analyse data for classification and regression purposes. Training data is called supervised learning. The algorithm outputs an optimal plane division of the data provided to categorize new data. The categorization takes place in the form of classes. However, there can be no perfect class for all the input data. Due to this a regularization parameter is decided, whereupon the data is expected to deviate as little as possible from the hyperplane and thereby cause the least deviation. This also means that certain outlier values need to be determined that need to be "let go" in order to achieve perfect parameterization. The tuning parameters are Kernel, Gamma, Regularization, and Margin. These parameters are used to compute the regression line's characteristics with respect to the classification of data. The idea of an ideal classification is nigh on impossible to obtain due to overlap of data. However, it is possible to obtain the best possible fit. This is what makes this learning model best suited for machine learning.

2.4 Previous Work

Research papers titled, "Malware Variants Detection Based on Opcode Image Recognition in Small Training Set"[2], "Detecting Android Malware by Applying Classification Techniques on Images Patterns"[3], "Malware Classification using Gray-scale Images and Ensemble Learning"[4] perform the methodology of malware detection and classification by dividing the malware binaries into opcode sequences. These opcode sequences are then converted to grayscale, image variants and enhanced to identify common malware patterns. Then, by using SVM these patterns are classified and the device identifies their strains as malicious software**.** The paper titled "Consortium Blockchain-based Malware Detection in Mobile Devices"[4] suggests using Blockchain technology to create a shared network for detection and classification of "known malware" using decoding methods on the malicious files.

2.5 Problems in Previous Works

The method of malware image variant detection has several problems as far as its implementation to Android systems is concerned, namely:

1. The system itself is designed around the fact that all the files are malicious in nature. However, in real life applications, such a luxury is not offered. Malware systems need to scan healthy files and determine them as a non-risk as well as scan infected files and quarantine them.
2. The system aims at providing machine learning via SVM to software programs. However, Android systems have limited processing power as well as storage capacity. Implementing complicated systems such as machine learning and maintaining a storage database for established malware variants will be very tough.
3. Android OS is an open-source operating system which means that any software code introduced is susceptible to tampering or modification due to enterprising users which could severely compromise system security.

4. The analysis made in image variant detection is made under static conditions where the total number of malicious files remained fixed throughout the testing environment. In real-life this number is subject to change which means that complete analysis of a system would prove to be very difficult.
5. Analyzing and classifying malware variants as well as teaching them to the system using machine learning is a time-consuming process especially when the system performance is limited to a few gigahertz.

The method of consortium blockchain is sound in its architecture, but has some issues in its implementation to Android systems as well as in its malware detection methodology:

1. The system claims to easily classify "known malwares" in a very less time. The problem with this ideology is that every second, a huge amount of malware types are created and distributed across the internet. This requires a rapid response method which it cannot provide.
2. The system also relies on Consortium Blockchain (CB) heavily. There is no central server to maintain a backup of the data classified and as a result is susceptible to data duplication or data loss.
3. The system aims to maintain a fact table in the storage layer which is shared between the nodes. However, each of these malwares are classified under a block which cannot be changed once the malwares are verified and confirmed. This poses a host of issues since some malwares are merely variants of an original, parent malware and therefore can be classified under the same block.
4. The system aims to decode every single malicious file provided to it. This is tedious and cumbersome even though the data is divided into parts. Some malware are mere variants and can immediately be classified as a threat if the information about the parent malware is available.
5. The increasing amount of new malwares would make it very difficult to maintain a fact-table between devices and effectively maintain a communication between the said devices.

3. Our solution

3.1 Architecture

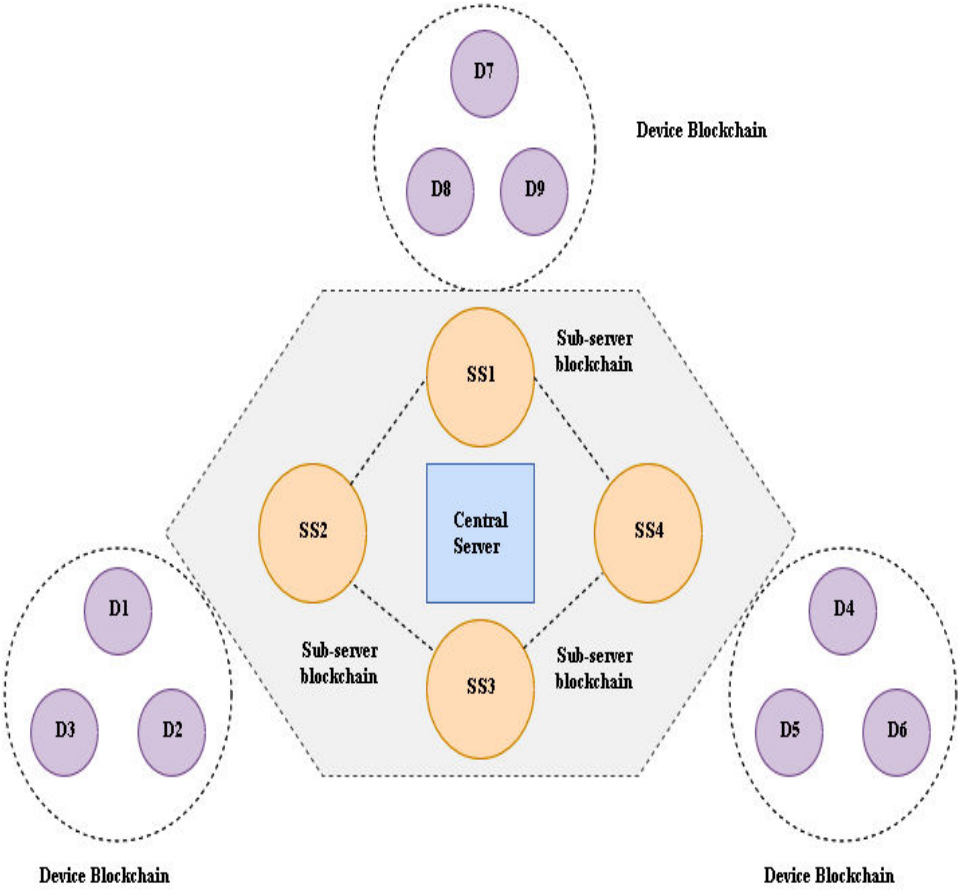

Fig. 1. Illustration of the architecture of the blockchain technology implementing the malware image variant detection method

3.2 Device blockchain (DB)

This sub-system is a collection of Android devices interconnected with the help of a P2P (peer-to-peer) network. The Android devices are the ones responsible for the conversion of the malware opcode to its image variant.

3.2.1 Working

The entire system of DB devices will have a specific sub-server (native) assigned to them. This will be their native server and all the personnel information associated with the devices will be stored on the SSB. Each of the devices will receive a cryptographic hash of the malware opcode sequence, having a specific header assigned for further assembly. The devices will convert the malware opcode into its corresponding image variant using the tools inbuilt in the software and send the data to its native server. In case the native server is unavailable, the devices will send the data to its nearest available server called the host server. If the device encounters any suspicious file during its working duration, it will forward the file directly to the native server which will then process the file.

3.2.2 Advantages

1. The Android devices only need to process a small part of the malware opcode which greatly reduces processing power consumed.
2. The devices also need to utilize very less amount of storage space which would be equivalent to the current storage used by antivirus software.

3.3 Sub-Server Blockchain (SSB)

The sub-server blockchain acts as the intermediary between the Central Server (CS) and the Device Blockchain (DB). It is here that the assembly of the image variants into a single image takes place which is then relayed to the central server. The SSB is in constant contact with the CS in order to facilitate a quick relay of information in case a malware pattern matches any other previous pattern then the analysis is stopped halfway and an associated risk factor is directly assigned to combat the threat rapidly.

3.3.1 Working

The SSB acts as a relay between both the DB and the CS. It also performs the task of converting the malware binary into opcode sequences. Then, it divides these opcode sequences into pieces and assigns identifying header information. The numbers of pieces are equivalent to the total amount of devices native to it. These pieces are then relayed onto the native device blockchain for further processing. Once the native device blockchain converts the malware opcode into its image variant, the SSB patches them together into a single file for pattern analysis. It is essential to note that the SSB is in constant contact with the CS. Very frequently, there will be times when a malware is found to be a variant of an already identified malware class. At this point any and all processing on the malware would be halted and a base risk factor (1 to 10) will be assigned to the suspicious file. This is done on a priority basis and the update is shared with all the SSB which is then relayed onto Android devices so that they can take action instantaneously. Once the quarantine of all such files is done, the malware strain would then be processed completely for further classification.When a malware file is classified completely, the information is relayed to the CS to be updated in the database.

3.3.2 Storage

Since the SSB is required to halt processing a malware if it's found to be a variant, it needs to require two storages within itself –

1. Current buffer: This will contain information about the current malicious file being processed. This will also contain the "halted" malware information so that it may be resumed once the malware is in quarantine.
2. Halt buffer: This will contain information about the malware that have been placed in "halt" state. Here, once the quarantine is complete the sample file will then be classified completely and updated into the database.

3.3.3 Advantages

1. The SSB acts as a central point that always stays online due to a "buddy" system of host sub-servers which the devices can connect to. This ensures that data is constantly being transferred and stored regardless of the native server's condition.
2. Once the native server comes back online, it can compare and verify file integrity and version. Then, it can update it files and continue its processing tasks. In this way, the entire file system remains concurrent.

3.4 Central Server (CS)

The central server acts as the relay point for the fact-table in the entire malware detection system. It is here that the image variant is compared with existing malware patterns until a match is found. The match is then assigned a threat classification which is then relayed to the device blockchain software system as an update.

3.4.1 Working

The CS is the focal point of the entire system. It is responsible for the fact table of malwares and their corresponding variants. This means that the database needs to be completely relational in nature. As such, it needs to be supremely robust and speedy enough to deal with multiple requests at a time. The CS will be responsible for accepting the classifications from the SSB to be stored into the database. It will also respond to the SSB's request to match a similar malware pattern in case of a "halt" request. The CS will then find the requested malware's original strain and provide information such as risk factor, pattern, malware family, etcetera to the SSB. Once the SSB completes assessing the risk factor of the halt buffer malware, it will relay this information to the CS. The CS in turn will send this information to the Android devices in the form of updates. Once the SSB completes the analysis of the halt buffer, the information of the malware is sent to the CS which will be updated. Unlike the consortium-blockchain method, the blocks of information are not locked. Each information piece can be updated, deleted or modified as necessary by the CS. The CS also is tasked with assigning the malware binaries to the corresponding SSB's. This makes it very vital to the entire system.

3.4.2 Storage

In order to store the information related to each malware program and its variants, it is essential that the database be relational in nature. In this way, it becomes very easy to traverse to the information and retrieve it as necessary.

3.4.3 Advantages

1. The CS always has an updated database which is very helpful in case of a massive SSB failure. Since the CS database is relational in nature, it can handle multiple SSB requests.
2. The CS doesn't need to take part in operational tasks and therefore won't be prone to any runtime crashes which makes it a secure working environment.

Conclusion

We propose a model using blockchain technology that enhances the functionality of the consortium-blockchain technology by combining malware image variant detection with it. In this way, the active threat monitoring of systems can take place with machines learning to detect new malware variants quickly and combat them effectively. This paper aims to provide a solution which bridges the gap between both the realms of the research with a new architecture.

Acknowledgment

We have taken efforts in the preparation of this paper. We are highly indebted to Prof. Archana Singh for their guidance and constant supervision as well as for providing necessary information regarding the project. We take this opportunity to thank all our friends and colleagues who started us out on the topic and provided extremely useful review feedback and for their all-time support and help in each and every aspect of the course of our project preparation.

References

[1] McAfee Lab Threat Report Q3, https://www.mcafee.com/us/resources/reports/rp-quarterly-threats-mar-2018.pdf
[2] Tingting Wang, Ning Xu, Malware Variants Detection based on Opcode Image Recognition in Small Training Set – 2017 the 2nd IEEE International Conference on Cloud Computing and Big Data Analysis
[3] Manzhi Yang, Qiaoyan Wen, Detecting Android Malware by Applying Classification Techniques on Images Patterns – 2017 the 2nd IEEE International Conference on Cloud Computing and Big Data Analysis
[4] Liu Liu, Baosheng Wang, Malware Classification Using Gray-scale Images and Ensemble Learning – The 2016 3rd International Conference on Systems and Informatics (ICSAI 2016)
[5] Jingjing Gu, Binglin Sun, XiaoJian Du, (Senior Member, IEEE). Jung Wang, Yi Zhuang, Ziwang Wang, Consortium Blockchain-based Malware Detection in Mobile Devices, IEEE Access 2018, Grant filed in China under Grant 61572253

Social IoT: Network of Smart Things with Social Connections

Zalak Butani[a*], Kajal Vadhiya[a], Brinda Pandit[a], Sejal Bhavsar[a]

[a]*Gandhinagar Institute of Technology, Moti Bhoyan, Gandhinagar, Gujarat, India 382781*

Abstract

In the Internet of Things (IoT) we can analyse the connection between different kinds of object. When they are connected with social networks objects became the smart objects. These all smart objects create an intelligent environment. It have a sense to analyse the surrounding activities. These smart objects operate as independent to provide and request information and services based on the user's requirement. We have to establish trustworthy relationship among the objects and objects to human for greatly increases the effective node interaction in the SIoT and helps to improve uncertainty and risks.

Keywords: social network, smart object, internet of things, social internet of things

1. Introduction

Internet of thing is a network of smart things which are capable of sensing the physical world and communicate with each other without human intervention.
Today we are connected with many digital things which makes our life more comfortable. In our day to day life there are many number of devices are growing rapidly. That devices are a sensor or any physical device which is capable to sense the environmental change. Then it collect data from that device and communicate with other device via wireless protocol. That's why it is known as smart device. There are so many examples of these devices like smart TVs, smart watches, medical devices, smartphones, sensors, security system, etc. [1].
IoT term is first used by Kevin Ashton in 1999.A Coca-Cola machine is a first IoT device. And afterword IoT term rarely popular after 2012-2013. Now a days, the convergence of the Social Network and the IoT is gaining importance. In this perspective, a new paradigm known as Social IoT (SIoT) has been announced where the social networks and IoT converge together to establish social collaboration in an independent way according to the rules set by the owner [2].
There is a requirement and proper understanding to define inter-connection between human and smart devices that devices work as per the instructions given by users. Internet is a medium which provide a platform to connect human to object and human to human [1].

The adoption of SIoT paradigm present several advantages:

- Increase the level of trustworthiness by established more interaction among several things.
- New discover services work very effectively and objects are scalable in social network of human.

2. Literature Review of SIoT

We collected some definitions from different sources to highlight the literature review of SIoT available in below table.

Sr. No	Description	Remark
[4]	The perception of 'describing human behaviour' using Big Data in SIoT by recommending structure design that processes and analyses real time big data.	It grab the challenge of understanding by providing response to the users that offer them the chance to increase their behaviour using the alert message taxonomy.
[5]	Secure authentication systems of social networking web sites like Facebook which monitors physical home environment of end user, taking into account which user can control the home environment and give home security remotely	Provides trustworthiness and security to control home system

* Zalak Butani Tel.: +91-9558399656
E-mail address: zalakbutani87@gmail.com

Sr. No	Description	Remark
[6]	Creating truthful associations among the objects greatly increases the efficiency of node interaction in the social IoT and helps nodes overcome perceptions of uncertainty and risk.	Discriminate the normal behaviour in a unfriendly environment from the Malicious behaviour.
[7]	The environment provided by wearable devices and smart cities that determine human behaviours as well as human dynamics using big data.	It increase the chance of their behaviour using alert message taxonomy.
[8]	A new algorithm to address the resource management issue so that Mobile crowd sensing maximize the lifetime of the task group.	Focus is on encompassing the resource allocation algorithm to other types of heterogeneous resources.
[9]	A level of trustfulness is permitted to navigate the communication among the billions of object.	It provides crowd management using level of trustfulness.
[10]	The possibility to implement a distributed approach for a low-complexity cooperation and the scalability feature in heterogeneous networks.	Wireless services will be provided by heterogeneous networks, and thus the problem of spectrum scarcity will be severer.

3. Why SIoT?

SIoT has smart objects which interact with object to object, object to human and human to human via internet. Current research is based on to find the objects which have fundamental role in human society. Therefore, try to build nature or functions of object which has potential to interact with human. In future many application and services should be connected with groups of objects and start to build a social relationship on the fundamental features of objects.
As we delve deeper in to SIoT, it generate large amount of data generated by the smart things enclosed by us. That will be see in veracity, volume and velocity of the data generated by smart things.
According to the Cisco [3], 2.5 quintillion bytes of data using social device is being generated by users per day. Datasets are generated by majority of the applications. These datasets are not fit for data processing technologies or relational databases, i.e., DB2, MySQL, and Oracle, due to which it is included in Big Data. The prospective of Big Data and smart environment improves the quantitative and qualitative understanding of smart objects and human behaviour.

There are so many advantages of SIoT like

- Main idea behind SIoT is that human doesn't want to involve to establish relationship between the objects. If objects are friendly towards each other, this will define the level of trustworthiness.
- It also include the security level which is measured by human.If large number of objects are connected to network then they become relevant to solve the problems.

Now a day's technology is an essential part of our life. For any purpose we are travelled or tour from one country to another country. We can't live without the social relation with technology.

- If we migrate from one place to another then some communication channel may block in other countries. Some time we have to adapt that countries technology without our choice because we have to communicate with other or complete our tasks. So the magical solution of this problem is SIoT. It gives to control everything as per your choice with efficient ways with solutions even when the place or locations are not static.
- As per our general life we complete our many needs by using mobile phones. We can store many thing in smartphones. SIoT allows you to connect your device with your smart cities, your transportation vehicles, smart home and many more. By using SIoT we easily communicate with different devices which are connected with us.
- In home there are many appliances present like oven, blender, refrigerator, electric kettle, mixture, smoke detector etc. Refrigerator will store many groceries. When we go for shopping then we have to check each and every item with quantity so we able to analyze that what things we have to purchase. If apply the concept of SIoT in this then refrigerator will tell us about that what groceries we need and which are the present groceries with its quantity. Even it will order groceries from your favorite store or nearby store.
- SIoT is also use for the general security purpose. In school, at the time of recess children's are coming towards ground or if any student go to the outside the school, then as per the student location teacher will instantly get message for that.
- If anyone is alone at home and some accident was done then automatically their neighbors get the message of that via email, text or any social media. This thing is also possible from SIoT.
- It is useful for any factories. There are many machines which are working continuously. We have to regularly provide servicing to that machines. By using SIoT when machines are in condition that service is required then they automatic send message to the service center for the services. So maintenance issue is solve. This concept is apply in many devices which are used in home, hospitals, transportations, agricultures, shopping centers and many more.

- In shopping malls or hospitals there are lifts or escalator is used. If any problems are occurred in that then in minimum time we have to find the solution for that. Apply SIoT in this then, that lifts or escalator are automatically send the message to the nearest or available engineering team to solve the problem.
- There is no country which have no any risks. Natural disasters, terror attacks, virus outbreaks etc. are come any time. Some time we have no time to deliver message to each and every person. Here we can use SIoT. It will identify the risk and send message to everyone using social media, TV channels, radio, emails etc. It is very much helpful to save the life of many peoples.

4. Application in the era of social object and its relationship

In the deployment of any application social object is a central role for it. Let us consider an example for this.
Amazon's most advance shopping technology is Amazon Go. It is a new kind of store which has no lines, no checkout and no cashier. You have to use Amazon Go app to access the store. When you open an entry gate then first scan a QR code in the Amazon Go app using smarts phones. It is just walk out technology which automatic detect products which are taken or return from the shelves. In virtual cart all selected products are track. It has special cameras, sensors and computer vision system that all work together and monitor your actions in the store as well as movement of items on shelves. .Once you leave the store your Amazon account is billed for the items you grabbed. Total amount and bill receipt of purchased products are automatically send into your amazon account.
To make this type of application, each object should be connected with any social relationship so as to discover other relevant objects from surrounding and established social relationship among them.
There are five types of relationships that govern the social internet of things

1. Parental Object Relationship (POR): This type of relationship is established between the same types of objects which have same generation with same manufacturer.
2. Co-location Object Relationship (C-LOR): This is established between same type of object or different type of objects which are included in same environment. Good example for this is smart home devices. It has different kind of sensors with different links but they all are work for one common system.
3. Co-work Object Relationship (C-WOR): This is established between two or more devices whose functionalities are combined to accomplish a common goal. This type of relationship occurs between objects that either need to touch each other to achieve that goal, or need to be in close proximity of one another
4. Ownership Object Relationship (OOR): It is between smart devices with same user. Good example for this is smartphones, video game etc.
5. Social Object Relationship (SOR): This relationship defines when the device is coming in touch with owner. For the business purpose companies are established this type of relationship.

5. IoT to Social IoT

Social infrastructure is converging with the Internet of Things creating a new phenomenon known as **Social IoT**, where IoT meets social infrastructure.
A simple example for this is household garbage picker. As per our daily routine garbage collector have a specific route with specific time to collect garbage. But when amount of garbage is differ with its quantity then usual then it will disturb the specific schedule. So making this thing easy we can attach sensor to that container so real time data will excess by the central office. By using that data they efficiently collect more amount of garbage. Currently this is working in Santander (Spain).
We can also apply SIoT concept with our smart home by transferring some power of one device to other which needs it. It is not necessary that they belongs to same type of object. We can establish relationship between the heterogeneous object so we can efficiently work with system.

6. Challenges in SIoT

IoT faces the biggest challenge due to large number of website present over the internet. It is also challenging task to handle all the things at same time. Technologies would be design to overcome these challenges so that it is easier to derive benefits of IoT in social media. If such technologies are implemented properly then businesses would be able to provide recommended services with ease along with providing better customer analytics.

Conclusion

This paper has introduced the fundamental role of SIoT, based on the integration of environment of IoT with Social Networking. Application situations are those where objects share preeminent practices. For instances, ACs in the same local area network can establish social relationships that can be used to find solutions to common setting problems, such as those related to the power or battery problems.So, we defined a new concept of the social IoT as a ubiquitous interaction paradigm for the information sharing in the Web of devices.

References

[1] Jara, Antonio J., Yann Bocchi, and Dominique Genoud. "Social Internet of Things: The Potential of the Internet of Things for Defining Human Behaviours."
[2] Atzori, Luigi, Antonio Iera, Giacomo Morabito, and Michele Nitti. "The social internet of things (SIoT) when social networks meet the Internet of things: Concept, architecture and network characterization." Computer Networks 56, no. 16 (2012)pp. 3594-3608.
[3] R. Pepper and J. Garrity, The Internet of Everything: How the Network Unleashes the Benefits of Big Data, Global Information Technology Report 2014, Cisco Systems, 2014; http://blogs.cisco.com/wp-content/ uploads/GITR-2014-Cisco-Chapter .pdf.
[4] Ahmad, Awais, etal."Defining human behaviors using big data analytics in social internet of things."Advanced Information Networking and Applications (AINA), 2016 IEEE 30th International Conference on. IEEE, 2016.
[5] Bhagayshree Jadhav and Dr. S. C Patil. " Wireless home monitoring using Social internet of things." International Conference on Autom atic control and dynamic optimization techniques IEEE, 2016:pp. 925-928.
[6] Shen, Chih-Ya, etal. "Task-Optimized Group Search for Social Internet of Things." EDBT. 2017.
[7] Paul, Anand, etal. "Smart buddy: defining human behaviors using big data analytics in social internet of things." IEEEWireless Commun ications 23.5 (2016): pp. 68-74.
[8] Rober to Girau, Luigi atzori, Salvatore Martis, Virginia Pillioni. "A SIoT Aware Approach to the resource manage mentissue in mobile c rowd sensing. IEEE, 2017.
[9] Atzori , Luigi, AntonioIera, and Giacomo Morabito. "Siot: Giving a social structure to the internet of things. "IEEE communications letters15.11(2011): pp. 1193-1195.
[10] Nitti, Michele, etal. " Exploiting social internet of things features in cognitive radio. "IEEE Access4 (2016): pp. 9204-9212.
[11] Campagna, Giovanni, etal. "Thing Talk: A Distributed Language for a Social Internet of Things. "Work in progress (2015).

Acknowledment

The authors would like to thank Dr.Kirit J Modi, Associate Professor,Ganpat University for his insightfull comments and discussion on improving overall quality of the paper.

AMBA Based RTL Design of AHB2APB Bridge

Akash Verma[a*], Hardik Bhatt[a]

[a]*Gandhinagar Institute of Technology, Moti Bhoyan, Gandhinagar, Gujarat, India 382781*

Abstract

The superior Microcontroller Bus structure (AMBA) is an on chip bus structure utilized to meet up the accessibility & reusability of IP and its miles one of the most widely incorporated interconnection standards highly recommended for system on chip (SoC). In parliamentary law to aid high-velocity latched facts transfers, it supports a deep circle of bus alerts, making the deep study of AMBA-based processor designs a hard inspiration. The AMBA specs has emerge as de-facto preferred for the VLSI industry, it has been taken up by extra than 90% of Advanced RISC Machine alliances and some of IP vendors.
The basis takes a look at of AMBA-primarily structures poses a hard design issues. The sole objective of this report is to optimize and synthesize a complex AHB_2_APB bridge among superior great overall performance Bus and Advanced Peripheral Bus called as "AHB_2_APB Bridge". in this file, synthesized internet listing of Bridge module is brought ahead. To carry out purposeful and Timing Simulation the use of EDA gear -Xilinx ISE and Questa Sim.

Keywords: AMBA; HDL; Verilog; EDA; AHB2APB

Abbreviations

HDL	Hardware Description language
AHB	Advanced High Performance Bus
APB	Advanced Peripheral Bus
SoC	System on Chip
RTL	Register Transfer Logic

1. Preface

The Advanced Microcontroller Bus Architecture's aim is to help the design maker of SoC devices to expend on complexities like layout for less strength consumption, to facilitate the correct-win-time improvement of Embedded systems with one or extra CPU or processors, to be generation-impartial and to promote the modular system design. Also to reduce the silicon footprint and infrastructure required helping green on chip and rancid-chip community for a better greener world.
This report typically concentrates at the synthesis and simulation of AMBA primarily based AHB_2_APB Bridge. AHB_2_APB Bridge connects the AHB and APB buses. it's far required to bridge the conversation hole among less peripherals in APB with the excessive Processors and/or other more-paced systems linked on the AHB. that is to make sure that there is no information loss between AHB_2_APB or APB on AHB statistics transfers. right here we used Hardware Description Language for defining the RTL code. Simulation are finished with the usage of EDA equipment - Questa Sim and Xilinx ISE.

2. AMBA Microcontroller

The AMBA architecture micro-controller includes a great-overall performance gadget bus, capable of preserve the external reminiscence bandwidth, on-chip reminiscence and different Direct Memory Access (DMA) gadgets reside. This bus affords some excessive-bandwidth connections between the additives which are required in most people of transports.
As properly put through the excessive performance bus is the bridge to enable the decrement of bandwidth bits of APB, where maximum of the connected devices within the corporation are positioned. AMBA APB presents the basic cell and its macros communications infrastructure as the only primary bus from the better bandwidth in phase principal bus. The parent beneath explains the typical AMBA based totally microcontroller summary stage design. The high performance buses, i.e. AHB, is related with the ARM processors, DMA Bus, On-chip RAM. those are termed as the Masters and then again, of the Bridge the Slaves are positioned.

* Akash Verma Tel.: +91-9909904785
E-mail address: 140120111001@git.org.in

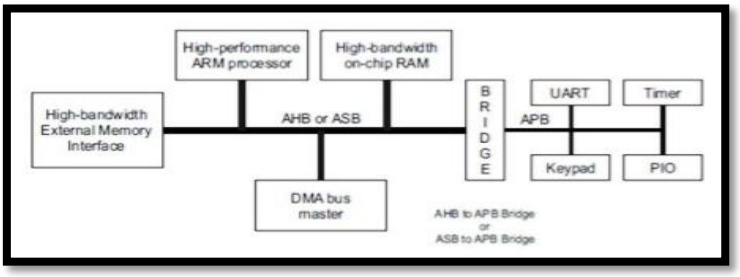

Fig. 1. AMBA Protocol design at abstract level

3. AHB2APB Bridge Properties

The AHB_2_APB connects the AHB and APB buses. It deals with acess and information from the AHB, also it gives the APB peripherals and return statistics alongside reaction signal to the AHB. The AHB_2_APB connections is written to perform when the AHB & APB operation possess the un sync combination of address phase & data cycles. The AHB2APB plays the transfer of facts from the design AHB_2_APB for writing cycle and APB to AHB for determining the state of operation.

The connections among the buses gives ordering in controls, addressing and facts indicators for the peripherals of the AHB_2_APB Bridge.

Reinforcements for the chase

- The slaves and its components
- Components requiring wait states

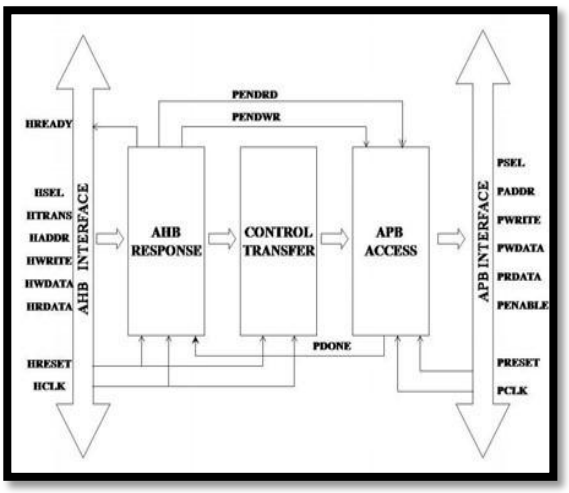

Fig. 2. Architecture of AHB2APB Bridge

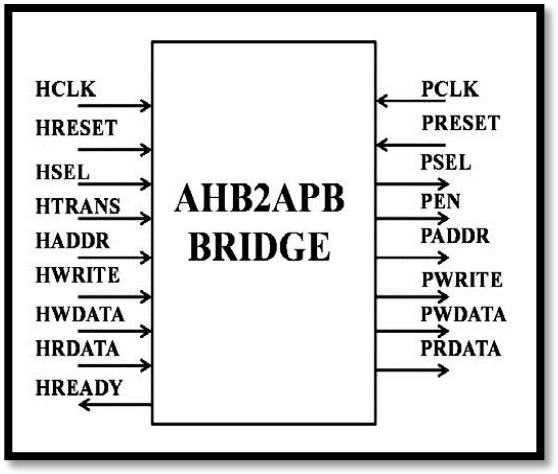

Fig. 3. Pin level information of AHB2APB Bridge

4. Synthesis

4.1 Bridge Layout

AHB_2_APB Bridge operates on H_CLK and APB get entry operating on P_CLK. AHB response and manipulate switch are together termed because the AHB connection and APB get entry to is called as an APB connection. To make certain a right generation of appropriate manage indicators and address we follow 3 signals in the design module, namely: PEND_WR (Pending Write), PEND_RD (Pending examine), P_DONE (Peripheral operation done). The seize of cope with & control, for Write or examine operation is executed while H_READY, H_TRANS and H_SEL are valid.
The sub modules function on extraordinary clock domains, particularly H_CLK and P_CLK, there may be a demand for interfacing these clock domain names. The design will become asynchronous on the boundary of connections, which force changes in setup and maintain timing analysis violation, metastability and unreliable information transfers. And so we want to exit for notable design and interfacing strategies. In this kind, we call for to perform records switch, there exist only a few strategies to acquire this and they are as follows:

- Handshake signalling approach
- The Asynchronous First in First Out

The design has both personal benefits and drawbacks. We used Handshake signalling method. Handshake signalling technique the AHB connection transfers facts to APB connections classified due to the handshake alerts PEND_WR (PEND_RD) and PDONE indicators. This makes use of the identical method that is installation with x86 chips primarily based on the handshake indicators Request and renowned. AHB connection asserts the PEND_WR (PEND_RD) signal, asking the APB connection to just either testify or to transfer the information alongside the statistics bus. APB connections asserts the P_DONE signal, preserving that it has popular or sent the records. This approach is easy, simply it has got loopholes: while APB connections samples the AHB connections, PEND_WR (or PEND_RD) line and AHB connections samples APB connections' P_DONE line, they're executed with regard to their inner time reference, hence there could be setup and preserve major timing analysis violation. To deflect this, we use twice degree sync managers and might be proof against metastability to a wide extent. The parent 4 below indicates how that is controlled

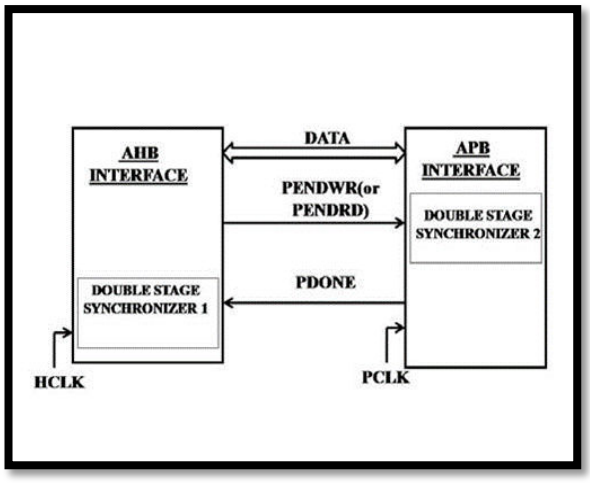

Fig. 4. Efficient handshake signaling method

4.2 AHB Driver Design

The AHB driver/reveal follows example that motivates the AHB_2_APB Bridge with AMBA manage alerts, information and cope with. also supervises the input statistics this is acquired from the bridge, in order that AHB master surroundings is produced. This module additionally controls the block for H_CLK era distributed to the module AHB_2_APB Bridge and RESETn technology distributed to the "2" different modules, namely AHB_2_APB Bridge bus and those two alerts generated are glaringly used in this module as properly.

4.3 APB Driver Design

The APB driving force/screen is that instance that motivates the AHB_2_APB Bridge with suitable records and induced control indicators and additionally monitors the manipulate indicators, cope with and facts that is fetched from the bridge module, so that it will create the pseudo test bench area of the APB Slave. This deal with and manipulate indicators that is fetched from the AHB_2APB bridge is certainly used within the module facts access the values from the design to this interface or the opposite also holds true, primarily based on

neither or not it is appending an explain and read operation. This layout incorporates instance block of P_CLK technology, which is made for the AHB_2_APB bridge module, and the P_CLK formed is manifestly utilized in this module as well.

5. Result and Observations

Netlist mapping through the transformation of a geared up layout to a static simulation containing the design constrained files having the design netlist. This changed into executed on the Xilinx ISE fashioned synthesis record for the AHB2APB example. on this research paper most effective bridge example is the synthesized module and APB reveal & AHB driving force had been simulated from the check bench.

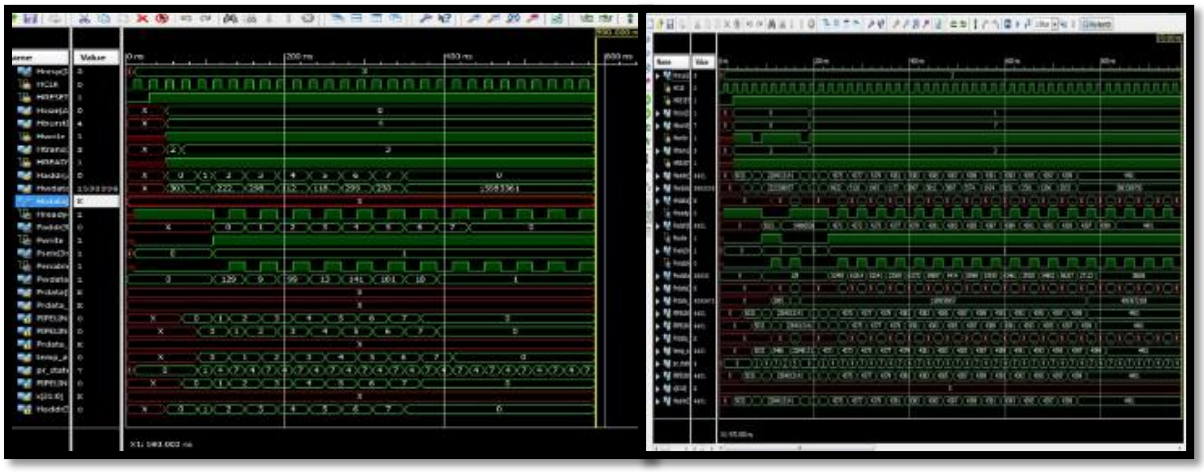

Fig. 5. AMBA Burst Read and Write Switch initiations

Conclusion

The simulation for the subsequent task has been verifies the use of the EDA equipment Xilinx ISE. The check bench had been validated and with tremendous code insurance. The AHB2APB Bridge has been substantiated and synthesised the use of TB named as AHB motive force/driver and APB motive force/monitor. The netlist has been efficaciously synthesised and established according to the Gate stage simulation with RTL simulation outcomes. hence, AHB2APB Bridge acts as the only option to extract the benefits because of ARM is primarily based on ARM AHB bus by means of interfacing.

References

[1] ARM Manual for AMBA Specification (Rev 2.0).
[2] AHB AMBA System; Technical Manual ARM 1999
[3] Xilinx ISE Synthesis Guide
[4] Wang Zhonghai,Ye Yizheng,Wang Jinxing, and Yu Mingyan, “Designing AHB/PCI Bridge,”in Proceedings of 4th International Conference on ASIC, Oct 2001,pp.578-580.
[5] Jaehoon Song, Student member, IEEE, Hyunbean Yi, Member,IEEE, Juhee Han, and Sungju Park, Member, IEEE,”An Efficient SOC Test Technique by Reusing On/OffChip Bus Bridge”IEEE Transcactions on Circuits and Systems-I:Vol,56,No.3,March2009

Modeling and Analysis of Overcurrent Relay using MATLAB

Abhishopek Harit[a*], Hitesh Manani[a], Satish Patel[a], Mohammad Silavat[a]

[a]*Gandhinagar Institute of Technology, Moti Bhoyan, Gandhinagar, Gujarat, India 382781*

Abstract

This paper is focussed on the modeling and analysis of overcurrent relays to understand their characteristics in abnormal conditions. Overcurrent relay senses the overcurrent in the system and trips the circuit breaker if the current increase from certain pre-set value. It is an important relay used to protect transmission and distribution feeders, transformer, bus etc., as main or backup protection. Modeling is an important tool in the research to attain the effects of network parameters and configurations of the operation. This research deals with modeling and simulation of various overcurrent relay like instantaneous, definite and inverse definite time overcurrent relay under different faulty conditions in the power system. Matlab/Simulink is used as a software platform.

Keywords: Over current Realy, Fault mitigation, Simulink Model, Tripping Time, MATLAB.

Nomenclature

TMS	Time Multiplier Setting
PSM	Plug Setting Multiplier
IDMT	Inverse Definite Minimum Time
LG	Line to Ground Fault
LLG	Double Line to Ground Fault
CT	Current Transformer
Subscripts	
f	Fault
p	*Pick up value*
op	*Operating*

1. Introduction

Relays are very important part of the power system. Relay is an electrical device which provides protection to the system in abnormal conditions. It plays a vital role in protection, whether for individual equipment or whole power system network. Sensitivity, selectivity, reliability and speed are the parameters to judge the characteristics of the relay [1] [2]. It should operate for specified area, in short time and with a good reliability. One relay can be operates as main protection or as backup protection.
On the basis of functionality relays are classified as overvoltage, overcurrent, undervoltage etc. [7]. Overcurrent relays can be further divided into following class:

1.1 Instantaneous Relay

It reacts instantaneously to the fault and passes the tripping signal to the circuit breaker, without any delay. It just depends on the current magnitude, which means whether in the condition of switching of heavy load or temporary fault or permanent fault it will operate in both the conditions. Instantaneous relay is can't discriminate the operation when fault current at two or more locations is the same. [2] [3]

1.2 Definite Time Overcurrent Relay

In the abnormal condition when current exceeds certain limit, relay operates after a predefined delay and passes the trip signal to the circuit breaker. Definite time overcurrent relay allows some time to the system to come into normal condition such as in switching of heavy load or temporary faults, and observe the system. After that delay, relay operates and isolates the unhealthy system from healthy system. The function of the relay can create a problem in three phase short circuit fault near generator (most severe fault), because in that condition generator faces a very large fault current and relay cannot operate before its delay time. [3] [7]

* Abhishek Harit Tel.: +91-8238694886
E-mail address: abhishek.harit@git.org.in

1.3 Inverse Time Overcurrent Relay

This relay plays a very important role in the system. In this relay provided predefined delay is inversely proportional to the current magnitude. It means for heavy fault current it provides less delay, and for low magnitude current it provides large delay. It allows adequate time to the system to mitigate the fault and to come into normal condition [3]. Hence, this relay overcomes mal operation of both the relays.

2. Modeling and Simulation

2.1 Instantaneous and Definite Time Overcurrent Relay

The Simulink model of Instantaneous relay and Definite time overcurrent relay are nearly same. Off Delay Block differentiate these two because practically Instantaneous relay operates without delay and definite time overcurrent relay operate with a predefine delay.

Table 1. Parameter used in Simulink Model of Instantaneous and Definite time Overcurrent Relay

Operating Parameter	Parameter Value
Operating Voltage	132 kV
Fault Timing	0.1 Sec
Delay Time	0.1 Sec for Definite Time Relay
Pick up Value for operating Relay	300 Amp

To understand the simulation of the relays, a fault (LG) has created at the instance of 0.1 second in the Simulink Model of the system as shown in Fig. 1. Overcurrent Relay compares the system current samples with the reference value, which is predefined by the user. In the faulty condition, the magnitude of the current drastically increases. Relay compares the heavy fault current with the reference value, and passes a trip signal to the circuit breaker. In Fig. 2 & 3, at 0.1 second the magnitude of fault current can been seen.

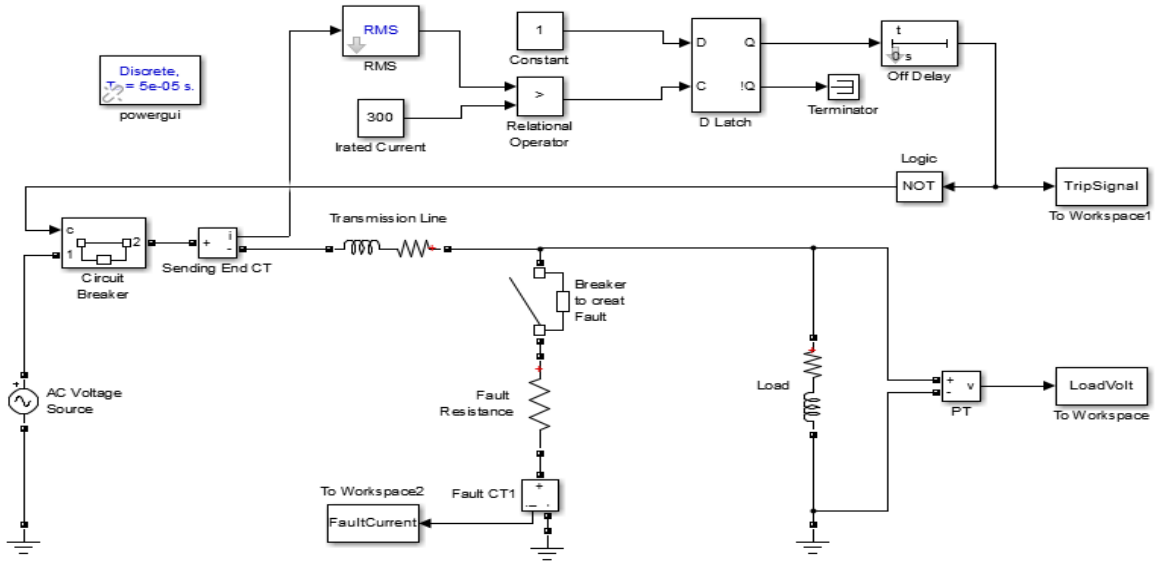

Fig. 1. Simulink Model of Single Phase Overcurrent Relay

The instantaneous relay operates without any delay and switches the trip signal state from 0 to 1 as shown in Fig. 2. This trip signal opens the circuit breaker to isolate the unhealthy system. Voltage profile can be seen in Fig. 2(b). In definite overcurrent relay, the delay of 0.1 second is introduced. In Fig. 3, after the occurring of fault, relay take an additional delay of prescribed time and then switches the trip signal from 0 to 1. Voltage profile can be seen in Fig. 3(b)

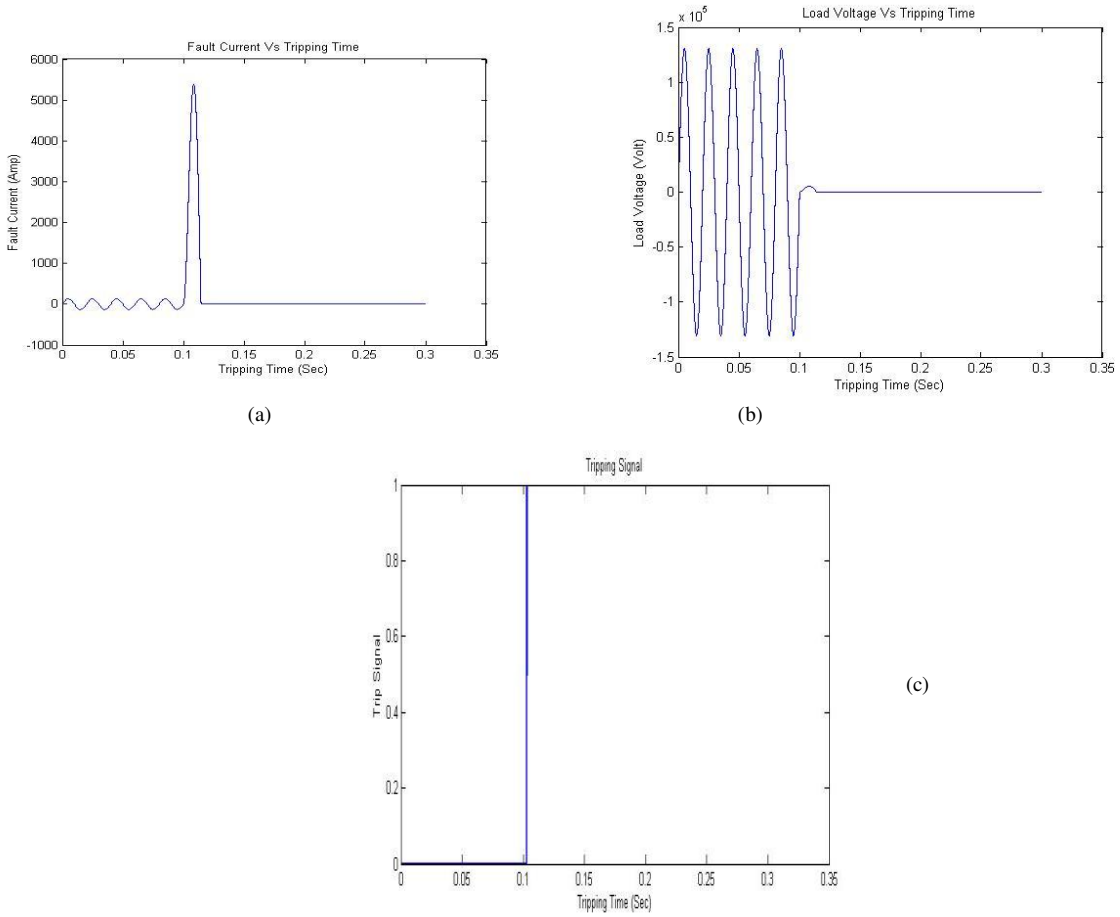

Fig. 2 Response of Instantaneous Relay (a) Fault Current Vs Tripping Time (b) Load Voltage Vs Tripping Time (c) Tripping Signal

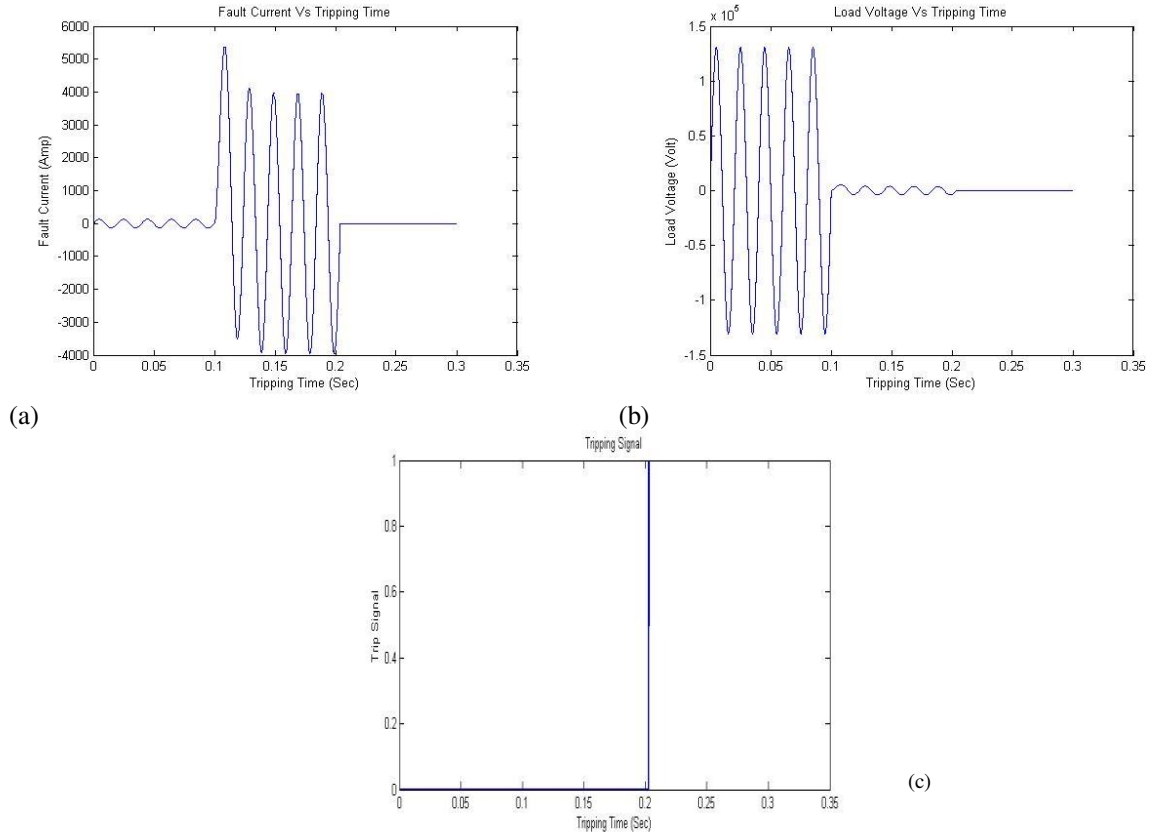

Fig. 3 Response of Definite Time Relay (a) Fault Current Vs Tripping Time (b) Load Voltage Vs Tripping Time (c) Tripping Signal (0.1 Sec Delay)

2.2 Inverse Definite Time Overcurrent Relay

The operating time of this relay depends upon the magnitude of the fault current. Both the quantities fault current and operating time is inversely proportional to each other. So, as the magnitude of current increases, time decreases. This property makes it very important, special and versatile relay. In Fig. 4 modeling of relay shown which contains the subsystem named IDMT Relay having the modeling of the equation of the different IDMT characteristics. [3]

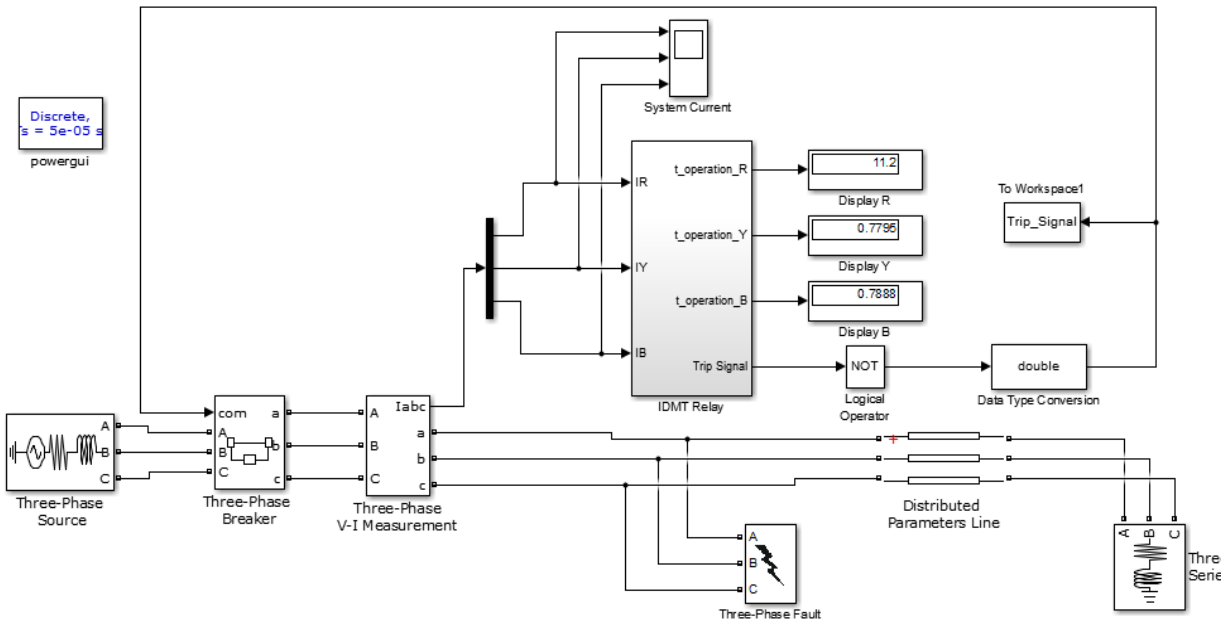

Fig. 4. Simulink Model of Inverse Definite Minimum Time Overcurrent Relay

On the basis of the reaction of operating time, IDMT are further classified as – [7]

- Long Time Inverse Overcurrent Relay
- Standard Inverse Time Overcurrent Relay
- Very Inverse Time Overcurrent Relay
- Extremely Inverse Time Overcurrent Relay

For better understanding of these different relay, the system is tested on double line to ground fault (R-Y-G) on the 3 phase supply, at the instance of 0.2 second. For the analysis following parameters are taken in the Simulink model.

Table 2. Parameter used in Simulink Model of IDMT Overcurrent Relay

Operating Parameter	Parameter Value
Phase to Phase Source Voltage	228.63 kV
Line Distance	50 km
Fault Timing	0.1 Sec
CT Ratio	1200/1 A
Plug Setting	1.2
Current Setting	120 %
Fault Type	L-L-G (R-Y-G)
Operating Frequency	50 Hz
TMS for Phase	0.35
TMS for Earth	0.35
X/R Ratio	7
Fault Resistance	0.01 M

The IDMT subsystem contains the modeling of all the three phases as shown in Fig. 5. This model itself contains a subsystem in which actual current for individual phase is the input and, trip signal for that respective phase and operation time is the output. This can be easily understood through the Fig. 5.

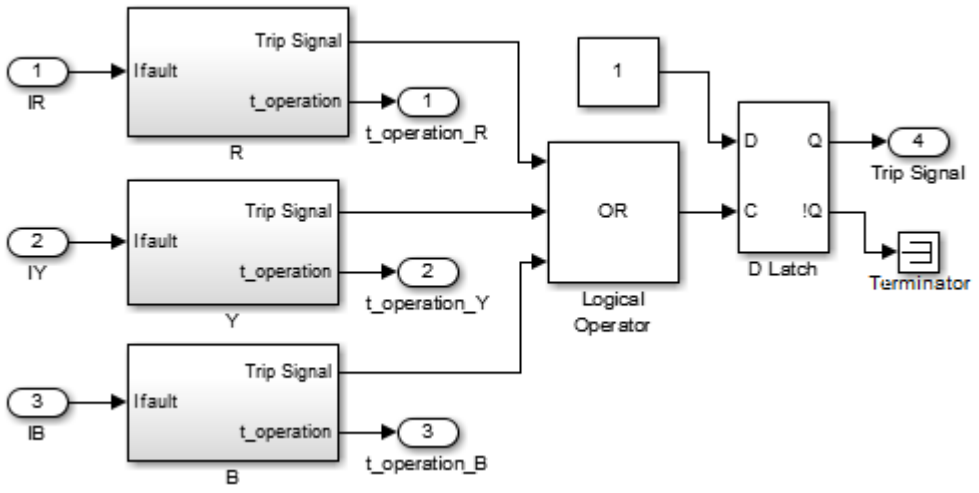

Fig. 5. Subsystem of IDMT Relay

Subsystem of individual phases (R,Y,B) in Fig. 6 contains identical model of relay. This subsystem is shown in Fig. 6. It can be seen in this subsystem, actual current is the input (fault current) and stepped down with the help of CT, which compares with user defined reference value of the current. For the different characteristics of IDMT, modeling of the equation [3] is required, which is shown in Fig. 6 denoted as T_{op}.

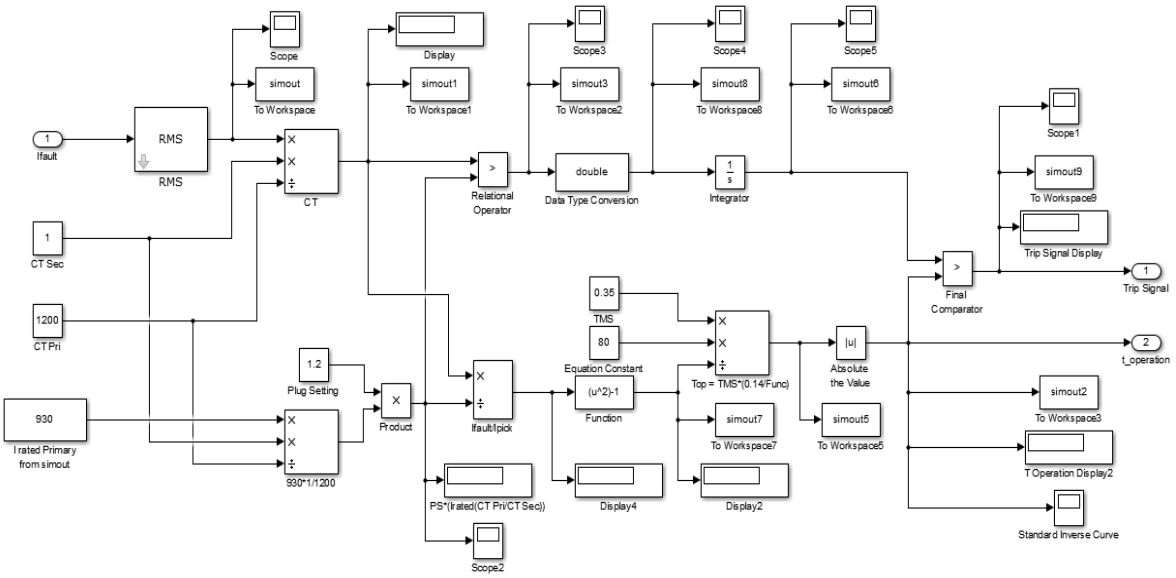

Fig. 6. Modeling of TMS & PSM in R Phase

Comparison of actual current and reference current is fed through the integrator to the final comparator and other input to the final comparator is modeling output of the specific equation of IDMT characteristics. Trip signal and the operating time is the output of the final comparator. It should be noted here that operating time is depend upon type of the IDMT characteristics. [2]

2.2.1 Long Time Inverse Time Overcurrent Relay

This relay takes maximum time to pass the trip signal to the circuit breaker. The time duration that relay takes to observe the system is depends upon the TMS, fault current and pick up value. Operating time can be given by: [3]

$$t_{op} = TMS \times \frac{120}{(\frac{I_f}{I_P}) - 1}$$

It can be seen from Fig. 5, fault is considered to be occurred at 0.2 second and after a duration of second, circuit breaker trips. Characteristics of trip signal is shown in Fig. 5(b), Phase current profile is shown for long time inverse relay is shown in Fig. 5(a).

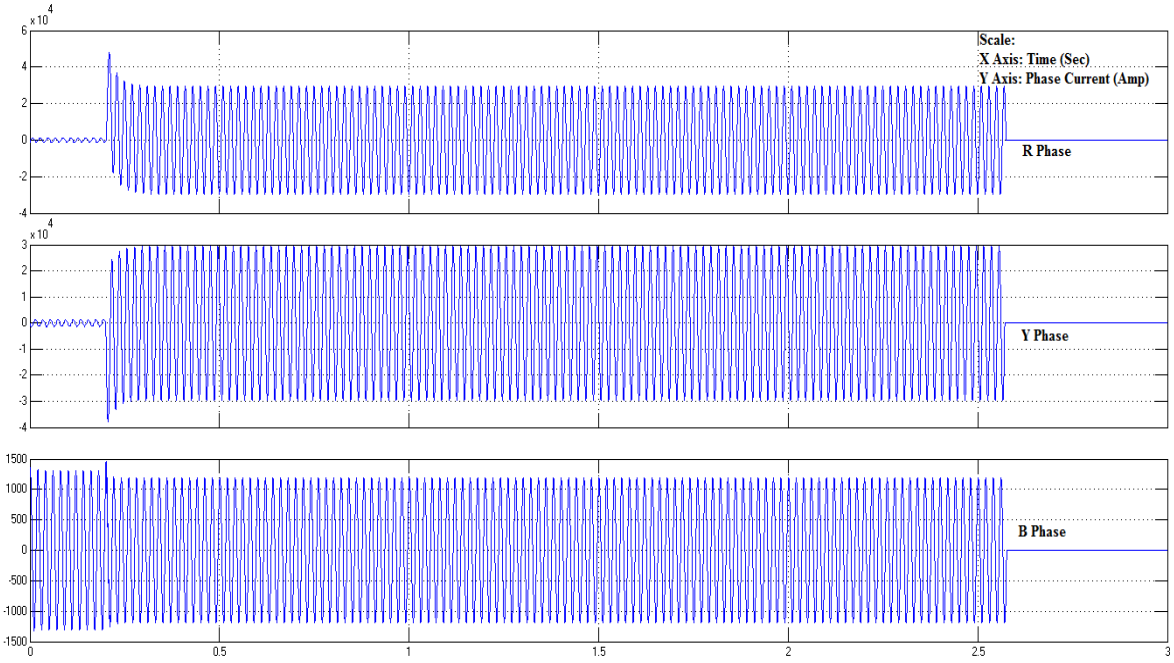

(a) Fig 6 Standard Inverse Response (a) Phase Current Vs Tripping Time (b) Tripping Signal (approx. at 1.05 Sec)

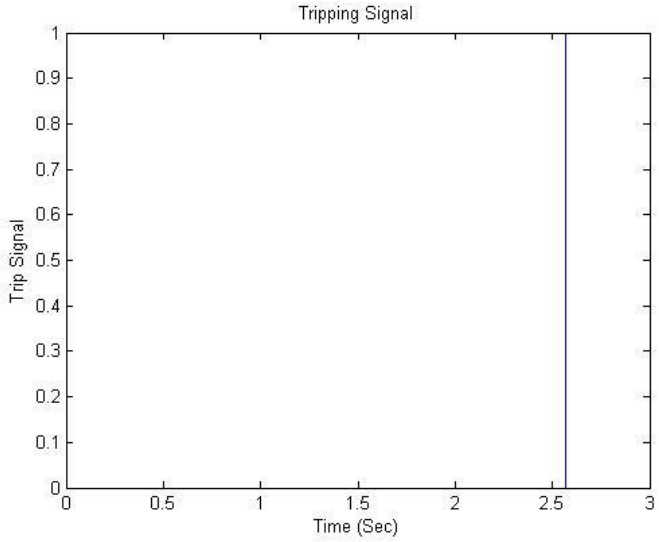

(b)

Fig 5 Long Time Inverse Response (a) Phase Current Vs Tripping Time (b) Tripping Signal (approx. at 2.6 Sec)

2.2.2 Standard Inverse Time Overcurrent Relay

This relay is having standard inverse characteristics. Thus it is also known as normal time inverse overcurrent relay. The operating time is given by following operating equation. [3] [4] The modeling and working of Definite time Overcurrent relay and normal time inverse overcurrent relay may seem same but operation of both the relay are very different. In definite time overcurrent relay, time is depend upon the delay, irrespective of the magnitude of fault current and in normal inverse time relay magnitude of fault have a significant role to play. This time may vary from 5 to 7.5% of the rated operating time. Simulink results of trip signal and current profile are shown in Fig. 5(a) and Fig. 5(b) respectively.

$$t_{op} = TMS \times \frac{0.14}{(\frac{I_f}{I_P})^{0.02} - 1}$$

(a)

(b)

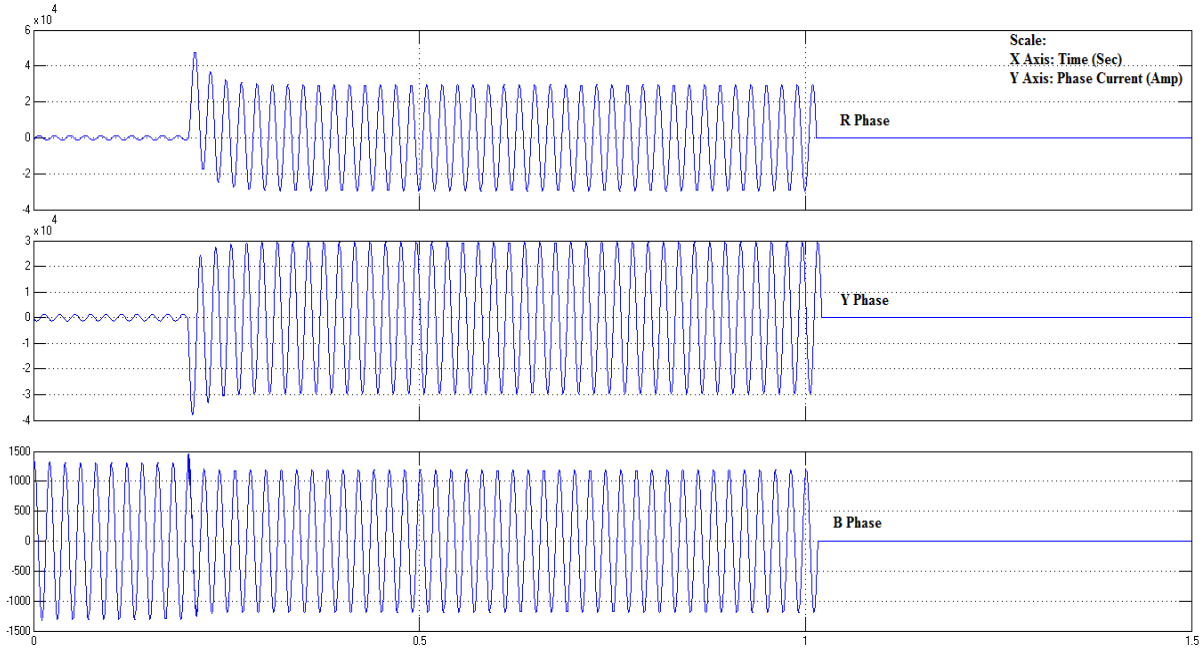

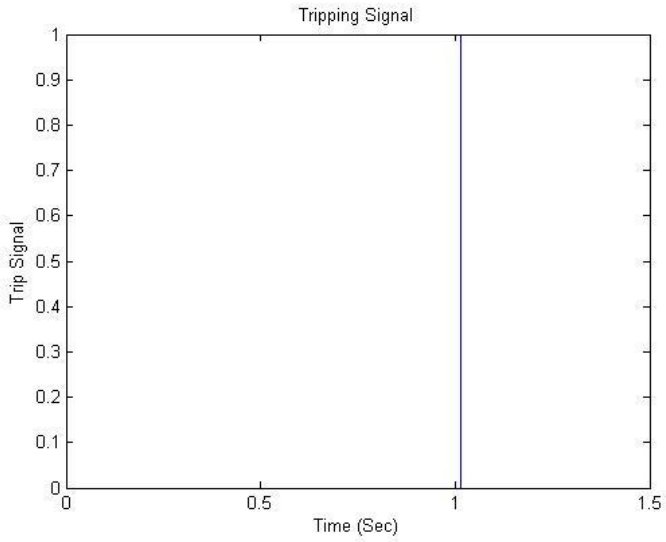

2.2.3 Very Inverse Time Overcurrent Relay

This relay shows fast and sharp inverse characteristics as compared to standard inverse IDMT. This kind of relay are generally used for short circuit current, with some distance from substation. Equation of operating time is given by following equation [3]. Simulink results of trip signal and current profile are shown in Fig. 7(a) and Fig. 7(b). From the tripping signal waveform, one can also see that the time required by relay to operate breaker is very small compare to Long time inverse and Standard time Overcurrent relay.

$$t_{op} = TMS \times \frac{13.5}{(\frac{I_f}{I_P}) - 1}$$

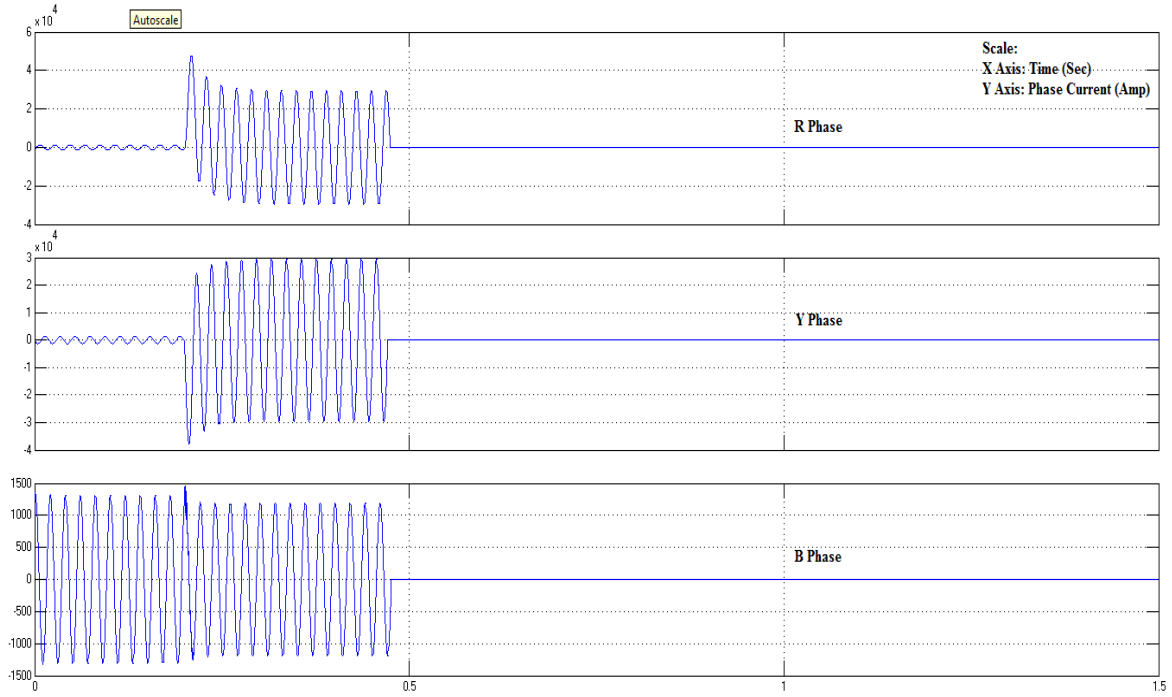

(a)

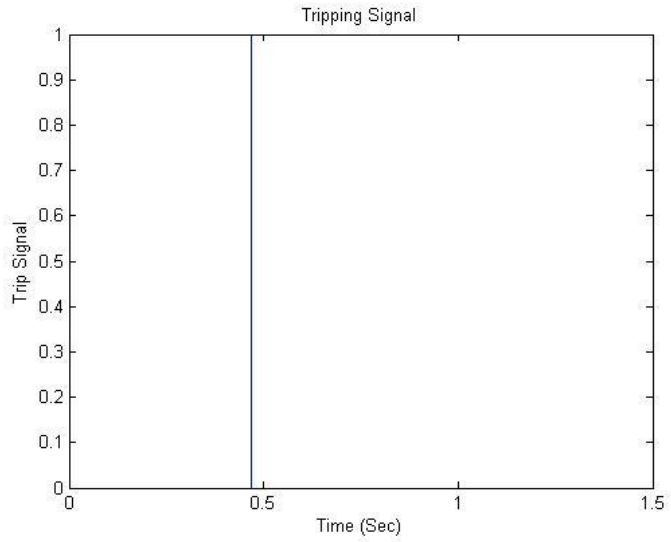

(b)

Fig 7 Very Inverse Response (a) Phase Current Vs Tripping Time (b) Tripping Signal (approx. at 0.481 Sec)

2.2.4 Extremely InverseTime Overcurrent Relay

This relay shows the extreme deep inverse characteristics with time. This relay takes the minimum time as compared to the others IDMT relays. The operating time is almost inversely proportional to the square of the current. Extreme Inverse IDMT relay are preferred for the protection of individual machines. Operating time for extreme inverse IDMT is given by following equation. [5] Simulink results of trip signal and current profile are shown in Fig. 8(a) and Fig. 8(b) respectively. Here, Relay operates very quickly compare to others as it takes delay of 0.055 Sec only.

$$t_{op} = TMS \times \frac{80}{(\frac{I_f}{I_P})^2 - 1}$$

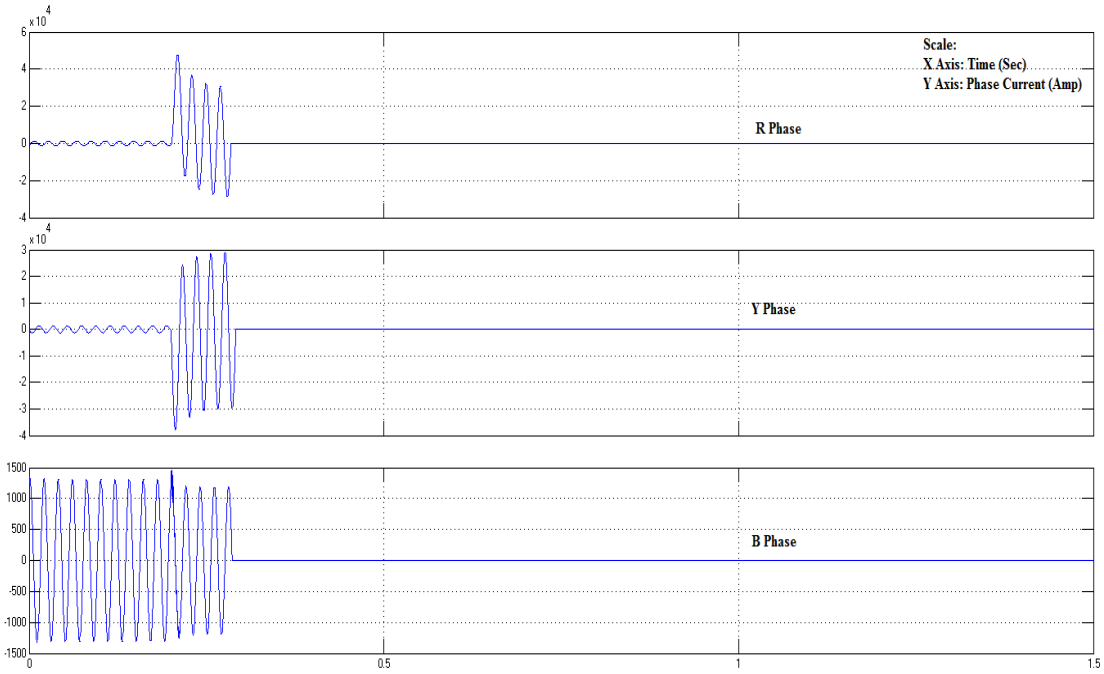

(a)

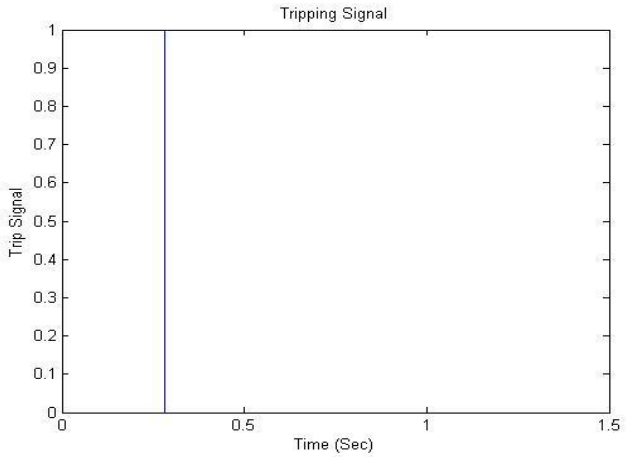

(b)

Fig 7 Extremely Inverse Response (a) Phase Current Vs Tripping Time (b) Tripping Signal (approx. at 0.255 Sec)

Conclusion

Proper functioning of power system needs strong protection mechanism. Reliability and stability of any power system depends upon the provided protection schemes which are made up of different relay connections in different manner. Overcurrent relay plays a vital role in the power system and analysis of its characteristics is important to understand. The simulation results of instantaneous, definite time and inverse time overcurrent relays are discussed. After analyzing the characteristics, it can be concluded that all overcurrent relays have their own importance and working mechanism. To provide better protection, it is very important to choose correct overcurrent relays with the specific requirements like location, magnitude etc.

References

[1] P. Maji, G. Ghosh, 2017, Designing Over-Current Relay Logic in MATLAB, International Journal of Scientific & Engineering Research, Volume 8, Issue 3, ISSN 2229-5518.

[2] Sergio Sebastián Martín, Mónica Bernabé Fernández, 2006, Model and Performance Simulation for Overcurrent Relay and Fault-Circuit-Breaker Using Simulink, International Journal of Electrical Engineering Education, volume 43, issue 1

[3] Nur Hazwani Hussin, Muhd Hafizi Idris, Melaty Amirruddin, Mohd Saufi Ahmad, Mohd Alif Ismail, Farrah Salwani Abdullah, Nurhakimah Mohd Mukhtar, 2016 Modeling and Simulation of Inverse Time Overcurrent Relay using Matlab/Simulink, IEEE International Conference on Automatic Control and Intelligent Systems (I2CACIS), Shah Alam, Malaysia.

[4] M. H. Idris, S. Hardi, and M. Z. Hasan,2013 "Teaching distance relay using Matlab/Simulink graphical user interface", Procedia Engineering, vol. 53, pp. 264–270.

[5] Muhammad Shoaib Almas, Rujiroj Leelaruji, Luigi Vanfretti, 2012, Over-current relay model implementation for real time simulation & Hardware-in-the-Loop (HIL) validation, IEEE IECON 2012 - 38th Annual Conference on IEEE Industrial Electronics Society, Montreal, QC, Canada.
[6] Wen-Hao Zhang, Seung-Jae Lee, Myeon-Song Choi,2011, Protectability Evaluation for Overcurrent Relay based on a Probabilistic Method, Journal of International Council on Electrical Engineering Vol. 1, No. 1, pp. 44-48.
[7] C. L. Wadhwa, Electrical Power System, New Age International Publishers, 6th Edition.

A Review on Metallurgy of ASTM-217 CAST GR. C12A or Modified 9Cr-1Mo Steel

Rohan Y. Modi[a]*, Hemant Panchal[a], S. N. Soman[a], Swapnil Daga[b]

[a]*The M. S.University of Baroda, Vadodara 390001, India*
[b]*Director at ShreeHans Alloys Ltd.*

Abstract

Modified 9Cr-1Mo (P91 or C12A) steel is considered an important high temperature creep resistant material which can maintain strength at a temperature up to 650 °C. In this study, We will learn about heat-treatment, chemistry, mechanical properties of C12A steel. Then optical and electron microscopy are used to understand the microstructural evolution. Heat-treatment of C12A is very critical because It may developed few amount of δ-Fe in fully martensitic microstrucutre. The microstructural evolution of the designed alloy tells regarding phase transformation and to correlate this information with mechanical properties. Study on presence of δ-Fe is also carried out. C12A were selected because of their best creep performance at temperature 600 °C for 9-12% Cr steel family.

Keywords: C12A; Carbides; δ-Fe; Normalizing; Thermodynamics; Alloying elements

1. Introduction

Modified 9Cr-1Mo steel developed in 1970's for manufacturing of pipes and vessels for fast breeder reactors. Before 1970's, 300 series of austenitic stainless steel was used for these applications [1]. C12A is a material of choice in fossil-fuel-power plants with increased efficiency, service life and reduction in emission of CO_2, NO_x, and SO_2[2]. The efficiency of fossil-fired power mainly depends on temperature and pressure of steam. Temperature of steam in coal fired power plant is expected to be in range of 550-720 °C[3]. This material has high creep strength. i.e.100000 hrs. creep strength of 100 MPa at 600 °C and also have high toughness as well as ultimate tensile strength[4,5]. It's microstructure and mechanical properties can improve by heat-treatment. This article covers thermodynamics, heat-treatment, chemical composition, effect of alloying element, microstructure and mechanical properties.
C12A steels are high strength alloys that normally transform completely to martensite during air cooling. Microstructure consist of low C lath martensite, carbides (like $M_{23}C_6$, NbC, M_3C etc.), and fine precipitates of niobium carbonitrides (Nb(C, N)). [2,6,7]

2. Lieterature Review

2.1. The alloy system

Austenitic stainless steels have some drawbacks like cost and less resistance to thermal fatigue. Modified alloy system is similar to conventional 9Cr-1Mo grades [2]. Modifications include additions of Vanadium, Niobium, and nitrogen as well as lower C content. This alloy has high thermal conductivity so it has good resistance to thermal fatigue than austenitic stainless steel.[8]

Table 1. ASTM and ASME specifications and grades for 9Cr-1Mo-V materials[2]

Form	ASTM	ASME	Grade designation
Forging	A182	SA182	F91
Seamless Tubing	A213	SA213	T91
Seamless Pipe	A335	SA335	P91
Forged Pipe	A369	SA369	FP91
Plate	A387	SA387	Grade 91
Piping Fitting	A420	SA420	WP91
Forging	A336	SA336	F91
Casting	A217	Code Case 2192-2	C12A

* Rohan Modi Tel.: +91-9687755885
E-mail address: rohanmodi9010@ymail.com

Table 2. Compositions for various forms[2]

Element	Wrought Grades F91, T9, WP91, P91, F91 and 91	Cast Grade C12A	Casting Per ASME Code Case 2192-2
C	0.08-0.12	0.08-0.12	0.08-0.12
Mn	0.30-0.60	0.30-0.60	0.30-0.60
P	0.020[a]	0.020	0.020
S	0.010[a]	0.010	0,010
Si	0.20-0.50	0.20-0.50	0.20-0.50
Cr	8.00-9.50	8.0-9.5	8.00-9.50
Mo	0.85-1.05	0.85-1.05	0.85-1.05
Ni	0.40	0.40	0.40
V	0.18-0.25	0.18-0.25	0.18-0.25
N	0.030-0.070	0.030-0.070	0.03-0.07
Nb(Cb)	0.06-0.10	0.060-0.10	0.06-0.10
Al	0.04	0.040	0.02
Ti	---	---	0.005

[a] 0.025 in ASTM A336 and ASME SA336

Table 3. Mechanical Property Requirement for Various Forms[2]

Property	Specification/Grade		
	A182/SA182 F91 A213/SA213 T91 A335/SA335 P91 A387/SA387 Gr91	A217 C12A	ASME Code Case 2192-2 Casting
Minimum Ultimate Tensile, Strength, ksi (MPA)	85(585)[a]	85(585)[a]	85(585)
Minimum Yield Strength, ksi (MPa)	60(415)	60(415)	60(415)
Minimum % Elongation	20[b]	20	20
Minimum % Reduction in Area	40(SA182)	45	---
Maximum Hardness (HB)	248(SA182)	---	---

[a] SA217, SA234 and SA387 include a maximum tensile strength requirement of 110 ksi (760 MPa).
[b] Minimum elongation per SA387 is 18% .

A microstructure of modified 9Cr -1Mo is depends on two factors. Firstly, the fine $M_{23}C_6$ precipitate particles nucleate on Nb(C,N) which initially appears during heat treatment and secondly Vanadium enters $M_{23}C_6$ and retards it's growth at service temperature. It will maintain structure for long time at service temperature [2,9].

2.3. Processing Issues

There are number of metallurgical issues that must be addressed with respect to deoxidation practices, heat treatment and welding process used in production of the material [2]. One important issue is specification of maximum tempering temperature which are limited by A1 temperature. Total amount of Ni and Mn as well as heating rate affect A1 temperature. However, Cr + Mo concentration increases A1 temperature.[1]

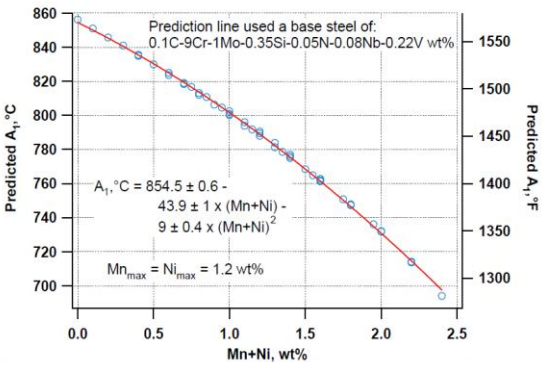

Fig. 1. Prediction based on equilibrium thermodynamics of the variation of A_1 with (Mn+Ni) concentration in P91 steel[1]

2.3. Matrix microstructure of creep steel

Resistance to creep deformation depends on presence of fine and highly stable dispersion of carbides and intermetallic compounds which precipitate during tempering or during elevated temperature service. Carbides interact with dislocations and retard coarsening rate of microstructure. There is also solid solution strengthening by substitutional solutes [10]. Add sufficient amount of those alloying elements which can increase hardenability. It will results in martensitic structure even at air cooling. Martensitic steels have to be temepered to get optimum combination of strength and toughness. [2]

2.4. Heat treatment

Microstructure is consist of δ-Fe, martensite, bainite, allotriomorphic ferrite, and retained austenite by normalizing and tempering treatments [10]. The phases were formed depends on composition and heat treatment cycle. As per ASTM std. A217 heat treatment cycle is ; i) normalized at 1040-1080 °C and ii) then tempered at 730-800 °C[11]. But main objective behind normalizing is austenization at high temperature in order to dissolve all alloying elements into solid solution as well as to dissolve stable precipitates and provide a natural cooling or forced air cooling for certain mm thickness. Sometimes in case of heavy sections we can go for a liquid quenching to get completely fine martensitic structure. Too low temperature gives incomplete dissolution of carbide and lead to loss in creep strength. While too high temperature gives undesirable formation of δ-Fe phase. Recent studies say that high A1 temperature leads to good creep strength.[10]
Normalizing followed by tempering to achieve desired mechanical properties. During tempering carbides and carbonitrides are precipitate as well as relive stresses [2]. Due to tempering hard martensite lath structure with high dislocation density converted into stress-free tempered martensite structure. As we increase tempering time; diffusion of carbon also increase and at the same time tensile as well as yield strength also decrease. That's why creep properties improves in tempering and then eventually degrade after the precipitation of large equilibrium alloy carbides[10]. Martensite start (Ms) temperature decided based on following equation[3].

$$Ms = 550\ °C - 450C - 33\ Mn - 20\ Cr - 17\ Ni - 10\ W - 20\ V - 10\ Cu - 11\ Nb - 11\ Si + 15\ Co \ldots (Eq.01)$$

2.5. Description of carbides

The evolution of microstructure in steel is a complex and dynamic process involving simulation transformation of different types of phases. Types of phases that can be found like possible phases such as martensite, δ-Fe, retained austenite; graphite; $Fe_{2.5}C$; Fe_3C; Chi Fe_2C; M_2X, M_6C, $M_{23}C_6$, M_7C_3 laves; M_5C_2, Z-phase, μ-phase, ϰ-phase, etc.[10]
Morphology of M_2X is fine needle like particles dispersed throughout the matrix and generally considered to nucleate on dislocations and martensite lath boundaries. It will give secondary hardening. Mo_2C usually play a major role in creep strength. Cr and Mo stabilize the M_2X carbides but form δ-Fe phase and this phase is detrimental to creep strength; So it should be stay in limits. M_7C_3 forms after formation of M_2X. It will nucleate in vicinity of Fe_3C or at Fe_3C/α-Fe interface. This phase generally observed in 2.25Cr-1Mo steel. This phase has been found to coarsen rapidly and gave no beneficial contribution to creep rupture strength. In over-aging; the formation of $M_{23}C_6$ and the dissolution of M_2X found. Vanadium stabilizes M_7C_3 and so decreases the rate of release of C and Cr into matrix for growth of $M_{23}C_6$. $M_{23}C_6$ is less effective in resistance of creep deformation. Precipitation of $M_{23}C_6$ is reduced by stabilizing fine M_2X and MX for longer time to increase creep strength[10].

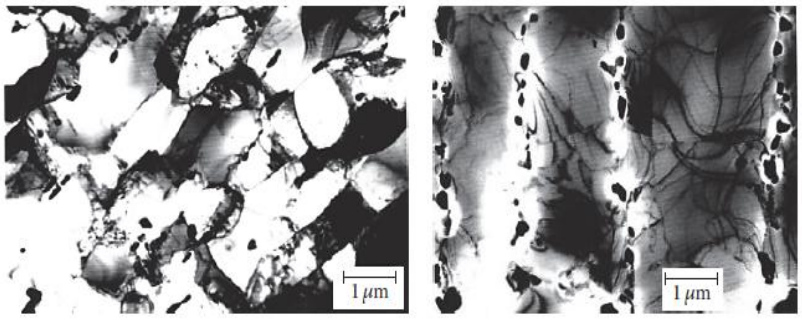

Fig. 2 TEM micrograph of 9Cr steel, a) shows tempered martensite having lath morphology and carbides (absence of coarsening); b) carbides aligned at martensite laths boundaries(Presence of Coarsening)[10]

Above certain amount of Ni and N will also accelerate microstructure degradation during creep at 650 °C by precipitation of Z-phase. After a long exposure to elevated temperature equillibrium laves phase precipitation at 600 °C and it has general composition Fe_2M, where the alloy content may be W, Mo or a combination of both. General chemistry of lave phase is Si= 11%, Mo = 44%, Cr = 17%, Fe = 28%[10,12].
This phase will form preferentially in Cr-depleted regions. Generally these regions are rich in Mo; Diffusion rate of Mo and Si control the formation and growth of laves phase; but Mn will retard laves phase formation [13]. Si at around 0.3% give best balance between recovery of microstructure and coarsening of precipitates. Another phase is Z-phase observed at greater than 550°C. This phase consist complex nitride phase containing Cr, V, and Nb in the form Cr(Nb,V)N by dissolving NbX particles. As this phase grows, it is seen to gradually replace MX and M_2X nitrogen riched phases which improve creep rupture strength. Study shows that large concentration of Nb (0.9%) enhances the precipitation of Z-phase[14,15,16]. Crystal structure of Z-phase is either cubic (Short time exposure) or tetragonal (long time exposure)[3]. Nucleation rate of Z-phase is higher at austenite grain boundry and at a temperature of 650°C [14,15,16]. In general, the precipitation of Z-phase, M_6X and Fe_2(W, Mo) laves phase during creep causes loss of creep strength because they consume existing fine M_2X, MX, and

$M_{23}C_6$ precipitates. Sequence of carbide formation is as given below. Some fine MX phase could be present.[3,10]

$$M_3C + M_2X \rightarrow M_3C + M_2X + M_{23}C_6 \rightarrow M_2X + M_{23}C_6 [10]$$

2.6. Effects of alloying elements

Role of alloying elements in creep steel is very important because if slightly changes has been done in composition it will directly affected on microstructure. Elements such as Mn, Mo, Cr, V, W, Ti, and Nb are present in form of stable carbides or in solid solution within ferrite [10].

a) Carbon; stabilizes austenite relative to α-Fe. It will form carbides which cause secondary hardening[10]. It usually has peak value because high levels of C lead to unacceptable reductions in mechanical properties such as toughness and may cause cracking after normalization and also after welding[17].
b) Manganese; stabilizes austenite but give adverse effect on creep strength. A phenomenon is retention of austenite which will be rich in C and nitrogen, so reducing secondary hardening[10]. If Mn present in excess amount then it may increase growth rate of M_6X, an undesirable and coarse phase which can remove W from solid solution and cause the dissolution of other more desirable precipitates [3].
c) Nickel; stabilizes austenite and promoting coarsening of carbide phase as well as laves phase. This coarsening reduces creep property so Ni concentration should be less than 0.4%. This is because Ni increases the rate of dissolution of M_2X as a consequence of precipitation of M_6X phase[10].
d) Cobalt; Co stabilized austenite field and doesn't show coarsening effect on microstructure like Mn and Ni because it will slow down diffusion process[3]. Study shows that Co strengthens the martensitic matrix by solid solution strengthening mechanism and improves stability of fine precipitates such as MX and μ-phase. Disadvantage of addition of Co is that it makes steel difficult to recycle because Co containing scrap has low scrap value [10].
e) Boron; additionStudy upto ≈0.01% will increase rupture strength on high temperature structure of 10 Cr steel by retardation of coarsening rate of precipitates. However, high B% detrimental to strength due to formation of dissolved boride phase. It will also create problems in weldability and forgeability[10].
f) Copper; is an austenite stabilizer. If Cu is added then it's only function is to retard δ-phase formation. Cu additions upto 2%, have been found to cause retarding the recovery of martensite[10].
g) Chromium; stabilizes ferrite and it is carbide former. It is also improve steam oxidation resistance. 9-10% Cr additions provide hardenability, good creep strength and resistance to corrosion. 11% Cr increase corrosion resistance at creep steel at 650 °C; however high percentage of Cr leads to formation of undesirable δ-Fe[10].
h) Silicon; is a α-Fe stabilizer and found to accelerate precipitation and coarsening of laves phase in 9Cr steel as well as promote δ-Fe phase. However Si can be very important in formation of protective oxidation layers. Optimum Si is 0.3% because it's give acceptable corrosion resistance and mechanical property. Study shows that 0.4% Si deteriorates tensile strength, creep strength and toughness due to δ-Fe formation.Study shows that 0.4% Si deteriorates tensile strength, creep strength and toughness due to δ-Fe formation. Graph of δ-Fe formation according to Cr and Si amount.[7,10]

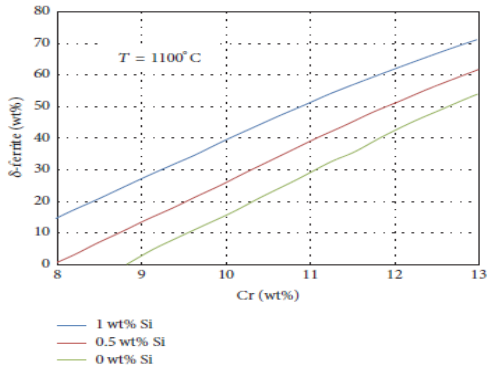

Figure.3 δ-ferrite volume fraction as a function of Cr wt% for a steel of composition 0.08C-0/1Si-0.5Mn 8/13Cr-3W-0.2V-0.005B-0.005N wt% [10]

i) Tungsten; is promoter of δ-Fe as well as laves phase. It is stabilize M_2X type carbide though less effective. W addition gives solid solution hardening. Study shows that increase W concentration in a 9Cr alloy reduced the coarsening rate of $M_{23}C_6$ precipitate and martensite laths but increasing coarsening rate of laves phase[10].

j) Vanadium; is a main element to form stable nitride. It will form VC thus leaving Mo in matrix, which will give solid solution strengthening[10].

k) Molybdenum; stabilizes M_2X phase and a phase given as $M_{23}C_6$ phase. It will also contribute as solid solution strengthening. Amount of Mo above 1% has been found to promote formation of M_6C, laves phase and δ-Fe in 9%Cr[3].
l) Titanium; improves creep strength by formation of carbide and nitride[10].
m) Niobium; gives the MX carbides and nitrides which are small and stable. These precipitates pin grain boundary and prevent grain growth. Effectiveness of this mechanism relies on dissolving Nb during austenization otherwise insoluble NbC remains and causing coalescence of precipitates, coarsening them and accelerating recovery[10].
n) Tantalum and Neodymium; are improve creep strength by formation of TaN and NdN precipitates. These are extremely stable and do not coarsen rapidly during welding and heat-treatment[3,10].
o) Aluminum; is detrimental to creep strength because of formation of AlN instead of VN or NbN. Behind reduction in creep strength the reason is that AlN is coarse phase[10].
p) Nitrogen; occupies interstitial sites in iron lattice and stabilizes austenite. It is also stabilize MX precipitate as CrN and this will increase creep strength[10].
q) Phosphorous; presence in excess amount is results in segregation to grain boundary which lead to embrittlement. P is interact with Mo and segregated at prior austenite grain boundary and results in loss of ductility in 9Cr-1Mo steel [10].
r) Sulfur; gives theformation of sulphides, such as MnS can provide preferential nucleation sites for cavitation. Cavitations caused by low interfacial adhesion between MnS and α-Fe matrix [10].

2.7 CCT diagram

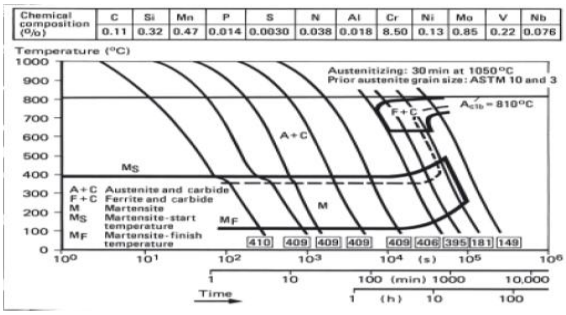

Fig.4 CCT diagram of P-91[18,19]

A1 temperature is lies between 800 to 830°C but mainly depend on Ni+Mn amount. Martensite start temperature is around 400°C and martensite finish temperature is around 100 °C. To achieve fully martensitic microstructure maintain cooling rate >0.1°C/s [19,20]. Typical microstructure after normalizing and tempering are as shown in Figure 5.[21,22]

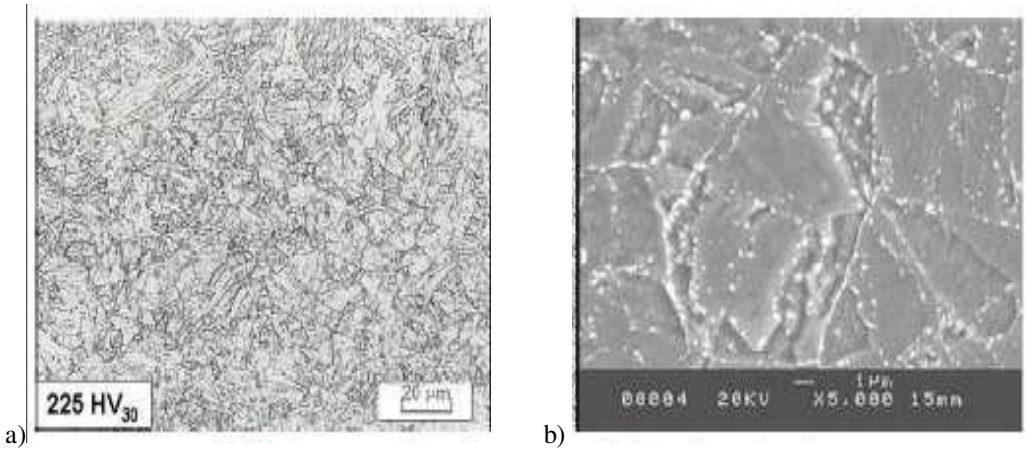

a) b)

Fig.5 Fully martensitic structure a)in optical microscope b) in SEM.[22]

2.8. Effect of δ-Fe

δ-Fe is the first solid solution phase to form during solidification as a primary solidification phase. It is nucleated upon heating steel to 1210°C at rate of 10°K/s. Upon cooling this δ-Fe transforms to austenite and austenite will convert to martensite[23,24]. This δ-Fe is much softer than martensite matrix and it can reduce mechanical properties like toughness, tensile strength, hardness and creep strength [12,25,26].

According to paul; if $Cr_{eq.}$ is greater than 9; then there is more chances of δ-Fe presence.[23,27]

$$Cr_{eq.} = Cr + 6Si + 4Mo + 1.5W + 11V + 5Nb + 12Al + 8Ti - 40C - 2Mn - 4Ni - 2Co - 30N - Cu \quad ...(Eq.02)$$

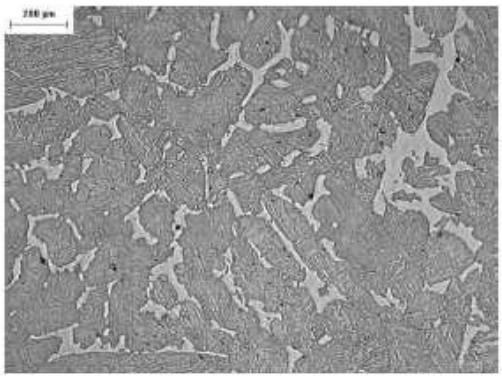

Fig.6 non-acceptable microstructure because δ-Fe is present in microstructure[23]

2.9 Thermodynamic and kinetic analysis

A thermodynamic analysis of nitride precipitation can be made based on Ellingham diagram of nitrides shown in Fig.7(a). Diagram shows greater tendency for AlN to form than either VN or NbN. However, the Ellingham diagram shows the standard state condition and doesn't consider the actual concentration of Al, V, Nb, and N in the welds[5].

The solubility products of all the nitrides decrease as the temperature decreases. AlN is precipitate first during cooling because it has lowest solubility at temperature above 863°C, as shown in Fig.7b. [5]

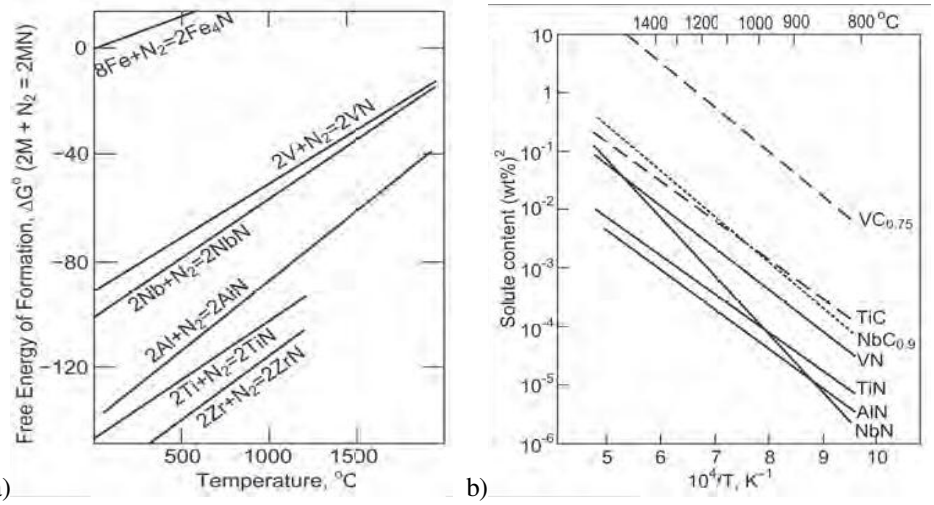

Fig.7 Effect of temperature on formation of nitirides[5]

3. Discussion

Austenitic stainless steel can be replaced by C12A because of it's stable microstructure. It possess good creep strength due to carbonitride precipitates as well as solid solution strengthening due to various alloying elements. According to various literatures; Laves phase, Z-phase, $M_{23}C_6$ and M_7C_3 type carbides will reduced creep strength. Alloying elements like Cr, Si, and Mo are major δ-Fe promoters. Critical cooling rate for C12A is 0.1°C/s to get fully martensitic structure which results in better creep strength. We can't use Al as a de-oxidiser because according to Ellingham diagram AlN is more stable than VN or NbN. AlN is coarse precipitates which reduces creep strength. That is why De-oxidation is carried out by Mn, Mg, Se and some amount of calcium silicide.

4. Summary

From the above work we can summarize following points:

1) Strength of C12A mainly depends on it's microstructure. So we have to precisely maintain chemical composition as well as heat-treatment parameters.

2) Precipitation of fine Nb(C, N) with MX and M_2X type carbides are necessary for long term creep strength.

3) In heat treatment air cooling is sufficient upto certain thickness to get fully martensitic structure but for heavy thickness (i.e. >3 in.) we can go for water quenching or oil quenching.

References

[1] M. L. Santella, R. W. Swindeman, R. W. Reed, and J. M. Tanzosh. Martensite formation in 9 Cr-1 Mo steel weld metal and its effect on creep behavior, Oak Ridge National Laboratory, pp.1-8
[2] Emel Taban, Erdnic Kaurluc, Tanil ATICI, 2012. 9%-12% Cr steel: Properties and weldability aspects, the situation in Turkish Industry; Uluslararasi, 2nd international conference on welding technologies and exhibition, pp.203-209.
[3] Zur Erlangung des Grades and Doktor-Ingenieur, 2011. 9-12% Cr heat resistant steels, alloy design, TEM characterisation of microstructure evolution and creep response at 650°C, Bochem-2011, pp.10-24.
[4] G.Golanski and J. Slania, 2013. Effect of different heat treatments on microstructure and mechanical properties of the martensitic grade GX12CrMoVNbN9-1 Cast steel, Archives of Metallurgy and materials vol.58, 2013, pp. 25-29.
[5] X.Chai, J. C. Bundy, M. A. Amata, C. Zhang, F. Zhang, S. Chen, S. S. Babu, And S. Kou, May-2015. Creep Rupture Performance of Welds of P91 Pipe Steel; AWS and Welding research council, Vol.94, pp. 145,146,150,151,153,154,155.
[6] Triratna Shrestha, Sultan F. Alsagabi, Indrajit Charit, Gabriel P. Potirniche and Michael V. Glazoff, 2015. Effect of Heat Treatment on Microstructure and Hardness of Grade 91 Steel; Metals,Vol.5, pp.131-138
[7] Emel Taban, Erdnic Kaurluc, Tanil ATICI, 2012. 9%-12% Cr steel: Properties and weldability aspects, the situation in Turkish Industry; Uluslararasi, 2nd international conference on welding technologies and exhibition, pp.203-209.
[8] Vinod K. Sikka. Development of modified 9Cr-1Mo steel for elevated temperature services, oak ridge national laboratory, 1981, pp.1-2.
[9] Huijun Li & David Mitchell, 2013. Microstructural characterization of P91 steel in the virgin, service exposed and post-service renormalized conditions; University of Wollongong, Steel research international, vol.84, pp.3-5.
[10] V. C. Igwemezie, C. C. Ugwuegbu and U.Mark, 2016. Physical Metallurgy of Modern Creep-Resistant Steel for Steam Power Plants: Microstructure and Phase Transformations, Journal of metallurgy, Vol.2016, pp. 6-20.
[11] SA-335, 2004. Specification for seamless Ferritic alloy-steel pipe for high temperature service, Section-II, pp. 574.
[12] Xiaotian Li, M. T. Cabrillat, and Y. Lejeail, 2002. Study of Modified 9Cr-lMo Welds, Institute of nuclear and new energy technology, pp.64-66.
[13] Zheng-Fei Hu.Heat-Resistant Steels, Microstructure Evolution and Life Assessment in Power Plants; School of Materials Science and Engineering in Toungi University, Intech-2012.
[14] Danielsen, Hilmar Kjartansson, 2016. Review of Z phase precipitation in 9–12 wt-%Cr steels; material science and technology, Vol.32(2), pp.2-5.
[15] Danielsen, Hilmar Kjartansson, Somers, Marcel A. J.,Hald, John, 2007. Z-phase in 9-12% Cr Steels; Technical University of Denmark, pp.3-12, 18-20.
[16] A. Di Gianfrancesco , S. Tiberi Vipraio, D. Venditti, 2012. Long term microstructural evolution of 9-12% Cr steel grades for steam power generation plants; Metal, BRNO-23, pp.1-3.
[17] R. Viswanathan & W. T. Bakker, 2000. Materials for Ultra Supercritical Fossil Power Plants; EPRI, TR114750, 2000.
[18] API, 2008. Use of 9Cr-1Mo-V (Grade 91) Steel in the Oil Refining Industry, API technical report, 938-B, 1st edition, 2008, pp.3-14.
[19] A. McGehee, & K. Coleman, 2003. Effect of Normalization and Temper Heat Treatment on P91 Weldment Properties. EPRI Fossil Repair Applications Center, 1004915, pp.1-5.
[20] J.R.Distefano& V.K.Sikka; Summary of modified 9Cr-1Mo steel development program;Oak Ridge National Laboratory, ORNL-6303, 1986, pp.17-40.
[21] Ng Guat Peng, Badrol Ahmad, Mohd Razali Muhamad, Mohd Ahadlin, 2013. Phase Transformation Of P91 Steels Upon Cooling After Short Term Overheating Above Ac1 & Ac3 Temperature, Advanced Materials Research, Vol.634-638, pp. 2-4.
[22] T.C. Totemeier, H. Tian, and J.A. Simpson, May-2006. Effect of Normalization Temperature on the Creep Strength of Modified 9Cr-1Mo Steel; metallurgical and materials transaction, Vol.37A, pp.1519.
[23] WRI, BHEL, and IIM. Fabrication and Processing of grade 91 material, International Workshop, 2011, pp.8-25.
[24] Masataka Yoshino, Yoshinao Mishima, Yoshiaki Toda, Hideaki Kushima, Kota Sawada and Kazuhiro Kimura, 2005. Influence of Normalizing Heat Treatment on Precipitation Behavior in Modified 9Cr-1Mo Steel; ECCC Creep Conference, pp.148-156.
[25] sung Ho Kim, Woo seog ryu & Hiun kuk, 1999. Microstructure and mechanical properties of Cr-Mo steels for Nuclear indusries applications; Journal of Korean nuclear society, pp.561-563.
[26] Peter Mayr, 2007. Evolution of microstructure and mechanical properties of the heat affected zone in B-containing 9% chromium steels; Dissertation at Graz university of technology, 2007, pp. 7-19.
[27] B.Arivazhagan& M. Kamaraj, 2013. A study on influence of DELTA-ferrite phase on toughness of P91 steel welds; steel grips, pp.21-22

Acknowledgement

Let us express our gratitude to all people who have helped us in this paper work. First of all, we are indebted to our guides Dr. S. N. Soman (H.O.D. of Metallurgy and Materials Engineering department at The M.S.U.) and Mr. Hemant Panchal for their kind guidance during progress of our work. We had invaluable, fruitful, and often joyful discussions. We are highly motivated by their positive attitude and greatly benefited by their wide experience and knowledge. Then we are indebted to Mr. Swapnil Daga (Director at Shree Hans Alloys Ltd.) for his valuable suggestions for selection of this project and during the progress of my work.

Experimental Investigation on effects of Exhaust Gas Recirculation (EGR) on the performance of CI Engine fueled with Biodiesel-Diesel Blends

Kapil Yadav[a], Nirav Joshi[a], N M Bhatt[a]*

[a]*Gandhinagar Institute of Technology, Gandhinagar, Gujarat 382721, India*

Abstract

Today majority of the stationary diesel engines are utilized for irrigation, power generation and as prime mover in countries like India, where cost effectiveness is the predominant criteria. From past few years, usage of diesel engines was increased which can be seen from the sales report of many engine manufacturing companies. The reason behind this growth could be cost of diesel fuel and efficiency of the diesel engine when compared to petrol engine. But on the other side, emissions from diesel engine are high especially NO_x emissions. There is a need for a technique which could reduce the emissions without affecting the performance of engine. By using the biodiesel blends, conventional fuel can be saved but NO_x emissions are increased due to presence of oxygen in biodiesel. Experimental investigation has been carried out to investigate the effect of Exhaust Gas Recirculation (EGR) to reduce the emission from multi cylinder diesel engine fuelled with biodiesel-diesel blend. Using B20, 20% diesel can be saved but on other side, to achieve same performance, more fuel is consumed with higher emissions. Hence the EGR is implemented to reduce the emissions from the engine. When engine is operated with B20 blend with 10% EGR, 56% reduction in NO_x can be achieved with 5% increase in HC emission in addition to 11% loss of efficiency. Hence a CI engine fuelled with 20% Biodiesel blend and operated at 10% EGR can replace the conventional CI engine with reduced NO_x emissions.

Keywords: Diesel, Biodiesel, CI Engine, Emission, NO_X, EGR, Engine Performance.

Nomenclature

CI	compression ignition
CO	carbon monoxide
CO_2	carbon dioxide
EGR	exhaust gas recirculation
HC	hydro carbon
NO_x	oxides of nitrogen
PM	particulate matter

1. Introduction

The present world is facing the crisis of fast depleting fossil reserves and increasing environmental threats. The higher consumption of fossil fuels demands search for alternative fuels. Fuels obtained from bio-origin can provide a feasible solution to this global petroleum crisis. Bio-diesel obtained from vegetable oil is comparable to diesel from the point of calorific value and emission quality. India imports about 40-50% edible oil to meet domestic need, and therefore production of biodiesel from edible oil resources is not justified [1] but for the same purpose non-edible oils can be considered. Feedstock of mainly neem, mahua, cotton seed, castor, rubber seed, tobacco, jojoba, kusum and jatropha curcas are the most prominent species for bio-diesel production. Compression Ignition engines can be operated with no design modification using this bio-diesels. [2-3] Jatropha and karanja crops can be grown on the wasteland and land on the road sides and railway tracks, in addition to check soil erosion and improve fertility of land. Jatropha curcas is a bush of up to 6 m height and is adapted to low rainfall, now available throughout the tropical and subtropical areas. Due to presence of toxic cursive and curcasive, the cattle do not graze the plant, seed and oil. The jatropha oil is unscented, colorless if fresh but becomes yellow on storing, a slow-drying oil. The jatropha seed contains oil in the ranges from 30 to 35 % by weight [4]. Calorific value of jatropha can be compared well to any bio-diesel as well as to diesel. It is reported that viscosity of the oil obtained from jatropha seed is more compared to petro-diesel, have higher cloud points with minimal sulphur content and more reactive to excess oxygen [5]. In jatropha oil longer carbon chain with less number double bond is responsible for higher viscosity, cetane number and calorific value. Due to incomplete combustion, the high viscous jatropha curcas oil forms carbon deposits and reduces life of the engine. Vegetable oil can be converted into bio-diesel by various methods e.g. transesterification, thermal cracking, micro-emulsions etc.

* N M Bhatt Tel.: +91-9904406000
E-mail address: nmbhatt19@gmail.com

Over recent past years, stringent emission laws have been imposed worldwide on NO_x, smoke and particulates emitted from diesel engines. Diesel engines are typically characterized by worldwide low fuel consumption and very low CO emissions. However, the NO_x emissions from diesel engines remains high. Hence, to meet the environmental legislations, it is highly desirable to reduce the amount of NO_x in the exhaust gas.

It is well-known fact that the CI engines are widely used because of their higher thermal efficiency and low maintenance [6]. Exhaust gases (HC, CO, CO_2, NO_x etc.) of diesel engine are very harmful and major source of air pollution hence contributing to global warming. Studies have found that over 60% of the total air pollution is caused by engine exhaust. Engineers and scientists have done lots of research and experiments to find alternatives for diesel engine and effective means to control emission which is contributing to air pollution. They found that biodiesel as a fuel can replace diesel and it can reduce the harmful exhaust gases to significant amount. Biodiesel contains oxygen as a part of its chemical composition which lead to higher NO_x emissions than diesel operated engine. Also, many researches have focused on blend concentration and finalization of engine parameters [7] and to fight "food to fuel crises" [8]. NO_x emission can be considerably reduced with the help of exhaust gas recirculation (EGR).

Biodiesel is a domestically produced, renewable fuel that can be produced from vegetable oils, animal fats or recycled restaurant oil for use in diesel vehicles. Biodiesel's physical properties are like those of petroleum diesel, but it is a cleaner-burning alternative. In many countries, this has led to the use of blends of biodiesel with conventional diesel instead of 100% biodiesel. Often blends with diesel are denoted by acronyms such as B20, which indicates a blend of 20% biodiesel with diesel on volume basis.Biodiesels are made from transesterification process in which vegetable oils, a triglyceride reacts with an alcohol in the presence of a strong acid or base, producing a mixture of fatty acids alkyl esters and glycerol. The overall process is a sequence of three consecutive and reversible reactions, in which di and mono glycerides are formed as intermediates. It is the most common method to produce biodiesel.

In EGR, the part of exhaust gases are recirculated as shown in Fig 1 which aids in reducing the NO_x emissions. Exhaust gas normally contains CO_2, NO_x etc. and mixture has higher specific heat compare to atmospheric air, thus recirculated exhaust gas displaces fresh air in combustion chamber and hence, it helps to reduce oxygen available for combustion and it also increases the specific heat of mixture entering the combustion chamber thus lowers flame temperature.

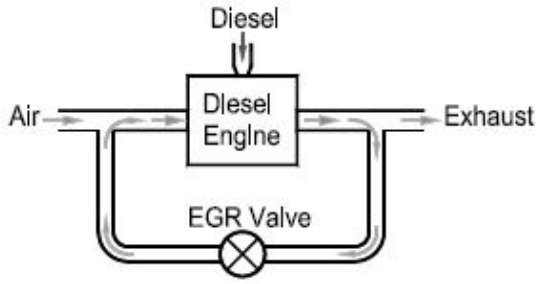

Fig 1 Exhaust gas recirculation

EGR is one of the most effective and economical method to reduce NO_x emissions. EGR helps in increasing the heat capacity, diluting the intake charge and reducing ignition delay. It cause increase in amount of inert gas in the mixture and hence reduces the adiabatic flame temperature.

Sapre et al. investigated effect of various exhaust gas recirculation rates on engine emission characteristics like NO_x, HC, CO, CO_2, and exhaust gas temperature. Experiments were performed on a single cylinder, naturally aspirated, 4-stroke, vertical, air cooled CI engine. They found that NO_x emission got reduced by 64.75% and HC emission increased by 15% with EGR. HC emission was observed less for the non EGR operations. They concluded that 20% EGR was optimum for NO_x reduction without significant change on brake specific fuel consumption and HC emission [9]. Selim studied the effects of EGR ratio, engine speeds, engine load, temperature of recycled exhaust gases, intake charge pressure and engine compression ratio on combustion noise and thermal efficiency. It was observed that 5% exhaust gas recirculation was increasing the thermal efficiency. The use of a low EGR ratio of 5% was also favorable for reduced combustion noise and reduced NO_x emission. However, increasing the EGR reduced the thermal efficiency [10]. Joshi et al. performed experiments and concluded that biodiesel was more viscous as compare to diesel hence for higher blends of biodiesel, the modification required in injection system of engine due to increase in viscosity of fuel. Due to less calorific value of biodiesel, higher consumption of fuel for biodiesel-diesel blend was noted. 10% biodiesel-diesel blend delivered acceptable performance with marginal decrease in BSFC and increase in BSEC and BTE [11]. Srinidhi et al. worked on CI engine fuelled with honne oil methyl ester for performance and emission determination. They observed that specific fuel consumption was reduced for 0%, 20%, 40%, 60%, 80% and 100% blending. The brake thermal efficiency increases with increase in load. The brake thermal efficiency for B20 is similar to diesel for all loads. NO_x emission of B100 was observed to be highest for all loads [12]. Mohebbi et al. studied the influence of EGR on NO_x and diesel engine combustion. NO_x, PM emissions, brake

specific fuel consumption (BSFC), engine thermal efficiency, cylinder pressure and heat release rate (HRR) were analyzed. The experiments were conducted on a turbocharged DI diesel engine under full load condition at two different injection timings to distinguish and quantify effects of EGR with various engine parameters. Experimental results proved that increase of EGR rate has a negative effect on air-fuel ratio. For a premixed combustion at constant pressure, ignition delay was increased leading to retardation of all combustion process, allowing more HRR and reduction of in-cylinder peak temperature. Use of EGR reduced NO_x emissions whereas PM emissions were increased. The advance of injection timing resulted in the reduction PM while both NO_x emissions and fuel consumption were increased. With increasing EGR rate, unequal EGR distribution was increased in inlet port of cylinders [13]. Patel et al. discussed about long run analysis of engine and reported that engine suffered problems such as carbon deposition, lubricating oil dilution, piston ring sticking and injector nozzle chocking running on pure plant oils. Without any change to oil or engine, short run test were likely to be successful. For long run utilization, to minimize these durability problems, the biofuels (esterified oil / blend with diesel/ blend with diesel in presence of additives) can be used as an attractive option [14].

2. Experimental setup

Experiments have been performed on two cylinder, direct injection, water cooled CI engine. The experimental setup is shown in Fig 2. An air box with orifice is connected to the inlet manifold and the air mass flow rate is measured using the U-tube manometer connected to the air box. The EGR system consists of a piping arrangement which connects the exhaust gas flow to the inlet charge in metered quantity. An orifice meter was used to measure the flow rate of the exhaust gases with the help of control valve. The amount of exhaust gas recycling into the inlet air was controlled by EGR control valve. 5 gas analyzer was used for emission measurement. The engine was coupled with electrical dynamometer which was connected to electrical load bank. Engine specifications are mentioned in Table 1. Table 2 contains the list of equipment used for various measurements.

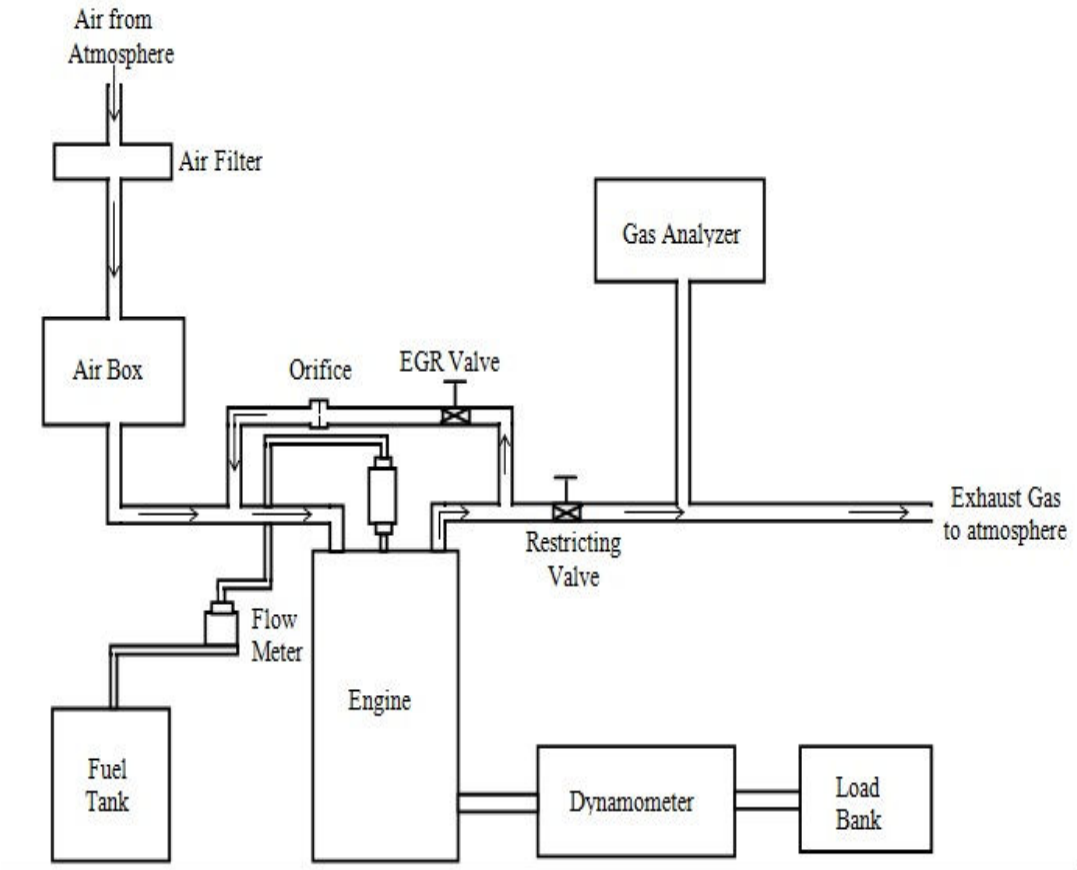

Fig 2 Schematic diagram of experimental setup

Table 1 Engine specifications

Type	2 cylinder, 4 stroke diesel engine	Rated power output	5 kW
Bore × Stroke	87.5 mm × 110 mm	Loading	Electrical dynamometer
Rated Speed	1500 rpm	Compression Ratio	16:1

Table 2 Equipment used in engine test

Parameter	Equipment	Accuracy	Parameter	Equipment		Accuracy
Engine Speed	Stroboscope	± 0.1 rpm	Engine Emissions	5-Gas Analyzer	NO_x	± 1 ppm
Temperature	Thermocouple	± 1°C			HC	± 1 ppm
Engine Load	Electrical load bank	± 0.4 kW			CO	± 0.1 %vol
Fuel Consumption	Burette	± 0.1 mm			CO_2	± 0.1 %vol
Gas/Air Flow	Orifice & manometer	± 1 mm of H_2O (± 0.001 m^3/h)			O_2	± 0.1 %vol

3. Results and Discussion

Experiments were carried out with diesel to get the base line data at varying load conditions. 5 gas analyzer was used to measure the emissions from exhaust gas. After getting base line readings with diesel, jatropha biodiesel has been blended with the diesel in various proportions by volume ranging from 0% to 30%. In addition to variation of fuel, EGR rate has been varied from 0% to 15%. Optimum biodiesel blend with optimum EGR rate has been obtained which gives acceptable engine performance with controlled emissions. Entire experimental work has been carried out as per IS 10001. Uncertainty in measurement of data has been considered. Biodiesel used has been procured from CSMCRI, Bhavnagar with certified properties.

3.1 Performance and Emissions without EGR

Brake Specific Fuel Consumption (BSFC): Fig 3 shows the effect of different blends on BSFC with respect to the varying engine load. The values of BSFC for different blends are higher than the base fuel diesel because of the higher density, higher viscosity and lower calorific value of biodiesel. For blend B20 the specific fuel consumption is reduced by 7 % compared to diesel.
Brake Thermal Efficiency (BTE): The effect of different blends on BTE at various engine loads is shown in Fig 4. BTE for different blends are lower than diesel because of lower calorific value of biodiesel. In comparison to other blends, it is reduced by only 4% for B20.

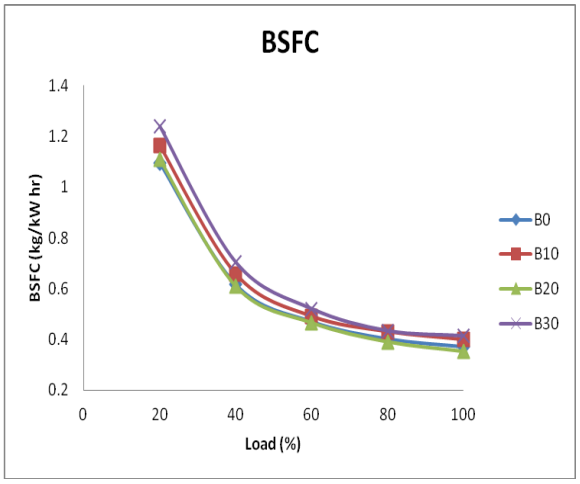

Fig 3 Effect of different diesel-biodiesel blends on BSFC with different load

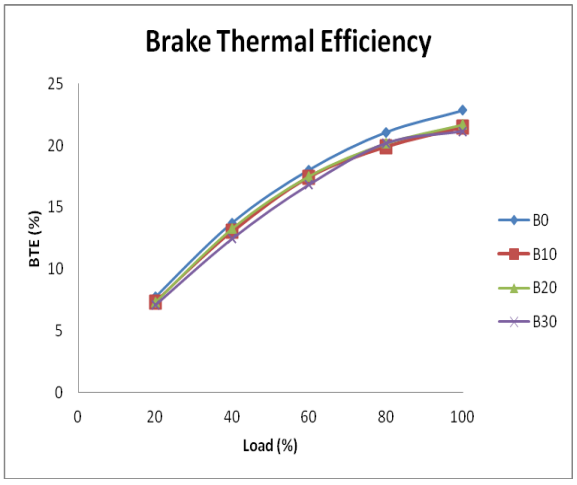

Fig 4 Effect of different diesel-biodiesel blends on BTE with different load

Exhaust Gas Temperature (EGT): Change of EGT with respect to the load for diesel and different diesel-biodiesel blends is plotted in Fig 5. From the results, it is observed that the value of exhaust gas temperature for different blends are lower than the diesel because of lower calorific values of fuel and poor combustion efficiency. For B20, EGT is reduced by 4 %.

Carbon monoxide (CO) Emission: The effects of different blends on CO emissions are shown in Fig 6. Carbon monoxide emissions for different blends are lower due to presence of oxygen in the biodiesel. For blend B20, CO emissions are lower by 5%.

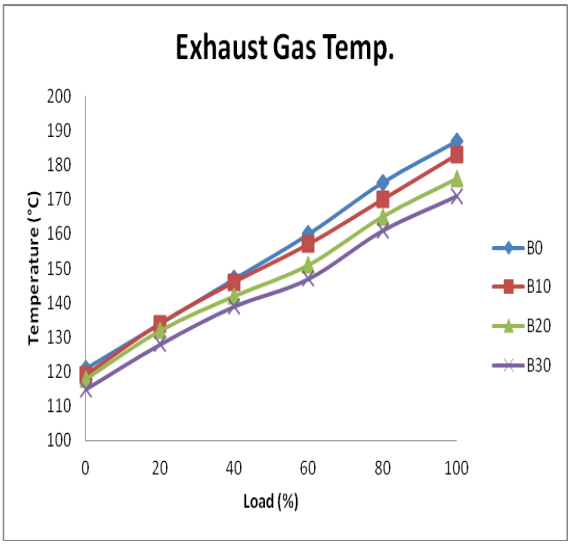

Fig 5 Effect of different diesel-biodiesel blends on EGT with different load

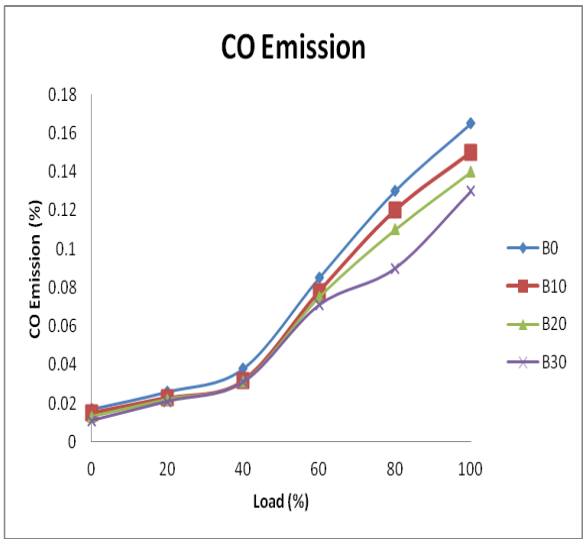

Fig 6 Effect of different diesel-biodiesel blends on CO emission with different load

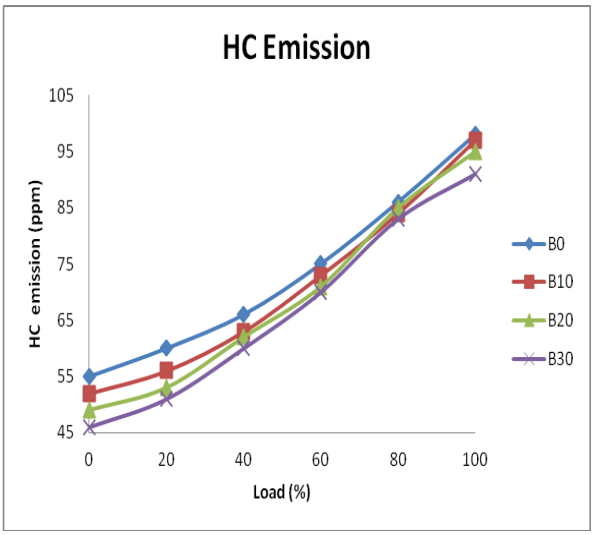

Fig 7 Effect of different diesel-biodiesel blends on HC emission with different load

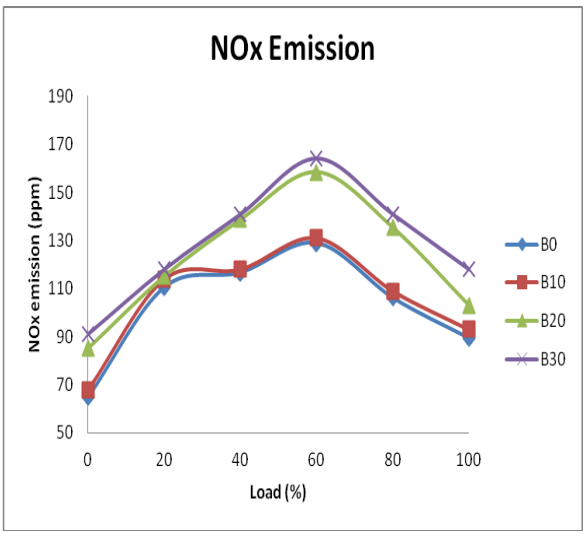

Fig 8 Effect of different diesel-biodiesel blends on NO_X emission with different load

Hydrocarbon (HC) Emission: When Biodiesel is used as fuel, due to proper combustion process and presence of extra oxygen, unburnt fuel particles are less. Hence lower HC emissions are observed during the tests. Fig 7 shows the drop in HC emission by 6% when B20 is used.

Oxides of nitrogen (NO_x) Emission: Effect of various biodiesel – diesel blends on NO_x emission with respect to load is plotted in Fig 8. Excess oxygen present in fuel reacts with nitrogen available in combustion chamber at higher temperature and generates noticeable amount of NO_x. For B20, the NO_x emissions are 18% higher than that of diesel.

From the experiments with diesel and different diesel-biodiesel blends, it is found that among all blends of biodiesel, B20 is the most optimum blend to continue the further experiments. Use of B20 in CI engine without any modification gives 7% reduction in BSFC, 4% reduction in BTE, 5% reduction in CO emissions, 6% reduction in HC emissions and 18% increase in NO_x emissions.

EGR replaces the excess amount of air present in combustion chamber with chemically inactive exhaust gases. It also lowers the combustion temperate as the specific heat of exhaust gases are higher than that of air. Less availability of excess oxygen at lower combustion temperature leads to reduction in NOx emissions.

3.2 Performance and Emissions with EGR

BSFC with Exhaust Gas Recirculation (EGR): Fig 9 shows the effect of EGR on BSFC. BSFC for optimum blends are higher than the diesel due to replacement of air by gases which effects the combustion due to lower calorific value. For blend B20 and 10% EGR, BSFC is 14% higher than diesel.

BTE with EGR: BTE is reduced by 11 % when 10% EGR is implemented as shown in Fig 10. This drop in efficiency is due to poor combustion and lower calorific value of biodiesel.

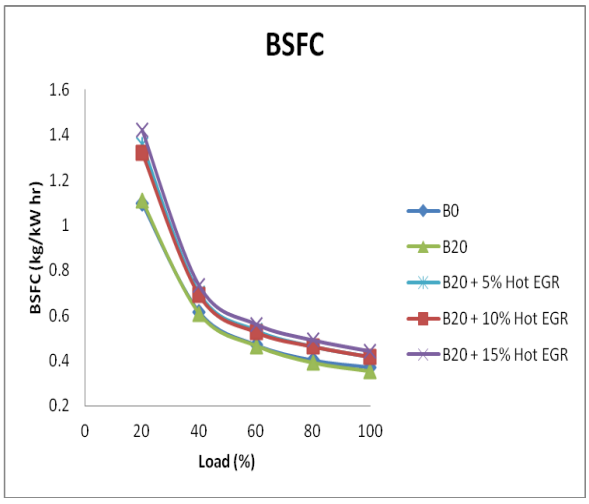

Fig 9 Effect of EGR on BSFC for B20

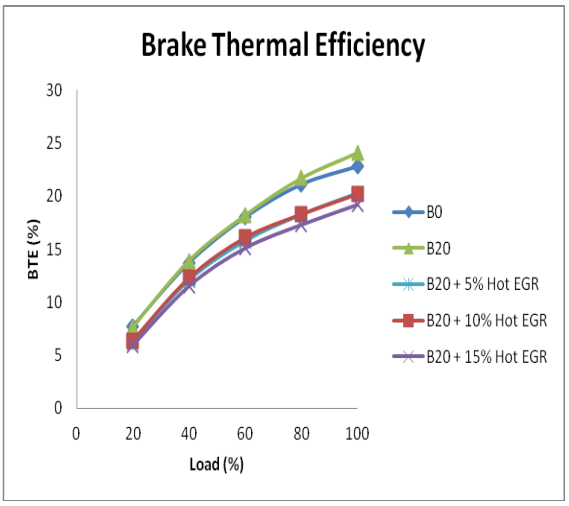

Fig 10 Effect of EGR on BTE for B20

Exhaust Gas Temperature (EGT) with EGR: EGT for optimum blends are lower than diesel with higher rate of EGR. For blend B20 and 10% EGR, the exhaust gas temperature is 9% lower with 10% EGR and 13% lower with 15% EGR as represented in Fig 11.

CO emission with EGR: In presence of EGR, CO emissions are increasing due to absence of excess air which has been replaced by exhaust gases. Fig 12 shows the increase in CO emissions by 14% as compare to diesel in presence of 10% EGR with B20 blend.

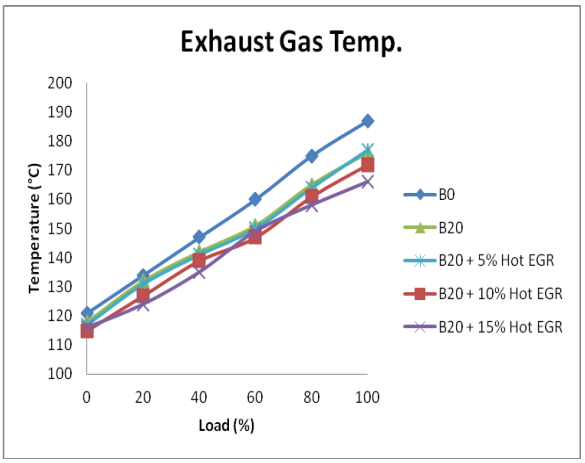

Fig 11 Effect of EGR on EGT for B20

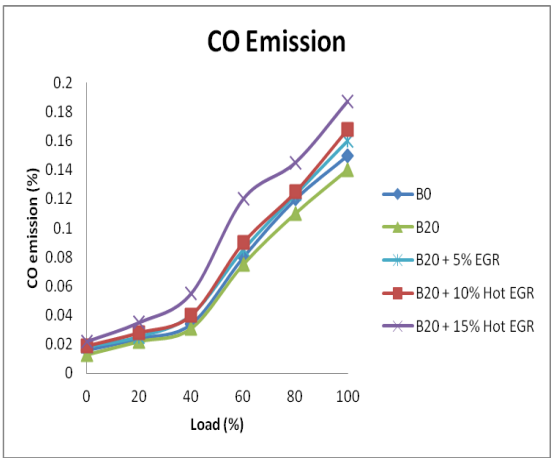

Fig 12 Effect of EGR on CO emission for B20

HC emission with EGR: Fig 13 shows the effect of exhaust gas recirculation (EGR) on Hydrocarbon (HC) emission. Results shows that the hydrocarbon emission are higher than the diesel with increase in rate of EGR as more and more air is replaced by exhaust gases. For blend B20 and 10% EGR, HC emissions are increased by 5%.

NO_x emission with EGR: Fig 14 describes the effect of different rate of exhaust gas recirculation (EGR) on NO_x emission. Results show that for B20 blend with 10% EGR, NO_x emissions are reduced by 56% as compare to B20 without EGR. Reduction in NO_x is due to lower combustion temperature and less availability of oxygen.

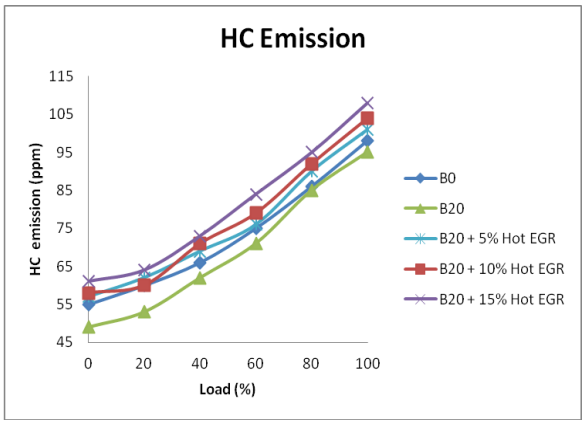

Fig 13 Effect of EGR on HC emission for B20

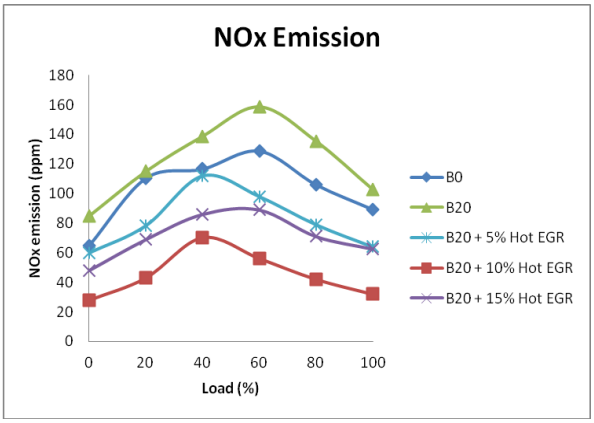

Fig 14 Effect of EGR on NO_X emission for B20

Conclusion

Blending of biodiesel with diesel gives us an opportunity to save the conventional fuel. Lower calorific value and higher viscosity limit the blending in the CI engine without any modification. With the use of biodiesel blends, thermal efficiency of engine drops. Various emissions are increased which can be addressed by EGR. After carried out the tests, following observations have been concluded for optimized performance of CI engine fuelled with biodiesel blends with EGR.

For blend B20 as compare to diesel, BSFC is 7 % higher, BTE is 4 % lower and EGT is 4 % lower. CO emission is 5 % lower, HC emission is 6 % lower and NO_x emission is 18 % higher for B20 blends as compare to Diesel. By using B20, 20% diesel can be saved but on other side, to achieve same performance, more fuel will be consumed with higher emissions due to low calorific value of biodiesel. Hence the EGR is implemented to reduce the emissions from the engine.

When engine is operated with B20 blend and various EGR rates, following observations are made. For 10% EGR, BSFC is 14% higher, Brake thermal efficiency is 11% lower and EGT is 9% lower as compare to diesel. When 10% EGR is applied, CO emission increases by 14% and HC emission is 5% higher. For 10% EGR rate, NO_x emission is 56 % lower for B20 as compared to diesel. Results prove that with 10% EGR, 56% reduction in NO_x can be achieved with 5% increase in HC emission in addition to 11% loss of efficiency.

Taking all the results into consideration, B20 blend gives optimum performance of CI engine with major increase in NO_x emission. This NO_x emissions can be taken care with 10% EGR which reduces it by 56%. Hence a CI engine fuelled with 20% biodiesel blend and operated at 10% EGR can be a good alternative to the convention CI engine with reduced emissions and saving of fuel.

References

[1] Ming Zheng, Mwila C. Mulenga, Graham T. Reader, Meiping Wang, David S-K. Ting, Jimi Tjong, 2008. Biodiesel engine performance and emissions in low temperature combustion, Fuel, Vol. 87, pp. 714-722.

[2] Magin Lapuert, Octavio Armas, Jose Rodri guez-Fernandez, 2008. Effect of biodiesel fuels on diesel engine emissions, Progress in Energy and Combustion Science, Vol. 34, pp. 198-223.

[3] A. Demirbas, 2007. Importance of biodiesel as transportation fuel. Energy policy, Vol. 35, pp. 4661–4670.

[4] Gaurav Paula, Ambarish Datta, Bijan Kumar Mandal, 2014. An Experimental and Numerical Investigation of the Performance, Combustion and Emission Characteristics of a Diesel Engine fuelled with Jatropha Biodiesel. Energy Procedia, Vol. 54, pp. 455-467.

[5] Y.Ali, M.A.Hanna, S.L.Cuppett, 1995. Fuel Properties of tallow and soya bean ester. Journal of American Oil Society, Vol. 72, pp. 1557-1564.

[6] Wang Ying, Zhou Longbao, 2008. Experimental study on exhaust emissions from a multi-cylinder DME engine operating with EGR and oxidation catalyst.Applied Thermal Engineering, Vol. 28, pp. 1589-1595.

[7] Anthony Dubreuil, Fabrice Foucher, Christine Mounai m-Rousselle, Guillaume Daym, Philippe Dagaut, 2007. HCCI combustion: Effect of NO in EGR. Proceedings of the Combustion Institute, Vol. 31, pp. 2889-2886.

[8] Nakka Satyanarayana, Vinaychandra Jha, Y.V Hanumantha Rao, 2017. Performance and Emission Characteristics of Diesel Engines fuelled With Jatropha oil Methyl Esters. International Journal of Emerging Trends in Engineering and Development, Vol. 2, pp. 134-141.

[9] Pratik G. Sapre, Kunal A.bahgat, 2014. Emission characteristics for single cylinder DI diesel engine with EGR system. International journal of engineering sciences & research technology, Vol. 3, pp. 315 – 323.

[10] Mohamed Y.E. Selim, 2003. Effect of exhaust gas recirculation on some combustion characteristics of dual fuel engine. Energy Conservation and Management, Vol. 44, pp. 707 -721.

[11] Joshi N, Lakdawala A, Shah N, Patel R, 2013.Effect of biodiesel diesel blends on the performance of compression ignition engine. Proceedings of International conference on alternative fuels for IC Engines, pp. 327 - 330.

[12] C. Srinidhi, S.V.Channapattana J.A. Hole, A.A. Pawar P.G. Kamble, 2014. Investigation on Performance and Emission Characteristics of CI Engine fuelled with honne oil Methyl Ester. International Journal of Engineering Science Invention, Volume 3, pp.59-66.

[13] A. Mohebbi S. Jafarmadar and J. Pashae, 2012. Performance Evaluation and Emissions improving of Turbocharged DI Diesel Engine with Exhaust Gas Recirculation (EGR). International Journal of Automotive Engineering, Vol. 2, pp. 35-47.

[14] Patel P, Lakdawala A, Chourasia S, Patel R, 2016. Bio fuels for compression ignition engine: A review on engine performance, emission and life cycle analysis. Renewable and Sustainable Energy Reviews, Vol. 65, pp. 24–43.

Load balancing Improvement through Flexible Assignment of Jobs in the Grid

Akash Mehta[a*], Prakash Patel[a], Jalay Maru[a]

[a]*Gandhinagar Institute of Technology, Gandhinagar, Gujarat 382721, India*

Abstract

Grid computing has emerged as a striking dividing concept due to the availability of high speed WAN & a low cost computing capital. This paper represents a novel load harmonising algorithm for network by consenting for node appeal. The set of partners are fashioned for apiece node using the prestige of the job. For each job, in the gird, the proposed algorithm uses the popularity of other nodes in the grid to arrangement k number of buddies and p time of nationals. The methods for constructing neighbours and buddies are prevailing. A new job received to a node is proximately dispersed to the originating node it or to its companion nodes. The load tuning is agreed unremittingly and common material government is used to minimize the communication overhead in the projected load balancing procedure. The proposed procedure is self-motivated, sender-initiated and decentralized.

Keywords: Grid computing, heterogeneous, load balancing, job, wide area network, nearest neighbour.

1. Introduction

The advances in computers and communications have distorted society noticeably. At the same time, the computers can pool resources with the budding high-speed networks by creating massive computing power which helps in running advanced computational exhaustive jobs, in a smallest time.
Several certain computers or workstations are supportive to form collection systems which shall be used to run disseminated tenders through a high speed system. The deficiency of using the cluster schemes is, they are constrained to a fixed area, construction the job immobile in terms of its presentation.
The geologically detached cluster systems associated by a network form computational grid for implementing distributed jobs .As compared with the predictable clustered systems, grid totalling uses internet connections to provide large scale resource sharing and improved resource utilisation. A Grid computing offers more processing power and quality of service in executing scientific jobs rather than the cluster systems. It also reduces the answer time of the jobs. Computing networks will appear as next cohort computing and it will a noteworthy substitute for the addition problems in engineering, academic and government clusters.
Resource organization models: There are two kinds of resource organisation models and consistent metrics.
System Centric: The grid comprises of autonomous jobs which are compiled at dissimilar periods and necessitate dissimilar extents and possessions for their employ. When a job influences at a lattice, the scheduler will examine the load complaint of every node and selects one lump to route the job. The expansion policy at this point must increase the total protest of the whole organisation. The development system must distinguish the load harmonising and increase the system material and resource feeding, if the grid system is profoundly loaded. In this paper, this type of development is private as "system-centric scheduling", for which the detached is to augment system routine. The main focus here is the system –level reserve.
Application Centric: The number of tasks of a parallel submission attains within a unit development time – slot, the preparation system will distribute a node and appearance it in terms of a distinct neutral. Usually, the disconnected is the minimal assumption time for the entire submission. Here the grounding policy is suggestion oriented and hence it is mentioned a bid centric arrangement.

2. Considerable transfer cost.

The transfer cost of unapproachable job performance at the local area network can be overlooked because the processors in the LAN are connected through a high speed system. However, the conversion cost is a concern for the scheduling process to execute the job in the inaccessible system in the grid, due to the low speed Internet links

* Akash Mehta. Tel.: 8460543289
E-mail address: akash.mehta@git.org.in

Uneven job arrival pattern: The operation of computers outdoes the maximum bulk at peak intervals and drops to a minimum in the night hours. A bursts traffic produced by the nodes in the grid atmosphere will be balanced by allotting the workloads to different clusters. Hence, load harmonising optimises the supply usage and conniving a load balancing procedure in a grid atmosphere is more complex. The main stimulation of this study is to commend, regionalized go-ahead load harmonising elucidations that can supply to these limited distinguishing of Grid totalling heaven.

2.1 Literature Review

There exists many load harmonising algorithms in the works. Cataloguing of the load balancing procedures is beneficial for the enterprise and scrutiny of new load matching developments.

2.2 Non-pre-emptive versus pre-emptive

Active load balancing strategies may be pre-emptive or non- pre-emptive. A non-pre-emptive load opposite policy allots a new job to a greatest node in the organisation. Once the job performance initiates at that bulge, it is not stimulated even if the bulge run time features modification. Though it is necessary that the load at each bulge need not be completely steady. This stuff allows inventing load complementary structures that deal with great grain separation of the assignment such as errands and it does not demand high rapidity declaration among nodes.

In distinction, a pre-emptive cargo harmonising will complete load harmonising between the nodes when an unevenness exists between the bulges. A work can be removed to added bulge even if the job is in its progression of accomplishment. Originally, nevertheless load circulations across nodes seem to be composed, they will developed unstable as shorter jobs comprehensive and leave behindhand a jagged distribution of lengthier jobs. Job immigration allows these disproportions to be amended among the nodes. However, job immigration in course of performance incurs more upstairs which consequences in performance dilapidation. If the pre-emptive guidelines are endeavoured in loosely coupled organisations, more communications are to be produced among the nodes and it will origin bottleneck in the announcement system which will outcome in the organisation recital poverty.

2.3 Node-level versus grid-level

When a job reaches to a node, the load –opposite procedure of the bunch will investigate the load condition of each and every node in the bunch and will choice an fitting node to route the work.

2.4 Centralised versus distributed

Load balancing policies can be classified as centralized or distributed. In centralized strategies, there will be one master node which will take choices about development. The master node assigns afresh incoming jobs to dissimilar dispensation bulges. The info gathering about job entrances and partings will be relaxed in the federal strategies. The main drawback of federal strategies is the conceivable recital and consistency blockage due to the conceivable hefty load on the principal lump. For this cause, federal strategies are untimely for great scale organisations.

The supply policy is raised as discrete optimum procedure, in that individually job improves its own answer time autonomously of others. [10, 3].

System Model

The trade prototypical defines the information about the job required by the load balancing algorithms. The load balancing algorithm is designed in such a way that it has to reduce the chances of job thrashing and starvation at any node. The performance objective of the load balancing algorithm will be system utilization and normal answer period of the works.

Architecture model

The clusters consist of N number of processors and the communication bandwidth is shared by all the processors. The previous research such as condor and Load sharing facility has addressed the management of the jobs at cluster level.

The heterogeneity in system can be expressed in terms of processors speed, remembrance and diskette I/O.

Announcement model

The nodes ***N*** are entirely organised and there occurs at least one announcement track among each two nodes in N. The message passing mechanism is used as a communication between the nodes and there exists a handover interruption on the communication system amongst the bulges. The handover delay is diverse among unlike pairs of lumps. The original network decorum pledges that letters sent across the system are customary in the command referred.

Two strictures such as a handover interruption and data programme rate are used to characterise the system recital between any two bulges (n_i,n_j). Transfer time compulsory for transfer a memo of Q bytes among two bulges is assumed by

$$TD_{ij} + \frac{Q}{BW_{ij}}$$

The above equation represents the whole time compulsory to cross all of the associations on the pathway among n_i andn_j. BW_{ij} is represented as active data relocating rate in bytes per unit spell or is categorised in rapports of kb/s. TD_{ij} contains a start-up charge and suspensions sustained by cramming at midway links on the path amongst $n_i$and n_j.

For a given node n_i ∈N, jobs will arrive to the nodes belong to C_i , where Ci denotes the cluster consisting of N nodes. The entrance of jobs are accidental with an normal delay,λ, among two succeeding entrances and shadow poisson rate and the delay among the onsets will be Exponential circulation. The jobs can be executed at any node and are computationally intensive. The execution of the jobs are not time common and can be implemented at any solitary protuberance. The job is allotted to accurately one node for performance and on achievement of job, the fallouts will be transported to the inventing bulge of the work. The set of all works produced at node S will be signified as J= $\{\{j_1, j_2 \ldots j_r\}\}$. The organisation mechanically generates the subsequent strictures associated near the job.

Performance objective

The major critical performance object in the grid computing is to minimize the response time of all jobs submitted in the system denoted by ART.

$$ART=\frac{\sum_{i=1}^{n} responsetime\ \ (j_i)}{n}$$

The performance of the projected procedure is gauged by its upgrading factor over the another algorithm X as trails in terms of normal answer time of professions

$\frac{ART\,(X)-ART\,(A)}{ART\,(X)}$, Where ART (A) signifies the normal answer time of jobs using procedure A and ART(X) denotes the normal answer time of jobs by procedure X. A positive value specifies an enhancement over the prevailing process and undesirable value suggests the dilapidation over the prevailing process.

3. Proposed Method

A novel load balancing procedure for heterogeneous systems has been accessible in this paper with deliberation of job passage to the remote nodes. Job immigration from a local node to remote node deliberates processing power of a remote node and the announcement delay to the remote node. The load harmonising algorithm for each node n_i forms a set of K partners and C neighbours and the material collection overhead from the national and partner nodes are reduced by using reciprocal information organization (RIM). The algorithm presented in this paper is dynamic, sender-initiated and regionalized. Job that arrives at each node n_i is allotted either to n_i or to its neighbouring nodes. The adjustment of loads has been made continuously among neighbours of noden_i.

Resource -aware load-balancing algorithm (RWLB)

Many prevailing courses in the text have second-hand a sudden run crocodile extent (the number of works actuality facilitated or to instigated for establishment at arranged instantaneous) as the weight guide. The time required for calculating the load index is based on the queue length of the node. The load index of a node consisting of more than one CPU is calculated based on the total queue length of that node divided by the number of CPUs at that node. The limitations such as average dispensation power and the assignment delay are used to assign a job to a node in the node.

The node- collecting procedure contemplates N number of nodes for the meting out power of each node n_i. The bulges are nominated haphazardly in such a procedure that the allowance influence of separately node swerves large adequate with extra node. The nodes are organized by exemption supremacy in descendent order former daubing node-clustering practice. A situation course $<d_1, d_2, d_3 .. d_n>$ is prearranged based on the modification in dispensation power Pi of node n_i to the other nodes in the scheme and nodes with comparable position vector adjacent to each other in terms of dispensation power are bunched into $c_1, c_2, c_3 .. c_m$ collections. Lastly empty

bunches in $c_1, c_2, c_3..c_n$ are uninvolved so that only $c_1, c_2, c_3..c_q$ ($q \leq m$) will continue in the order of lessening regular dispensation power.

Partners

Each node n_i has K number of companion nodes P_{set} used by the scheduler to choice companion nodes for conveying newly arrived jobs. When a node connexions the lattice organisation, it will regulate its cohorts. An unassuming empirical is employed to find partner nodes including heterogeneous nodes in terms of their computing power. An algorithm to select associates for the protuberances is accessible in the below procedure.
A preferable gathering of nodes of Nof methods a set Q_i used in planned Associates Alteration Policy have greater or analogous meting out power to node n_i .The set of favourite nodes Q_i will be rationalised by the process as essential. The above method may not promise in conclusion the optimum cohorts, however it may provide ascendable and effectual method in the initial development of companion nodes.

Neighbours

The set N_{seti} maintains C number of neighbouring nodes by each node n_i . The scheduler will reduce the communication cost by selecting the neighbouring nodes for migrating the jobs and hence reduces the transfer delay for the weight undertaking and permit quick answer to load disparities. The nationals have been nominated in such a way that bulges are lightly encumbered and smallest transfer delay amongst the sender node and the earpiece node. n_j is considered as neighbouring node to n_i if the communication delay between the nodes n_i and n_j is minimum. The neighbouring nodes are sorted in the ascending order based on the transfer delay and the least ranked node is chosen as the nearest node. The transfer delay is described as follows:

$$\varepsilon = \frac{TD_{ji}}{TD_{near}}$$

The transfer delay from node n_j to node n_i is denoted by TD_{ji} . The transfer delay from the nearest node of n_i is denoted by TD_{near} .

Information policy

The reciprocal information management system restricts the load information exchange to partner and neighbouring nodes ton$_i$. When a node n_i handover a job j_x to its national or partner node n_j for processing,. Node n_i affixes load material to itself, r_p , accidental nationals or allies who have sent the job handover request TR to n_j . The load material is rationalised by n_j by associating the timestamp, by examining whether a demand is from it is nationals or associates. Also n_j inserts its contemporary load material and r_p radon protuberances from its N_{seti} and P_{seti} in the job recognise AR or completions reply CR to n_i, So n_i can bring up-to-date its state matters.
Transfer policy and location policy
The handover and position strategies used in the planned algorithm are combination of instantaneous and load adjustment policy.

Instantaneous Distribution Policy

The instantaneous distribution policy is used to decide whether a new job is assigned to the originating node or one of its neighbour nodes. If the existing neighbour nodes of n_i are overloaded then the job is put in the global queue of n_i which is later scheduled to run on the partner nodes. This policy will attempt to regulator the job dispensation amount at respectively node and extremely computing jobs are route on the tall end protuberances or very less loaded bulges. If there are two companion nodes with the same smallest load, the adjoining companion node is selected for implementing the job and this can lessen the announcement interruption. Algorithm 4.4 designates the IDP for n_i

Load Adjustment Policy

The Load modification procedure reduces the load difference between nodes i and its neighbour nodes by relocating jobs from profoundly loaded nodes to the informally loaded bordering nodes. This strategy is generated when the freight material is received by node I from its neighbouring nodes. This policy uses the most recent load information to decide to initiate the transfer of jobs. The threshold policy used in this method is dynamically adjusted based on the system load and the nodes with loads developed than the regular load of the organisation are measured as dispatchers and the last job to originated in the bulge I is measured as the applicant

for transfer to the remote node. If the neighbouring nodes have the same minimum load, then the candidate node for transporting the job is chosen based on the network delay. The node with less transfer delay as considered for transferring the job.

4. Results And Discussion

In this paper, Sender-Initiated algorithms are used aimed at routine estimation. The planned procedure (RWLA) is associated with two of the dominant algorithms in the literature. Aimed at the NB, each protuberance is limited to collect load gen after inside its personal sphere, which entails of herself and its nationals. The load harmonising deed is invented if a load of protuberance outdoes the normal load of its scope.

Table 2: Heterogeneous system configurations

Heterogeneous systems	Average processing power
1 To 8 nodes	0.1
9 to 16 nodes	0.2
17 to 24 nodes	0.5
25 to 32 nodes	1.0

Effect of system size

The simulations have been carried out for varying system sizes to check for the stability of the proposed and existing algorithms. Both algorithms are scalable and stable. However the average response time offered by the proposed algorithm is better than the diffusive load balancing algorithm. The results are shown in the figure 4.2

Conclusion

The resource aware dynamic load balancing algorithm (RWLB) proposed in this paper by considering the scalability of the grid system which consists of heterogeneous processing nodes and addressed considerable communication overhead involved in collecting the information from the various nodes in the grid. The simulation revealed the performance of the proposed load balancing algorithm equated with the prevailing distribution load harmonising procedure and the untried results show that the proposed algorithm has done recovering than the dissemination load harmonising process and diminishes the typical rejoinder time of the trades.

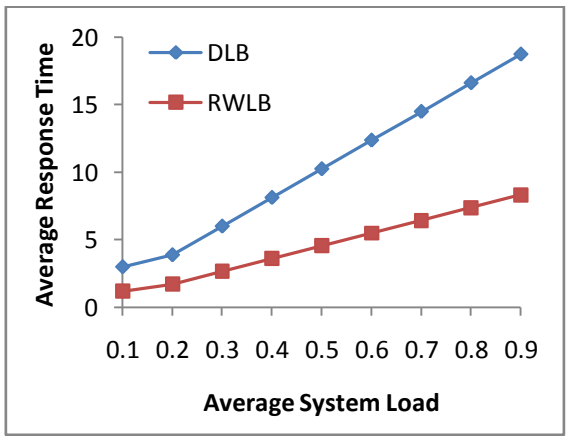

Figure 4.1: Effect of System heterogeneity

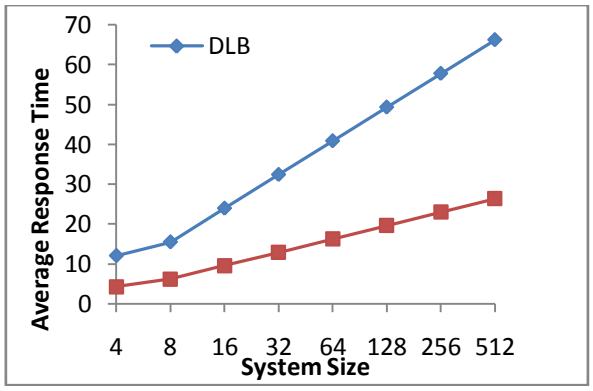

Figure 4.2: Effect of System Size

References

[1] Robert Elsässer, Burkhard Monien, and Robert Preis. 2000. Diffusive load balancing schemes on heterogeneous networks. In *Proceedings of the twelfth annual ACM symposium on Parallel algorithms and architectures* (SPAA '00). ACM, New York, NY, USA, pp. 30-38. DOI: https://doi.org/10.1145/341800.341805

[2] S. F. El-Zogdhy, H. Kameda, and J. Li, Numerical studies on a paradox for noncooperative static load balancing in distributed computer systems, Computers andOperations Research, 33(2) (2006) pp. 345-355.

[3] S. Penmatsa, A.T. Chronopoulos, Cooperative load balancing for a network of heterogeneous computers, in: Proceedings of the 20th IEEE International Parallel and Distributed processing Symposium, 25-29 April 2006 Page(s):8.

[4] Z. Zeng and B. Veeravalli, Design and analysis of a non-preemptive decentralized load balancing algorithm for multi-class jobs in distributed networks, Computer Communications, 27(7) (2004) pp. 679-694.

[5] K. Lu, R. Subrata**,** and A. Y. Zomaya, An efficient load balancing algorithm for heterogeneous grid systems considering desirability of grid sites, in: Proceedings of the 25th IEEE International Conference on Performance, Computing, and Communications, 10–12 April 2006, Phoenix, Arizona, USA.

[6] K. Lu, R. Subrata**,** and A. Y. Zomaya, Towards decentralized load balancing in a computational grid environment, in: Proceedings of the first International Conference on Grid and Pervasive Computing, May 3-5, 2006, Taichung, Taiwan, Lecture Notes in Computer Science (LNCS), Vol. 3947, pp. 466- 477, Springer-Verlag Press.

[7] K. Lu and A. Y. Zomaya, A hybrid policy for job scheduling and load balancing in heterogeneous computational grids, in: Proceedings of the 6th IEEE International Symposium on Parallel and Distributed Computing, 5-8 July 2007, Hagenberg, Austria.

[8] Jia Z. A Heuristic clustering-based task deployment approach for load balancing using Bayes Theorem in cloud environment. IEEE Transactions on Parallel and Distributed Systems. 2016; 27(2): pp. 305–316.

[9] Kunjal G, Goswami N, Maheta ND. A performance analysis of load Balancing algorithms in Cloud environment. 2015 International Conference on Computer Communication and Informatics (ICCCI), IEEE; 2015.pp. 4–9.

[10] Ashok, A.S., Hari, D.P., 2012. Grid Computing: various job scheduling strategies, emerging trends in computer science and information technology. In: Proceedings of the International Conference on Emerging Trends in Computer Science and Information Technology-2012 (ETCSIT-2012), Mar.

[11] Ruay-Shiung Chang , Chih-Yuan Lin , Chun-Fu Lin, An Adaptive Scoring Job Scheduling algorithm for grid computing, Information Sciences: an International Journal, 207, pp.79-89, November, 2012.

Bandwidth utilization scheme for MIMO Co-operative Networks with 3G/4G Networks

Mohit Bhadla[a*], Swapnil Panchal[b], Dhaval Vaja[b]

[a]*Research Scholar, Rai University, Saroda, Dholka -382260, India*
[b]*Gandhinagar Institute of Technology, Gandhinagar- 382721, India*

Abstract

Cooperative systems administration is known to have noteworthy potential in expanding system limit and transmission unwavering quality. Presently in a day's impromptu systems, most works are constrained to the fundamental three-hub hand-off plan and single-antenna wire frameworks. These two constraints are interconnected and both are because of a restricted hypothetical comprehension of the ideal power designation structure in MIMO Cooperative Networks (MIMO-CN). We additionally measure the execution increase because of helpful transfer and build up an association between agreeable hand-off and unadulterated hand-off. In this postulation, proposed philosophy has been introduced. This proposed framework is executed in Matlab 2013a. It will show to us some influenced parameters are Network Capacity, offloading movement, covered cell with one zone to another region we utilized here in calculation DR calculations and Reduce Overhead Signaling. The intermittent scope of macrocell causes the expanded enrollment flagging overhead in the femtocell and macrocell organize where the thick femtocellls covered with a macrocell are divided into little Tracking Areas (TAs). After examination another approach known as Delay Registration (DR) calculation is proposed for overhead diminishment with the cost of giving up the activity offloading capacity of the femtocell and macrocell in such case.

Keywords: Famtocell, Macrocell, DR Algorithm,MIMO-CN,DF-DT System.

1. Introduction

Cooperative correspondence is like the hand-off channel model to some degree yet varies fundamentally in that every remote client is expected to both transmit information and additionally go about as a cooperative operator for another client. At the end of the day, cooperative flagging conventions ought to be planned so clients can help different clients while as yet having the capacity to send their own particular information [1]. Collaboration prompts intriguing tradeoffs in code rates and transmits control. On account of energy, it might appear that more power is required on the grounds that, in cooperative mode, every client is transmitting for both itself and an accomplice. In any case, the point to be made is that the pickup in assorted variety from participation enables the clients to decrease their transmit controls and keep up a similar execution. Notwithstanding this exchange, one trust in a net decrease of transmits control, given everything else being consistent. In cooperative correspondence, every client transmits the two its own bits and in addition some data for its accomplice, so it might give the idea that every client requires more bandwidth. Then again the phantom effectiveness of every client enhances in light of the fact that, because of collaboration assorted variety, the channel code rates can be expanded. Accordingly, in non-cooperative correspondence clients send specifically to a typical goal, without rehashing for each other. In cooperative communications, autonomous ways between the client and the base station are created by means of the hand-off channel. The transfer channel can be thought of as a helper channel to the immediate channel between the source and goal. A key part of the cooperative correspondence process is the preparing of the flag got from the source hub done by the hand-off. These distinctive handling plans result in various cooperative communications conventions. The preparing at the hand-off contrasts as indicated by the utilized convention. Cooperative communications conventions can be for the most part arranged into intensify and forward and interpret and forward transferring plans. [2]

2. System Analysis and Problem Outcomes

Consider a multi-source and multi-hand-off system with M source hubs and N transfer hubs as appeared in Fig.1. [8]. Here it is accepted that, immediate transmission isn't conceivable and one source has just a single accomplice to help for data transmission, i.e. single hand-off choice. The convention utilized by hand-off is interpret and forward. (DF). In this technique, each source hub is associated with one hand-off. The channels from source hubs to transfers and the channels from transfers to goal are unidirectional. [4]

* Mohit Bhdla Tel.: +91-7600403738
E-mail address: mohit.bhadla@git.org.in

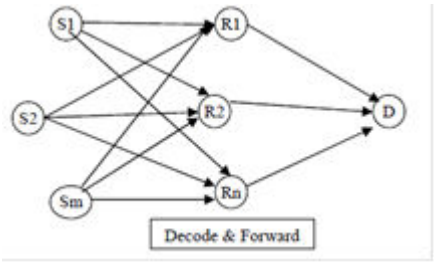

Fig 1: Wireless networks and M Sources and N Relays [3]

The sources are assigned to relays in such a way to minimize the total power consumption in the network. The problem of power minimization can be stated state mathematically as follows:

$$min\left(\sum_{i=1}^{M} P_{s,i} + \sum_{j=1}^{N} P_{r,j}\right)$$

$$\text{s.t.} \quad P_{s,i} > 0, \quad P_{r,j} > 0$$

$$\sum_{i=1}^{M} P_{s,i} \leq P_{s,max}$$

$$\sum_{j=1}^{N} P_{r,j} \leq P_{r,max}$$

Fig 2: power minimization [4]

3. Related Work

Above all else, for the hand-off choice, control framework is created, in which transmission control for each source with each transfer is ascertained [8]. At that point introduce the components in the transmission control network, which can be communicated as demonstrated as follows.

$$\begin{bmatrix} P_{1,1} & \cdots & P_{1,N} \\ \vdots & \ddots & \vdots \\ P_{M,1} & \cdots & P_{M,N} \end{bmatrix} \ldots.[1]$$

Fig 3 : components in the transmission control network [4]

This calculation can be utilized to choose suitable hand-off hub in the cooperative condition with a specific end goal to limit the transmission energy of source-hand-off sets and in addition the transmission energy of the entire system. The stream diagram of calculation is appeared in fig 2. Set of source hubs is meant by S and set of transfer hubs are signified by R individually. P1 means the underlying transfer distribution, P2 indicates the middle of the road hand-off portion and P3 signifies last hand-off designation. The calculation comprises of three stages: Initial stage, Intermediate stage and last stage. [3]

The transfer designation in Initial stage is known as introductory hand-off allotment, (Fig.2) which is meant by P1. In this stage, for one source the transfer is being chosen such that the source-hand-off combine has least power utilization. Along these lines transfer choice is done until the point when all the source hubs have been assigned. The hand-off designation in Intermediate stage is known as Intermediate hand-off distribution, (Fig.2) which is signified by P2. In this stage, trade of hand-off is done M times for the power diminishment. From P1 the most extreme power expending pair (I, j) is chosen. At that point another source and hand-off combine (y, z) from beginning stage, which can swap the transfer to get the greatest power sparing, is being found. On the off chance that the source and hand-off combine (y, z) is found, erase past sets from P1, and include new matches in P2 and P1 individually. Rehash this procedure until the point when P1 is vacant. The transfer portion in Final stage is known as Final hand-off distribution, (Fig.2) which is signified by P3. Last stage utilizes a stage

comprising of a check to distinguish whether the aggregate power utilization because of source-transfer allotment in Intermediate Phase. [4]

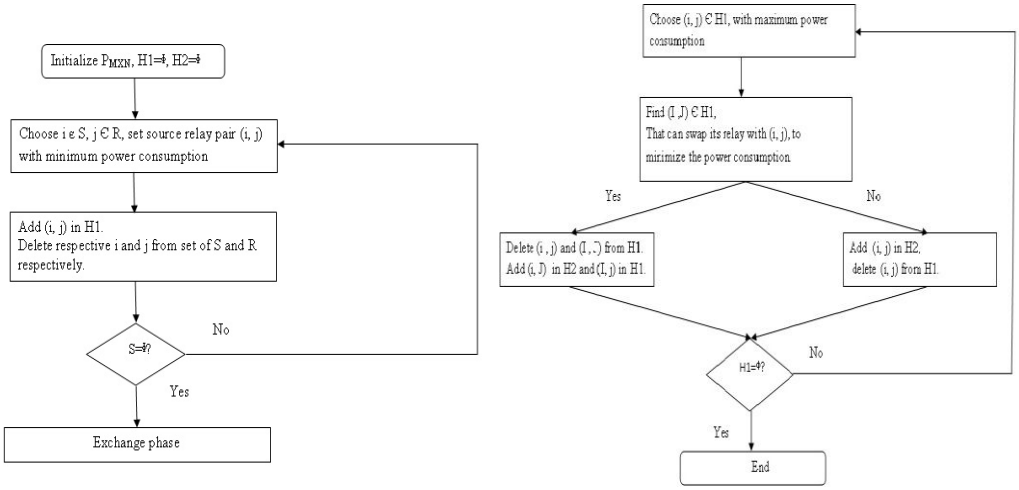

(a) (b)

Fig. 4: (a) Greedy Phase (b) Exchange Phase [6]

Is lesser than the corresponding power consumed in the Initial phase or not. And then relay selection is done based on the initial relay allocation or intermediate relay allocation which has lesser power consumption.

4. Simulations Results

Reproduction of this calculation is performed in recreation instrument MATLAB. In DF condition, expecting that the power assignment is as of now done; we consider 5 sources and 5 transfers for the reenactment reason, which can be changed according to necessity later on. From the recreation of the calculation it has been discovered that, it functions admirably in DF-DT framework. In DF-DT framework, Direct Transmission from source hub to goal is conceivable notwithstanding the transferred transmission. In the Second stage when a most extreme power expending pair (I, j) in P1 swaps its transfer with other combine (y,z) shaping pair (I, z), at that point source y stays without hand-off. In this way, now it can either made match with the transfer j which is left by the source I, or it can co-work with the rest of the transfers in the system, or can even decide on coordinate transmission. The impediment with calculation is that if there should be an occurrence of DF framework, where no immediate transmission is conceivable, the moderate stage designation tends to expand the aggregate power transmission. This is on account of, when match (I, j) i.e most extreme power devouring pair in P1, swaps its hand-off with (y, z) shaping (I, z), at that point the source y is compelled to make combine with j attributable to the way that there is no immediate transmission conceivable and different transfers are involved by various sources. This can build the aggregate power utilization of the source y transmission to the goal by means of hand-off j. So as to conquer this confinement of the first and second stage, we propose a last stage which wipes out the likelihood of increment in control utilization in the middle of the road stage. Table 1 demonstrates the source-hand-off combine and their relating power utilization and aggregate power in Initial Phase. Add up to control in First Phase is the aggregate transmission energy of the system. [4]

Table1: First Phase relay allocation

Source	Relay	Power Consumption
2	5	1.0714
1	2	2.9262
3	1	3.8096
4	3	14.5613
5	4	28.7848

Total Power in initial Phase=51.1532

Table 2: Second Phase relay allocation

Source	Relay	Power Consumption
2	5	1.0714
5	1	18.9708
4	3	14.5613
3	2	16.4064
1	4	4.2566

Total power in intermediate stage=55.2664

Table 2 demonstrates the source-hand-off match and their relating power utilization and aggregate power in second Phase. Add up to control in First Phase is the aggregate transmission energy of the system. As observed from Table 1 the greatest power devouring source-transfer match is 5-4 in P1 expending 28.7848 unit control. In Second stage as show in Table 2, source 5 trades it transfer with source 3 influencing pair to source hand-off 5-1 devouring 18.9708 unit control which is not as much as pervious combine 5-4. Be that as it may, however we prevailing with regards to decreasing force utilization of source 5, second stage has unwittingly expanded power utilization of source 3 from 3.8096 to 16.4064 units which in turns builds the aggregate transmission energy of the system from 51.1532 to 55.2664 units. In Fig.3, the code is keep running for 5 continuous circumstances with a specific end goal to see the impact of energy level of first Phase and second Phase; and the relating comes about have been appeared as Bar-chart. The cautious perception (Fig 3) of the diagram demonstrates that at first in the principal, third, fourth and fifth run the power in first Phase is successfully diminished yet in second run, it neglects to do as such. The explanation behind this is, second stage's endeavor to limit the power utilization of greatest power expending source hand-off match by hand-off trade, has expanded the general power utilization of the system. Subsequently Final hand-off determination isn't made based on P2, yet it is made based on P1 i.e introductory transfer distribution in beginning stage. From fig.5 we watch that the power utilization in definite stage never surpasses that in the second Phase.

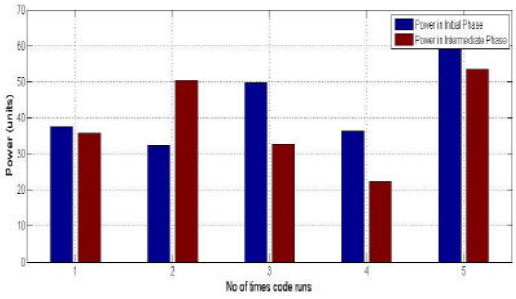

Fig 5: Power consumption in First phase and Second phase

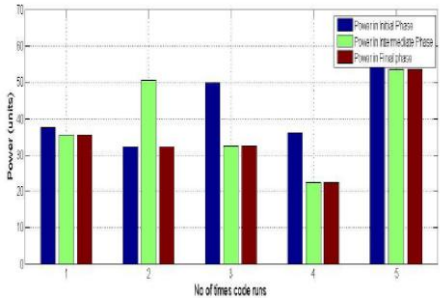

Fig 6: Power consumption in final phase

5. Final Investigations

We propose another arrangement for negligible exertion region organization in the femtocell and macrocell networek. It declines the phone reselection from the macrocell to femtocell, however keeps the most sensible femtocell data available at the Mobile Station which is used to trigger the handover to femtocell for development offloading when call arrives. It lessens the flagging cost incurred significant injury in the meantime securing the development offload capacity of the femtocell, however requires no any adjustment on the present system. The execution examination between our outcome and another approach named as DR calculation is directed with together the examination and recreation. The examination shows that our proposition better DR figuring in the cost diminish with the considerable adaptability to the differing Mobile Stations (MS) lead in high movability. Our last outcome is approving against the reproduction tests. They can be used for the execution evaluation on other multitier portable systems other than the femtocell/macrocell systems.

References

[1]J. Laneman, D. Tse, and G. Wornell, "Cooperative Diversity in Wireless Networks: Efficient protocols and Outage Beha vior," IEEE Trans. Info. Theory, vol. 50, no. 12, 2015, pp. 3062–80.
[2] P. H. J. Chong et al., "Technologies in Multihop Cellular Network," IEEE Commun. Mag., vol. 45, Sept. 2016, pp. 64–65.
[3] K. Woradit et al., "Outage Behavior of Selective Relaying Schemes," IEEE Trans. Wireless Commun., vol. 8, no. 8, 2016, pp. 3890–95.
[4] Y. Wei, F. R. Yu, and M. Song, "Distributed Optimal Relay Selection in Wireless Cooperative Networks with Finite-State Markov Channels," IEEE Trans. Vehic. Tech.,vol. 59, June 2016, pp. 2149–58.
[5] Q. Guan et al., "Capacity-Optimized Topology Control for MANETs with Cooperative Communications," IEEE Trans. Wireless Commun., vol. 10, July 2017, pp. 2162–70.
[6] P. Santi, "Topology Control in Wireless Ad Hoc and Sensor Networks," ACM Computing Surveys, vol. 37, no. 2, 2017, pp. 164–94.
[7] T. Cover and A. E. Gamal, "Capacity Theorems for the Relay Channel," IEEE Trans. Info. Theory, vol. 25, Sept. 2018, pp. 572–84.
[8] Q. Guan et al., "Impact of Topology Control on Capacity of Wireless Ad Hoc Networks," Proc. IEEE ICCS, Guangzhou, P. R. China, Nov. 2016.
[9] P. Gupta and P. Kumar, "The Capacity of Wireless Networks," IEEE Trans. Info. Theory, vol. 46, no. 2, 2017, pp. 388–404.
[10] M. Burkhart et al., "Does Topology Control Reduce Interference?" Proc. 5th ACM Int'l. Symp. Mobile Ad Hoc Networking and Computing, Tokyo, Japan, May

Study on Impact of Biodiesel on Various Metals used in CI Engine with Static Immersion Test: A Review

Sajan Kumar Chourasia[a*], Nilesh Sharma[a], Abhishek Pandey[a]

[a]Gandhinagar Institute of Technology, Gandinagar, Gujarat - 382721, India.

Abstract

Biodiesel has emerged as alternative fuel because of its environmental friendliness and it is biodegradability. Moreover, corrosion of metals in biodiesel is the major problem related to biodiesel compatibility with automobiles.In automobile engine, fuel is exposed to variety of engine parts including fuel injector, fuel pump, filters, gaskets, fuel liners, bearing, piston rings, piston, etc. Copper alloy based parts like fuel pump, bearing, bushing, etc. are mostly damaged by the fuel. Copper & its alloys, mild carbon steel, aluminium and stainless steel are few important metals widely used in diesel engines. Corrosion rate of metals in biodiesel diesel blends were found in the order of aluminium < mild steel < copper at different temperature conditions based on static immersion test as per ASTM G 31-72.

Keywords: Biodiesel, Corrosion and Immersion test

Nomenclature

ASTM	American Society for Testing and Materials
B0	0% Biodiesel 100% Diesel
B5	5% Biodiesel 95% Diesel
B20	20% Biodiesel 80% Diesel
B50	50% Biodiesel 50% Diesel
B100	100% Biodiesel 0% Diesel
B20D70E10	20% Biodiesel 70% Diesel and 10% Ethanol
B20D75E5	20% Biodiesel 75% Diesel and 5% Ethanol
BHT	Butylated hydro-oxy toluene
EDA	Ethylenediamine
mpy	Milli-inch per year
nBA	n-butylamine
PY	Pyrogallol
RME	Rapeseed methyl easter
TBA	Tert-butylamine
ULSD	Ultra low sulphur diesel

1. Introduction

Biodiesel is an alternative fuel to petroleum diesel. It is renewable and biodegradable fuel source consist of long chain of fatty acid methyl esters. Biodiesel can be produced from edible and non-edible vegetables, animal fat and waste cooking oils by the process of transesterification in which vegetable/animal oil is reacted with methanol/ethanol forming methyl/ethyl esters and glycerin. All the products and bi-products are utilized. Biodiesel is non-toxic, environmental friendly and biodegradable. As the petroleum diesel emits harmful gases after burning like oxides of sulfur, oxides of carbon, oxides of nitrogen etc. The high proportion of sulfur in diesel fuel generates great environmental problems. Biodiesel has low proportion of sulfur contents and it can eliminate these problems through its properties like inherent lubricity and environmental friendliness. Biodiesel has high tendency to get unsaturated. As compared to diesel, biodiesel absorbs more water which leads to corrosion and may result in choking.In automobile engine, fuel comes in contact with a variety of engine parts like fuel pump, fuel injector, gaskets, filters, piston, bearing, piston rings, fuel liners etc. Parts based on copper alloy like fuel pump, bearing, bushing, etc. are mostly affected by biodiesel. Copper, aluminium, mild carbon steel and stainless steel are important metals widely used in diesel engines. Auto-oxidation of biodiesel also affects its corrosive characteristics and also degradation of fuel properties. When oxidation of biodiesel occurs, it converts esters into different mono-carboxylic acids such as formic acid, acetic acid etc. which are mainly responsible for corrosion of automotive parts.

* Sajan Chourasia Tel.: +91-8347557041
E-mail address: sajan.chourasia@git.org.in

This process also increases the free water content. Free water is undesirable in automobiles because it promotes micro-bacterial growth and corrode fuel system components and also decreases compatibility with engine metals. Furthermore problems connected with biodiesel is that it is great sensitive towards light, moisture and working temperature.
The corrosion properties towards biodiesel can only be described using copper coupon corrosion test, such as ASTM D130 and for identification of corrosion rate ASTM G 31-72 which is "Laboratory Immersion Corrosion Testing of Metals" can been used. The results of these tests can be useful and supportive in identifying the application, suitable way of storage and transportation of biodiesel. The review is based on Static immersion test.

2. Effect of biodiesel on Copper & Copper alloys:

Nowadays, biodiesel is widely used as B5 blend (5% vol biodiesel). Due to some properties like incompatibility ofmaterials of fuel system, biodiesel in high proportion cannotbeen used. Corrosiveness is one ofthe major drawback to the biodiesel compatibility. If high concentration of free water and fatty acid are present, biodieselbecomes more reactive. Due to incomplete transesterificationreaction, freefatty acid may present in biodiesel. Corrosive property is also affected by auto-oxidation of biodiesel.In engine, fuel comes in contact with different engine parts like fuel pump, fuel injector, gaskets, filters, piston, bearing, piston rings, fuel liners etc. Fuel is highly reactive to copper alloy based parts [1]. Recent studies shows that copper, aluminium, zinc, brass and bronze are not suitable to biodiesel [2]. Geller et al. [3] observed that copper alloys are more aggressive to corrosion as compared to ferrous alloys. On bronze filters in oil nozzle after 10 h of operation with biodiesel at 70 °C pitting corrosion was observed [4]. Lower biodiesel (2%) blend are also showing corrosive properties [5].Due to oxidation, attack by microbes, humidity absorption, etc. bio oil degradation happens and it becomes extra corrosive. According to Tsuchiya. et. al. [5], at the time of oxidation bio oil changes esters into various mono-carboxylic acid like acetic acid , caproic acid, formic acid , , propionic acid, etc those are leading factors for the corrosive nature of bio oil. This method also rises the quantity of free content of released water. Concentration of released water quantity is unwanted because it endorses micro-bacterial development and also it disturbs the fuel pipe system [6,7]. As per Maleque. et al. [8] and Kalam. and Masjuki. [9], rate of wear in bio oil was found to be reasonably higher the main reason behind this is its corrosive and oxidative properties. Rate of Corrosion directly dependent on its supply feedstock [10,11]. Diaz-Ballote. et al. [12] observes that if minimum amount of impurities are present after processing the rate of corrosion bio oil is decreased. Further down in the presence of dissolved oxygen, aeration in side bio oil upsurges the rate of corrosion [5]. The main aim of the current analysis is to identify the oxidation and corrosion nature of bronze and copper in the palm methyl Easter bio oil. Static immersion tests has been conducted at normal room temperature ranging from 25 °C to 30 °C) and a other at a temperature of 60 °C. Outcomes of this test will help in behavior understanding of corrosion with respect to fuel line system for that working temperature is ranged between 44°C and 86 °C [13].

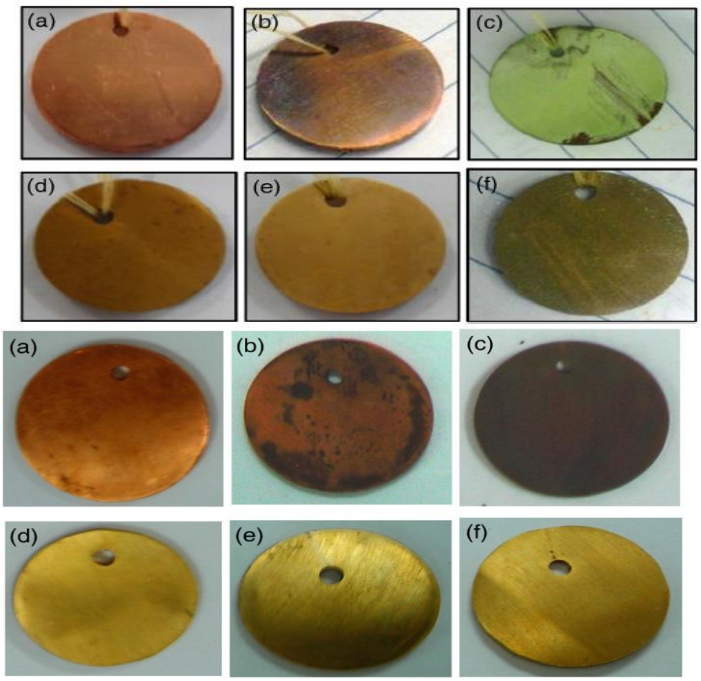

Fig. 1. Image of exposed metal above surface after the coupon immersion test at normal room temperature: Left side : a.) Copper in B0, b.) Copper in B50, c.) Copper in B100, d.) Bronze in B0, e.) Bronze in B50, and f.) Bronze in B100 & same for exposed metals at 60 ^{0}C right side image [14].

Corrosive nature of copper (99.9% industrial grade) and bronze with lead content (87.1% Cu, 6.2% Sn, 5.8% Pb etc.) on palm based bio oil has been examined by a immersion test at 2 temperatures (room temperature and 60 °C). In the case of normal room temperature ranging from 25 °C to 30 °C, static immersion tests in B0 (pure diesel), B50 (50% bio oil in mineral diesel) and B100 bio fuels were gone for the test for a duration of 2640 hrs. Similar static immersion tests was also performed with B0, B100 and oxidized B100 fuels at a temperature of 60 °C for 840 hrs. The rate of corrosion for leaded bronze and copper at normal room temperature and 60 °C are shown in Figs. 1. For both the metals, by increasing concentration of biodiesel in the blend its rate of corrosion increases. Biodiesel is more corrosive due to the existence of higher proportion of unsaturated and free fatty acids in palm bio oil like, linoleic acid and oleic acid which plays major role for vulnerability to react with metal surface. Rate of corrosion for each metal is relatively greater at 60 °C than at normal room temperature for both bio oil and diesel. The rate of reaction increases with increased temperature and it could lead to increased corrosion. It can also be said that total condensation of oxygen inside biodiesel from atmosphere compare to that at closed room temperature is more. If we see the temperature almost equivalent to room, rate of corrosion of bronze and copper in 100% pure biodiesel is obtained to be 0.018 and 0.042 mpy separately. Comparatively, at 60 °C, the corrosion rate for individually metals are relatively more, 0.0232 mpy for bronze and 0.0531 mpy for copper. Improved resistance towards corrosion bronze metal is due to presence of alloys such as tin (Sn). Kaul. et al. [11] perform a test of corrosion for piston metal at normal room temperature (15 to 40 °C because of climatically variation) for 7200 hrs in order to examine the reactiveness in terms of corrosion of biodiesel taken from various feed stocks. They identify that the rate of corrosion for piston (aluminum alloy) in curcus, mahua, salvadora, jatropha, kanarja, bio oil were found to be 0.0057 mpy, 0.01235 mpy, 0.0116 mpy, and 0.0057mpy, whereas in the case of diesel it was found to be 0.0057 mpy. A green colored oxide layer has been found on Copper surface which was immersed in B100 at normal room temperature, although it changes from green to black at the temperature of 60 °C. For the case of leaded bronze, coupons for test which were immersed at a temperature of 60 °C was found to be very much cleaner and having shining appearance compared to the test taken at normal room temperature. The layer of oxide colour depends on combine effect of testing temperature and coupon matal. Huang. and Tsai. [15] have advised that change in colour is an sign of changing copper into its own oxides and carbides due to temperature of reaction and dissolved oxygen quantity on the medium. At normal temperature, the reacted deposit oxide layer in copper for pure biodiesel appears to be carbonates of copper (CuCO3) of having pale green in colour. For related test coupon of metals were placed at a temperature of 60 °C, the layer of cupric oxide (CuO) having black colour texture were obtained at the surface of metal coupon is probably due to presence of high oxygen dissolved inside the biodiesel. M.A. Fazal et al. [37] examined the effect of mixing additives in palm biodiesel on copper, leaded bronze and phosphorus bronze. This experiment was conducted at normal room temperature (25 °C to 27 °C) for a duration of 90 days. For this experiment pure palm biodiesel B100 with and without additives, they have use additive with a maximum concentration of 500 ppm, the additives including benzotriazole, tert-butylamine, pyrogallol, propyl gallate, and butylated hydroxytoluene. They found that corrosion rate of copper was found to be significantly greater than those of the other copper metal alloys. XRD (X-ray diffraction) analysis shows the existence of copper carbonate and cupric oxide on the copper surface that was in contact with biodiesel. The existence of above mentioned composites could be attributed to the high composition of CO_2 and O_2 in the biodiesel when additive was not used. They claims and found that benzotriazole and tert-butylamine significantly enhanced the sustainability of biodiesel by reducing surface degradation of metals. Another work by same author claims that corrosion rates of copper was found to be meaningfully reduced by the use of PY addition as associated to that of BHT addition. It has been found that the corrosion inhibition efficiency of PY for copper is 93% while it is 73% for BHT. This result proposes that PY is more effective in corrosion reduction of copper in biodiesel compare to BHT, the main reason for this might be the organic molecules which donates electron like hydroxyl or methoxy can behave as free radical trapping agents which make them efficient corrosion inhibitors. [38].

3. Effect of biodiesel on Cast Iron:

Kaul et al. [8] claimed that biodiesel made from salvadora and jatropha curcas werehighly reactive for the material of piston liner in comparison to the metal of piston. Theconcentration the different metals for that alloys were not mentioned in that paper. On the baseof density claimed by the researcher in the paper, it seems that the density of piston metalwill be nearer to 2.221 g/cm^3 which is an alloy of aluminum while the metal of piston linerhaving a density of 6.10 g/cm^3 is a alloy of ferrous, maybe cast iron. From the immersion test based on both diesel and 5.0% methyl Easter fatty acid diesel blended, Tsuchiya et al. [17] examined corrosion rate of sheetsteel (Lead-8.0% tin layered rolled steel sheet) which is usually used forfabrication of take made for storage of fuel. Corrosion in the form of Pitting were found on the exposed samplewhich directly come in contact with biodiesel- diesel blended fuel. As researcher claims amine based additive fuel are commonly found to be more effective for both biodiesel and diesel, among the variety of amine only three of these been chosen for this investigation they are tert-butylamine (TBA), n-butylamine (nBA) and ethylenediamin (EDA). Cast iron has been selected in this review because it is widely used in manufacturing of various automotive based engine components like cylinder liner, piston ring, piston, etc. [18]. Corrosion rate of high graphite cast iron (C: 3.0%, Si: 1.83%, Mn: 0.821%, P: 0.097%, S: 0.09%, Fe: remaining) in existence or lack of various corrosion inhibitors

obtained in biodiesel were examined by static immersion test. Every coupon test were performed for a duration of 1200 hrs at normal room temperature. In the coupon corrosion test the average rate of corrosion was measured from two identical coupons made from high graphite cast iron, after the exposure with biodiesel made from palm for a duration of 1200 hrs at normal room temperature was obtained to be of 0.077 mpy. Rate of Corrosion of alike metal after the static immersion test in fatty biofuel- diesel blend 80% biodiesel in diesel for approximate 10 months at a temperature of 38.0 °C was found to be 0.193 mpy by Geller et al. [20]. They also found that the rate of corrosion for mild steel in mineral diesel and biodiesel were 0.045 and 0.0521 mpy respectively at normal room temperature. Rate of corrosion at a temperature of 80 ^{0}C found to be 0.049 mpy in mineral diesel and 0.06 mpy in biodiesel. Due to presence of water content, oxygen, fatty acid and impurities residual after treatment appears to rise the rate of corrosiveness in biodiesel in comparison with diesel fuel [16]. Higher rate of corrosion found in both biodiesel and diesel with increment in temperature could possibly be the reason for fast formation and suspension of product obtained in corrosion. Among this due to the presence of higher concentration of unsaturated acid components the rate of corrosion also increases [19]. On exposure to 1440 h exposure in biodiesel with and without antioxidants. It was found that the corrosion rates of mild steel upon addition of PY and BHT in biodiesel were almost similar. For mild steel, 33% inhibition efficiency was found with the addition of PY. They found that PY has significantly reduced the corrosion rate compare to BHT. This could be attributed to the fact that organic molecules incorporating an electron donating groups (hydroxyl), which can act as free radical trapping agents and make them efficient corrosion inhibitors. Hydroxyl radical corrosion inhibition efficiency of the compounds were mainly related to its antioxidant properties [38.]

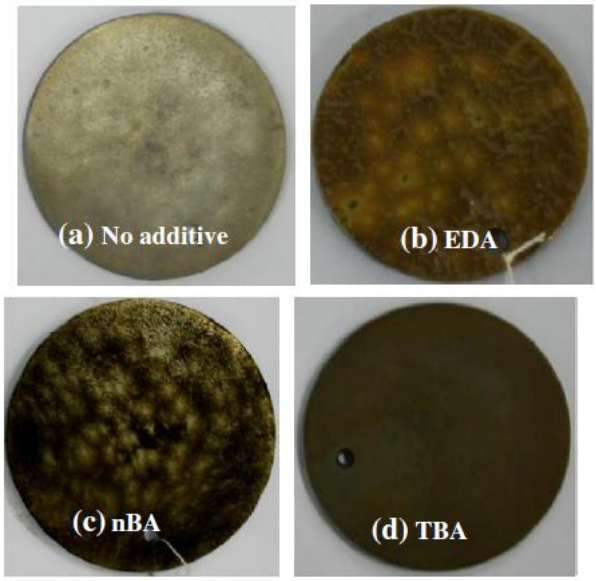

Fig. 2. Image of cast iron above surface which is exposure to palm biodiesel in the presence and absence of different inhibitors for corrosion. [21]

4. Effect of biodiesel on Aluminium:

M.A. Fazal et al. [23] used biodiesel of palm oil to different engine materials like stainless steel, aluminium andcopper and concluded that copper is a strong catalyst for oxidation in biodiesel. They stated that aluminium is less reactive as compared to other metals. Aluminiumand copper are used because they are widely used in engine parts and they are in constant contact with fuel. For example the composition of cylinderheads, engine block and piston are pure aluminum and aluminum alloys having percentages of Aluminum of 70%, 19% and 100% respectively [23,24]. Corrosiveness of copper and aluminum were examined bystatic immersion test at a temperature of 80 °C for a duration of 600 hrs. The corrosive test were performed in the fuel mixture of RME and ULSD, 8 testsample were taken for four rapeseed oil (RME) having percentages concentration of 0%, 50%,75% and 100 vol.% and two different metals coupons of aluminum were exposed with the fuel. The coupons made from metal were immersedinside the diesel- biodiesel blend for around 600 hrs at a temperature of 80 °C. Due to huge concentration of unsaturated fattyacids for oleic acid (C18:1) (68.791%) and linoleic acid (C18:2) (19.492%), it can increase the corrosion rate of rapeseed biodieselcompared to low sulphur diesel fuel. Due to presenceof oxygen particles in biodiesel, it can increase the corrosiveness. Kaul et al. [22] reported that due to unsaturatedfatty acids in the biodiesel it has higher corrosivenesscompared with diesel. Also Fazal et al. [23] reported that unsaturated fattyacids increases the corrosiveness of palm biodiesel.Slightlywarm temperature for the test was selected to simulate the real enginesituations as several fuel chain systems in mineral diesel engines are operated at a temperatureof80 °C. Rate of corrosion for aluminumexposed to rapeseed biodiesel, the test was conducted at a temperature of 43 °C for a duration of 60 days was obtained to be0.0033 mm/y. likewise by various authors who claimed for normal room temperature, the corrosion rate for aluminium was found to be 0.0681 mpy and 0.0614 mpy immersed in B20D70E10 and B20D75E5, which issomewhat greater in

comparison to pure diesel 0.0514 mpy. As associated to earlierstudies [26,28,30], values were found lower. At the temperature of 60 ^{0}C, the corrosion rate of aluminium is found to be 0.217 mpy and 0.211 mpy in B20D70E10 and B20D75E5. The claimed values are equivalent to Fazal et al. [25] and Huet al. [27]; furthermore, these results are found to be lesserthan Cursaru et al. [16] and Norouzi et al. [29].According to Hu et al. [27], aluminium is best alternative for evolutionof metal oxide films which stops the oxidation. The metal oxide film protects aluminium from oxygen which stop the fuel connectionwith metal surface and it results in low corrosiveness. Fig. 3 shows the analysis of metal corrosion products subjected to fuel blends at room temperature (25-30 ^{0}C) and 60 ^{0}C. The surface of the metal was damaged due to corrosion on metal surface when exposed to Biodiesel diesel ethanol (BDE) blends as compared to the metal surface received originally (as shown in Fig. 3). A layer of oxides covers the aluminum metal surface, which protects the aluminum metal from corrosion.

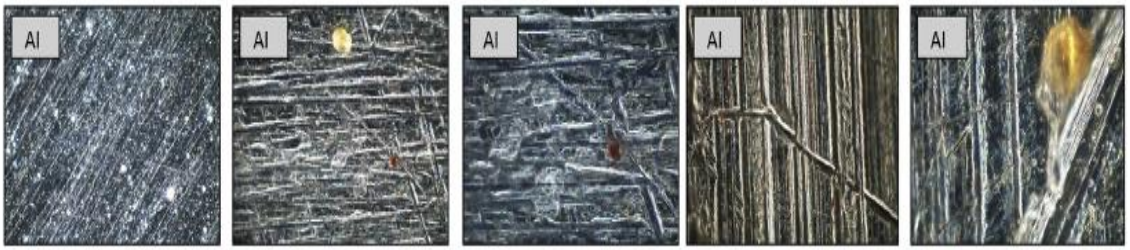

Fig. 3. Microscopic Image of Aluminium at (100X) magnification presenting the morphology of corrosion on the above surface of aluminium metals after immersion at normal room temperature and at 60 ^{0}C [31].

5. Effect of biodiesel on Magnesium:

Recently the development in automobile sector is related to the problems due to fuel consumption and weight reduction. Therefore researches are carried on for the light-weight metals [32]. Light metal can enhance the engine performance and ir can decrease the energy consumption. At present, light-weight non-ferrous metals such as Al, Mg are widely used to replace the heavy-weight like cast iron blocks. Use of light metals results in the decreased fuel consumption and enhanced engine performance. Magnesium is relatively 35% lighter than aluminium and shows similar level of strength [33,34]. The research has been carried out for corrosion characteristics of aluminium and magnesium in palm biodiesel. The static immersion tests were conducted at normal room temperature between (25 to 27 ^{0}C) for a duration of 720 hrs and 1440 hrs. For the static immersion test with a duration of 720 hrs, 3 coupons and 60.0 ml of biodiesel were taken out from each glass container.
Rate of corrosion for aluminium with a duration of 720 hrs and 1440 hrs were found to be 0.123 mpy and 0.0526 mpy. Rate of corrosion for magnesium is very much high around 3.091 mpy for 720 hrs and 2.6564 mpy for 1440 hrs. With the increase of immersion test time, the rate of corrosion decrease for both aluminium and magnesium. Fazal et al. [36] also studied that rate of corrosion of aluminium slightly decreases with immersion time. It can be concluded from the above data that magnesium shows higher corrosion rate compared to aluminium.

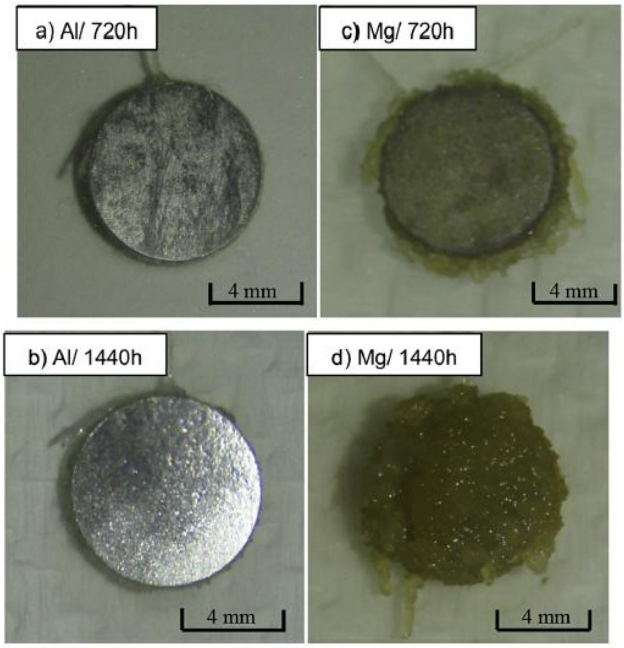

Fig. 4. Image of aluminium (a & b) and magnesium (c & d) surfaces after the exposure to bio oil at normal room temperature for a duration of 720 hrs and 1440 hrs.[3]

This is due to higher reactivity of magnesium with biodiesel. Magnesium is less noble compared to aluminium in the galvanic series. Fig. 4. Shows the appearances of magnesium and aluminium metal coupons which were used for static immersion test for duration of 720 hrs and 1440 hrs. Huge variation between the surface analysis of both metals can be found. Due to biodiesel exposure, a gel like mass get sticked on magnesium coupon, while aluminium coupon surface remained somewhat same. Gel-like mass has yellowish colour texture and sticky in nature.

Conclusion

Although biodiesel is a promising replacement to petroleum diesel fuel in terms of biodegradability, renewability, environmental friendliness, better lubrication, it shows some major concerns to the engine components in terms of wear and friction. Biodiesel properties changes due high temperature, storage, metal contamination and moisture absorption. The chemical properties of biodiesel are as per the ASTM standard, many properties has been found to be changed with the regular usage upon its dilution. There are few important conclusion mentioned below:

- Corrosion inhibitors can be used to reduce the corrosion in biodiesel. The effectiveness of corrosion inhibitors as inhibitor decreases in following order EDA > TBA >nBA.
- Corrosion of mild steel in both diesel and biodiesel increases with increase of temperature.
- Depletion of fuel properties in palm biodiesel increases with increase of temperature subject to mild steel. Exposure of mild steel in biodiesel increases its oxidation instability.
- Corrosion rate is more in biodiesel compared to diesel fuel for metal surfaces.
- Both copper and leaded bronze showed more corrosion rate in biodiesel as compared to that in diesel.
- Rate of corrosion of copper is more than compared to leaded bronze.
- Corrosiveness of B20D70E10 fuel is more than B20D75E5 fuel. At the temperature of 60 ^{0}C, the rate of corrosion is found more in BDE blends compared to normal room temperature. Rate of corrosion of metals in BDE blends is in the order of aluminium < mild steel < copper at various temperature conditions.
- Magnesium shows higher corrosion rate compared to that of aluminium in biodiesel.
- The surface analysis of magnesium coupon changed significantly while aluminium did not showed any symbolic changes.

References:

[1] Kenneth, P., McCromick, R.., Chandler, K., Buchholz B., 2005. Operating experience and teardown Analysis for engines operated on biodiesel blends (B20),NREL/CP-540-38509, SAE International 01-3641.
[2] BiodieselHandling and Guidelines,U. Department of Energry,DOE/GO-102006-2356, Third edition, September 2006.
[3] Geller D.P., Adams T.T., Goodrum J.W., Pendergrass J., 2008. Storage stability of poultry fat and diesel fuel mixtures: specific gravity and viscosity, Fuel 87 pp. 92–102.
[4] Sgroi M., Bollito G., Saracco G., Specchia S., 2005.BIOFEAT: Biodiesel fuel processor for a vehicle fuel cell auxiliary power unit - study of the feed system, Journal of Power Sources 149 pp. 8–14.
[5] Tsuchiya T., Shiotani H., Goto S., Sugiyama G., 2006.A. Maeda, Japanese standards for diesel fuel containing 5% fame blended diesel fuels and its impact on corrosion,SAE Technical pp.01-3303.
[6] Kamisnki J., Kurzydlowski K.J., Use of impedance spectroscopy on testing corrosion resistance of carbon steel and stainless steel in water–biodiesel configuration, Worsaw University of Technology, Faculty of materials Science and Engineering, Woloska 141Warsaw, Poland. Project KBN-3T08C00428, pp. 02-507.
[7] Klofutar B., Golob J., 2007. Microorganisms in diesel and in biodiesel fuels, Acta Chimica Slovenica 54 pp. 744–748.
[8] Maleque M.A., Masjuki H.H., Haseeb A.S.M.A., 2000. Effect of mechanical factors on tribological properties of palm oil methyl ester blended lubricant,Wear 239 pp. 117–125.
[9] Kalam M.A., Masjuki H.H., 2002. Biodiesel from palmoil - an analysis of its properties and potential, Biomass and Bioenergy 23 pp. 471–479.
[10] Maru M.M., Lucchese M.M., Legnani C., Quirino W.G., Balbo A., Aranha I.B., Costa L.T., Vilani C., De Sena L.A., Damasceno J.C., Cruz T.S., Lidízi L.R., Silva R.F., Jorio A., Achete C.A., 2009. Biodiesel compatibility with carbon steel and HDPE parts, Fuel Processing Technology 90 pp. 1175–1182.
[11] Kaul S., Saxena R.C., Kumar A., Negi M.S., Bhatnagar A.K., Goyal H.B., Gupta A.K., 2007. Corrosive behavior of biodiesel from seed oils of Indian origin on diesel engine parts, Fuel Processing Technology 88 pp. 303–307.
[12] Diaz-Ballote L., Lopez-Sansores J.F., Maldonado-Lopez L., Garfias-Mesias L.F., 2009. Corrosion behavior of aluminum exposed to a biodiesel, Electrochemistry Communications 11 pp. 41–44.
[13] Hasimoglu C., Ciniviz M., Ozsert I., Icingu Y., Parlaka A., Salman M.S., 2008. Performance characteristics of a low heat rejection diesel engine operating with biodiesel, Renewable Energy 33 pp. 1709–1715.
[14] Haseeb A.S.M.A., Masjuki H.H., Ann L.J., Fazal M.A., 2010. Corrosion characteristics of copper and leaded bronze in palm biodiesel, Fuel Processing Technology 91 pp. 329–334.
[15] Huang T.J., Tsai D.H., 2003. CO oxidation behavior of copper and copper oxides, Catalysis Letters 87 pp. 3–4.
[16] Haseeb A.S.M.A., Fazal M.A., Jahirul M.I., Masjuki H.H., 2011. Compatibility of automotive materials in biodiesel: a review, Fuel 90 pp. 922–931.
[17] Tsuchiya T., Shiotani H., Goto S., Sugiyama G., Maeda A., 2006. Japanese Standards for Diesel Fuel Containing 5% FAME blended diesel fuels and its Impact on Corrosion, SAE Technical pp. 3303.
[18] Kaul S., Saxena R.C., Kumar A., Negi M.S., Bhatnagar A.K., Goyal H.B., Gupta A.K., 2007. Corrosion behavior of biodiesel from seed oils of Indian origin on diesel engine parts, Fuel Processing Technology 88 pp. 303–307.
[19] Rajasekar A., Maruthamuthu S., Palaniswamy N., Rajendran A., 2007. Biodegradation of corrosion inhibitors and their influence on petroleum product pipeline, Microbiological Research 162 pp. 355–368.

[20] Geller D.P., Adams T.T., Goodrum J.W., Pendergrass J., 2008. Storage stability of poultry fat and diesel fuel mixtures: specific gravity and viscosity, Fuel 87 pp. 92–102.
[21] Fazal M.A., Haseeb A.S.M.A., Masjuki H.H., 2011. Effect of different corrosion inhibitors on the corrosion of cast iron in palm biodiesel, Fuel Processing Technology 92 pp. 2154–2159.
[22] Kaul S., Saxena R.C., Kumar A., Negi M.S., Bhatnagar A.K., 2007. Corrosion behavior of biodiesel from seed oils of Indian origin on diesel engine parts, Fuel Processing Technology 88 pp. 303–307.
[23] Fazal M.A., Haseeb A.S.M.A., Masjuki H.H., 2010. Comparative corrosive characteristics of petroleum diesel and palm biodiesel for automotive materials, Fuel Processing Technology 91 pp. 1308–1315.
[24] Ogawa T., Kajiya S., A., Ohshima and Atsushi Murase, 2006. Analysis of the Deterioration of Nylon-66 Immersed in GTL Diesel Fuel Part 1. Analysis and Test of Nylon and GTL Diesel Fuel Before and After Immersion. s.l.: SAE Technical Paper 3326.
[25] Fazal M.A., Haseeb A.S.M.A., Masjuki H.H., 2010. Comparative corrosive characteristics of petroleum diesel and palm biodiesel for automotive materials, Fuel Process. Technol. 91 pp. 1308-1315.
[26] Fazal M.A., Haseeb A.S.M.A., Masjuki H.H., 2012. Degradation of automotive materials in palm biodiesel, Energy 40 76-83.
[27] Hu E., Xu Y., Hu X., Pan L., Jiang S.,2012. Corrosion behaviors of metals in biodiesel from rapeseed oil and methanol, Renew. Energy 37 pp. 371-378.
[28] Cursaru D.L., Branoiu G., Ramada I., Miculescu F., 2014. Degradation of automotive materials upon exposure to sunflower biodiesel, Ind. Crop. Prod. 54 pp. 149-158.
[29] Norouzi S., Eslami F., Wysynski M.L., Tsolakis A., 2012. Corrosion effects of RME in blends with ULSD on aluminium and copper, Fuel Process. Technol. 104 pp. 204-210.
[30] Chew K.V., Haseeb A.S.M.A., Masjuki H.H., Fazal M.A., Gupta M., 2013 Corrosion of magnesium and aluminum in palm biodiesel: a comparative evaluation, Energy 57 pp. 478-483.
[31] Saravana Kannan Thangavelu Abu Saleh Ahmed , Farid Nasir Ani, 2016. Impact of metals on corrosive behavior of biodiesel-diesel-ethanol (BDE) alternative fuel, Renewable Energy 94 pp. 1-9.
[32] Wohlecker R, Johannaber M, Espig M., 2007. Determination of weight elasticity of fuel economy for ICE, hybrid and fuel cell vehicles. In: SAE world congress, 2007 Detroit, Michigan. SAE International; SAE paper no.0343.
[33] Pagerit S, Sharer P, Rousseau A., 2006. Fuel economy sensitivity to vehicle mass for advanced vehicle powertrains. In: SAE 2006 world congress Detroit, Michigan. SAE International; SAE paper no. 0665.
[34] Blawert C, Hort N, Kainer KU,. 2004. Automotive applications of magnesium and its alloys. Trans Indian Inst Met:57: pp.397-8.
[35] Chew K.V., Haseeb A.S.M.A.,Masjuki H.H., Fazal M.A., Gupta M., 2013. Corrosion of magnesium and aluminum in palm biodiesel: A comparative evaluation, Energy 57 pp. 478-483.
[36] Fazal MA, Haseeb ASMA, Masjuki HH,. 2010. Comparative corrosive characteristics of petroleum diesel and palm biodiesel for automotive materials. Fuel Process Technol 91 pp. 1308-15.
[37] Fazal M.A, Suhaila N.R, Haseeb A.S.M.A, Rubaiee Saeed,. 2018. Sustainability of additive-doped biodiesel: Analysis of its aggressiveness toward metal corrosion, Journal of Cleaner Production.
[38] Fazal M.A, Jakeria M.R, Haseeb A.S.M.A, Rubaiee Saeed,. 2017. Effect of antioxidants on the stability and corrosiveness of palm biodiesel upon exposure of different metals, Energy 135: pp. 220-226.

Object Detection System Using Smart Navigation For Blind People

Parin Patel[a*], Hitesh Patel[a]

[a]Gandhinagar Institute of Technology, Moti Bhoyan, Gandhinagar, Gujarat, India 382781

Abstract

Vision is one in every of the terribly essential human senses and it plays the key role in human perception about surroundings. The standard and oldest quality aids for persons with visual impairments area unit the walking cane (also referred to as white cane or stick) and guide dogs. The foremost vital drawbacks of those aids area unit necessary skills and coaching part, vary of motion and really very little info sent. With the speedy advances of contemporary technology, each in hardware and software package front have brought potential to supply intelligent navigation and language capabilities. In planned system we have a tendency to use camera to capture the image then the image are going to be processed to extract the options of the thing victimization 2 algorithms. The simulation results victimization SIFT formula and also the SOBEL formula is employed to extract edge key points matching showed sensible accuracy for police investigation objects. Object detection deals with extracting embedded details, patterns and their relationship in pictures. The captured image are going to be compared with the images that area unit already hold on within the datasets. The Images that area unit matched with the dataset images area unit reborn into text message and so the text is reborn into voice notes. All the process are going to be done by victimization MATLAB.

Keywords: Cloud Camera capture, Intelligent navigation, Different language processing, MATLAB.

1. Introduction

According to the UN agency (World Health Organization), there are nearly 285 million individuals, UN agency are visual impairments, 39 million of them are blind and 246 million have a decrease of acuity. Virtually ninetieth UN agency are visually impaired are living in low-income countries.[1] During this context, African country has known thirty thousand individuals with visual impairments; including13.3% of them are blind. The way of life of the blind individuals won't be that abundant straightforward as we expect. With the assistance of the development within the technology, several devices were serving to them to guide their life. The prevailing system isn't that abundant economical for detection the seriousness of the spirited object. It will predict the thing with its potency, however the planned system can predict the thing with ninety fifth potency. Here we have a tendency to are exploitation 2 algorithms particularly, SIFT and SOBEL. By merging these 2 algorithms in MATLAB, the options of the thing are extracted. MATLAB (matrix laboratory) could be a multi-paradigm computing atmosphere and fourth-generation artificial language. A proprietary artificial language developed by scientific discipline Works, Virtualization Technologies

2. Overview

Image segmentation is the base of the object recognition and image vision. Image noise ought to be eliminated through image preprocessing. And there's some specifically given work for image marking and region extraction to try when the most operation in this for the sake of recuperating visual result. There are two major image vision issues, image segmentation and visual perception, are historically handled with strict instruction, bottom-up ordering. This is the method of subdividing a digital image into multiple purposeful regions or sets of pixels regions with relation to a selected application. It is depends on measurements taken from the image and may be grey level, color, texture, depth or motion. The results of this method could be a set of segments that jointly cowl the all image. In relation to some characteristic of computed properties like color, intensity and texture every pixels in region are similar. With relation to this characteristics adjacent regions disagree. In digital image process edge detection technique is one method that sometimes used. The task of finding a given object in an image or video stream is Visual perception. There are several description of the article about the features. This description extracted from a coaching image will then be accustomed determine the article once making an attempt to find the article during a check image containing several different objects.

* Parin Patel Tel.: +91-7600030582
E-mail address: parin.patel@git.org.in

2.1 Image

A picture is associate degree array or a matrix of sq. pixels (picture elements) organized in columns and rows. a picture (from Latin: imago) is associate degree object, for instance a two-dimensional image, that incorporates a similar look to some subject sometimes an entity.

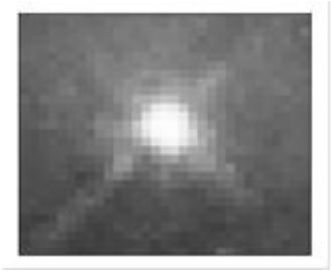

Fig. 1. An image – array or a matrix of pixels arranged in columns and rows.

2.2 Pixel

Image process may be a set of the electronic domain wherever within the image is born-again to associate degree array of little integers, referred to as pixels, representing a physical amount adore scene radiance, keep in an exceedingly digital memory and processed by pc or alternative digital hardware.

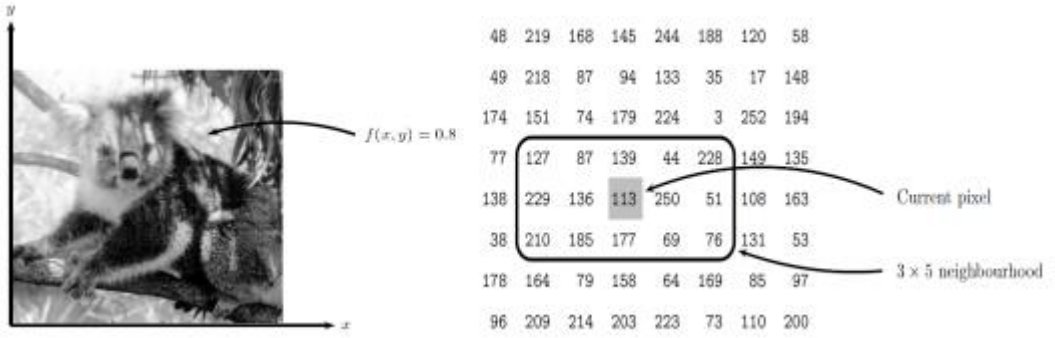

Fig. 2. A gray scale image and pixel representation

2.3 Image Resolution

Pixels remodel into inches through what's referred to as "resolution", the amount of element per area unit on a pc. Resolution permits you to remodel element into inches and back once more[6].
There are two resolution definitions area unit usually utilized in place of 1 another. Element resolution is that the size (in bytes) of your image or its look on a monitor. This variety is tied on to however huge your image is on your drive. The computer memory unit –size of the image file is directly proportional to the element count and its size on your monitor, which merely displays all the pixels in an exceedingly fastened matched grid.

2.4 Image Brightness

Brightness really describes however we have a tendency to expertise light-weight and not 'how it is'. If we have a tendency to area unit reaching to describe light-weight and 'brightness' properly, there are a unit 2 essential terms:
1. Luminance: Luminance is that the light-weight we have a tendency to see: mirrored or divergent from objects. It's measured in candlepower unit per center.
2. IL physical property: IL physical property is light-weight we have a tendency to can't see directly – it's alleged close light-weight. It's measured in illumination unit.

2.5 Contrast

The Image distinction magnitude relation refers to the distinction between the physical properties of the white a part of a picture, divided by the black half. Thus if the white half is 100 times brighter than the black half, it'll be 100:1, and so on. Element count and its size on your monitor, which merely displays all the pixels in an exceedingly fastened matched grid.

2.6 Image Processing

In process of image input can be a picture, photograph or video frame. Picture, group of characteristics or parameters of image can be the output of the image. There are some techniques which treat image as a dimensional signal and applying normal signal-processing techniques[8].
The example in figure three operate 256 gray-scale pictures. this implies that every picture element within the image is keep as variety between zero to 255, wherever zero represents a black picture element, 255 represents a white picture element and values mediate represent reminder grey.

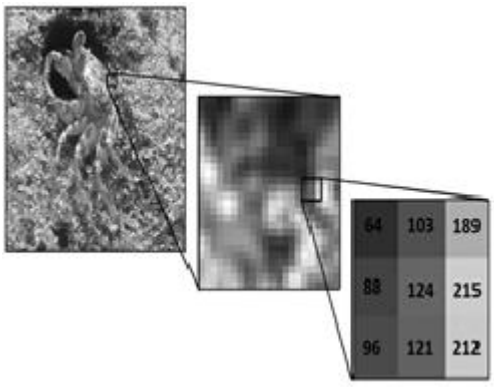

Fig. 3. Structure of grey-scale image

3. Proposed System

Maximum vision structures square measure supported rules for converting pictures into records sensory substitution tactile or exteroception stimuli. Certainly, an outsized half dedicated to the blind gadget attaches on to the cane as a supplement for detection. Sensory substitution structures rectangular degree extraordinarily encouraging due to in recent times they'll locate and renowned objects from pics with terribly trustworthy conversion's regulations. But, they will entirely be accustomed localize truthful styles and can't be used as gear of substitution in herbal environments. Those systems had been economical for exceptional and localization of gadgets this is commonly with a decrease exactness, consequently they want a few obstacles that we would like to surmount them[4]. In fact, they are doing now not establish items (e.g. whether or now not it's a table or chair) and that they have in some instances an overdue detection of tiny gadgets. Additionally, some obtain more exteroception, others need a sufficiently lengthy learning quantity. The importance of making plans a gadget supported the recognition and localization of items to fulfill the important thing challenges of the blind is in three major classes of desires: displacement, orientation and visible perception.[4]
In our technique, we tend to advocate to investigate the frame of photographs victimization the alternatives selection's algorithmic software so as to translate detected item. Then for each body we've got to use the noted algorithmic software. Alternatives extracted for each object square measure stored within the data[5]. We have a tendency to cipher key factors in the target frame. We tend to construct correspondence between options extracted from the body and people saved inside the information. If frames rectangular measure a similar, the list of detected items that turned into hold can seem, else if they're wonderful, options from the goal body are matched with the ones of items stored at the info, on the way to spot the new list of detected gadgets. If the matching among totally exceptional options suggests the detection of some gadgets, we have a tendency to keep the list of detected objects and extracted options from the body into the info. Then the textual content is born-once more into voice message to factor the seriousness for the blind oldsters.

3.1 SIFT

The value of extracting options of objects is reduced by way of taking a cascade filtering approach, during which the costlier operations square measure carried out totally at locations that pass partner in nursing preliminary check. Following rectangular degree the most vital tiers of computation wont to generate the set of photograph functions:

1. scale-area extrema detection: the number one degree of computation searches over all scales and image places. it's enforced with efficiency with the aid of employing a difference-of-Gaussian operate to identify capacity interest factors that square degree invariant to scale and orientation.
2. Key factor localization: key point's square measures stability and intensive model with verification of object place.[9]
3. Orientation challenge: one or extra orientations square degree assigned to every key factor location supported native photograph gradient directions. All future operations square measure done on picture records that has been remodeled relative to the assigned orientation, scale, and placement for every feature, thereby supplying

invariability to those variations.
4. Key point descriptor: the native picture gradients square degree measured at the chosen scale within the place round every key point.

Those rectangular measure remodeled into an illustration that enables for vital stages of native shape distortion and modify in illumination. This technique has been named the dimensions invariant characteristic remodel (sift), because it transforms photograph facts into scale-invariant coordinates relative to local options. An essential side of this technique is that it generates large numbers of options that densely cover the image over the overall range of scales and locations. a regular photograph of length 500x500 pixels can concerning to approximately 2000 strong alternatives (despite the fact that this variety relies upon on each photograph content material and selections for various parameters)[11]. The wide variety of options is specifically essential for visible notion, wherever the energy to be aware little gadgets in untidy backgrounds needs that a minimum of three options be nicely matched from each object for reliable identity.
For picture matching and reputation, sift options square degree 1st extracted from a group of reference snap shots and maintain in a very facts. a substitute picture is matched by means of severally examination each function from the new picture to the contemporary preceding information and locating candidate matching options supported Euclidian distance in their characteristic vectors[7]. The Keypoint descriptors square measure extremely special that permits one function to search out its accurate match with clever likelihood in a very giant data of alternatives. But, in a totally untidy image, several alternatives from the background might not have any correct match within the facts, giving upward push to several false matches additionally to the right ones. The proper fits could be filtered from the entire set of fits via distinguishing subsets of key points that agree on the article and its region, scale, and orientation inside the new picture. The likelihood that many options can agree on these parameters with the aid of twist of fate is a ways below the likelihood that any individual characteristic match are in blunders. The determination of those regular clusters can be finished speedily by means of victimization accomplice in nursing cost-effective hash desk implementation of the generalized though redesign. Every cluster of 3 or extra options that agree on associate in nursing item and it's create is then situation to any problematic verification. First, a least-squared estimate is formed for associate in nursing affine approximation to the item create. The alternative photograph alternatives in line with this create square degree known, and outlier's square measure discarded. Finally, an intensive computation is fashioned of the probability that a specific set of options shows the presence of associate in nursing object, given the accuracy of labor and variety of likely false suits. Object suits that skip of those exams may be referred to as correct with high confidence.

4. SOBEL

Sobel operator is hired in picture process and laptop vision, especially inside facet detection algorithms wherever it creates a photograph emphasis edges. Its miles supported convolving the photo with a bit, separable, and integer-valued filter out inside the horizontal in phrases of computations[12]. It's a distinct differentiation operator, computing associate in nursing approximation of the gradient of the image intensity operate. The kernels rectangular degree designed to reply maximally to edges strolling vertically and horizontally relative to the constituent grid, one kernel for every of the two perpendicular orientations. Those will then be blended along to hunt down absolutely the magnitude of the gradient at every purpose and also the orientation of that gradient.
This is less sensitive to noise for larger quality. The operator moreover generally produces notably better output values for similar edges, as compared with the Roberts cross. As with the Roberts cross operator, output fees from the operator will in reality overflow the maximum allowed constituent value for picture types that solely help small entire range constituent values (e.g. eight-bit entire range photos). As soon as this occurs the exceptional practice is to without difficulty set overflowing output pixels to the most allowed charge. The problem may be avoided with the aid of victimization a photograph type that supports constituent values with a larger vary. The photograph suggests a much less complex scene containing certainly one flat darkish object in opposition to a lighter heritage. Making use of the sobel operator produces. All edges in the picture are detected and might be nicely separated from the heritage using a threshold of one hundred fifty. Although the sobel operator isn't as sensitive to noise because the Roberts go operator, it still amplifies excessive frequencies. The picture is that the results of adding Gaussian noise with an average deviation of fifteen to the preliminary photo[10]. Applying the sobel operator yields and keeping the end result at a rate of one hundred fifty produces the edge points.

4.1 Image processing

Reputation and class of objects are topics of extraordinarily energetic analysis. They're accomplished on many virtual media corresponding to pictures or videos. In a totally visible scene of world, visual perception mission is commonly specialize in the general project of the linguistics interpretation. Picture and video facts can be perceived in any other case growing it terribly hard to keep whole content data of pix or video[2]. There are 2 huge instructions of general visual belief, particularly instance reputation and class recognition. The preceding entails re-

recognizing a famous 2d or 3D inflexible item, in all likelihood being viewed from a completely unique standpoint, against a littered heritage, and with partial occlusions. The class-stage or time-honored visible notion is the hard downside of recognizing any instance of a particular popular class corresponding to cat, car, or bicycle. Seeking out objects in a totally video scene may be conjointly performed using rule of alternatives extraction and descriptor for matching signatures of objects. Function-based totally machine operates a variety of faster than a pixel-based totally machine. To analyze the content of films, the number one step is to extract data that characterizes every frame. the maximum cause of exploitation alternatives in place of raw component values due to the fact the input to a gaining knowledge of rule, is to lessen/growth the in-elegance class variability as compared to the raw input document, and so creating classification less complicated.

4.2 Features Extraction

Capabilities extraction is that the technique by means of that certain options of interest inner a photograph are detected and represented for added method. It's an essential step in maximum computer imaginative and prescient and image method solutions as a result of it marks the transition from pictorial to non-pictorial (alphanumerical, commonly quantitative) facts illustration. Varieties of options a good way to be extracted from picture rely upon the type of photograph (e.g. binary, gray-level, or coloration), the quantity of graininess (entire picture or person regions) favored, and therefore the context of the equipment. Once the options are extracted, they're generally diagrammatic in accomplice diploma alphanumeric technique for extra process. The unique example relies upon on the approach used. The alternatives extraction technique need to be precise, just so consistent alternatives are extracted on two snap shots showing steady object. It is composed on five steps[7]:
1) Notice a collection of distinctive keypoints.
2) Outline a vicinity around every keypoint in a very scale- orAffine-invariant manner.
3) Extract and normalize the region content.
4) Figure a descriptor from the normalized region.
5) Match the native descript.

Feature extraction may be obtained by VI factors:

1) Mean:
The mean of an information set is solely the arithmetic average of the values within the set, obtained by summing the values and dividing by the amount of values.
2) Variance:
The variance of the info set is that the arithmetic average of the square variations between the values and therefore the mean.
3) Standard Deviation:
The standard deviation is that the root of the variance.
4) Skewness:
It is a measure of symmetry, or additional exactly, the dearth of symmetry. A distribution, or information set, is centrosymmetric if it's constant to the left and right of the middle purpose.
5) Kurtosis:
It is live of whether or not the info ar heavy-tailed or light-tailed relative to a traditional distribution.
6) Entropy:
Entropy is outlined because the quantitative live of disorder or randomness in a very system.delta-S = Q/T

4.3 Descriptors

Extracted options represent the fascinating points found within the image to check them with alternative fascinating points. Descriptors are won't to describe these options[1]. They're usually based mostly around points of interest of the image and often related to a detector of key points .The descriptors may be international, native or semi-local:
1) International image descriptor: options overall image are typically supported color indices and therefore the most noted Global color descriptor is that the color bar graph.
2) Native image descriptors: native options are ones that have received the foremost attention in recent years. The main plan is to specialize in the areas containing the foremost discriminated data.
3) Semi-local image descriptor: most form descriptors comprise this class. This descriptor relies on extracting accurate contours of shapes within the image or within the region of interest. During this case, image segmentation is usually helpful as a preprocessing step. Many strategies for options localization and outline are planned within the literature. during this paper, we tend to aim to use options extraction rule SIFT.

Conclusion

Visual substitution systems square measure typically specializing in the quality, the redirection and also the detection of obstacles. Our goal is to produce a sturdy and simple system permitting the blind folks or visual impaired to explain their environments by objects identifiers. This method is predicated on the analysis of images that square measure keep in dataset. Then it'll endure a picture process to spot totally different objects detected. In this paper, we've evaluated SIFT and SOBEL, the celebrated ways for options extraction for objects detection. so as to ameliorate and increase the article recognition rate, we are going to contemplate the color whereas distinguishing objects associate degreed add an sense modality translation for known objects.

References

[1] Petros Maragos and Iasonas Kokkinos, (2012),"Synergy between Object Recognition and image segmentation using Expectation and Maximization Algorithm"., IEEE Trans. on Pattern Analysis and Machine Intelligence (PAMI), Vol. 31(8), pp. 1486-1501, 2012.
[2] Wen-Xiong Kang, Qing-Qiang Yang, Run-Peng Liang (2015), "The Comparative Research on Image Segmentation Algorithms," First International Workshop on Education Technology and Computer Science.
[3] V. Ferrari, T. Tuytelaars, and L.V. Gool(2015), "Simultaneous Object Recognition and Segmentation by Image Exploration," Proc. Eighth European Conf. Computer Vision, 2015.
[4] B. Leibe, A. Leonardis, and B. Schiele(2014), "Combined Object Categorization and Segmentation with an Implicit Shape Model," Proc. ECCV Workshop Statistical Learning in Computer Vision, 2014.
[5] Y.Ramadevi, B.Kalyani, T.Sridevi(2017), " Synergy between Object Recognition and Image Segmentation", International Journal on Computer Science and Engineering, Vol. 02, No. 08, 2017, pp. 2767-2772.
[6] N.Senthilkumarn, R.Rajesh(2017), "Edge Detection Techniques for Image Segmentation- A Survey of Soft Computing Approaches", IJRTE, vol1,No2, 2017, pp. 250-254.
[7]. A. Petrosino, "Moving Object Detection for RealTime Applications," in Proc. IEEE 14th Int. Conf. Image Analysis and Processing, Modena, Italy, Sep. 2007, pp. 542-547.
[8] G. Zhang, J. Jia, W. Xiong, T. T. Wong, P. A. Heng, and H. Bao, "Moving Object ",2017
[9] Implementation of an Automated Single Camera Object Tracking System Using Frame Differencing and Dynamic Template Matching'Karan Gupta1, Anjali V. Kulkarni2 Indian Institute of Technology, Kanpur, India
[10] 'MOTION OBJECT DETECTION OF VIDEO BASED ON PRINCIPAL COMPONENT ANALYSIS 'Proceedings of the Seventh International Conference on Machine Learning and Cybernetics, Kunming, 12-15 July 2017.
[11] Moving object detection tracking system: a real time implemented, SEIZIÈME COLLOQUE GRETSI — 15-19 SEPTEMBER 1997 — GRENOBLE
[12] Segmentation and tracking of multiple video objects Received 7 June 2005; received in revised form 23 February 2006; accepted 14 July 2016`

Retailer's Optimal Ordering and Credit Period Policy for Items with Ramp type Demand

Mihir S. Suthar[a*], Kunal T. Shukla[b]

[a]*PDPIAS, Charotar University of Science and Technology, Changa-388421*
[b]*Lukhdhirji Engineering College, Morbi-363642*

Abstract

In recent competitive market, to boost demand of an item or to attract more customers, the retailer offers a credit period to his customers. Ordering strategy is presented for the inventory system for items, where market needs (i.e. demand rate) follows ramp type pattern. This means that demand of an item is assumed to be increasing with time over certain time duration. Then it becomes constant throughout the planning horizon. Shortages are not allowed. Mathematical model and numerical examples with sensitivity analysis, is presented to discuss the ordering strategy in detail.

Keywords: Ramp Type Demand, Credit Period Policy

Nomenclature

$I(t)$	Inventory level at any instant time t
T	Length of ordering cycle time
β	Credit period elasticity
M	Credit period offered by supplier
δ	Scaling parameter
Q	Economic order quantity (decision variable)
P	Selling price per unit
C	Purchase cost per unit
h	Holding cost per unit per time unit
A	Ordering cost per order
K	Average profit of the supplier

1. Introduction

In current global and competitive market, retailer offers a delay period without any interest charges to attract more customers on the purchase made. This results in to increase in sale. On the other hand, this delay period offer leads to a default risk for the retailer, when the customer declares that he is unable to pay back.
It is clear that, default risks are in direct proportion with length of delay period. Goyal (1985) gave an inventory model with permissible delay in payments. Shah et al. (2010) carried out review article on inventory systems with trade credits. Shah et al. (2014) discussed optimal ordering and purchase quantity model when demand is depending upon credit period offered.
Ghare and Schrader (1963) proposed exponentially decaying inventory system. Covert and Philip (1973), Philip (1974) and Tadikamalla (1978) extended the model of Ghare and Schrader (1963) by using Weibull distribution and Gamma distribution. In reality, most commodities maintain its quality or original conditions over a span. i.e., during this span deterioration does not occur. Normally, it is observed that food stuffs, first hand vegetables and fruits have a short span of maintaining fresh quality, in which there is almost no spoilage. Whereas in items like volatile liquids, radio-active chemicals, trendy goods, electronic goods have more span of marinating their quality or freshness. For the first time, Hill (1995) formulated an inventory model with ramp type demand rate. In case of ramp type demand rate, the rate of demand increases linearly at the beginning, then it goes constant until the end of replenishment cycle. Such demand pattern is mostly observed in new brand consumer goods which are likely to be introduced in market.

* Mihir Suthar Tel.: +91-8141845402
E-mail address: mihirsuthar86@gmail.com

The demand rate of such products is generally increasing function of time at some extent, and then it becomes constant. Many researchers have studied inventory models with ramp type demand. Cheng and Wang (2009) extended this idea from ramp type demand to trapezoidal type demand. Cheng et al. (2011) extended the model for deteriorating items and by allowing shortages, with partial backlogging. Research articles on ramp type demand are Mandal & Pal (1998), Wu et al(1999), Wu(2001), Chung and Huang(2003), Giri et al.(2003),Manna and Chaudhuri(2006), Deng et al(2007), Panda et al.(2008), Skouri et al(2009), Skouri et al(2011) formulated the inventory system having ramp type demand. Huang (2003), Chung and Liao (2004), Huang (2008), Liao (2008), Gor and Shah (2008), Gupta et al(2011), Seifert et al(2013) developed inventory system under trade credit policies.

Here, proposed model deals with retailer's inventory system. It is assumed that retailer deals with an item having ramp type and credit period trended demand rate, i.e. demand of an item increases first up to some level and then it stabilize over a planning horizon. It also depends upon credit period offered to the customer. Shortages are not expected during ordering cycle.

2. Assumptions

The following assumptions and notations are used in the formulation of mathematical form of the proposed model.

(1) The inventory system deals with a single item. Rate of replenishment rate is assumed to be infinite and lead time considered to be zero or negligible. The length of planning horizon for is infinite. Inventory system does not possess shortages.

(2) The function $I(t)$ represents level of an inventory at any instant of time t during $[0,T]$, where T is length of ordering cycle.

(3) To boost demand of an item supplier offers a credit period M to the buyers. The demand is assumed to be ramp type and depending upon credit period, say $R(t,M)$, defined as under:

$$R(M,t)=\begin{cases} f(t)M^{\beta}, 0<t<\lambda \\ f(\lambda)M^{\beta}, \lambda<t<T \end{cases} \quad (1)$$

Demand of an item increases during $[0,\lambda]$, thereafter it remains stable during $[\lambda,T]$, $\beta>0$ is credit period elasticity.

(4) The item does not deteriorate during cycle time.

(5) It is observed that, longer the credit period offered to the buyer, increases default risk to the supplier. Rate of default risk due to credit period offered, is assumed to be $F(M)=1-M^{-\delta}$, where $\delta>0$ is scaling parameter.

3. Formulation of Model:

Mathematical formulation for an inventory system is developed from supplier's stance. The supplier's inventory level depletes due to demand on λ is the time up to which demand of an item increases, thereafter demand remains constant up to cycle time T.

The differential equation governing inventory system can be written as follows:

$$\frac{dI(t)}{dt}=\begin{cases} -f(t)M^{\beta} & ; \quad 0\le t\le\lambda \\ -f(\lambda)M^{\beta} & ; \quad \lambda\le t\le T \end{cases} \quad (2)$$

with $I(T)=0$ (3)

Using boundary condition (3), continuity of $I(t)$ at time $t=t_d$, $t=\lambda_1$, we solve equation (2). And solution is

$$I(t)=\begin{cases}-M^{\beta}\int_{\lambda}^{t} f(x)dx+f(\lambda)M^{\beta}(T-\lambda) & ; \quad 0\le t\le\lambda \\ f(\lambda)M^{\beta}(T-t) & ; \quad \lambda\le t\le T\end{cases} \tag{4}$$

Using (3), supplier's initial stock level is Q,

$$Q=I(0)=-M^{\beta}\int_{\lambda}^{0} f(x)dx+f(\lambda)M^{\beta}(T-\lambda) \tag{5}$$

Total profit of an inventory system comprises following cost components:

1. Net sales revenue after default risk SR:

$$SR=P\cdot(1-F(M))\left(\int_0^{\lambda} f(t)M^{\beta}dt+\int_{\lambda}^{T} f(\lambda)M^{\beta}dt\right)=PM^{-\delta}\begin{pmatrix}\int_0^{\lambda} f(t)M^{\beta}dt \\ +M^{\beta}(T-\lambda)f(\lambda)\end{pmatrix} \tag{6}$$

2. Ordering Cost OC: $OC=A$ (7)

3. Purchase cost PC:

$$PC=C\cdot Q=-CM^{\beta}\int_{\lambda}^{0} f(x)dx+f(\lambda)M^{\beta}(T-\lambda) \tag{8}$$

4. Inventory holding cost HC:

$$HC=h\int_0^T I(t)dt=h\left(\int_0^{\lambda} I(t)dt+\int_{\lambda}^{T} I(t)dt\right)$$
$$=\frac{hM^{\beta}}{2}\left((T-\lambda)^2 f(\lambda)-2\int_0^{\lambda}\left((\lambda-T)f(\lambda)+\int_{\lambda}^{t} f(x)dx\right)dt\right) \tag{9}$$

So, Supplier's yearly profit per time unit is,

$$K(T,M)=\frac{1}{T}[SR-OC-PC-HC] \tag{10}$$

To evaluate optimal solution for $K(T,M)$, we use fundamental calculus and computational algorithm given as under:

3.1. Computational Algorithm:

Step 1 Assign parametric values to the parameter.

Step 2 Solve $\frac{\partial K}{\partial M}=0$ and $\frac{\partial K}{\partial T}=0$ to find optimal values M^* and T^* provided $\frac{\partial^2 K}{\partial M\,\partial T}<0$

Step 3 Using M^* and T^* find EOQ Q and maximum value of $K(T^*,M^*)$

3.2. Numerical Example

To illustrate above formulation and computational algorithm, we consider following examples.

Example 1 We consider $f(t) = a_1 + b_1 t$ which is a linear function, where the standard value of parameters are $A = \$100$/order, $C = \$10$/unit, $h = \$2$/unit/time unit, $P = \$12$/unit, $\lambda = 100/365$ years, $a_1 = 1000$, $b_1 = 0.5$, $\delta = 2$, $\beta = 4$. With this set of parameters, optimal credit period and cycle time are $M^* = 0.7539019822$ years and $T^* = 0.5565245396$ years respectively. Using these optimal values EOQ $Q = 179.799$ units and maximized total profit is $K = \$3230.875$. The graph given in Figure 1 indicates that the total profit per time unit is strictly concave. Variation of profit with respect to T and M is exhibited in Figure 2 and Figure 3 respectively.

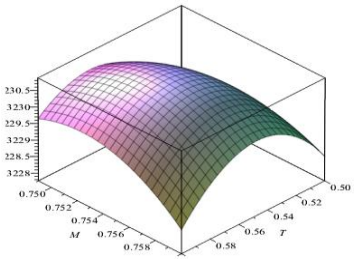

Figure 1 Total profit/time unit

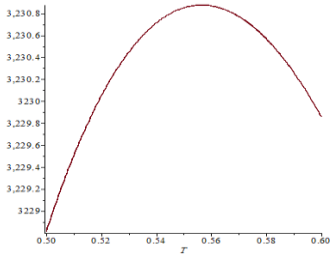

Figure 2 $T \to K(M,T)$

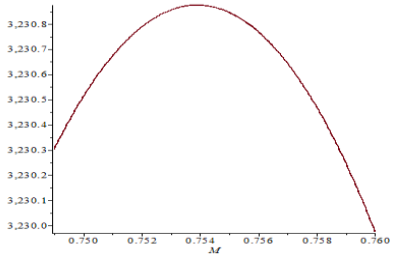

Figure 3 $M \to K(M,T)$

3.3. Sensitivity Analysis

Variations in optimal values, EOQ and total profit per time unit with respect to variation in major parameters, like a_1, C, P, h, β, δ and A are exhibited in Figure 4-7.

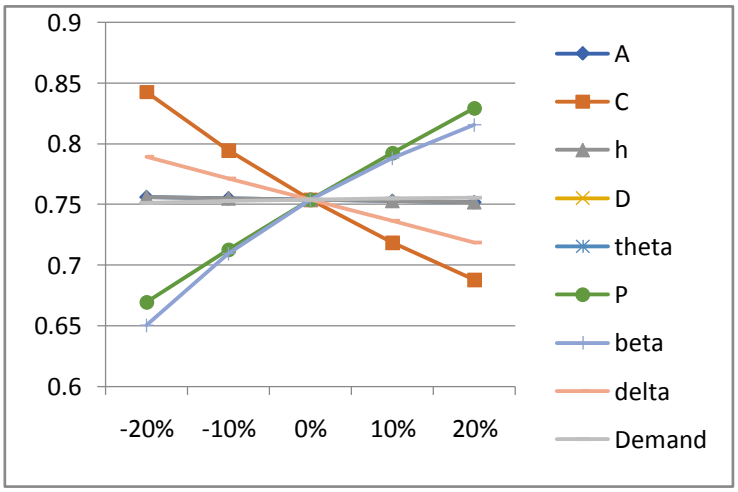

Figure 4 Variation in M

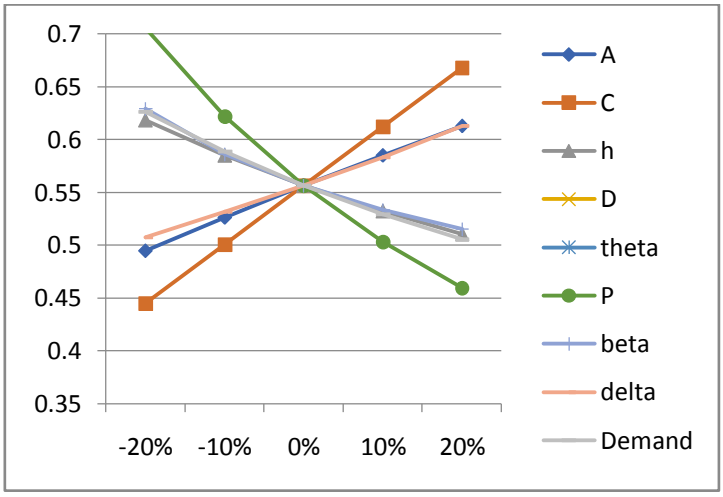

Figure 5 Variation in T

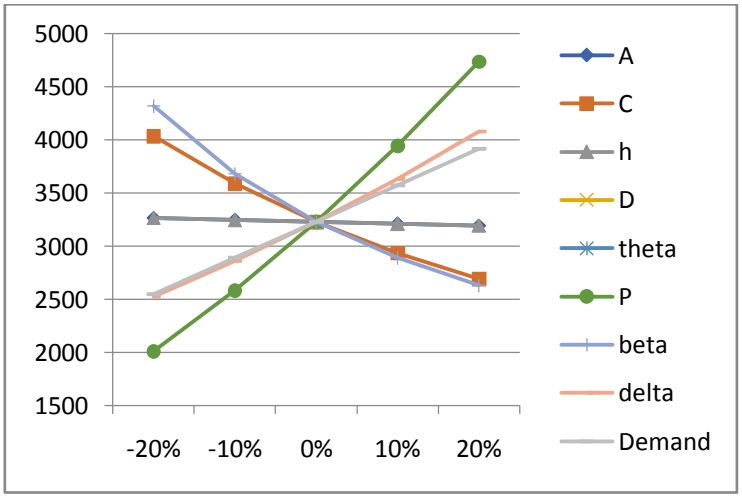

Figure 6 Variation in $K\left(M,T\right)$

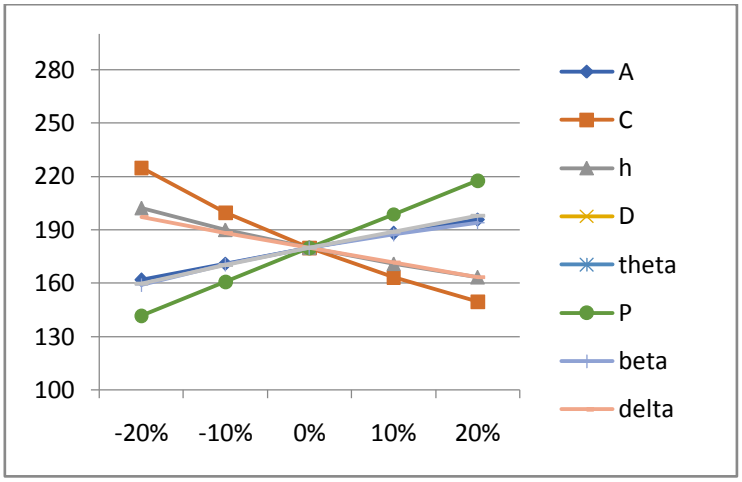

Figure 7 Variation in Q

3.3.1. Managerial Insights:

Using sensitivity analysis, following managerial issues were observed.

1. From figure 4, it is observed that credit period M has positive impact with respect to selling price, credit period elasticity and demand rate. Also, opposite impact with ordering cost, holding cost, purchase cost and scaling parameter δ .
2. From figure 5, it is observed that cycle time T has positive impact over increase in ordering cost, purchase cost and scaling parameter δ . And opposite impact over increase in holding cost, selling price, credit period elasticity and demand rate.
3. From figure 6, it is observed that the total profit of an inventory system K has opposite impact over increase in ordering cost, purchase cost, holding cost and credit period elasticity. Also, positive impact over increase in selling price, demand rate and scaling parameter δ .
4. From figure 7, it is observed that economic order quantity Q has positive impact over increase in ordering cost, credit period elasticity, demand rate and selling price. Also, opposite impact over increase in purchase cost, scaling parameter δ and holding cost.

Conclusion:

It is difficult for the supplier to decide permissible credit period to be offered to the retailer. Increase in the credit period offered, increases the default risks. An optimal ordering and credit period policy for the item having ramp type demand is presented here from the point of supplier. During cycle time shortages are not allowed. A solution procedure is discussed with support of various numerical examples. Computational algorithm is illustrated through examples and managerial insights were presented using sensitivity analysis.

References:

[1] Cheng, M., Wang, G., 2009. A note on the inventory model for deteriorating items with trapezoidal type demand rate, Computers and Industrial Engineering 56, pp. 1296-1300.
[2] Cheng, M., Zhang B., Wang, G., 2011. Optimal policy for deteriorating items with trapezoidal type demand and partial backlogging, Applied Mathematical Modelling, 35, pp. 3552-3560.
[3] Chung, K.J., Huang, Y.F., 2003. The optimal cycle time for EPQ inventory model under permissible delay in payments. International Journal of Production Economics, 84, pp. 307 – 318.
[4] Chung, K.J., Liao, J.J., 2004. Lot – sizing decisions under trade credit depending on the order quantity. Computers and Operations Research, 31, pp. 909 – 928.
[5] Covert, R. P., Philip, G. C. 1973.An EOQ model for items with Weibull distribution deterioration, AIIE transactions 5 (4), pp. 323-326.
[6] Deng, P.S., Lin, R.J., Chu, P., 2007. A note on the inventory model for deteriorating items with ramp type demand rate. European Journal of Operation Research 178, pp. 112-120.
[7] Ghare, P. M., Schrader, G. F. ,1963. A model for exponentially decaying inventory, Journal of Industrial and Engineering Chemistry, 14 (2), pp. 238-243.
[8] Giri, B.C., Jalan, A.K., Chaudhuri, K.S., 2003. Economic Order Quantity model with Weibull deterioration distribution, shortage and ramp type demand. International Journal of Systems Science 34(4), pp.237-243.
[9] Gor, R. and Shah, N. H., 2008. A time dependent deteriorating EOQ model with selling price and stock dependent demand during inflation under supplier credits. ICFAI University Journal of Operations Management, 7(4), pp. 6 – 20.
[10]Goyal, S.K., 1985. Economic order quantity under conditions of permissible delay in payments. Journal of the Operational Research Society, 36, pp. 335 – 338.
[11] Gupta, O.K., Shah, N.H., Shukla, K.T., 2011. Supply chain inventory model for deteriorating items under two-level credit policy in declining market, International Journal of Applied Management Science, 3(2),pp. 143-173.
[12]Hill, R., M., 1995. Inventory model for increasing demand followed by level demand. Journal of Operation Research Society 46, pp. 1250-1259.
[13]Huang, Y.F., 2003. Optimal retailer's ordering policies in the EOQ model under trade credit financing. Journal of the Operational Research Society 54, pp. 1011 – 1015.
[14]Liao, J. J., 2008. An EOQ model with non-instantaneous receipt and exponentially deteriorating items under two-level trade credit. International Journal of Production Economics 113, pp. 852–861.
[15] Mandal, B., Pal, A.K., 1998. Order level Inventory system with ramp type demand demand rate for deteriorating items. Journal of Interdisciplinary Mathematics 1, pp.49-66.
[16] Manna, S.K., Chaudhuri, K.S., 2006. An EOQ model with ramp type demand rate, time dependent deterioration rate, unit production cost and shortages. European Journal of Operation Research 171(2), pp.557-566.
[17] Panda, S., Senapati, S., Basu, M., 2008. Optimal replenishment policy for perishable seasonal products in a season with ramp type time dependent demand. Computers and Industrial Engineering 54(2), pp. 301-314.
[18]Philip, G, C., 1974. A generalized EOQ model for items with Weibull distribution, AIIE transections 6(2), pp. 159-162.
[19]Seifert, D., Seifert, R.W., Seifert, M., P.S., 2013. A review of trade credit literature: Opportunities for research in operations, European Journal of Operational Research 231(2), pp. 245-256.
[20] Shah, N. H., Shah, D. B., Patel, D. G., 2014. Optimal credit period and ordering quantity for credit dependent trended demand and deteriorating items with maximum lifetime, Control and Cybernetics 42 (2), pp. 311-320.
[21] Shah, N. H., Gor, A.S., Wee, H.M., 2010. An Integrated Approach for Optimal Unit Price and Credit Period for Deteriorating Inventory System when the Buyer's Demand is Price Sensitive, American Journal of Mathematical and Management Sciences 30(3-4), pp. 317-330.
[22]Skouri, K., Konstantaras, I., Papachristos, S., Ganas, I., 2009. Inventory models with ramp type demand rate, partial backlogging and Weibull deterioration rate, European Journal of Operation research,192, pp.79-92.

[23] Skouri ,K. , Konstantaras, I., Papachristos, S., Teng, J.T., 2011. Supply Chain models for deteriorating products with ramp type demand rate under permissible delay in payments, Expert Systems with Applications 38(12) , pp.14861-14869.
[24] Tadikamalla, P.R. (1978): An EOQ inventory model for items with gamma distribution, AIIE Transections, 10 (1), pp. 100-103.
[25] Wu, J.W., Lin, C., Tan, B., Lee, W.C., 1999. An EOQ Inventory Model with Ramp Type Demand Rate for Items with Weibull Deterioration. Information and Management Sciences 10(3), pp. 42-51.
[26] Wu, K.S.,2001. An EOQ inventory model for items with Weibull distribution deterioration, ramp type demand rate and partial backlogging. Production Planning and Control, The Management of Operations 12, pp. 787-793.

Acknowledgement

The authors are very thankful to reviewers for their valuable comments to improve quality of this article. Also, they are thankful to editor for his continuous and caring support.

Structural and Thermophysical Properties of Al-Li intermetallic alloy

N. Y. Pandya[a*], Adwait Mevada[b], P. N. Gajjar[c]

[a]*Gandhinagar Institute of Technology, Moti-Bhoyan, Khatraj-Kalol Road, Ta: Kalol, Dist: Gandhinagar, Gujarat, India*
[b]*President college of Science, Ghatlodia, Ahmedabad-380 061, Gujarat, India*
[c]*Department of Physics, University School of Sciences, Gujarat University, Ahmedabad-380 009, Gujarat, India*

Abstract

Aluminium-Lithium alloys are best option to fulfil the need of light weight alloys for using as structural in aerospace applications. Better mechanical properties e.g. higher specific strength, enhanced resistance to high cycle fatigue and fatigue crack growth are found for Al-Li alloys as compared to conventional Al alloys. Present paper report various finite temperature/pressure thermophysical properties of B2 structured Al-Li using DFT as used in Quantum ESPRESSO code in consonance with quasi harmonic Debye model. Calculated equilibrium lattice constants and isothermal bulk modulus are in consonance with other theoretical results. Conclusions based on the various finite temperature/pressure thermophysical properties like room temperature thermal equation of stateand Grüneisen parameter are outlined. Our presently calculated results may serve as a reliable set of data of structural and thermophysical properties of B2 structured Al-Li alloy.

Keywords: Al-Li; Pseudopotential; Thermophysical properties, Quantum Espresso

1. Introduction

Despite the fact that both elements aluminium and lithium are quite normal metals, their alloys manifest rather unusual thermodynamic and electrochemical properties which have lately prompted a number of theoretical studies of the Al-Li system [1]. If the net weight of the structure is reduced considerably, the substantial improvements in structural efficiency, fuel saving and payload in aerospace can result. Aluminium-Lithium alloys are the best light weight alloys for using as structural in aerospace application compared to other structural materials. Al-Li alloys exhibit superior mechanical properties as compared to conventional Al alloys [2]. The desire for more efficient aircraft materials has given the force to the research of Al-Li alloy and are technologically more important as compared to costly structural materials such as Ti alloys and composites [2]. Present work reports the thermal equation of state and Grüneisen parameter of B2 structured Al-Li alloy using DFT as used in Quantum ESPRESSO [3] in consonance with quasi harmonic Debye model[4]. Present work is discussed as follows. Methodology of the present work is reported in section 2. The results and discussion are discussed in section 3 followed by conclusions in section 4.

2. Computational Methodology

In the present work, ground state and thermophysical properties of B2 structured Al-Li are calculated using DFT as used in Quantum ESPRESSO [3] in consonance with quasi harmonic Debye model. The calculation is performed using ultrasoft pseudopotential with non linear core correction within generalized gradient approximation (GGA) [5]. The Aluminium Lithium (Al-Li) crystallizes into Cesium chloride (B2) structure at ambient condition and remains stable up to very high pressures. The Al and Li atoms occupy positions (0, 0, 0) and (0.50, 0.50, 0.50), respectively, in a SC primitive cell. Total energy calculation of B2 structured Al-Li is performed at different lattice constants in the increment of 0.1 a.u. (atomic unit). The convergence test gave an 8x8x8 Monkhorst-Pack (MP) k-point grid [6] for Brilliouin-zone (BZ) sampling along with the kinetic energy cutoff as 116 Ry. This ensures the convergence of total energy to 0.1 mRy. Total energy in other two cubic phases namely rock salt (B1) and zinc blende (B3) is also calculated. Fitting of computed total energies were done by Murnaghan equation of state [7], concerning to determine equilibrium lattice constant, isothermal bulk modulus and its pressure derivatives. For the analysis of thermal effect in the present study, we used quasi-harmonic Debye model implemented in pseudo code Gibbs. **[4]**. Basicconcept used here is the replacement of true phonon density of states (p-dos), g (ω) by ~ ω2 term. In Quasi harmonic Debye model, Debye temperature depends on the scaling function f (σ). Hence the Poisson's ratios σ have to be inserted concerning to define f (σ). Due to the absentees of definite Poisson's ratio for Al-Li alloy, we used 0.32 which is the value of Poisson ration for Al alloy [8]. Further, the other thermophysical properties can also be studied by using the consonant equilibrium volume in the applicable expressions as mentioned in **[4]**.

* Nirav Pandya Tel.: +91-9904405945
E-mail address: nirav.pandya@git.org.in

We obtain the finite temperature/pressure thermophysical properties likethe thermal equation of state and Grüneisen parameter of B2 Al-Li for computed equilibrium lattice parameter. The cohesive energy of all three cubic phases i.e. B1, B2 and B3 were also reported in our previous work [9].

3.Results and Discussion

Only B2 structure of Al-Li were studied out of three cubic phases because it has the lowest energy at equilibrium. The ground state properties of B2 structured Al-Li are calculated by minimizing the total energy with respect to the cell volume by means of Murnaghan equation of state [7]. As a result, we obtained the equilibrium lattice constant, isothermal bulk modulus and first order derivative of bulk modulus for B2 structure Al-Li, which is presented in table 1, together with the other available theoretical data [10]. We notice that, there is an excellent consistent of present results with the other theoretical findings [10].

Table 1. Calculated structural properties of B2 structured Al-Li alloy

Structure	Properties	Present	Theory [10]	Exp.
CsCl (B2)	a_0 (Å)	3.217	3.175	---
	B_0 (GPa)	37.1	40.7	---
	B_0'	3.67	4.37	---

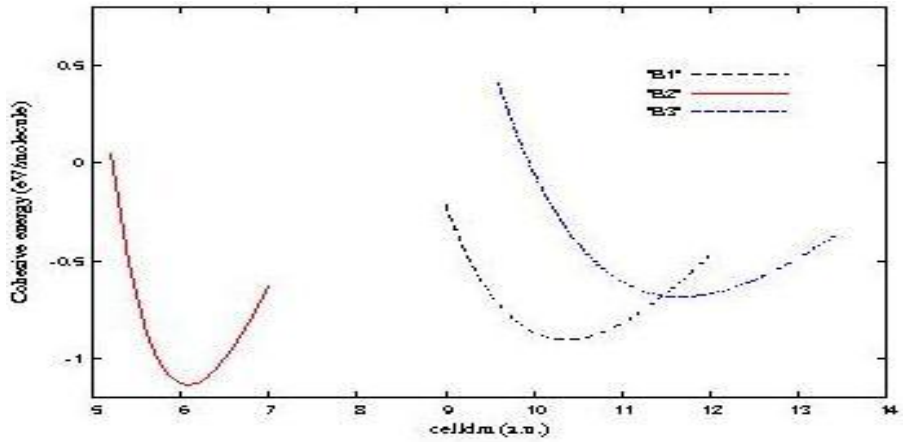

Fig.1 Cohesive energy of Al-Li as a function of celldm

Cohesive energy of all three cubic phases i.e. B1, B2 and B3 of Al-Li are presented in fig.1, where B2 (CsCl) structure exhibit lowest cohesive energy compare to B1 and B3 structure of Al-Li. This significantly indicates the structural stability of B2 (CsCl) structure of Al-Li alloy at equilibrium. In our previous work [9], we reported full phonon dispersion and electronic band structure along with total and projected density of states of B2 structure Al-Li at theoretically obtained equilibrium lattice constant along major symmetry directions of the Brillion zone using DFT as used in Quantum ESPRESSO [3]. In the present work, we extend the investigation on Al-Li by computing thermophysical properties such as thermal equation of state and Grüneisen parameter of B2 and B3 Al-Li.

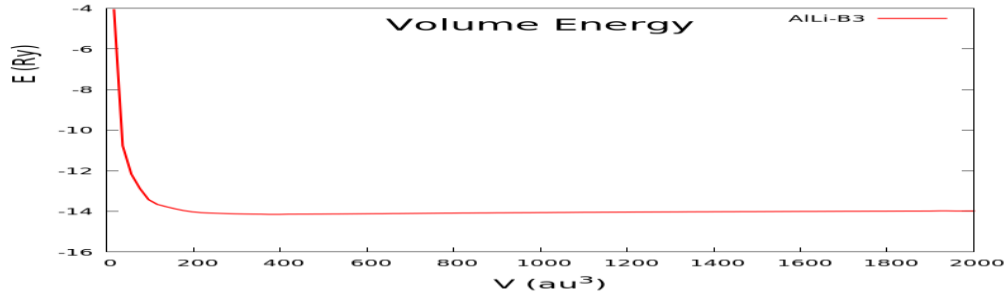

Fig.2 Energy - Volume graph for B2 Al-Li

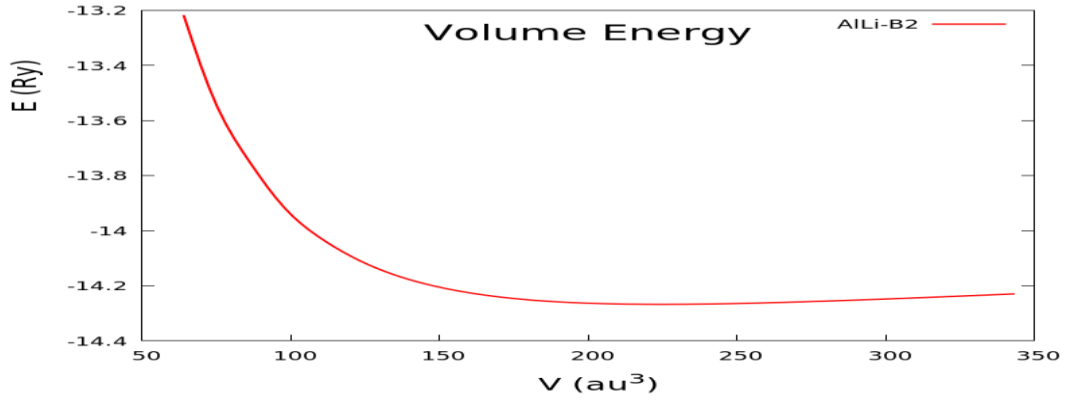

Fig.3 Energy - Volu me graph, for B3 Al-Li

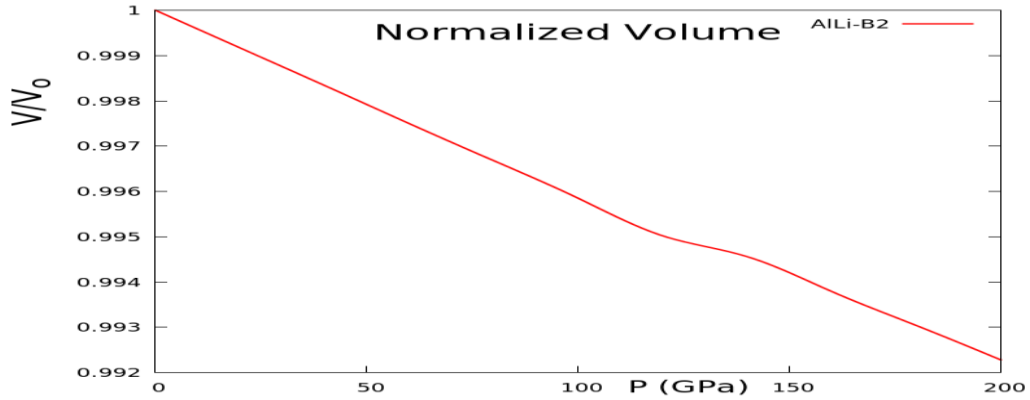

Fig.4 Thermal equation of states of B2 Al-Li

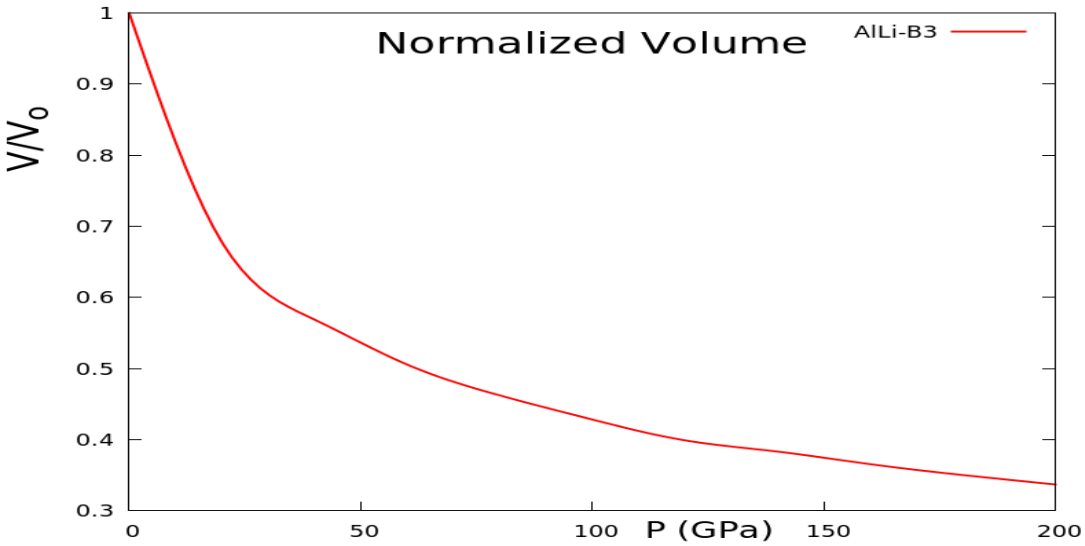

Fig.5 Thermal equation of states of B3 Al-Li

Different thermophysical properties of B2 Al-Liwere investigated for computed optimize cell parameters a = 3.217Å using GIBBS programme [4].For the comparative study, the said thermophysical properties are also computed for B3 structure of Al-Li. Figs. 2 and 3 indicate the energy versus volume diagram for the B2 and B3 structure of Al-Li, respectively. Using an obtained *E (V)*data, and an equation of states (EOS), the thermophysical properties are found for computed optimize cell parameters and atomic positions.

Figures 4 and 5 show the normalized volume-pressure diagram for B2 and B3 Al-Li, respectively. The smooth decrease in unit cell volume and constant behaviour of unit cell volume with increase in pressure is observed which indicates that the crystal structure of the B2 Al-Li is stable up to a pressure of 200 GPa. It is observed that linearity between normalized volume $V/V_0$and pressure P of B2 Al-Libased on our optimize results is more compared to that for B3 Al-Li which signifies the more stability of B2 Al-Li. The in volume of B2 Al-Li based on our optimize results is 62.8 % less compared to that for B3 Al-Li, which is due to the higher bulk modulus of B2 Al-Li compared to B3 Al-Li.

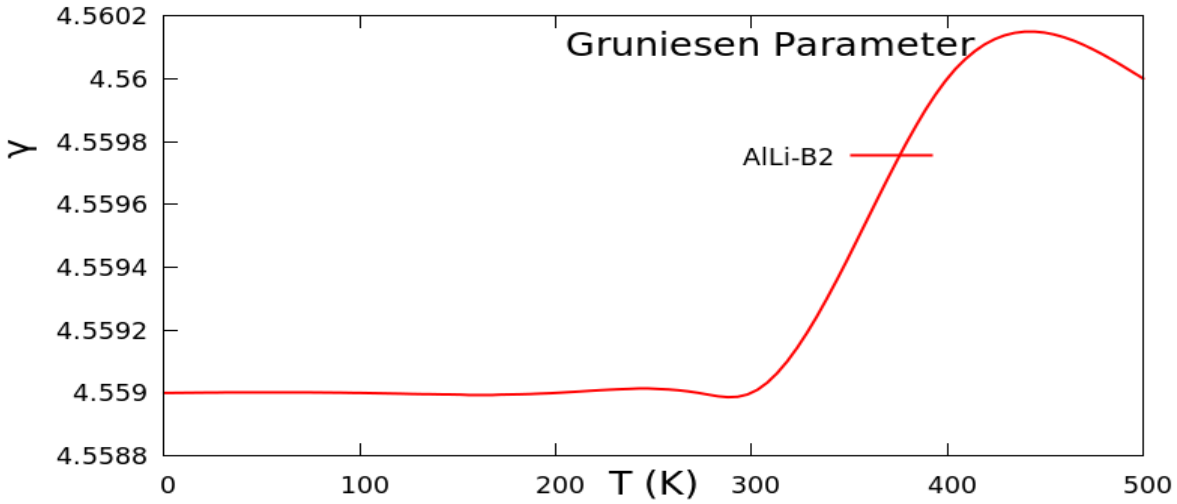

Fig.6 γ_g as a function of T for B2 Al-Li

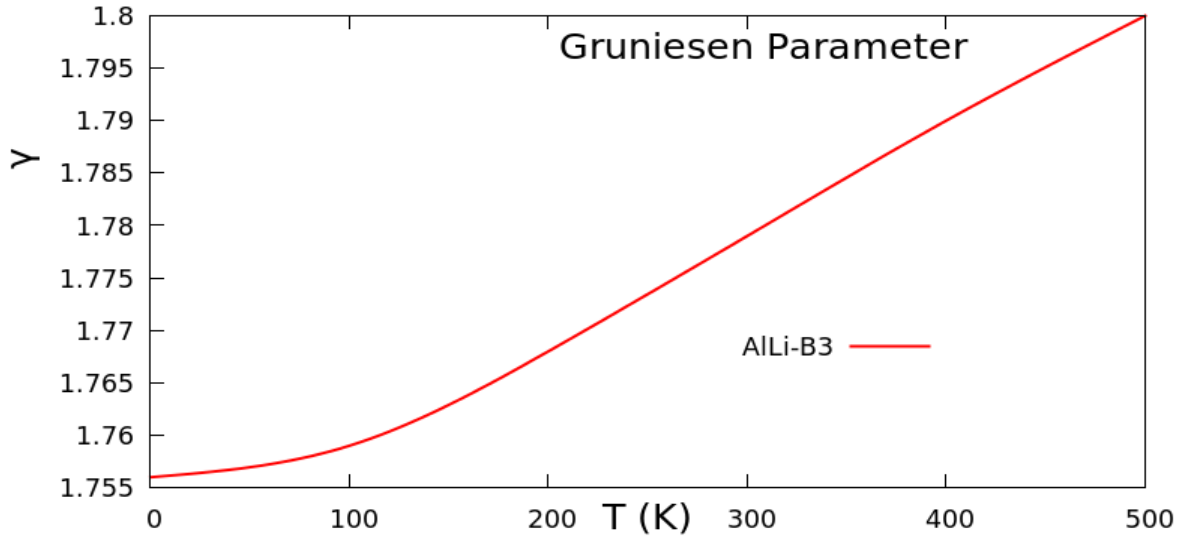

Fig.7 γ_g as a function of T for B3 Al-Li

In Figs. 6 and 7, the computed Grüneisen parameters ofB2 and B3 Al-Li are plotted for the different temperature values at pressure P = 0. Grüneisen parameter varies from 4.5590 to 4.5600 for B2 structure Al-Liand from 1.7500 to 1.800 for B3 structure Al-Li, with the temperature variation from 0 K to 500 K which indicates extremely small change in $\gamma_g$with the temperature variation. The weak change in $\gamma_g$with temperature is in consonance with Grüneisen's assumption [11].

Conclusions

Present results report various ground states and thermophysical properties of B2 (CsCl) structured Al-Li. For the comparative study, thermophysical properties of B3 structure of Al-Li are also computed. Our calculated equilibrium lattice constant and isothermal bulk modulus for B2 (CsCl) structured Al-Li agrees well with the other theoretical findings [10]. Calculated cohesive energies for three cubic phases clearly reveal the structural stability of B2 structure Al-Li at equilibrium. Computed thermal equation of states presumes the stable structure of B2 Al-Li up to a pressure of 200 GPa. Variation in Grüneisen parameter with the temperature indicates the weak temperature dependence of $\gamma_g$with the temperature changes even up to 500 K.

Acknowledgements

Computer facility developed under DST-FIST Level-I program from DST, Government of India, New Delhi and financial assistance under DRS-SAP-I from UGC, New Delhi is highly acknowledged.

References

[1] Korzhavyi, P. A., Ruban, A. V., Simak, S. I., and Vekilov, Yu.Kh., 1994. Phys. Rev. B 49, pp. 14229
[2] Eswara Prasad, N., Gokhale A. A., and Rama Rao, P., 2003, Mechanical Behaviour of Aluminium-Lithium Alloys, Sadhana 23, pp. 209-246
[3] www.quantum-espresso.org
[4]Blanco, M. A., Francisco, E. and V. Luana, V., 2004, Comp. Phys. Commu. 158, pp. 57
[5] Perdew, J. P., Burke, K. and Ernzerhof, M., 1996. Phys. Rev. Lett. 77, pp. 3865
[6] Monkhorst, H. J. and Pack, J. D., 1976. Phys. Rev. B 13, pp. 5188
[7] Murnaghan , F. D., 1944. Proc. Natl. Acad. Sci. USA 30, pp. 244
[8] https://en.wikipedia.org/wiki/Poisson%27s_ratio
[9] Pandya, N. Y., Mevada, A. D., and Gajjar, P. N., 2015, GIT JET 8, pp.178
[9] Kohn, W., Sham L.J., 1965. Phys. Rev. 140, pp. 1133
[10] Khambholja, S. G., Ph.D. thesis, S.P. University, Gujarat (India), pp. 101, (2012)
[11] Grüneisen, E., 1912,Annals Physik 12, pp. 257